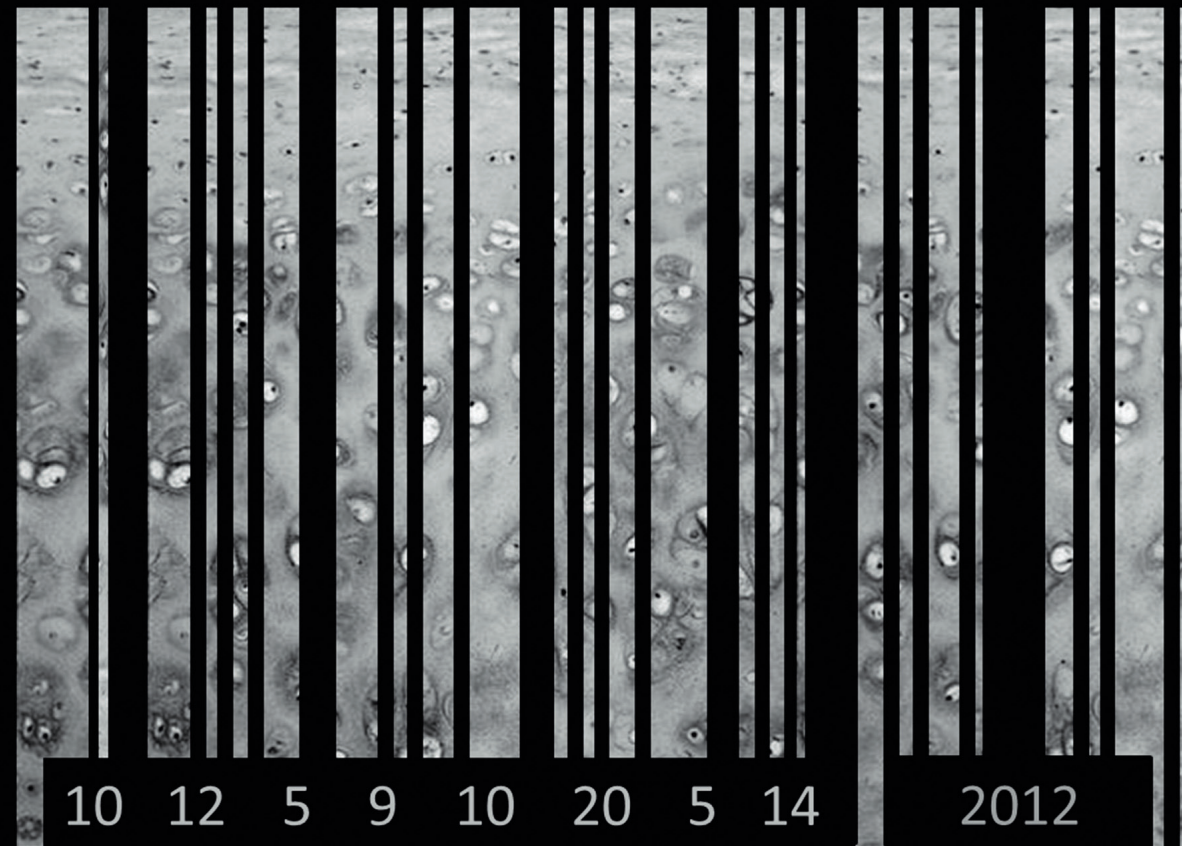


Regulators of Articular Cartilage Homeostasis J. Leijten 2012

Regulators of Articular Cartilage Homeostasis



Jeroen Leijten

Invitation

To attend the public
defence of my
dissertation

Regulators
of articular
cartilage
homeostasis

On Wednesday
25th of May,
2012, at 16:30

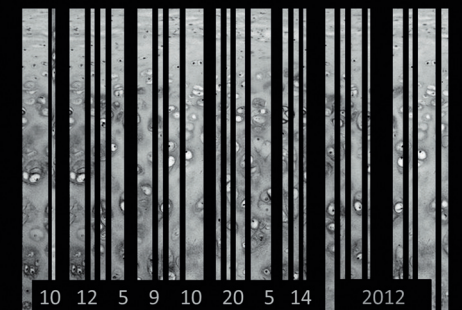
In the Prof. Dr. G. Berkhoff-
zaal (Collegezaal 4),
building De Waaijer, at
the University of Twente,
Drienerlolaan 5, Enschede,
The Netherlands

Jeroen Leijten

j.c.h.leijten@utwente.nl
Tel: 0031-(0)618086235

Paranymphs:
Jim Swildens
Paula van Rossum

ISBN 978-94-6191-308-1



Regulators of articular cartilage homeostasis

Jeroen Leijten

2012

Members of the Graduation Committee

Chairman:

Prof. Dr. G. van der Steenhoven

Promoter:

Prof. Dr. C.A. van Blitterswijk (University of Twente)

Co-promoter:

Prof Dr. M. Karperien (University of Twente)

Members:

Prof. Dr. Floris Lafeber (University Medical Center Utrecht)

Prof. Dr. Gerjo van Osch (Erasmus Medical Center)

Dr. Peter van der Kraan (University Medical Center St Radboud)

Dr. Pieter Emans (Maastricht University Medical Center)

Prof. Dr. Jan de Boer (University of Twente)

Prof. Dr. Leon Terstappen (University of Twente)

Regulators of articular cartilage homeostasis

Jeroen Christianus Hermanus Leijten

PhD Thesis, University of Twente, Enschede, The Netherlands

This publication was supported by the Dutch Arthritis Foundation

This publication was supported by the NBTE (Dutch association for Biomaterials and Tissue Engineering)

ISBN: XXX-XX-XXXX-XXX-X

Copyright: J.C.H. Leijten, 2012, Enschede, The Netherlands. Neither this thesis nor its parts may be reproduced without written permission of the author.

Cover design: L.S. Moreira Teixeira. The barcode shaped cartilage symbolizes the zonal finger printing described within this thesis. It represents a method to identify articular cartilages key features using a zonal approach. The numbers found at the bottom of the barcode numerically encrypt the authors name and year in which this thesis was published.

Regulators of articular cartilage homeostasis

DISSERTATION

to obtain
the doctor's degree at the University of Twente,
on the authority of the rector magnificus,
Prof. Dr. H. Brinksma
on account of the decision of the graduation committee,
to be publicly defended
on Friday, May 25th, 2012, at 16.45 hrs

by

Jeroen Christianus Hermanus Leijten

Born on October 22th, 1982
in Breda, The Netherlands

Promoter:

Prof. Dr. C.A. van Blitterswijk (University of Twente)

Co-promoter:

Prof. Dr. M. Karperien (University of Twente)

Summary

Prevention of hypertrophic differentiation is essential for successful cartilage repair strategies. Although this process is essential for longitudinal growth, it also is part of degenerative cartilage diseases such as osteoarthritis. Moreover, it limits the use of cell types prone to this process for articular cartilage repair; cartilage that becomes hypertrophic can be transformed into endochondral bone. Therefore, fundamental knowledge on hypertrophic differentiation might prove crucial for cartilage repair strategies.

In this thesis we have focused on: i) revealing the mechanism that prevents healthy articular chondrocytes from undergoing hypertrophic differentiation, ii) exploring whether this mechanism is disturbed in joint disease (model), iii) investigating the effect of cartilage's environmental factors on this mechanism and iv) pioneering novel cartilage repair strategies that are not confounded by hypertrophic differentiation.

To set the stage, we provided a literature review in chapter 2 that focuses on existing and emerging cartilage repair strategies and emphasized the cellular behavior in cell-based therapies in chapter 3 by offering an overview of all cell sources that have been studied for cartilage repair.

In Chapter 4 we revealed that the unknown molecular mechanism preventing hypertrophic differentiation of healthy mature articular cartilage is at least partially based on expression of the secreted antagonists *GREM1*, *FRZB* and *DKK1*. In chapter 5 we demonstrated that *GREM1*, *FRZB* and *DKK1* protein levels are affected by sterile inflammation. In chapter 6 we proved that factors related to hypertrophic differentiation can influence the mRNA expression of *GREM1*, *FRZB* and *DKK1*.

In chapter 7 we revealed that oxygen levels regulate longitudinal growth by regulating the speed of hypertrophic differentiation. Moreover, we showed that *GREM1*, *FRZB* and *DKK1* expression levels were inversely correlated with hypertrophic differentiation. In chapter 8, we reported that lowered oxygen levels during in vitro chondrogenic differentiation of mesenchymal stromal cells induced *GREM1*, *FRZB* and *DKK1* expression.

In chapter 9 we capitalized on the chondrocyte's ability to prevent hypertrophic differentiation by mixing low amounts of chondrocytes with larger amounts of mesenchymal stromal cells, which if used alone become hypertrophic. We demonstrated that the MSCs improved cartilage formation by stimulating chondrocytes to proliferation and deposit matrix. In chapter 10 we designed a cost-effective approach that enhanced the cartilage formation by forming micro-aggregates of chondrocytes on a

novel high throughput platform.

Finally, chapter 11 reflects on the overall results presented in this thesis and provides an outlook for a future directive for the utilization of fundamental cartilage knowledge in cartilage repair strategies.

Table of Contents

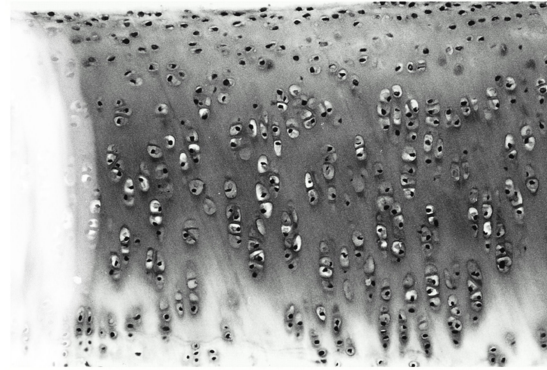
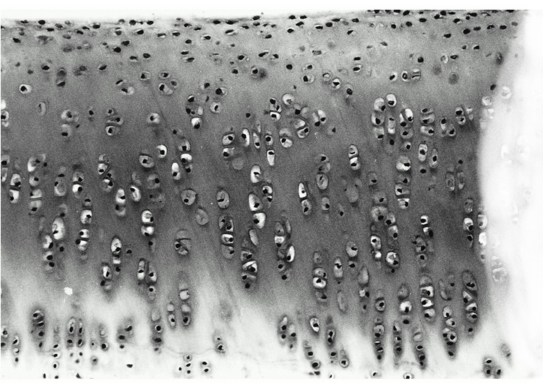
1	General introduction	1
1.1	Cartilage	2
1.2	Development of hyaline cartilage	3
1.3	Hyaline cartilage repair	4
1.4	Aims and outline of this thesis:	5
2	Cartilage tissue engineering	9
2.1	Introduction	11
2.2	Development of cartilage	11
2.2.1	Joint formation	11
2.2.2	Growth plate cartilage	12
2.2.3	Articular cartilage	13
2.3	History of clinical applications in cartilage repair	13
2.4	Cell sources for cartilage engineering	15
2.5	Biomaterials for cartilage repair	17
2.5.1	Chondro-conducting scaffolds: natural and synthetic biomaterials	17
2.5.2	Emerging "smart" biomaterials	20
2.6	Future of cartilage tissue engineering	21
3	Cell sources for cartilage repair	25
3.1	Introduction	27
3.2	Autologous articular chondrocytes: cell number versus dedifferentiation	27
3.3	Non-autologous articular chondrocytes: morbidity versus immune re- sponse	28
3.4	Non-articular chondrocytes: morbidity versus phenotype	29
3.5	Non-chondrocyte cell sources: morbidity versus differentiation control	30
3.6	Co-cultures: combinatorial advantages versus current knowledge . . .	32
3.7	Discussion	34
4	Natural brakes of articular cartilage hypertrophy	43
4.1	Introduction	45
4.2	Materials and methods	46
4.2.1	Origin samples	46
4.2.2	Total RNA extraction	46

4.2.3	Cell isolation and cultivation	46
4.2.4	Organ cultures	46
4.2.5	Histology and immunohistochemistry	46
4.2.6	Microarray processing and Quantitative real-time reverse transcriptase- polymerase chain reaction	47
4.2.7	Genetic Study population	47
4.3	Results	47
4.3.1	Differential gene expression between articular and growth plate cartilage	47
4.3.2	Wnt signaling and cell cycle pathways are less active in articular cartilage	48
4.3.3	Chondrogenically differentiating MSCs resemble growth plate chondrocytes	51
4.3.4	Grem1, Frzb and Dkk1 inhibit longitudinal growth of explanted fetal tibiae dose dependently	53
4.3.5	Addition of GREM1, FRZB or DKK1 during chondrogenic dif- ferentiation of MSCs inhibits terminal hypertrophic differentiation	54
4.3.6	Preserved antagonist expression in expanded articular chondro- cytes	56
4.3.7	GREM1 transcription decreased in degenerating osteoarthritic cartilage	57
4.3.8	SNP rs12593365 is associated with radiographic osteoarthritis .	58
4.4	Discussion	59
5	Grem1, Frzb and Dkk1 as biomarkers	65
5.1	Introduction	67
5.2	Materials and methods	67
5.2.1	Experimental animals	67
5.2.2	Induction of sterile synovitis	68
5.2.3	Collection of blood and synovial fluid	68
5.2.4	Quantification of Grem1, Frzb and Dkk1 protein levels	68
5.2.5	Statistical analysis	68
5.3	Results	68
5.3.1	Synovial fluid protein levels of Grem1, Frzb and Dkk1 during sterile synovitis	68
5.3.2	Serum protein levels of Grem1, Frzb and Dkk1 during sterile synovitis	69
5.3.3	Effect of morphine treatment on synovial fluid protein levels of Frzb and Dkk1 during sterile synovitis	70
5.4	Discussion	70
6	Regulation of GREM1, FRZB and DKK1	75
6.1	Introduction	77
6.2	Materials and methods	78
6.2.1	Chondrocyte isolation and culture	78

6.2.2	Oxygen levels	78
6.2.3	Tonicity	78
6.2.4	Mechanical stimulation	78
6.2.5	Recombinant protein and compound stimulation	79
6.2.6	Quantitative real-time reverse transcriptase-polymerase chain reaction (qRT-PCR)	79
6.2.7	Cell viability	79
6.2.8	Statistical analysis	80
6.3	Results	80
6.3.1	BMP2 enhances transcription of Wnt antagonist FRZB and DKK1	80
6.3.2	Canonical Wnt-signaling down regulates GREM1, FRZB and DKK1 expression	80
6.3.3	Canonical Wnt-signaling regulates <i>GREM1</i> , <i>FRZB</i> and <i>DKK1</i> mRNA levels in bovine chondrocytes, MG63, SAOS2, and MSCs	81
6.3.4	Inhibition of Canonical Wnt signaling induces mRNA expression of GREM1, FRZB and DKK1	84
6.3.5	Effects of PTHrP, IHH and cyclopamine on <i>GREM1</i> , <i>FRZB</i> and <i>DKK1</i> mRNA expression	85
6.3.6	Effects of IL1B stimulation on <i>GREM1</i> , <i>FRZB</i> and <i>DKK1</i> mRNA expression	86
6.3.7	Effects of physiological factors on <i>GREM1</i> , <i>FRZB</i> and <i>DKK1</i> mRNA transcription	87
6.4	Discussion	88
7	Oxygen level regulates hypertrophic differentiation	95
7.1	Introduction	97
7.2	Materials and Methods	98
7.2.1	Tibiae organ cultures	98
7.2.2	Histological analysis	98
7.2.3	Total RNA isolation	98
7.2.4	Quantitative real-time reverse transcriptase-polymerase chain reaction (qRT-PCR)	98
7.2.5	Enzyme-linked immunosorbent assay (ELISA)	99
7.2.6	Statistical analysis	99
7.3	Results	99
7.3.1	Hypoxia mitigates longitudinal growth	99
7.3.2	Normoxia stimulates endochondral ossification	100
7.3.3	Normoxia increases hypertrophic zone's length	100
7.3.4	Hypoxia decreases hypertrophy markers' mRNA expression	100
7.3.5	Hypoxia enhances Frzb and Dkk1 protein levels	103
7.4	Discussion	104
8	Oxygen level steers chondrogenesis	109
8.1	Introduction	111

8.2	Materials and Methods	112
8.2.1	Patient material	112
8.2.2	Total RNA extraction	112
8.2.3	Chondrogenic differentiation of MSCs	112
8.2.4	Histological analysis	113
8.2.5	Quantitative glycosaminoglycan and DNA assay	113
8.2.6	Determination of GREM1, FRZB and DKK1 protein levels	113
8.2.7	Microarray processing and statistical analysis	113
8.2.8	Quantitative real-time reverse transcriptase-polymerase chain reaction (qRT-PCR)	114
8.2.9	Statistical analysis	114
8.3	Results	114
8.3.1	Hypoxia stimulates chondrogenic differentiation of MSCs	114
8.3.2	Effect of oxygen on gene expression profile of chondrogenically differentiating MSCs	114
8.3.3	Gene networks regulated by oxygen levels	116
8.3.4	Hypoxia induces chondrogenically differentiating MSCs to express hyaline cartilage-enriched genes	116
8.3.5	Hypoxia up regulates articular cartilage-enriched and decreases growth plate cartilage-enriched mRNA levels in chondrogenically differentiating MSCs compared to normoxia	118
8.3.6	Continued hypoxia is needed to retain chondrogenic stimulus	120
8.3.7	Delayed hypoxia stimulus is sufficient to induce a shift in gene expression profile	120
8.4	Discussion	121
9	MSC secreted factors stimulate chondrocytes	125
9.1	Introduction	127
9.2	Materials and Methods	128
9.2.1	Cell culture and expansion	128
9.2.2	Histology	128
9.2.3	Quantitative GAG and DNA assay	128
9.2.4	DNA isolation, RNA isolation and quantitative PCR	128
9.2.5	Cell tracking with organic fluorescent dyes	129
9.2.6	EdU and TUNEL staining	129
9.2.7	Image acquisition and analysis	129
9.2.8	Preparation of conditioned medium	129
9.2.9	Short Tandem Repeats (STR) analysis	129
9.2.10	Statistical analysis	130
9.3	Results	130
9.3.1	Co-culturing hMSCs with hPCs enhanced cartilage matrix formation	130
9.3.2	Xenogenic co-culture of hMSC and bPCs show enhanced chondroinduction	130
9.3.3	Chondrocytes are located at the periphery of the cell pellet	132

9.3.4	iMSCs co-cultured with bPCs die via apoptosis	134
9.3.5	iMSCs stimulate chondrocyte proliferation in pellet co-cultures	134
9.3.6	iMSC conditioned medium increases bPCs proliferation and matrix formation	136
9.4	Discussion	139
10	Microaggregates stimulate neocartilage formation	147
10.1	Introduction	149
10.2	Materials and Methods	149
10.2.1	Tissue source and preparation	149
10.2.2	Mold design and micro-aggregate formation	150
10.2.3	Dextran-Tyramine hydrogels (Dex-TA)	150
10.2.4	Metabolic activity and chondrocyte viability	151
10.2.5	In vivo implantation	151
10.2.6	Histological analysis	151
10.2.7	Whole genome gene expression microarray analysis	151
10.2.8	Real time PCR analysis	152
10.2.9	Statistical analysis	152
10.3	Results	152
10.3.1	High-throughput generated chondrocyte micro-aggregates resemble chondrocyte clusters in OA	152
10.3.2	Micro-aggregation stimulates cartilage matrix formation	153
10.3.3	Micro-aggregated cell clusters remain viable after embedding in a hydrogel	156
10.3.4	Cell cluster formation enhanced cartilage matrix deposition	156
10.3.5	Microarray analysis confirmed increased expression of cartilage-related genes in human chondrocyte clusters	160
10.4	Discussion	160
11	Reflections and outlook	169
11.1	Abstract	170
11.2	Cell complexity	171
11.3	Tissue complexity	172
11.4	Organ complexity	172
11.5	Valorization complexity	173
	Acknowledgements	177
	Curriculum Vitae	179
	List of Publications	181



Chapter 1

General introduction and thesis outline

When a distinguished but elderly scientist states that something is possible, he is almost certainly right. When he states that something is impossible, he is very probably wrong.

Arthur C. Clarke, Clarke's first law

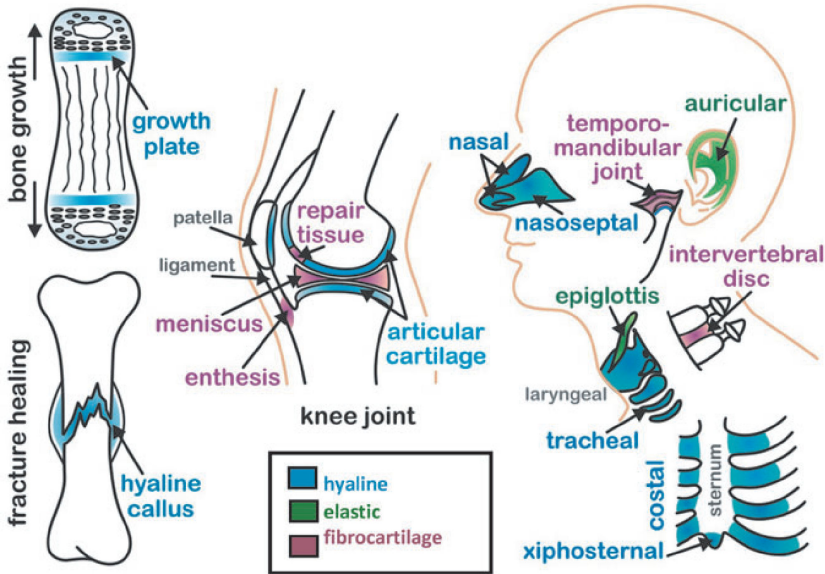


Figure 1.1: Schematic overview of the anatomical locations of different cartilages. Reproduced from (1).

1.1 Cartilage

Cartilage is a connective tissue that is located at a variety of anatomical sites. In general, cartilage can be divided in three types: hyaline cartilage, fibrocartilage and elastic cartilage (figure 1.1) [1]. In this thesis we will primarily focus on hyaline cartilage as articular cartilage belongs to this family of cartilage. Regardless of its subtype, cartilage predominantly consists of extracellular matrix. This matrix is typically composed of a collagen and proteoglycans [2]. Collagen is the backbone of cartilage in which proteoglycans are woven. The proteoglycans are comprised of multiple proteoglycan monomers that are attached end-on-end to a molecule of hyaluronan. This effectively forms a brush-shaped proteoglycan aggregate (figure 1.2). These aggregates are able to retain high amounts of water.

When pressure is exerted, by for example joint movement, the negatively charged proteoglycan aggregates are pushed closer together, which adds to the compressive stiffness of the cartilage. Moreover, the deformation of cartilage by mechanical stresses drive interstitial fluid away from the compressed cartilaginous matrix [3]. Although these mechanisms are able to absorb most of the mechanical stress, the collagenous network slowly accumulates. This results in a progressive decline of the compressive stiffness, as the aggregated proteoglycans are less efficiently contained by the collages. Within the extracellular matrix rests a sparse population of native cells: the chondrocytes. Despite their low metabolic activity in adults, these cells maintain the cartilage by delicately regulating extracellular matrix remodeling [4]. The fragile balance be-

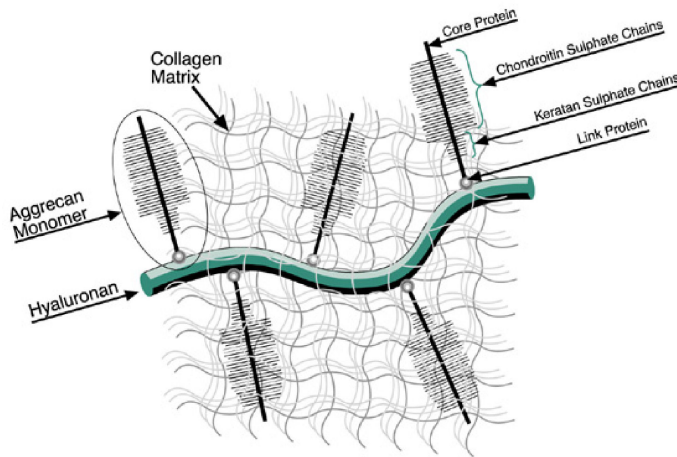


Figure 1.2: Schematic overview of cartilage's extracellular matrix. Reproduced from (15).

tween anabolism (i.e. matrix formation) and catabolism (i.e. matrix degradation) of the cartilage matrix is referred to as homeostasis.

1.2 Development of hyaline cartilage

When cartilage is irreparably damaged external intervention in the form of cartilage repair is desired. Most cartilage repair strategies are designed for the hyaline cartilage of the limbs. Therefore, it is of importance to understand how the limbs are formed. In human embryogenesis the limb buds are formed of a core of somatic mesoderm and an outer layer of ectodermal cells during the 4th week of gestation [5]. The outgrowth of the limb bud is a high-paced process that can be divided in three phases: initiation, propagation and termination. All of these phases are regulated by a tightly orchestrated molecular network of growth factors that includes members of the wntless/int (Wnt), bone morphogenetic proteins (BMP) and fibroblast growth factor (FGF) families, as well as SHH, GREM1 and DKK1 [5] (figure 1.3).

Chondrogenic differentiation starts with compaction of mesenchymal stromal cells within the center of the outgrown limb bud forming a prechondrogenic condensation. Subsequently the joints are formed via apoptosis in the middle layer of an area called the interzone (figure 1.4A) [5]. This efficiently separates the future stylopod, zeugopod and autopod. Cells in the mesenchymal condensates differentiate in immature hyaline chondrocytes and give rise to the developing long bones. During the maturation process, hyaline chondrocytes in the middle of the bone proliferate in a columnar fashion, become hypertrophic, undergo apoptosis and leave a mineralized cartilaginous template that is transformed in endochondral bone in which the bone marrow will be formed [6]. Postnatally, secondary centers of ossification are formed in both

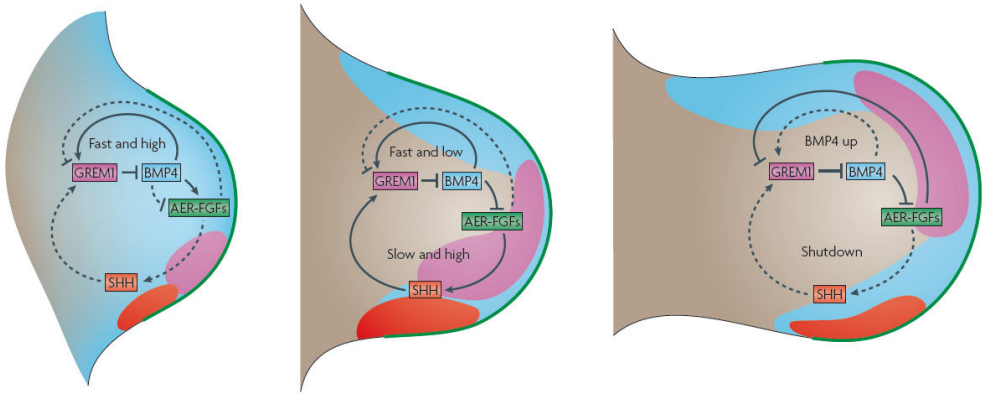


Figure 1.3: Schematic overview of limb bud formation. This process is regulated by a complex time-dependent interplay between gremlin1 (GREM1), bone morphogenetic protein 4 (BMP4), apical ectodermal ridge-derived fibroblast growth factor (AER)-FGF. Limb bud formation is initiated by the BMP4 driven up regulation of GREM1 (A). This allows the establishment of a signaling network that controls the distal progression of the limb bud (B). As the gap between SHH and GREM1 widens, together with the onset of AER-FGF-mediated inhibition of GREM1, it terminates the signaling network that drives limb bud formation (C). Broken lines indicate inactive signals, solid lines indicate active signals. Reproduced from [18].

cartilaginous heads of the long bone, which separates the articular cartilage from the growth plate cartilage (figure 1.4B) [6]. The growth plate continues to undergo the process of hypertrophic differentiation and endochondral ossification that drives the longitudinal growth of an individual. Around puberty the growth plate disappears; the remaining part of the growth plate cartilage is transformed into endochondral bone [7]. In contrast, healthy mature articular cartilage is highly resistant to hypertrophic differentiation and lasts throughout life. Articular cartilage can be divided into three zones: the superficial zone, the mid-zone and the deep zone (figure 1.4C). The collagen fibers have a distinct orientation, which supports the absorption of mechanical shocks [8]. Additionally, the superficial zone provides lubrication that allows near-frictionless and painless joint movement [9].

1.3 Hyaline cartilage repair

Articular cartilage is avascular and aneural and has consequently a limited repair capacity. Accordingly, severe damage to articular cartilage can only be repaired by external intervention. Severe articular cartilage damage can be inflicted acutely e.g. focal defects due to sports injuries or chronically via degenerative diseases e.g. osteoarthritis [10]. Young and active patients with focal cartilage defects can be considered for regenerative procedures such as autologous chondrocyte implantation. This

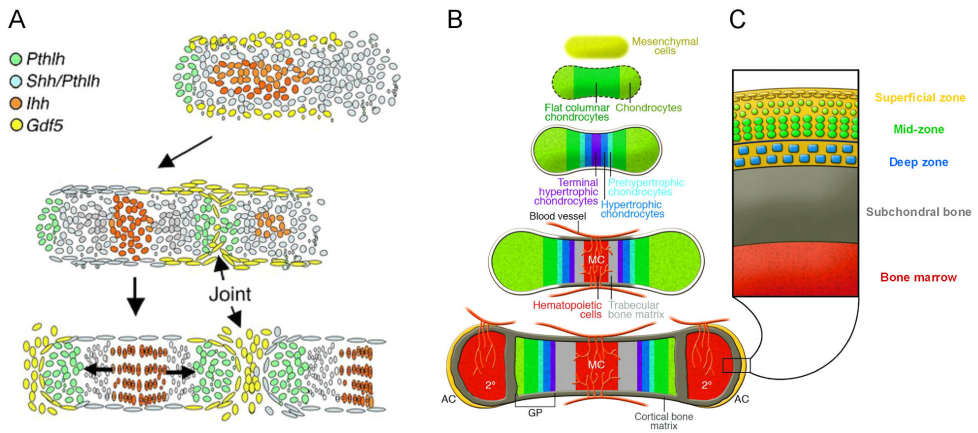


Figure 1.4: Schematic overview of joint formation and long bone development. Joint formation is regulated by indian hedgehog (IHH), parathyroid hormone-like hormone (PTH LH) and growth differentiation factor 5 (GDF5). *Ihh* induces *Pthlh* at a distance, which regulates the distance to the developing joint space. Although *Gdf5* is first expressed around the condensing cells of the cartilaginous anlage, it is later expressed in the future joint space, where it regulates cell recruitment and proliferation (A). The (pre)chondrogenic condensation of mesenchymal cells ultimately results in the development of long bones via hypertrophic differentiation and subsequent endochondral ossification. The growing long bones are composed of articular cartilage, secondary ossification center, growth plate consisting of resting zone, proliferative zone and hypertrophic zone, trabecular endochondral bone and bone marrow (B). Articular cartilage is comprised of superficial zone, mid-zone and the deep zone (C). Adapted from [6] and [19].

procedure is based on a two-step surgery [11]. In the first surgery a small cartilage biopsy is taken, from which the residing chondrocytes are isolated. However, to obtain sufficient amounts chondrocytes *in vitro* culture expansion is essential. Unfortunately, this expansion diminishes the chondrogenic potential of the isolated chondrocytes [12].

To circumvent this clinical problem, the use of the multipotent mesenchymal stromal cells for cartilage repair strategies was ventured. Although mesenchymal stromal cells demonstrated to possess several advantages over expanded chondrocytes, their use as cartilage forming cells is hindered by their proneness to undergo hypertrophic differentiation and subsequent endochondral ossification [13-15].

1.4 Aims and outline of this thesis:

Fundamental knowledge on the process of hypertrophic differentiation might prove crucial for cartilage repair strategies. In particular, it might result in methods to prevent this process from occurring. In consequence, such developments pave the way

for the use of non-chondrocyte cell sources, which are prone to undergo hypertrophic differentiation, for cartilage repair. Additionally, it might allow for the restoration of joint homeostasis as it has been postulated that, in at least a subset of patients, hypertrophic differentiation is an essential step in the progression of several cartilage diseases including osteoarthritis [16].

1

This thesis focuses on: i) acquisition of fundamental knowledge regarding how healthy articular chondrocytes are able to prevent hypertrophic differentiation, ii) determine whether such mechanisms are affected when joint homeostasis is perturbed and iii) pioneer novel approaches to improve upon cartilage regeneration strategies that are not confounded by hypertrophic differentiation. The current chapter gives a general introduction that allows the reader to understand the scope and aims of the thesis. Chapter two summarizes the history of cartilage repair and how the fundamental understanding of cartilage can drive the development of improved cartilage repair strategies.

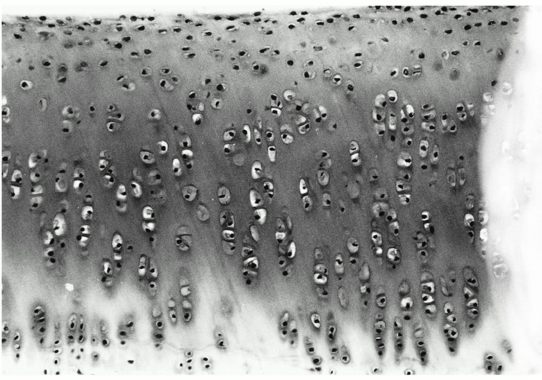
Chapter three reviews all cell sources that have been studied for cartilage repair with a special focus on their advantages and disadvantages. Chapter four describes an alternative approach using a novel platform to elucidate the unknown molecular mechanism that is responsible for the difference in propensity to undergo hypertrophic differentiation between human articular and growth plate cartilage. We postulate that the secreted antagonists *GREM1*, *FRZB* and *DKK1* are key elements in the prevention of hypertrophic differentiation in articular cartilage. In chapter five the effect of joint homeostasis perturbation on *GREM1*, *FRZB* and *DKK1* protein levels was studied. In chapter six we explored the effect of factors related to hypertrophic differentiation on the mRNA expression of *GREM1*, *FRZB* and *DKK1*.

In chapter seven we revealed that oxygen levels have profound effects on longitudinal growth, which is driven by hypertrophic differentiation and endochondral ossification. Moreover, it demonstrated that *GREM1*, *FRZB* and *DKK1* expression levels were inversely correlated with hypertrophic differentiation. In chapter eight, we reported that *GREM1*, *FRZB* and *DKK1* expression is regulated by oxygen tension during chondrogenic differentiation.

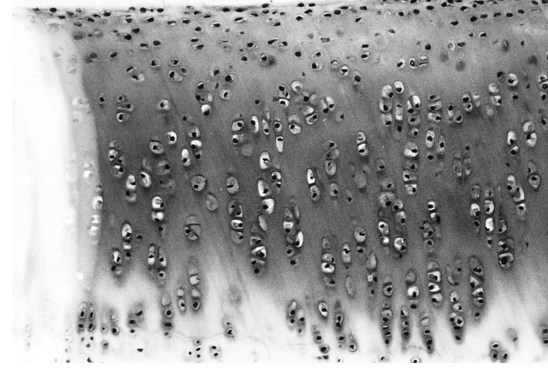
In chapter nine we capitalized on the chondrocyte's ability to prevent hypertrophic differentiation via these secreted factors by pursuing a co-culture strategy. Low amounts of chondrocytes were mixed with a larger amount of mesenchymal stromal cells. Remarkably, this dilution of chondrocytes resulted in an improved cartilage formation that was based on enhanced matrix deposition by and proliferation of chondrocytes. In chapter ten we designed an alternative cost-effective approach to enhance cartilage formation without the use of additional cell sources or exogenous recombinant proteins. Moreover, this bio-inspired cartilage repair strategy is not confounded by hypertrophic differentiation. Our methodology was based on high throughput formation of chondrocyte aggregates. We demonstrated that this bio-inspired approach improved cartilage formation compared to the standard use of an identical amount of single cell chondrocytes. In chapter eleven the current thesis is reflected with regards to its relevance to the current state-of-the-art in cartilage repair and provides an outlook for future directives for the utilization of fundamental cartilage knowledge in cartilage repair strategies.

References

1. El Sayed, K., et al., Heterotopic autologous chondrocyte transplantation—a realistic approach to support articular cartilage repair? *Tissue Eng Part B Rev*, 2010. 16(6): p. 603-16.
2. Morrison, E.H., et al., The development of articular cartilage: I. The spatial and temporal patterns of collagen types. *J Anat*, 1996. 189 (Pt 1): p. 9-22.
3. Soltz, M.A. and G.A. Ateshian, Interstitial fluid pressurization during confined compression cyclical loading of articular cartilage. *Ann Biomed Eng*, 2000. 28(2): p. 150-9.
4. Archer, C.W. and P. Francis-West, The chondrocyte. *Int J Biochem Cell Biol*, 2003. 35(4): p. 401-4.
5. !!! INVALID CITATION
6. Zuscik, M.J., et al., Regulation of chondrogenesis and chondrocyte differentiation by stress. *J Clin Invest*, 2008. 118(2): p. 429-38.
7. van der Eerden, B.C., M. Karperien, and J.M. Wit, Systemic and local regulation of the growth plate. *Endocr Rev*, 2003. 24(6): p. 782-801.
8. Arokoski, J.P., et al., Normal and pathological adaptations of articular cartilage to joint loading. *Scand J Med Sci Sports*, 2000. 10(4): p. 186-98.
9. Jay, G.D., et al., The role of lubricin in the mechanical behavior of synovial fluid. *Proc Natl Acad Sci U S A*, 2007. 104(15): p. 6194-9.
10. Bhosale, A.M. and J.B. Richardson, Articular cartilage: structure, injuries and review of management. *Br Med Bull*, 2008. 87: p. 77-95.
11. Brittberg, M., et al., Treatment of deep cartilage defects in the knee with autologous chondrocyte transplantation. *N Engl J Med*, 1994. 331(14): p. 889-95.
12. Yang, K.G., et al., Impact of expansion and redifferentiation conditions on chondrogenic capacity of cultured chondrocytes. *Tissue Eng*, 2006. 12(9): p. 2435-47.
13. van Laar, J.M. and A. Tyndall, Adult stem cells in the treatment of autoimmune diseases. *Rheumatology (Oxford)*, 2006. 45(10): p. 1187-93.
14. Scotti, C., et al., Recapitulation of endochondral bone formation using human adult mesenchymal stem cells as a paradigm for developmental engineering. *Proc Natl Acad Sci U S A*, 2010. 107(16): p. 7251-6.
15. Pelttari, K., et al., Premature induction of hypertrophy during in vitro chondrogenesis of human mesenchymal stem cells correlates with calcification and vascular invasion after ectopic transplantation in SCID mice. *Arthritis Rheum*, 2006. 54(10): p. 3254-66.
16. Pitsillides, A.A. and F. Beier, Cartilage biology in osteoarthritis—lessons from developmental biology. *Nat Rev Rheumatol*, 2011. 7(11): p. 654-63.
17. Preprotech. Cartilage, Related Cytokines, and Osteoarthritis. 2011; Available from: <http://www.peprotech.com/content/focusarticles.htm?id=72>.
18. Zeller, R., J. Lopez-Rios, and A. Zuniga, Vertebrate limb bud development: moving towards integrative analysis of organogenesis. *Nat Rev Genet*, 2009. 10(12): p. 845-58.
19. Niedermaier, M., et al., An inversion involving the mouse *Shh* locus results in brachydactyly through dysregulation of *Shh* expression. *J Clin Invest*, 2005. 115(4): p. 900-9.



2



2

Chapter 2

Cartilage tissue engineering

Jeroen Leijten*, Liliana Moreira Teixeira*, Nicole Georgi*, Ling Wu, Marcel Karperien

* Shared first co-authorship

I am always doing that which I cannot do, in order that I may learn how to do it.

Pablo Picasso

Abstract

Cartilage tissue engineering is the art aimed at repairing defects in the articular cartilage which covers the bony ends in the joints. Since its introduction in the early 90'ties of the past century, cartilage tissue engineering using autologous chondrocyte implantation (ACI) has been used in thousands of patients to repair articular cartilage defects. This review focuses on emerging strategies to improve cartilage repair by incorporating fundamental knowledge of developmental and cell biology in the design of optimized strategies for cell delivery at the defect site and to locally stimulate cartilage repair responses.

2.1 Introduction

Tissue engineering is the art of utilizing (biological) material to generate a new tissue that will replace worn out or lost native tissue that mimics its original function. Mature joint cartilage is unable to repair itself sufficiently when damaged. This results in degeneration of the cartilage and inevitably to joint failure. The need to intervene in this progressive degeneration and to restore or replace the affected cartilage effectively has created the field of cartilage tissue engineering. The main aim of cartilage tissue engineering is to repair joint or articular cartilage. Like epiphyseal growth plate cartilage, articular cartilage is a hyaline cartilage of which the extracellular matrix is rich in glycosaminoglycans and collagen type 2 as the most abundant protein. Unlike for articular cartilage, there is no clear clinical need for epiphyseal cartilage tissue engineering. Thus if one speaks about cartilage tissue engineering, we are specifically talking about articular cartilage.

This review first discusses the development of cartilage focusing on the development of long bones, the growth plate and in particular articular cartilage. Many of the molecular mechanisms identified in the developing long bones can be applied in tissue engineering strategies. In addition to the biological knowledge, it is important to understand the history of clinical applications of articular cartilage repair and how this led to presently used tissue engineering strategies. Another essential element for the creation of an optimal and effective therapy is, in case cells are used, the cell source. For this the focus will be on historically used cell sources, the current trend and options for future therapy. The use of currently available commercial biomaterials and their use in cartilage tissue engineering, as well as emerging smart materials that are adapted to certain selected requirements are highlighted. Finally this review gives a perspective on the future of cartilage tissue engineering.

2.2 Development of cartilage

2.2.1 Joint formation

The main purpose of tissue engineering is to generate new tissue that can mimic the original functions to replace worn out or lost native tissues. Fundamental knowledge on the tissue of interest, as well as its natural development, is therefore of paramount importance. Chondrogenesis is heralded from three different origins: the cranial neural crest that forms craniofacial cartilage, the somites leading to the axial skeleton and the lateral plate mesoderm resulting in the formation of limbs. From here on we will focus on the latter, since cartilage tissue engineering mostly focuses on the joints of the limbs [1].

Secretion of fibroblast growth factor (FGF) 7 from the lateral plate mesoderm initiates the formation of the limb organizing apical ectodermal ridge (AER). Subsequently a signalling loop between FGF 10 in the limb mesoderm and FGF 8 in the AER directs the proximal distal outgrowth of the limb buds. Cartilage formation starts with the mesenchymal condensations in these developing limb buds and is formed from a seemingly heterogeneous cell population. The up-regulation of

TGFB, a member of the BMP superfamily, leads to enhanced expression of numerous molecules including N-cadherin, N-CAM, fibronectin and Tenascin-C, which are all implicated in the condensation of the mesenchymal cells [2].

Initiation of the expression of the cartilage master regulator SOX9 instigates chondrogenesis and is associated with the expression of collagen type IIA and at a later stage its splice variant collagen type IIB. Under the influence of a growth factor cocktail, including amongst others insulin growth factor 1, FGF2 and BMPs 2/4/7/14, the mesenchymal condensation develops into a cartilage anlage.

The determination of the location of the joint is dependent on a site called the interzone. Although the mechanism behind this phenomenon is largely unknown, the involvement of several molecules such as WNT14, growth differentiation factor 5 and chordin has been implicated. The cells in the interzone start producing lubricin, which is suggested to play a role in the cavitation and separation of the original cartilage anlage resulting in the formation of the joint itself [3]. When fully formed, the articulated ends of the joints are still lined with lubricin producing cells that will allow almost frictionless movement. In the mid-section of the remaining cartilage anlage the primary centre starts to mineralize and is eventually replaced by bone in a process called endochondral ossification. Postnatally, a second centre of ossification appears in the primary growth plate that effectively separates the articular cartilage covering the distal ends of the long bone from the epiphyseal growth plate cartilage entrapped between the epiphysis and metaphysis. Unlike epiphyseal growth plate cartilage which disappears at the end of puberty by growth plate fusion, healthy articular cartilage is resistant to endochondral ossification and does not disappear after puberty.

2.2.2 Growth plate cartilage

Being primarily responsible for longitudinal growth, the activity of the epiphyseal growth plate is tightly orchestrated by multiple autocrine, paracrine and endocrine factors. After the initial mesenchymal condensation and chondrogenic differentiation, the chondrocytes in the centre of the cartilage anlage start to undergo hypertrophic differentiation. This terminal differentiation allows for the formation of a mineralized matrix, in growth of blood vessels and eventually chondrocyte death, most likely via apoptosis. On the remaining cartilage anlage, osteoblasts start producing bone, forming the primary spongiosa. At the opposing end of the hypertrophic chondrocytes, chondrocyte proliferation continues in vertical columns further lengthening the long bones. These proliferating chondrocytes are recruited from the resting zone which covers the distal ends of the long bones. After the formation of the secondary ossification center the resting zone is located directly adjacent to the epiphysis [4] and contains the growth plate stem cells. The continuous cycle of stem cell recruitment, proliferation, hypertrophic differentiation and chondrocyte death is tightly regulated by a plethora of signalling molecules. The feedback loop between Indian Hedgehog and Parathyroid Hormone-related Protein is demonstrated to be one of the key regulators of endochondral ossification. Additionally, many other factors have been shown to play (major) roles in endochondral ossification including paracrine factors like Fi-

broblast Growth Factors (FGFs), Bone Morphogenetic Proteins (BMPs), WNTs, and endocrine regulators such as Thyroid Hormone, Growth Hormone, Insulin-like Growth Factor 1, testosterone and estrogens [5]. Many of these factors are currently explored for application in tissue engineering strategies for cartilage repair.

2.2.3 Articular cartilage

As already indicated, the main focus of cartilage tissue engineering is on restoration of the articulated surface of the joint, the articular cartilage. In its healthy mature form the tissue has an extremely high matrix/cell ratio: only 2-3 percent of its mass consists of chondrocytes, the only residing cells in articular cartilage. For the remaining it consists out of 65-80 percent of water, 12-21 percent of collagens being predominantly collagen type II, 6-10 percent of proteoglycans and approximately 2-3.5 percent other proteins. The arch-like orientation of collagen type II fibrils, being almost horizontal in the superficial zone and almost fully vertical in the deep zone, gives the articular cartilage its anisotropic nature and allows it to transduce mechanical forces throughout the entire tissue. Additionally, the different zones do not contain the same (ratio of) molecules, having different (levels of) glycosaminoglycans and collagens as well as other more characteristic features such as the calcification of the cartilage near the subchondral bone and the production of lubricin in the superficial zone [6]. An important characteristic of healthy articular cartilage is that they are resistant to endochondral ossification. In joint degenerative diseases such as osteoarthritis, this resistance disappears and it is described that the degeneration is, at least in part, caused by endochondral ossification [7]. Articular and epiphyseal chondrocytes have many features in common and it has been long believed that they have a common progenitor. In the past years, however, preliminary proof has been provided that articular and epiphyseal growth plate chondrocytes arise from distinct cell populations. At present, the mechanisms by which articular chondrocytes are formed and by which they are able to resist hypertrophic differentiation and subsequent endochondral ossification remains unknown.

2.3 History of clinical applications in cartilage repair

The clinical and biological need to develop new cartilage repair strategies arises from the fact that cartilage has a low capacity of self repair. When damaged by either trauma or degenerative diseases it will progressively degrade and thereby destabilizing the joint. The majority of cartilage engineering strategies focus on the repair of cartilage lesions induced by trauma, since progressively diseased cartilage, such as seen in osteoarthritis needs different repair approach.

If left untreated, acute trauma will inevitably result in joint degeneration necessitating unicompartamental or total joint replacement as the only possible solution to treat the degenerated joint. To avoid total joint replacement the surgeon has a number of treatment options all with inherent drawbacks. The most popular clinical cartilage repair approaches of the last 20 years are osteochondral transplantation (OT),

marrow stimulation techniques e.g. microfracture (MF) and autologous chondrocyte implantation (ACI).

OT can be divided into autologous mosaicplasty and allograft osteochondral transplantation. In the more recently developed mosaicplasty, [8] cylindrical osteochondral grafts are harvested from a non-load bearing site of the donor and will then be press fitted in pre-drilled osteochondral holes of the defect area. During the healing process, space between the grafts will be filled with fibrocartilaginous tissue. This strategy carries the risk of bone collapse at the donor and recipient site but shows acceptable results in long term follow up. Since mosaicplasty can only be applied to smaller lesions, allograft osteochondral transplantation with matching fresh or frozen cartilage pieces from organ donors is an alternative option.

During MF the subchondral bone of the affected cartilage is perforated leading to blood clot formation at the defect site and, after the invasion of progenitor cells, to cartilage matrix formation. This cost saving and fast technique, based on the self-healing capacity of invading bone marrow cells, was first introduced by Steadman et al [9] in the early 90s. The procedure of MF leads to satisfactory outcome, but has been reported to induce fibrous cartilage formation with poor mechanical properties in some cases, questioning the long term performance of the de novo formed tissue. Next to MF, ACI gained popularity after its introduction by Brittberg et al in 1994. ACI is the first cell based therapeutic cartilage tissue engineering strategy [10]. This two step surgical procedure requires donor cartilage harvest from a non-load bearing site for chondrocyte isolation, followed by upto 6 weeks of cell expansion *ex vivo* and finally re-implantation of the expanded cells at the defect site. During re-implantation, the cartilage defect is first covered with a periosteal flap sealed with fibrin glue before injecting the cultured chondrocytes underneath the periosteal flap (Figure 2.1). This time consuming and costly technique has been shown to promote the formation of hyaline like cartilage with functional improvement in most patients, whereas other studies provide evidence for the abundance of substantial amounts of fibrous cartilage [11]. In the last decade, various studies compared microfracture to ACI with conflicting results. The findings indicate that ACI and MF lead to similar outcomes in the repair of small lesions, but the repair of large defects might have a superior outcome after ACI. In 2008, Saris et al [12] introduced characterised chondrocyte implantation (CCI) to overcome existing problems with the quality of the engineered cartilage obtained by ACI. The strategy of this CCI relies on the pre-assessment of chondrocyte populations with a greater potential to form hyaline cartilage. Compared with MF, this technique was shown to result in noticeably better clinical outcome after 36 months [13].

Although all these described cartilage repair strategies support enhanced joint function and pain relief for the patient, they do not succeed in restoring the natural cartilage structure with its associated biomechanical properties. Recent cartilage tissue engineering approaches include established methods in combination with the delivery of cells and/or bioactive molecules via a biomaterial scaffold. Bartlett et al described two variations of the traditional ACI. In the first variation, periosteal flap is replaced with a porcine-derived type I/type III collagen (ACI-C) matrix. In the second variation, before implantation chondrocytes were first seeded in a collagen

bilayer (matrix-induced ACI-MACI). Both methods resulted in an improvement of ACI based on the Cincinnati knee score and International Cartilage Repair Society score, which provide both a measure for cartilage and joint quality.

2.4 Cell sources for cartilage engineering

Presently, cartilage tissue engineering is primarily based on the use of two cell types: chondrocytes or mesenchymal stromal cells (MSCs). As the most intuitive cell source for cartilage regeneration, autologous chondrocytes, have been successfully used in many studies of cartilage repair with or without the use of a scaffold [10]. However, using chondrocytes in cartilage repair applications obviously has some disadvantages. One problem could be injury of healthy cartilage from which chondrocytes are harvested. Although donor cartilage is taken from low weight bearing sites of joint, this procedure often results in morbidity at donor sites. Another problem of using autologous chondrocytes in cartilage engineering is that they can only be harvested from small biopsies of articular cartilage. To obtain sufficient chondrocytes for cartilage repair, *in vitro* expansion is necessary. Culture expansion of chondrocytes results in a gradual loss of the chondrocyte phenotype with increasing passage number, a process known as chondrocyte dedifferentiation.

After several passages of expansion in two-dimensional culture environment, chondrocytes lose their initial characteristics and become fibroblast-like cells [14]. Expanding chondrocytes on microcarriers instead of tissue culture plastic can omit subculture steps in flask, thus can prevent dedifferentiation of chondrocytes. It is also believed that dedifferentiated chondrocytes may regain the ability to produce cartilage matrix when cultured in a 3D environment (e.g., suspension in hydrogel), or in chondrogenic differentiation medium containing transforming growth factor β (TGF β). This growth factor plays an important role in cartilage formation during organogenesis in the embryo. However, the cartilage phenotypes obtained by these treatments are significantly inferior when compared to native cartilage [15]. Yet the complex molecular events occurring in the induction and maintenance of the chondrogenic phenotype should still be enlightened for further identification of the bioactive levels and kinetics of the key factors involved in cartilage repair. Moreover, integration of repair cartilage with the native tissue and reestablishment of the zonal organization of articular cartilage are still challenging and only partly resolved. To improve the quantity of regenerated cartilage, mesenchymal stromal cells (MSC) are considered to be a promising alternative cell source. MSCs are adult stem cells isolated from somatic tissue. They have been found to be multipotent, showing the ability to differentiate into chondrocyte, osteoblast, adipocytes and endothelial cells. MSCs isolated from different origins like bone marrow, fat tissue, synovium and muscles all show potency of chondrogenic differentiation and may have possible applications in cartilage tissue engineering [16]. Most clinical studies use autologous MSCs, though allograft MSCs may be used in some cases. Traditionally, *ex vivo* chondrogenic differentiation of MSCs is induced by culturing high-density cell pellets in serum-free medium containing TGF β . High-density pellets mimics the first step of cartilage formation in the

embryo, namely the condensation of mesenchymal cells. For MSCs isolated from fat tissue, bone morphogenetic protein 6 (BMP6) is often added to the differentiation medium. In recent years, it has been reported that culturing MSCs in gel-like biomaterials made of collagen or fibrin increases chondrogenic differentiation of MSCs when compared with pellet culture [17]. When using MSCs for cartilage engineering, the greatest challenge is not the differentiation of the cells into chondrocytes per se but to prevent the chondrogenically differentiated MSCs from undergoing endochondral ossification. Substantial evidence indicates that the chondrogenically differentiated MSCs acquire an epiphyseal growth plate phenotype rather than an articular phenotype [18]. To direct differentiation of MSCs in the articular cartilage lineage instead of a growth plate lineage is an active area of research.

2

To reduce the number of chondrocytes needed for cartilage engineering, MSCs started to be co-cultured with chondrocytes. Interestingly, it was reported that co-cultures of bone marrow MSCs with articular chondrocytes produced more matrix compared to chondrocytes alone [19]. This phenomenon of increased cartilage formation was not only observed in differentiation medium containing TGF β , but also in medium without any growth factors. Enhancement of cartilage matrix formation was also found in co-culture of articular chondrocytes with other sources of MSCs [20]. This effect has been attributed to the chondrogenic differentiation of MSCs stimulated by the chondrocytes. In recent years, it has been suggested that lineage commitment of MSCs, however, cannot fully explain their benefits on tissue remodelling and repair. Many studies have suggested a role for MSCs in secreting trophic mediators that stimulate local tissue repair mechanisms. These factors promote tissue specific cells to restore the damaged or lost tissue. A combination of MSCs and autologous chondrocytes may be a promising strategy for cartilage engineering in which the trophic effects of MSCs support and facilitate the chondrocytes to repair cartilage defects. The strategy also reveals possibility of omitting *in vitro* expansion of chondrocytes in traditional ACI procedures. The mixture of chondrocyte and MSCs may lead to a single step surgery for cartilage treatment, in which chondrocytes are isolated, mixed with bone marrow cells from the same patient, loaded on a scaffold and directly re-implanted into the patient.

Many aspects of ACI still need further optimization. For example, the integration of the neo tissue is still far from optimal. It can be hindered by cell loss, either by apoptosis or necrosis caused by, for example inflammatory cytokines or mechanical stress, or due to leakage of the cells. The relatively limited ECM production by the implanted cells, and the dissimilarities in structure and/or composition compared to native cartilage can also lead to integration failure. Thus, strategies that circumvent these complex molecular events, such as the delivery of anti-apoptotic or anti-dedifferentiating factors, combined with a structural orchestration of cells and soluble factors is thought to play an essential role in future therapies.

2.5 Biomaterials for cartilage repair

The commonly used strategy of tissue engineering is, in general terms, to seed cells in a scaffold that can be implanted into the damaged site, as illustrated in figure 2.1. Initially, the main purpose of the scaffold is to provide structural support and allow attachment, proliferation and differentiation of cells in a 3D environment. The mechanical support provided by the scaffold would lead to a decrease in the rehabilitation time for the patient. Nowadays, tissue engineered scaffolds may be developed to trigger, interact and instruct cells by mimicry of key molecular features of the native extracellular matrix (ECM), conferred by both macromolecules (proteoglycans, collagens, fibronectin and laminins) and sequestered growth factors [21].

2.5.1 Chondro-conducting scaffolds: natural and synthetic biomaterials

A myriad of biomaterials has been used as scaffolds for 3D culture of chondrocytes *in vitro* and *in vivo*, as well as for medical applications. Scaffolds can vary depending on material chemistry, 3D geometry, structure, mechanical properties and speed of degradation. The structure, mainly described in terms of pore distribution, orientation and connectivity, should maximize exchange of nutrients, metabolites and regulatory factors, as well as limit oxygen gradients and influence cell-cell interactions. The chemistry can play an instructional role and, overall, the scaffold should be biocompatible and biodegrade at a similar rate as ECM deposition, to ensure continuity and stability of the neo-tissue [22]. Additionally, the scaffolds' mechanical integrity and integration should not only be sufficient to support or match the native tissue, but also mediate mechanical stimulus to the cells during loading [23].

Scaffold materials for cartilage repair can be distinguished according to their source: natural or synthetic, as shown in table 2.1. Natural biomaterials can also be divided in of two types: protein- and polysaccharide-based. Many of these natural materials can be degraded by human enzymes, with non-toxic degradation products. Yet these materials have some drawbacks, mainly related to batch variation, processing and potential pathogen transfer. The main natural materials used for cartilage tissue engineering are collagen, hyaluronic acid, chitosan, agarose, alginate and fibrin glue [24]. These materials can be used either as temporary scaffolds and/or vehicles for cell and drug delivery or can be directly implanted or injected into the defect site.

Synthetic polymers are widely used in tissue engineering due to their flexibility in design and absence of the possibility of disease transmission; yet the disadvantages are related to their relatively poor biocompatibility for example of degradation products, which can lead to severe inflammatory responses. Synthetic materials, such as polylactide, polyglycolide and polyurethane, have been explored as suitable candidates for cartilage repair [24]. Figure 2.2 shows some protein-based membranes and gels which are currently explored in ACI procedures. Scaffolds developed for cartilage tissue engineering can be either solid, like foams meshes or sponges, or gel-like, also termed as hydrogels. Hydrogels have been largely explored for cartilage repair strategies, because they consist of 3D hydrophilic networks and their high water content mimics

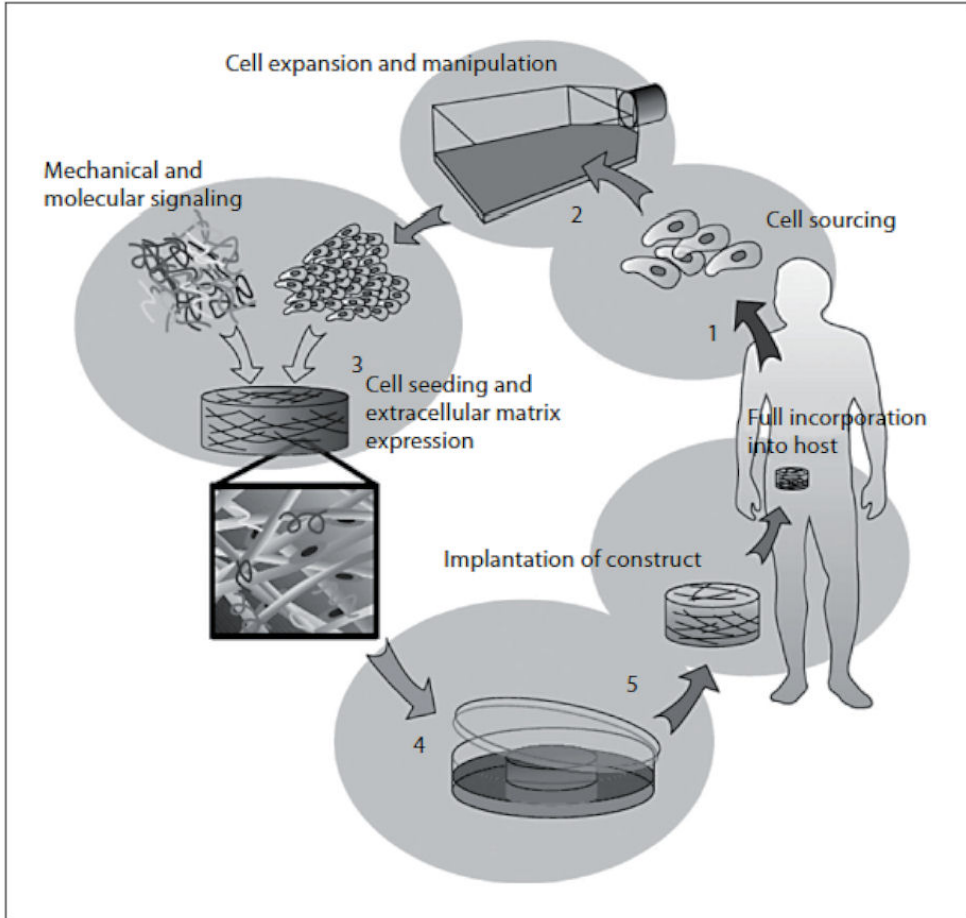


Figure 2.1: The tissue engineering approach. Adapted from: C.A. v Blitterswijk, *Tissue Engineering*. Academic Press Series in Biomedical Engineering [Elsevier / Academic press, Amsterdam; London, 2008] pp. xvi, 740 p.

Material source	Examples	Advantages/disadvantages
Natural	Collagen based	Advantage: providers of molecular cues to the cells, stimulating them to produce more collagen. Disadvantage: poor mechanical properties and can undergo contraction due to interactions with cells when not combined with other materials.
	Hyaluronic acid	Advantage: bioactive properties, with the ability of interacting with chondrocytes (via CD44). Disadvantage: poor mechanical properties of the unmodified hyaluronic acid; the combination or engraftment with other materials, such as polyethylene glycol or dextran, allowed optimization of the biomechanical properties of the hyaluronic acid-based scaffolds.
	Fibrin glue	Advantage: extensively used for wound healing and, additionally for its use as fixative for scaffolds to native tissue. It can also be used as a matrix. Disadvantage: enhancement of cartilage repair is limited.
	Chitosan, agarose and alginate	Advantage: used as either hydrogels, sponges or pads. Disadvantage: still not available for clinical applications.
Synthetic	Poly lactide, polyglycolide, polyethylene glycol and polyurethane	Advantage: no batch variation. Disadvantage: possible inflammatory response against degradation products.

Table 2.1: Scaffold materials for cartilage repair.

native cartilage, unlike solid-type materials. Additionally, due to high diffusion rates, hydrogels allow efficient transport of nutrients and waste products. Hydrogels can be composed of natural and/or synthetic polymers that form a gellified network by physical, ionic or covalent crosslinking. Some hydrogels can be thermo-reversible (liquid at approximately 25 degrees Celsius or below, only solidifying at body temperature, around 37 degrees Celsius), be chemically crosslinked (for example by enzymes), or by photo-polymerization (using visible or ultraviolet light). *in situ* forming hydrogels allow for replacement of open surgeries by a minimal invasive procedure that offers great advantages in integration with native tissue and limits the trauma caused by surgery.

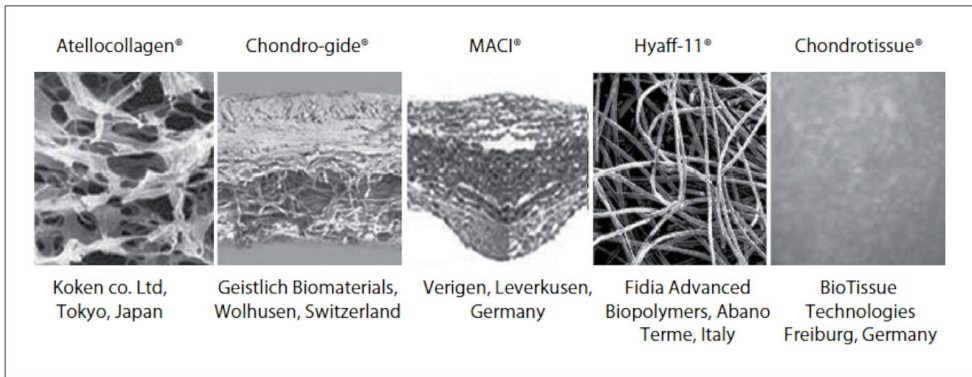


Figure 2.2: Protein-based membranes and gels already available for autologous chondrocyte implantation.

2.5.2 Emerging "smart" biomaterials

Novel scaffolds based on modification of natural polymers, such as dextran, silk, heparin and cellulose, or of synthetic polymers, such as polycaprolactone or co-polymers of polyether-esters have been studied to support cartilage regeneration. Several of these studies have focused on the optimization of these materials and have shown that the combination of different materials may improve properties [24]. Hybrid materials can be designed to mimic ECM structure, for example by adding hyaluronic acid or chondroitin-6-sulfate, and, therefore, providing direct interaction with the chondrocytes by the enabling necessary signals to trigger tissue repair. The communication between the cells and ECM can also be mediated by integrins, surface-specific receptors that react with proteins, such as collagens, fibronectin and laminin, which affect cell survival, proliferation and differentiation. To facilitate these type of interactions, short synthetic peptides such as the Arg-Gly-Asp (RGD) sequence, can be incorporated into scaffolds to increase the interaction between biomaterials and cells. These recognition sequences have proven to be of great value in the case of synthetic materials that lack cell-attachment signals. Yet the involvement of the RGD sequence in inducing or supporting chondrogenic differentiation of MSCs is still controversial. In addition to these peptides, the controlled local delivery of growth and differentiation factors, including Insulin-like Growth Factor 1 (IGF1), Transforming Growth Factor β (TGFB1 and TGFB3) or Bone Morphogenic Proteins (BMP2 and BMP6), have been successfully combined with scaffolds. These growth factors have been selected based on their proven role during cartilogenesis in the developing embryo. Hybrid scaffolds can either be designed to locally release the bioactive factors or produced in such a way that they mimic properties of the ECM. The release of growth factors by synthetic polymers is still highly dependent on the diffusion and degradation rates of the polymers.

Recently, surface-eroding scaffolds and materials of which the release occurs by cellular demand have been developed to allow a better and more effective control of

the release profiles. By incorporation in the scaffold of peptide sequences which can be recognized by e.g. matrix metalloproteinases (MMPs), release of growth factors can be locally controlled [25]. This responsive feature of the scaffold can be of great interest as the release of the growth factor in these cases can be tailored to depend on the disease-activity. For example, MMP13 is a factor that is significantly elevated in osteoarthritis and can be used as a trigger to release scaffold bound drugs [24].

Other strategies to improve scaffold design include the development of biphasic scaffolds. Such scaffolds can also be used *in vitro* for tissue formation prior to implantation, where the design prevents cell migration between regions of the scaffold [23]. Like the growth plate, articular cartilage has a zonal organization. Strategies have been developed that use predefined geometries (for example by using rapid prototyping technologies), or have incorporated physical and chemical gradients in the scaffold to recreate the zonal organization in tissue engineered constructs [26]. Using these strategies, the mimicry of the native cartilage-tissue anisotropy can be achieved. Gene therapy approaches can also be taken into account in scaffold design. In recent years promising results for cartilage repair strategies have been obtained by transfecting chondro-generative growth factor genes and/or chondro-protective cartilage catabolic inhibitor genes [23].

Starting from structural variations from nano to macroscale, the new generation of scaffolds often with a bioinspired design, aim at creating the optimal microenvironment for the formation of a *de novo* extracellular cartilaginous matrix by either chondrocytes, MSCs or a combination of both cell types.

2.6 Future of cartilage tissue engineering

Although a wide range of possible cartilage repair strategies have been described, none of them successfully restores the function and organisation of cartilage in long term studies. At the moment, numerous possible novel repair strategies arise. In general, the optimal approach will be determined by three major components: cells, biomaterials and bioactive compounds.

Cellular and molecular studies including improved cell culture, co-culture, cell tracking, gene therapy, gene arrays and proteomics will provide further cues for possible strategies in joint surface regeneration. The complex molecular events occurring in the induction and maintenance of the chondrogenic phenotype during embryogenesis may lead to the identification of novel mechanisms involved in cartilage formation. It seems promising to translate the findings from developmental biology into strategies for cartilage tissue formation. Beside optimised allogenic and autologous cartilage or cell transplants, progenitor cells, like autologous bone marrow derived stromal cells (MSCs), are likely to play an important role in future strategies for cartilage tissue repair being an alternative or supplementary cell source. Until now, however, the fate of these cells, the choice of cell fraction and optimal culture parameters are not determined and additional research is needed to clarify their applicability to articular cartilage engineering.

As indicated above, growth factors may play an important role in further opti-

mization of cartilage tissue engineering. Presently, application of growth factors in cartilage tissue engineering is controversial and more robust studies are needed to demonstrate their applicability. The choice of the optimal combination of growth factor and method of delivery will very likely depend on the used cell type. For example different growth factors may be needed when MSCs or expanded primary chondrocytes are used for cartilage repair. Improvements in growth factor delivery should reflect an extended release profile, with protection of the proteins against fast degradation and must aim at targeting specific cell types. Multistep release, as a poly-therapy approach instead of single delivery systems, could be an additional improvement for cartilage repair strategies.

2

The third pillar of cartilage tissue engineering is formed by biomaterials. At the moment evermore biomaterials are being developed that show better bioaffinity and manage to mimic the native environment of cartilage. An example of these new generations of biomaterials are *in situ* gelating hydrogels, which mimic the natural ECM and can perfectly fill up irregular defect sites. Importantly, *in situ* gelating hydrogels can be used in minimal invasive strategies, which will significantly reduce the burden for the individual patient. Smart” hydrogels sensitive to external stimuli such as temperature, pH or certain biomolecules, that can trigger swelling or degradation, have been developed. Recently, dynamic hydrogels have been investigated, offering the ability to precisely control temporal and spatial behaviour of the cells, by creating a tissue-like hierarchical organization. This strategy can be combined with tailored delivery of bioactive signals that stimulate tissue repair.

Translating fundamental knowledge in chondrogenesis and articular cartilage homeostasis into the design of novel smart materials is an active field of research, which undoubtedly will result in the development of improved strategies for cartilage repair in the near future.

References

1. Olsen BR, Reginato AM, Wang W. Bone development. *Annu Rev Cell Dev Biol* 2000;16:191-220.
2. Chimal-Monroy J, Diaz de Leon L. Expression of N-cadherin, N-CAM, fibronectin and tenascin is stimulated by TGF- β 1, β 2, β 3 and β 5 during the formation of precartilage condensations. *Int J Dev Biol* 1999;43:59-67.
3. Pacifici M, Koyama E, Iwamoto M. Mechanisms of synovial joint and articular cartilage formation: recent advances, but many lingering mysteries. *Birth Defects Res C Embryo Today* 2005;75:237-48.
4. Zuscik MJ, Hilton MJ, Zhang X, Chen D, O'Keefe RJ. Regulation of chondrogenesis and chondrocyte differentiation by stress. *J Clin Invest* 2008;118:429-38.
5. Grumbach MM. Estrogen, bone, growth and sex: a sea change in conventional wisdom. *J Pediatr Endocrinol Metab* 2000;13 Suppl 6:1439-55.
6. Poole AR, Kojima T, Yasuda T, Mwale F, Kobayashi M, Laverty S. Composition and structure of articular cartilage: a template for tissue repair. *Clin Orthop Relat Res* 2001:S26-33.
7. Kawaguchi H. Regulation of osteoarthritis development by Wnt- β -catenin signaling through the endochondral ossification process. *J Bone Miner Res* 2009;24:8-11.
8. Hangody L, Kish G, Karpati Z, Szerb I, Udvarhelyi I. Arthroscopic autogenous osteochondral mosaicplasty for the treatment of femoral condylar articular defects. A preliminary report. *Knee Surg Sports Traumatol Arthrosc* 1997;5:262-7.
9. Steadman JR, Rodkey WG, Briggs KK, Rodrigo JJ. [The microfracture technic in the management of complete cartilage defects in the knee joint]. *Orthopade* 1999;28:26-32.
10. Brittberg M, Lindahl A, Nilsson A, Ohlsson C, Isaksson O, Peterson L. Treatment of deep cartilage defects in the knee with autologous chondrocyte transplantation. *N Engl J Med* 1994;331:889-95.
11. McNickle AG, L'Heureux DR, Yanke AB, Cole BJ. Outcomes of autologous chondrocyte implantation in a diverse patient population. *Am J Sports Med* 2009;37:1344-50.
12. Saris DB, Vanlauwe J, Victor J, et al. Characterized chondrocyte implantation results in better structural repair when treating symptomatic cartilage defects of the knee in a randomized controlled trial versus microfracture. *Am J Sports Med* 2008;36:235-46.
13. Saris DB, Vanlauwe J, Victor J, et al. Treatment of symptomatic cartilage defects of the knee: characterized chondrocyte implantation results in better clinical outcome at 36 months in a randomized trial compared to microfracture. *Am J Sports Med* 2009;37 Suppl 1:10S-9S.
14. Schnabel M, Marlovits S, Eckhoff G, et al. Dedifferentiation-associated changes in morphology and gene expression in primary human articular chondrocytes in cell culture. *Osteoarthritis Cartilage* 2002;10:62-70.
15. Mukaida T, Urabe K, Naruse K, et al. Influence of three-dimensional culture in a type II collagen sponge on primary cultured and dedifferentiated chondrocytes. *J Orthop Sci* 2005;10:521-8.
16. Sakaguchi Y, Sekiya I, Yagishita K, Muneta T. Comparison of human stem cells derived from various mesenchymal tissues: superiority of synovium as a cell source. *Arthritis Rheum* 2005;52:2521-9.
17. Mueller MB, Tuan RS. Functional characterization of hypertrophy in chondrogenesis of human mesenchymal stem cells. *Arthritis Rheum* 2008;58:1377-88.
18. Tsuchiya K, Chen GP, Ushida T, Matsuno T, Tateishi T. The effect of coculture of chondrocytes with mesenchymal stem cells on their cartilaginous phenotype *in vitro*. *Mat*

Sci Eng C-Bio S 2004;24:391-6.

19. Hildner F, Concaro S, Peterbauer A, et al. Human Adipose-Derived Stem Cells Contribute to Chondrogenesis in Coculture with Human Articular Chondrocytes. *Tissue Eng Pt A* 2009;15:3961-9.

20. Gnechi M, He H, Liang OD, et al. Paracrine action accounts for marked protection of ischemic heart by Akt-modified mesenchymal stem cells. *Nat Med* 2005;11:367-8.

21. Place ES, Evans ND, Stevens MM. Complexity in biomaterials for tissue engineering. *Nat Mater* 2009;8:457-70.

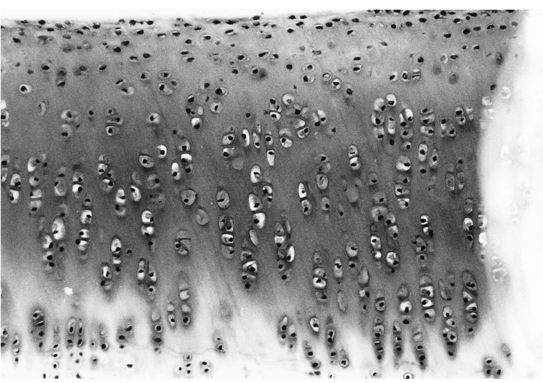
22. Vunjak-Novakovic G. The fundamentals of tissue engineering: scaffolds and bioreactors. *Novartis Found Symp* 2003;249:34-46; discussion -51, 170-4, 239-41.

23. Woodfield TB, Bezemer JM, Pieper JS, van Blitterswijk CA, Riesle J. Scaffolds for tissue engineering of cartilage. *Crit Rev Eukaryot Gene Expr* 2002;12:209-36.

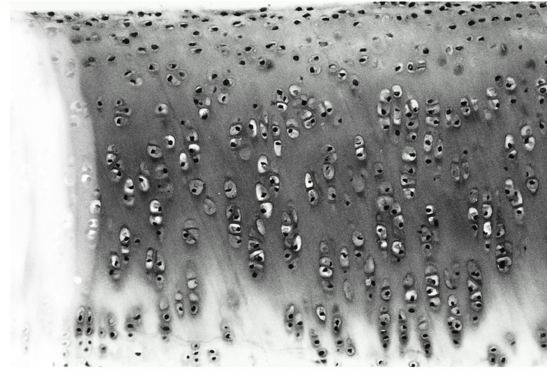
24. Stoop R. Smart biomaterials for tissue engineering of cartilage. *Injury* 2008;39 Suppl 1:S77-87.

25. Raeber GP, Lutolf MP, Hubbell JA. Mechanisms of 3-D migration and matrix remodeling of fibroblasts within artificial ECMs. *Acta Biomater* 2007;3:615-29.

26. Klein TJ, Malda J, Sah RL, Hutmacher DW. Tissue engineering of articular cartilage with biomimetic zones. *Tissue Eng Part B Rev* 2009;15:143-57.



3



3

Chapter 3

Cell sources for articular cartilage repair strategies: shifting from mono-cultures to co-cultures

Jeroen Leijten*, Nicole Georgi*, Clemens van Blitterswijk and Marcel Karperien

* both authors contributed equally

It is the mark of an educated mind to be able to entertain a thought without accepting it.
Aristotle

Abstract

The repair of articular cartilage is challenging due to the sparse native cell population combined with the avascular and aneural nature of the tissue. In recent years cartilage tissue engineering has shown great promise. As with all tissue engineering strategies, the possible therapeutic outcome is intimately linked with the used combination of cells, growth factors and biomaterials. However, the optimal combination has remained a controversial topic and no consensus has been reached. In consequence, much effort has been dedicated to further design, investigate and optimize cartilage repair strategies.

This review will give a comprehensible overview on the cell sources that have been investigated for articular cartilage repair strategies with emphasis on the advantages of combining multiple cell types.

3.1 Introduction

Mature articular cartilage is composed of an abundant extracellular matrix that is sparsely populated by chondrocytes. Articular cartilage is avascular and aneural and the native chondrocytes are largely in cell cycle arrest. As a consequence, it is challenging for this tissue to suitably respond to traumatic injury. Injury inevitably results in altered biomechanics of the joint and joint instability, which shift joint homeostasis towards catabolism [1, 2]. If left unchallenged, this may ultimately lead to joint failure. As a result, the recalcitrant capacity of articular cartilage to self-heal acquired injuries drives research focused on (novel) cartilage reparative and regenerative treatments.

Current treatments of traumatic cartilage defects include osteochondral grafting, bone marrow stimulation techniques and more recently cell based therapies [3-6]. Osteochondral autografting is particularly suitable for smaller lesions, but is associated with donor-site morbidity [7]. Osteochondral allografting can be considered for larger defects, but is associated with graft failure [8]. Bone marrow stimulation techniques such as micro-fracturing and micro-drilling are used for defects smaller than 2-4 cm² with little or no bone loss and are associated with the formation of fibrocartilage [9]. The most common form of cell based therapies is autologous chondrocyte implantation (ACI). This treatment is based on the implantation of *in vitro* expanded autologous chondrocytes, which were isolated from a biopsy that was obtained in a first surgery. ACI is typically used with defects larger than 2-4 cm², but recent evidence suggest that it also yields superior results in smaller defects compared to a bone marrow stimulation technique [10]. Since ACI is dependent on the violation of intact cartilage for the isolation of chondrocytes, it is associated with donor-site morbidity [4].

Consequently, a myriad of alternative cell sources other than culture expanded articular chondrocytes has been investigated to circumvent this side-effect and to improve the therapeutic outcome of cartilage repair strategies. In addition to several types of chondrocytes derived from a number of hyaline cartilage subtypes, the use of multi-potent cells with chondrogenic potential derived from various sources has been proposed.

This review will discuss the different cell sources dominating the field of cartilage tissue engineering and highlights recent advances of co-culture approaches.

3.2 Autologous articular chondrocytes: cell number versus dedifferentiation

Conventional cell-based cartilage repair therapies characteristically use autologous articular chondrocytes. These cells are harvested from biopsies of macroscopically intact cartilage derived from a non-weight bearing part of the joint [11]. Removal of a biopsy from healthy articular cartilage can potentially lead to secondary osteoarthritis. However, to understand the full extent of the consequences more thorough studies with longer follow up are required [12]. To minimize the chance of developing secondary

3 osteoarthritis the biopsy size is limited. In consequence, the biopsy yields insufficient amounts of chondrocytes to allow for direct reimplantation. Therefore, chondrocytes are expanded *in vitro* before reimplantation. Unfortunately, expansion is associated with progressive loss of the chondrogenic phenotype and results in dedifferentiated fibroblast-like chondrocytes [13]. We recently demonstrated that articular chondrocyte dedifferentiation is a continuous, progressive and multi-signaling-pathway-based process. Moreover, the potential to redifferentiate is also gradually lost and might be in part caused by epigenetic regulation such as DNA methylation. The loss of chondrocyte phenotype during mono layer expansion is suggested to be depended on the matrix elasticity of the culture environment [14]. Indeed, integrin $\alpha 5 \beta 1$ is suggested to play an important role in the dedifferentiation of chondrocytes [15]. As this process can impede the therapeutic outcome, the prevention of dedifferentiation or the induction of redifferentiation has been intensively investigated. Investigated strategies include exposure to optimized environmental properties like oxygen levels [16] and tonicity of the culture medium [17], dynamic non-adherent culturing [18], three dimensional expansion of cells using e.g. microcarriers [19], varying the elasticity [14] or pore-size of expansion material [20], culture on predeposited extracellular matrices of e.g. synovium-derived stem cells [21], the use of medium preconditioned by culturing e.g. primary chondrocytes or mesenchymal stromal cells (MSCs) [22-24] and supplementation of the expansion medium with exogenous recombinant growth factors [25].

Dedifferentiation can also be limited or prevented by reducing or omitting the expansion phase. This idea is based on implanting fewer chondrocytes that are less expanded and have therefore a higher cell performance [26-28]. Although this approach indeed demonstrated to be able to regenerate cartilage, it as of yet results in mechanically weaker cartilage when compared to implantation of higher densities of further expanded chondrocytes in the same defect size. However, it provides the opportunity to reduce the tediousness of currently used protocols. By reducing or omitting the amount of dedicated cell culture time, it might be possible to improve the costs-effectiveness of chondrocyte-based cell therapy.

3.3 Non-autologous articular chondrocytes: morbidity versus immune response

Allogenic, or even xenogenic, articular chondrocytes can be considered as an alternative cell source of which the isolation does not inflict additional damage to the afflicted joint. Advantageously, a larger number of chondrocytes can be obtained by taking larger biopsies and/or pooling different donors. This might limit or obsolete the expansion phase and could potentially reduce inter-patient variation of the therapeutic outcome. Naturally, serious consideration should be given to drawbacks such as disease transmission and immune rejection [29]. Indeed, chondrocytes constitutively express histocompatibility complex class I at their cell surface and demonstrate cytokine inducible expression of histocompatibility complex class II [30]. Moreover, it has been shown that chondrocytes can interact with immune cells [31]. Several

reports have described serious immune responses after allogenic chondrocyte implantation in full thickness defects where the access to the bone marrow increases the risk for immunological reactions [32-34]. Consequently, the clinical feasibility of allogenic chondrocytes implantation is severely hindered. In contrast, osteochondral allograft demonstrated only minor immunogenic signs in human clinical trials [35, 36]. This might at least be partially explained by the protective environment of the native cartilage. The avascular and highly dense nature of the extra cellular matrix might be able to limit or prevent the invasion of immune cells from the joint. Indeed, isolated chondrocytes appear to be protected from an immune response when encapsulated in biocompatible biomaterials or when allowed to form a new extracellular matrix *in vitro* [37, 38]. Therefore, non-autologous articular chondrocytes can be still considered as a potentially interesting cell source for matrix assisted chondrocyte transplantations.

3.4 Non-articular chondrocytes: morbidity versus phenotype

Next to articular chondrocytes, several alternative chondrocyte sources have been investigated to design cartilage repair strategies that do not impose additional damage to the articular cartilage. In adults, other sources of (non-articular) hyaline cartilage are located in the nose, ribs, larynx, trachea and bronchi. In particular, costal and nasoseptal chondrocytes have been extensively investigated [29, 39-41]. Both costal and nasoseptal cartilage biopsies grant a higher cell yield of chondrocytes. The proliferation rate of these chondrocytes is increased compared to articular chondrocytes [42]. Although they both undergo dedifferentiation during expansion they appear more sensitive to redifferentiation [43, 44]. Moreover, transplantation of costal chondrocytes in full thickness defects results in the production of neocartilage [45]. Unfortunately, both costal and nasoseptal chondrocytes are known for their ability to ossify when reimplanted [40, 46, 47].

Auricular chondrocytes derived from elastocartilage of the ear are as well considered as a possibly interesting cell source for cartilage repair strategies. Native and freshly isolated auricular chondrocytes typically express elastin. Although, upon *in vitro* culture the expression of elastin is gradually lost [41, 48], it has been reported that the elastin expression can be regained when implanted *in vivo* [49]. Whether the expression of elastin will negatively influence the mechanical properties of neocartilage in an articular cartilage defect remains to be clarified. Like nasoseptal and costal chondrocytes, isolated auricular cartilage provide a higher cell yield per gram of biopsied tissue and have a higher proliferation rate compared to articular chondrocytes. Auricular chondrocytes are prone to dedifferentiation and are susceptible to redifferentiation [42, 50]. Mild forms of ossification have been observed after reimplantation [40]. Interestingly, it has been found that auricular chondrocytes express lubricin, a mucinous glycoprotein essential to lubrication of the joint [41]. Therefore, auricular chondrocytes are a cell source of considerable interest, in particular for repair or reconstruction of the articular cartilaginous superficial zone.

Meniscal chondrocytes derived from the meniscal fibrocartilage as well express lubricin and have been investigated in cartilage repair strategies [41, 51]. However,

meniscal chondrocytes scarcely express collagen II, and have limited potential to secrete glycosaminoglycans. Consequently they generate neocartilage with inferior mechanical properties as compared to articular cartilage or other chondrocyte cell sources [52]. Like ACI, the use of meniscus chondrocytes is based on cells isolated from a biopsy and may predispose to secondary OA, as it can induce joint instability [53]. Additionally, the meniscus is partially exposed to the same catabolic environment as the articular cartilage, which deteriorates the chondrogenic behavior of the meniscal chondrocyte [54]. As meniscal chondrocytes have similar disadvantage compared to articular chondrocytes and produce inferior neocartilage compared to these cells, they are an unlikely cell source for articular cartilage repair strategies.

3 3.5 Non-chondrocyte cell sources: morbidity versus differentiation control

In recent years much research has been dedicated to cell sources other than chondrocytes for articular cartilage repair strategies. These cell sources include amongst others synovial fibroblasts, periosteocytes and multipotent progenitor cells.

Synovial fibroblasts are a part of the natural repair response to articular defects, as these cells tend to fill up non-treated defects with a fibrous matrix [55]. Unfortunately, this matrix is, like the matrix produced by meniscal chondrocytes, mechanically weak [56].

Periosteocytes, depending on their isolation site, contain a chondrogenic potential that allows the formation of neocartilage [57]. However, it has been suggested that this potential is inversely correlated with age. [58].

Pluripotent cells such as embryonic stem cells and induced-pluripotent stem cells are able to form *de novo* articular-like cartilage and can in theory be considered for cartilage repair strategies [59, 60]. However, gaining absolute control on the prevention of teratoma formation is paramount when using these cells [61, 62]. Until such control is acquired, it is unlikely that these cell sources will be clinically approved for treatment of non-lethal diseases such as articular cartilage repair.

The best characterized progenitor cell sources for articular cartilage repair include mesenchymal stromal cells (MSCs) derived from amongst others bone marrow, periosteum, synovium, synovial fluid, adipose tissue, bucal fat pad, infrapatellar fat pad and osteoarthritic cartilage [63-67]. Many other MSCs sources have remained largely uninvestigated for cartilage repair strategies and include umbilical cord blood, menstrual blood, muscles, ligaments, wartons jelly, amnion, chorion, breast milk, tonsil, etc [68-75]. Important factors deciding on the applicability of this plethora of MSCs should not only be based on chondrogenic potential and phenotype, but also on cell yield, accessibility, availability, age-related function decline, donor-site morbidity and acquisition costs.

Large inter-donor variation is a general complication encountered in all multipotent cell sources [76, 77]. This is exacerbated by the influence of temporal culture conditions, methods of harvest and disputably age of the donor [57, 78-81]. It has been suggested that distinct gene expression profiles might reflect their (chondrogenic)

differentiation potential [82]. However, the highly desired markers for chondrogenic differentiation potential of undifferentiated MSCs have so far remained undiscovered. Additionally, expansion of multipotent cells negatively affects chondrogenesis and might thereby possibly further confound therapeutic outcome [83, 84].

Both the maintenance of multipotency and chondrogenic potential of MSCs are greatly influenced by culture conditions in the expansion phase and optionally the differentiation phase. The classical view on optimizing the culture of mammalian cells is based on medium composition; much research has been focused on medium type and medium supplements [85-90]. Non-autologous medium supplements might hamper the clinical applicability of tissue engineering strategies. Presently much attention is paid towards optimizing physiological factors, which influence cell behavior and thus therapy outcome, such as mechanical stress, substrate stiffness, substrate coating or chemistry and incubator gas composition in particular oxygen levels [91-99]. Other physiological variables such as tonicity have remained largely uninvestigated.

Rather than using MSCs for chondrogenic differentiation and direct production of neocartilage, one can also take advantage of the immunomodulatory or trophic properties of MSCs [100]. It is suggested that after reimplantation differentiated MSCs continue to modulate the immune response [101]. This may be of high importance for allogeneic treatments [102]. However, whether this modulation proves to be sufficient in tissues that are scarce in cells and rich in matrix, such as articular cartilage, remains to be further studied. Nonetheless, using allogeneic strategies allows for a potential decrease in the therapeutic inter-donor variation via the use of pools of multiple donors or selection of well performing donors.

Intra-articular injection of MSCs in a degenerating joint improves joint function and retards the development of osteoarthritis compared to untreated controls [103]. However, tracking experiments have shown that only a fraction of the injected MSCs are integrated in or located near the affected cartilage [104]. In fact, most MSCs are located in the joint capsule or migrated from the joint to seemingly unrelated tissues such as thymus, tongue, stomach, duodenum, jejunum and colon [105]. Together this suggests that the MSC at least partially act via an indirect mechanism, most likely via the secretion of trophic factors. Indeed, *in vitro* co-culture experiments demonstrated the anabolic effects of MSCs-derived trophic factors on chondrocytes [23]. However, whether the same trophic factors are responsible for the anabolic effects observed *in vivo* remains to be proven.

Although MSCs can be differentiated in many different cell types, it remains to be noted that their differentiation process cannot be fully controlled *in vivo*. Spontaneous sarcoma formation has been observed in long term expanded MSCs and after injection in mice [106, 107]. Although this has not yet been reported in humans, the lack of full control over the behavioral phenotype of the MSCs remains a potential concern. For example, injections of MSCs in cancer therapy has both been described to restrict tumor growth by decreasing the division rate of benign cells as well as augment tumor growth by stimulating the angiogenesis [108]. These types of contradictions are not uncommon and underline the lack of deep understanding of the *in vivo* behavior of MSCs. Absolute control of the differentiation process of MSCs is essential if MSCs are to be used routinely for cell therapy such as articular cartilage repair. It can be

conceived that more stringent selection criteria for the isolation of MSCs will result in a more homogenous and controllable cell source. However, this would also result a more prolonged expansion phase as many cell will be discarded, which might lead to (partial) loss of multipotency.

Chondrogenic differentiation of multipotent cells such as MSCs typically results in the formation of neocartilage that is dissimilar to mature articular cartilage. However, it bears striking phenotypical resemblance to fetal cartilage [109, 110]. Moreover, differentiation of MSCs results in a gene expression profile that more resembles growth plate chondrocytes, which can differentiate into hypertrophic cartilage, rather than articular cartilage [Chapter 4]. Indeed, the newly formed cartilage displays typical signs of hypertrophic differentiation [111-113]. In line with this, standard differentiation protocols currently used for chondrogenic differentiation of MSCs *in vitro*, are not able to induce the expression of genes that are enriched in articular chondrocytes and are able to prevent hypertrophic differentiation [Chapter 8]. Consequently, chondrogenically differentiated multipotent and pluripotent cells undergo endochondral ossification upon subcutaneous implantation [60, 114, 115]. Although this phenomenon is of notable interest for bone repair strategies, it is highly undesirable for cartilage repair strategies. Moreover, it demonstrates that current differentiation protocols, at least *in vitro*, are insufficient to yield articular-like cartilage and require improvement for reproducible cartilage repair strategies.

3.6 Co-cultures: combinatorial advantages versus current knowledge

Performance of the used cell sources can be augmented by making use of co-culture strategies. Co-cultures of different cell sources is based on the idea that the multi-signal events *in vivo* cannot be perfectly mimicked by adding a limited variety of growth factors to a mono-culture of which the optimal cocktail remains largely elusive. This problem can be circumvented by the introduction of another cell source in the culture. In this way, cells are exposed to wider variety of stimuli. Moreover, the stimuli are based on autologous non-recombinant (secreted soluble) factors. As such, they should be considered as a preferred way of stimulation, as it omits the remaining issues regarding the use of non-autologous recombinant factors in clinical settings.

Three decades ago, the first co-culture experiments for cartilage tissue engineering were performed. These experiments mainly focused on revealing the pathological mechanisms of cartilage destruction by mixing chondrocytes with cell types that are potentially involved in cartilage catabolism [116, 117]. More recently, co-cultures that include chondrocytes have been investigated for their potential to boost neocartilage formation. In general three (partially overlapping) categories can be identified: i) co-cultures with unilateral beneficial effect for one cell type on neocartilage formation; ii) co-cultures with mutually beneficial effects on neocartilage formation; iii) co-cultures based on cell types with unique features that do not (directly) affect the behavior of the other cell type.

Expansion of isolated autologous chondrocytes is commonly required to obtain

sufficient amount of cells for reimplantation. This expansion induces dedifferentiation of the chondrocytes. Interestingly, co-culturing expanded dedifferentiated chondrocytes with (previously frozen) primary chondrocytes can (partially) reverse their loss of phenotype [118, 119]. This redifferentiation appears to induce a stable phenotype; withdrawal of the exposure to primary chondrocytes does not lead to reversal of the effect [120]. Alternatively, articular chondrocytes have been co-cultured with non-articular chondrocytes [121]. However, so far little attention has been focused on these types of chondrocyte-chondrocyte co-cultures. In consequence, many questions still linger before an in-depth understanding of their actual therapeutic value can be obtained.

Presently, the most common co-cultures experiments investigate the influence on the differentiation state of employed cell types, as well as in improving the tissue formation of engineered constructs. In 1999 Jikko et al. showed that co-culturing growth plate chondrocytes with articular chondrocytes inhibited the terminal differentiation of growth plate chondrocytes [122]. In line with this, it has been demonstrated that addition of articular chondrocytes to MSCs inhibits hypertrophic differentiation of the latter. Although the mechanism behind this phenomenon remains largely unknown, it is suggested that this effect is mediated via parathyroid hormone-related protein [123]. However, alternative explanations such articular cartilage enriched secreted soluble factors negatively involved in hypertrophic chondrocyte differentiation in both articular chondrocytes and MSCs cultures have remained uninvestigated [Chapter 4].

The first studies in which MSCs were combined with different cell sources to provide a distinct effect e.g. vascularisation of bone tissue engineered constructs [124, 125] and improvement of matrix deposition in degenerative discs (MSCs and degenerative disc cells [126]. In contrast, in cartilage repair strategies MSCs were initially used to reduce the amount of chondrocytes needed or to omit their use all together. Fascinatingly, *chondro-induction* was observed in these experiments; superior neocartilage formation was formed by the combination of two different cell-types as compared to either cell type alone [23, 127]. In this context, the co-culture of articular chondrocytes and MSCs is most commonly studied in the present. It is claimed that this phenomenon can be explained by the induction of chondrogenic differentiation of MSCs by articular chondrocytes [65, 128-130]. Indeed, the addition of articular chondrocyte-conditioned medium is able to instigate chondrogenic differentiation of MSCs [131]. However, recent findings demonstrate that chondrocyte proliferation is enhanced by the presence of MSCs [23, 130]. The MSCs accomplish this effect by acting as a trophic mediator. Moreover, while chondrogenic differentiation of MSCs can be triggered by chondrocytes, it also induces apoptosis in the MSCs [23]. This results in a progressive disappearance of the MSCs from the original co-culture. Further investigation has to demonstrate if MSCs eventually completely vanish from the co-culture. If indeed this holds true, it might be a beneficial factor for the use of (pools of) allogeneic MSCs as an immune response, if it occurs at all, could be of a temporal nature. Moreover, if MSCs indeed predominantly stimulate neocartilage formation indirectly by acting as a source of trophic factors, one might consider MSC implantation sites within the joint other than the cartilage defect as the secreted factors diffuse to the cartilage via the synovial fluid. Regardless, in light of these

novel findings the direct contribution of the MSCs to cartilage matrix deposition has become unclear. In addition, the question whether chondro-induction is induced due to exposure of factors normally produced by the opposite cell type or whether the co-culturing induces the expression of factors otherwise not expressed in either cell type remains to be answered.

Alternative strategies to improve neocartilage formation using co-cultures include the generation of articular cartilage's zonal architecture. In recent years novel cartilage repair strategies have been designed that aim at mimicking this anisotropic organization [132, 133]. Co-cultures in combination with multilayer three-dimensional printing or layer-by-layer methodology using hydrogels that are able to covalently link by residual reactive residues e.g. dextran-tyramine gels [134-136] can further enhance these strategies. Calcifying cells can be used for the deep zone, intensive extracellular matrix producing calcification resistant cells for the middle zone, and less intensive extracellular matrix producing and lubricin secreting cells for the superficial zone. Furthermore, For example, osteoblasts and chondrocytes can be co-cultured in different regions of a construct to allow the formation of an osteochondral interface [137, 138]. However, as only a scarce number of studies have been reported on such an approach, the feasibility remains to be determined.

3

3.7 Discussion

The therapeutic outcome of cell based therapies does not solely rely on the performance of the implanted cells. It also heavily relies on the expansion conditions, exogenous stimuli and (functionalized) biomaterials in case the cells are co-implanted with a scaffold. All these factors greatly influence therapeutic outcome. Moreover, they can result in dissimilar responses in different cell sources. Moreover, much research remains to be performed in order to identify the combinations leading to optimal clinical results. The wide range of cell sources available to cartilage tissue engineers grants an optimal starting point for future improvement of cartilage repair strategies. Specifically, the combination of different cell sources currently holds great promise as it is able to grants combinatorial advantages by combining the benefits while mitigating the disadvantages of unique cell types.

References

1. Roos, H., et al., Osteoarthritis of the knee after injury to the anterior cruciate ligament or meniscus: the influence of time and age. *Osteoarthritis Cartilage*, 1995. 3(4): p. 261-7.
2. Jacobsen, K., Osteoarthrosis following insufficiency of the cruciate ligaments in man. A clinical study. *Acta Orthop Scand*, 1977. 48(5): p. 520-6.
3. Beiser, I.H. and I.O. Kanat, Subchondral bone drilling: a treatment for cartilage defects. *J Foot Surg*, 1990. 29(6): p. 595-601.
4. Brittberg, M., et al., Treatment of deep cartilage defects in the knee with autologous chondrocyte transplantation. *N Engl J Med*, 1994. 331(14): p. 889-95.
5. Steadman, J.R., et al., [The microfracture technic in the management of complete cartilage defects in the knee joint]. *Orthopade*, 1999. 28(1): p. 26-32.
6. Hangody, L., et al., Autologous osteochondral grafting—technique and long-term results. *Injury*, 2008. 39 Suppl 1: p. S32-9.
7. Paul, J., et al., Donor-site morbidity after osteochondral autologous transplantation for lesions of the talus. *J Bone Joint Surg Am*, 2009. 91(7): p. 1683-8.
8. Williams, S.K., et al., Analysis of cartilage tissue on a cellular level in fresh osteochondral allograft retrievals. *Am J Sports Med*, 2007. 35(12): p. 2022-32.
9. Steinwachs, M.R., T. Guggi, and P.C. Kreuz, Marrow stimulation techniques. *Injury*, 2008. 39 Suppl 1: p. S26-31.
10. Saris, D.B., et al., Treatment of symptomatic cartilage defects of the knee: characterized chondrocyte implantation results in better clinical outcome at 36 months in a randomized trial compared to microfracture. *Am J Sports Med*, 2009. 37 Suppl 1: p. 10S-19S.
11. Jackson, D.W. and T.M. Simon, Chondrocyte transplantation. *Arthroscopy*, 1996. 12(6): p. 732-8.
12. Matricali, G.A., G.P. Dereymaeker, and F.P. Luyten, Donor site morbidity after articular cartilage repair procedures: a review. *Acta Orthop Belg*, 2010. 76(5): p. 669-74.
13. Lin, Z., et al., Gene expression profiles of human chondrocytes during passaged monolayer cultivation. *J Orthop Res*, 2008. 26(9): p. 1230-7.
14. Schuh, E., et al., Effect of matrix elasticity on the maintenance of the chondrogenic phenotype. *Tissue Eng Part A*, 2010. 16(4): p. 1281-90.
15. Fukui, N., et al., $\alpha 5$ Integrin promotes dedifferentiation of monolayer-cultured articular chondrocytes. *Arthritis Rheum*, 2011. 63(7): p. 1938-49.
16. Schrobback, K., et al., Effects of oxygen and culture system on in vitro propagation and redifferentiation of osteoarthritic human articular chondrocytes. *Cell Tissue Res*, 2011.
17. van der Windt, A.E., et al., Physiological tonicity improves human chondrogenic marker expression through nuclear factor of activated T-cells 5 in vitro. *Arthritis Res Ther*, 2010. 12(3): p. R100.
18. Lee, T.J., et al., Spinner-flask culture induces redifferentiation of de-differentiated chondrocytes. *Biotechnol Lett*, 2011. 33(4): p. 829-36.
19. Schrobback, K., et al., Adult human articular chondrocytes in a microcarrier-based culture system: expansion and redifferentiation. *J Orthop Res*, 2011. 29(4): p. 539-46.
20. Stenhamre, H., et al., Influence of pore size on the redifferentiation potential of human articular chondrocytes in poly(urethane urea) scaffolds. *J Tissue Eng Regen Med*, 2010.
21. Pei, M. and F. He, Extracellular matrix deposited by synovium-derived stem cells delays replicative senescent chondrocyte dedifferentiation and enhances redifferentiation. *J Cell Physiol*, 2011.
22. Ahmed, N., et al., Soluble signalling factors derived from differentiated cartilage tissue affect chondrogenic differentiation of rat adult marrow stromal cells. *Cell Physiol Biochem*,

2007. 20(5): p. 665-78.

23. Wu, L., et al., Trophic effects of mesenchymal stem cells increase chondrocyte proliferation and matrix formation. *Tissue Eng Part A*, 2011. 17(9-10): p. 1425-36.

24. Taylor, D.W., et al., Proteoglycan and collagen accumulation by passaged chondrocytes can be enhanced through side-by-side culture with primary chondrocytes. *Tissue Eng Part A*, 2010. 16(2): p. 643-51.

25. Yang, K.G., et al., Impact of expansion and redifferentiation conditions on chondrogenic capacity of cultured chondrocytes. *Tissue Eng*, 2006. 12(9): p. 2435-47.

26. Chaipinyo, K., B.W. Oakes, and M.P. Van Damme, The use of debrided human articular cartilage for autologous chondrocyte implantation: maintenance of chondrocyte differentiation and proliferation in type I collagen gels. *J Orthop Res*, 2004. 22(2): p. 446-55.

27. Jiang, C.C., et al., Repair of porcine articular cartilage defect with a biphasic osteochondral composite. *J Orthop Res*, 2007. 25(10): p. 1277-90.

3

28. Chiang, H., et al., Comparison of articular cartilage repair by autologous chondrocytes with and without in vitro cultivation. *Tissue Eng Part C Methods*, 2010. 16(2): p. 291-300.

29. Revell, C.M. and K.A. Athanasiou, Success rates and immunologic responses of autogenic, allogenic, and xenogenic treatments to repair articular cartilage defects. *Tissue Eng Part B Rev*, 2009. 15(1): p. 1-15.

30. Jobanputra, P., et al., Cellular responses to human chondrocytes: absence of allogeneic responses in the presence of HLA-DR and ICAM-1. *Clin Exp Immunol*, 1992. 90(2): p. 336-44.

31. Kuhne, M., et al., HLA-B27-restricted antigen presentation by human chondrocytes to CD8+ T cells: potential contribution to local immunopathologic processes in ankylosing spondylitis. *Arthritis Rheum*, 2009. 60(6): p. 1635-46.

32. Malejczyk, J., et al., Effect of immunosuppression on rejection of cartilage formed by transplanted allogeneic rib chondrocytes in mice. *Clin Orthop Relat Res*, 1991(269): p. 266-73.

33. Green, W.T., Jr., Articular cartilage repair. Behavior of rabbit chondrocytes during tissue culture and subsequent allografting. *Clin Orthop Relat Res*, 1977(124): p. 237-50.

34. Moskalewski, S., A. Hyc, and A. Osiecka-Iwan, Immune response by host after allogeneic chondrocyte transplant to the cartilage. *Microsc Res Tech*, 2002. 58(1): p. 3-13.

35. Gross, A.E., N. Shasha, and P. Aubin, Long-term followup of the use of fresh osteochondral allografts for posttraumatic knee defects. *Clin Orthop Relat Res*, 2005(435): p. 79-87.

36. Emmerson, B.C., et al., Fresh osteochondral allografting in the treatment of osteochondritis dissecans of the femoral condyle. *Am J Sports Med*, 2007. 35(6): p. 907-14.

37. Fujihara, Y., T. Takato, and K. Hoshi, Immunological response to tissue-engineered cartilage derived from auricular chondrocytes and a PLLA scaffold in transgenic mice. *Biomaterials*, 2010. 31(6): p. 1227-34.

38. Shangkai, C., et al., Transplantation of allogeneic chondrocytes cultured in fibroin sponge and stirring chamber to promote cartilage regeneration. *Tissue Eng*, 2007. 13(3): p. 483-92.

39. El Sayed, K., et al., Heterotopic autologous chondrocyte transplantation—a realistic approach to support articular cartilage repair? *Tissue Eng Part B Rev*, 2010. 16(6): p. 603-16.

40. Lohan, A., et al., In vitro and in vivo neo-cartilage formation by heterotopic chondrocytes seeded on PGA scaffolds. *Histochem Cell Biol*, 2011. 136(1): p. 57-69.

41. Zhang, L. and M. Spector, Comparison of three types of chondrocytes in collagen scaffolds for cartilage tissue engineering. *Biomed Mater*, 2009. 4(4): p. 045012.

42. Isogai, N., et al., Comparison of different chondrocytes for use in tissue engineering of cartilage model structures. *Tissue Eng*, 2006. 12(4): p. 691-703.

43. Lee, J., et al., Comparison of articular cartilage with costal cartilage in initial cell yield,

degree of dedifferentiation during expansion and redifferentiation capacity. *Biotechnol Appl Biochem*, 2007. 48(Pt 3): p. 149-58.

44. Asawa, Y., et al., Aptitude of auricular and nasoseptal chondrocytes cultured under a monolayer or three-dimensional condition for cartilage tissue engineering. *Tissue Eng Part A*, 2009. 15(5): p. 1109-18.

45. Szeperowicz, P., et al., Comparison of cartilage self repairs and repairs with costal and articular chondrocyte transplantation in treatment of cartilage defects in rats. *Rocz Akad Med Bialymst*, 2004. 49 Suppl 1: p. 28-30.

46. Moskalewski, S. and J. Malejczyk, Bone formation following intrarenal transplantation of isolated murine chondrocytes: chondrocyte-bone cell transdifferentiation? *Development*, 1989. 107(3): p. 473-80.

47. Landis, W.J., et al., Tissue engineering a model for the human ear: Assessment of size, shape, morphology, and gene expression following seeding of different chondrocytes. *Wound Repair and Regeneration*, 2009. 17(1): p. 136-146.

48. Ruszymah, B.H.I., et al., Pediatric auricular chondrocytes gene expression analysis in monolayer culture and engineered elastic cartilage. *International Journal of Pediatric Otorhinolaryngology*, 2007. 71(8): p. 1225-1234.

49. Ruszymah, B.H., et al., Pediatric auricular chondrocytes gene expression analysis in monolayer culture and engineered elastic cartilage. *Int J Pediatr Otorhinolaryngol*, 2007. 71(8): p. 1225-34.

50. Chung, C., et al., Effects of auricular chondrocyte expansion on neocartilage formation in photocrosslinked hyaluronic acid networks. *Tissue Eng*, 2006. 12(9): p. 2665-73.

51. Schumacher, B.L., et al., Proteoglycan 4 (PRG4) synthesis and immunolocalization in bovine meniscus. *J Orthop Res*, 2005. 23(3): p. 562-8.

52. Wilson, C.G., J.F. Nishimuta, and M.E. Levenston, Chondrocytes and meniscal fibrochondrocytes differentially process aggrecan during de novo extracellular matrix assembly. *Tissue Eng Part A*, 2009. 15(7): p. 1513-22.

53. Englund, M., The role of the meniscus in osteoarthritis genesis. *Med Clin North Am*, 2009. 93(1): p. 37-43, x.

54. Sun, Y., et al., Calcium deposition in osteoarthritic meniscus and meniscal cell culture. *Arthritis Res Ther*, 2010. 12(2): p. R56.

55. Hjelle, K., et al., Articular cartilage defects in 1,000 knee arthroscopies. *Arthroscopy*, 2002. 18(7): p. 730-4.

56. Hunziker, E.B. and L.C. Rosenberg, Repair of partial-thickness defects in articular cartilage: cell recruitment from the synovial membrane. *J Bone Joint Surg Am*, 1996. 78(5): p. 721-33.

57. Gallay, S.H., et al., Relationship of donor site to chondrogenic potential of periosteum in vitro. *J Orthop Res*, 1994. 12(4): p. 515-25.

58. Nakahara, H., V.M. Goldberg, and A.I. Caplan, Culture-expanded human periosteal-derived cells exhibit osteochondral potential in vivo. *J Orthop Res*, 1991. 9(4): p. 465-76.

59. Medvedev, S.P., et al., Human induced pluripotent stem cells derived from fetal neural stem cells successfully undergo directed differentiation into cartilage. *Stem Cells Dev*, 2011. 20(6): p. 1099-112.

60. Jukes, J.M., et al., Endochondral bone tissue engineering using embryonic stem cells. *Proc Natl Acad Sci U S A*, 2008. 105(19): p. 6840-5.

61. Yamashita, T., et al., Tumorigenic Development of Induced Pluripotent Stem Cells in Ischemic Mouse Brain. *Cell Transplant*, 2010.

62. Tang, C., et al., An antibody against SSEA-5 glycan on human pluripotent stem cells enables removal of teratoma-forming cells. *Nat Biotechnol*, 2011.

63. Koelling, S., et al., Migratory chondrogenic progenitor cells from repair tissue during the later stages of human osteoarthritis. *Cell Stem Cell*, 2009. 4(4): p. 324-35.
64. Pittenger, M.F., et al., Multilineage potential of adult human mesenchymal stem cells. *Science*, 1999. 284(5411): p. 143-7.
65. Lee, J.S. and G.I. Im, Influence of chondrocytes on the chondrogenic differentiation of adipose stem cells. *Tissue Eng Part A*, 2010. 16(12): p. 3569-77.
66. Jones, E.A., et al., Synovial fluid mesenchymal stem cells in health and early osteoarthritis: detection and functional evaluation at the single-cell level. *Arthritis Rheum*, 2008. 58(6): p. 1731-40.
67. Farre-Guasch, E., et al., Buccal fat pad, an oral access source of human adipose stem cells with potential for osteochondral tissue engineering: an in vitro study. *Tissue Eng Part C Methods*, 2010. 16(5): p. 1083-94.
68. Witkowska-Zimny, M. and E. Wrobel, Perinatal sources of mesenchymal stem cells: Wharton's jelly, amnion and chorion. *Cell Mol Biol Lett*, 2011. 16(3): p. 493-514.
69. Patki, S., et al., Human breast milk is a rich source of multipotent mesenchymal stem cells. *Hum Cell*, 2010. 23(2): p. 35-40.
70. Lee, O.K., et al., Isolation of multipotent mesenchymal stem cells from umbilical cord blood. *Blood*, 2004. 103(5): p. 1669-1675.
71. Allickson, J.G., et al., Recent Studies Assessing the Proliferative Capability of a Novel Adult Stem Cell Identified in Menstrual Blood. *Open Stem Cell J*, 2011. 3(2011): p. 4-10.
72. Hu, G., et al., Supernatant of bone marrow mesenchymal stromal cells induces peripheral blood mononuclear cells possessing mesenchymal features. *Int J Biol Sci*, 2011. 7(3): p. 364-75.
73. Wei, Y., et al., Human skeletal muscle-derived stem cells retain stem cell properties after expansion in mysosphere culture. *Exp Cell Res*, 2011. 317(7): p. 1016-27.
74. Matsumoto, T., et al., Isolation and Characterization of Human Anterior Cruciate Ligament-Derived Vascular Stem Cells. *Stem Cells Dev*, 2011.
75. Janjanin, S., et al., Human palatine tonsil: a new potential tissue source of multipotent mesenchymal progenitor cells. *Arthritis Res Ther*, 2008. 10(4): p. R83.
76. Estes, B.T., et al., Isolation of adipose-derived stem cells and their induction to a chondrogenic phenotype. *Nat Protoc*, 2010. 5(7): p. 1294-311.
77. Siddappa, R., et al., Donor variation and loss of multipotency during in vitro expansion of human mesenchymal stem cells for bone tissue engineering. *J Orthop Res*, 2007. 25(8): p. 1029-41.
78. Phinney, D.G., et al., Donor variation in the growth properties and osteogenic potential of human marrow stromal cells. *J Cell Biochem*, 1999. 75(3): p. 424-36.
79. Tokalov, S.V., et al., A number of bone marrow mesenchymal stem cells but neither phenotype nor differentiation capacities changes with age of rats. *Mol Cells*, 2007. 24(2): p. 255-60.
80. Tokalov, S.V., et al., Age-related changes in the frequency of mesenchymal stem cells in the bone marrow of rats. *Stem Cells Dev*, 2007. 16(3): p. 439-46.
81. De Bari, C., F. Dell'Accio, and F.P. Luyten, Human periosteum-derived cells maintain phenotypic stability and chondrogenic potential throughout expansion regardless of donor age. *Arthritis Rheum*, 2001. 44(1): p. 85-95.
82. Jansen, B.J., et al., Functional differences between mesenchymal stem cell populations are reflected by their transcriptome. *Stem Cells Dev*, 2010. 19(4): p. 481-90.
83. Vacanti, V., et al., Phenotypic changes of adult porcine mesenchymal stem cells induced by prolonged passaging in culture. *J Cell Physiol*, 2005. 205(2): p. 194-201.
84. Tan, Q., P.P. Lui, and Y.F. Rui, Effect of In Vitro Passaging on the Stem Cell-Related

Properties of Tendon-Derived Stem Cells-Implications in Tissue Engineering. *Stem Cells Dev*, 2011.

85. Chen, T., Y. Zhou, and W.S. Tan, Influence of lactic acid on the proliferation, metabolism, and differentiation of rabbit mesenchymal stem cells. *Cell Biol Toxicol*, 2009. 25(6): p. 573-86.

86. Goedecke, A., et al., Differential effect of platelet-rich plasma and fetal calf serum on bone marrow-derived human mesenchymal stromal cells expanded in vitro. *J Tissue Eng Regen Med*, 2011. 5(8): p. 648-54.

87. Chase, L.G., et al., A novel serum-free medium for the expansion of human mesenchymal stem cells. *Stem Cell Res Ther*, 2010. 1(1): p. 8.

88. Perez-Illarbe, M., et al., Comparison of ex vivo expansion culture conditions of mesenchymal stem cells for human cell therapy. *Transfusion*, 2009. 49(9): p. 1901-10.

89. Fan, X., et al., Optimization of primary culture condition for mesenchymal stem cells derived from umbilical cord blood with factorial design. *Biotechnol Prog*, 2009. 25(2): p. 499-507.

90. Lund, P., et al., Effect of growth media and serum replacements on the proliferation and differentiation of adipose-derived stem cells. *Cytherapy*, 2009. 11(2): p. 189-97.

91. Engler, A.J., et al., Matrix elasticity directs stem cell lineage specification. *Cell*, 2006. 126(4): p. 677-89.

92. Weijers, E.M., et al., The Influence of Hypoxia and Fibrinogen Variants on the Expansion and Differentiation of Adipose Tissue-Derived Mesenchymal Stem Cells. *Tissue Eng Part A*, 2011.

93. Muller, J., et al., Hypoxic conditions during expansion culture prime human mesenchymal stromal precursor cells for chondrogenic differentiation in three-dimensional cultures. *Cell Transplant*, 2011.

94. Karlsen, T.A., et al., Effect of three-dimensional culture and incubator gas concentration on phenotype and differentiation capability of human mesenchymal stem cells. *J Cell Biochem*, 2011. 112(2): p. 684-93.

95. Dos Santos, F., et al., Ex vivo expansion of human mesenchymal stem cells: a more effective cell proliferation kinetics and metabolism under hypoxia. *J Cell Physiol*, 2010. 223(1): p. 27-35.

96. Lozoya, O.A., et al., Regulation of hepatic stem/progenitor phenotype by microenvironment stiffness in hydrogel models of the human liver stem cell niche. *Biomaterials*, 2011. 32(30): p. 7389-402.

97. Winer, J.P., et al., Bone marrow-derived human mesenchymal stem cells become quiescent on soft substrates but remain responsive to chemical or mechanical stimuli. *Tissue Eng Part A*, 2009. 15(1): p. 147-54.

98. Kisiday, J.D., et al., Expansion of mesenchymal stem cells on fibrinogen-rich protein surfaces derived from blood plasma. *J Tissue Eng Regen Med*, 2011. 5(8): p. 600-11.

99. Curran, J.M., et al., The use of dynamic surface chemistries to control msc isolation and function. *Biomaterials*, 2011. 32(21): p. 4753-60.

100. Caplan, A.I. and J.E. Dennis, Mesenchymal stem cells as trophic mediators. *Journal of Cellular Biochemistry*, 2006. 98(5): p. 1076-1084.

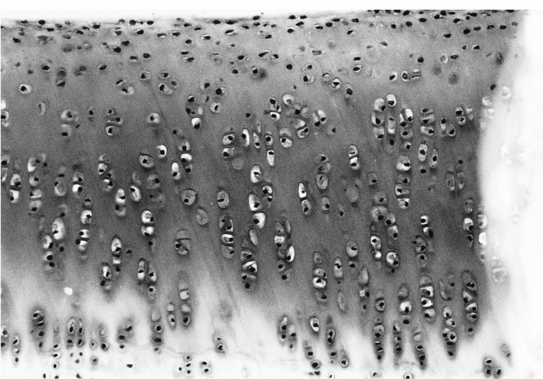
101. Le Blanc, K., et al., HLA expression and immunologic properties of differentiated and undifferentiated mesenchymal stem cells. *Exp Hematol*, 2003. 31(10): p. 890-6.

102. Chen, X., M.A. Armstrong, and G. Li, Mesenchymal stem cells in immunoregulation. *Immunol Cell Biol*, 2006. 84(5): p. 413-21.

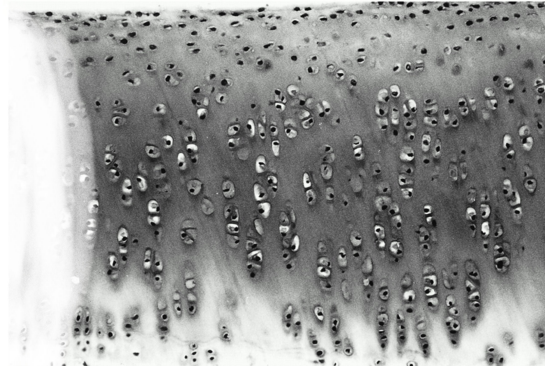
103. Lee, K.B., et al., Injectable mesenchymal stem cell therapy for large cartilage defects—a porcine model. *Stem Cells*, 2007. 25(11): p. 2964-71.

104. Murphy, J.M., et al., Stem cell therapy in a caprine model of osteoarthritis. *Arthritis and Rheumatism*, 2003. 48(12): p. 3464-3474.
105. Wood, J.A., et al., Periocular and Intra-Articular Injection of Canine Adipose-Derived Mesenchymal Stem Cells: An In Vivo Imaging and Migration Study. *J Ocul Pharmacol Ther*, 2011.
106. Helman, L.J. and P. Meltzer, Mechanisms of sarcoma development. *Nat Rev Cancer*, 2003. 3(9): p. 685-94.
107. Tolar, J., et al., Sarcoma derived from cultured mesenchymal stem cells. *Stem Cells*, 2007. 25(2): p. 371-9.
108. Suzuki, K., et al., Mesenchymal stromal cells promote tumor growth through the enhancement of neovascularization. *Mol Med*, 2011. 17(7-8): p. 579-87.
109. Zhai, L.J., et al., Mesenchymal stem cells display different gene expression profiles compared to hyaline and elastic chondrocytes. *Int J Clin Exp Med*, 2011. 4(1): p. 81-90.
110. Hillel, A.T., et al., Characterization of human mesenchymal stem cell-engineered cartilage: analysis of its ultrastructure, cell density and chondrocyte phenotype compared to native adult and fetal cartilage. *Cells Tissues Organs*, 2010. 191(1): p. 12-20.
111. Scotti, C., et al., Recapitulation of endochondral bone formation using human adult mesenchymal stem cells as a paradigm for developmental engineering. *Proc Natl Acad Sci U S A*, 2010. 107(16): p. 7251-6.
112. Mueller, M.B. and R.S. Tuan, Functional characterization of hypertrophy in chondrogenesis of human mesenchymal stem cells. *Arthritis Rheum*, 2008. 58(5): p. 1377-88.
113. Abrahamsson, C.K., et al., Chondrogenesis and mineralization during in vitro culture of human mesenchymal stem cells on three-dimensional woven scaffolds. *Tissue Eng Part A*, 2010. 16(12): p. 3709-18.
114. Pelttari, K., et al., Premature induction of hypertrophy during in vitro chondrogenesis of human mesenchymal stem cells correlates with calcification and vascular invasion after ectopic transplantation in SCID mice. *Arthritis Rheum*, 2006. 54(10): p. 3254-66.
115. Koga, H., et al., Synovial stem cells are regionally specified according to local microenvironments after implantation for cartilage regeneration. *Stem Cells*, 2007. 25(3): p. 689-96.
116. Huybrechts-Godin, G., P. Hauser, and G. Vaes, Macrophage-fibroblast interactions in collagenase production and cartilage degradation. *Biochem J*, 1979. 184(3): p. 643-50.
117. Goldring, S.R., J.M. Dayer, and S.M. Krane, Rheumatoid synovial cell hormone responses modulated by cell-cell interactions. *Inflammation*, 1984. 8(1): p. 107-21.
118. Ahmed, N., et al., Passaged human chondrocytes accumulate extracellular matrix when induced by bovine chondrocytes. *J Tissue Eng Regen Med*, 2010. 4(3): p. 233-41.
119. Gan, L. and R.A. Kandel, In vitro cartilage tissue formation by Co-culture of primary and passaged chondrocytes. *Tissue Eng*, 2007. 13(4): p. 831-42.
120. Ahmed, N., et al., Cartilage tissue formation using redifferentiated passaged chondrocytes in vitro. *Tissue Eng Part A*, 2009. 15(3): p. 665-73.
121. Kuhne, M., et al., Characterization of auricular chondrocytes and auricular/articular chondrocyte co-cultures in terms of an application in articular cartilage repair. *Int J Mol Med*, 2010. 25(5): p. 701-8.
122. Jikko, A., et al., Inhibition of chondrocyte terminal differentiation and matrix calcification by soluble factors released by articular chondrocytes. *Calcif Tissue Int*, 1999. 65(4): p. 276-9.
123. Fischer, J., et al., Human articular chondrocytes secrete parathyroid hormone-related protein and inhibit hypertrophy of mesenchymal stem cells in coculture during chondrogenesis. *Arthritis Rheum*, 2010. 62(9): p. 2696-706.
124. Villars, F., et al., Effect of human endothelial cells on human bone marrow stromal cell

- phenotype: role of VEGF? *J Cell Biochem*, 2000. 79(4): p. 672-85.
125. Hofmann, A., et al., The effect of human osteoblasts on proliferation and neo-vessel formation of human umbilical vein endothelial cells in a long-term 3D co-culture on polyurethane scaffolds. *Biomaterials*, 2008. 29(31): p. 4217-26.
126. Le Visage, C., et al., Interaction of human mesenchymal stem cells with disc cells: changes in extracellular matrix biosynthesis. *Spine (Phila Pa 1976)*, 2006. 31(18): p. 2036-42.
127. Bian, L., et al., Coculture of human mesenchymal stem cells and articular chondrocytes reduces hypertrophy and enhances functional properties of engineered cartilage. *Tissue Eng Part A*, 2011. 17(7-8): p. 1137-45.
128. Aung, A., et al., Osteoarthritic chondrocyte-secreted morphogens induce chondrogenic differentiation of human mesenchymal stem cells. *Arthritis Rheum*, 2011. 63(1): p. 148-58.
129. Bigdeli, N., et al., Coculture of human embryonic stem cells and human articular chondrocytes results in significantly altered phenotype and improved chondrogenic differentiation. *Stem Cells*, 2009. 27(8): p. 1812-21.
130. Acharya, C., et al., Enhanced chondrocyte proliferation and mesenchymal stromal cells chondrogenesis in coculture pellets mediate improved cartilage formation. *J Cell Physiol*, 2012. 227(1): p. 88-97.
131. Hwang, N.S., et al., Chondrogenic priming adipose-mesenchymal stem cells for cartilage tissue regeneration. *Pharm Res*, 2011. 28(6): p. 1395-405.
132. Klein, T.J., et al., Tissue engineering of articular cartilage with biomimetic zones. *Tissue Eng Part B Rev*, 2009. 15(2): p. 143-57.
133. Klein, T.J., et al., Strategies for zonal cartilage repair using hydrogels. *Macromol Biosci*, 2009. 9(11): p. 1049-58.
134. Jin, R., et al., Enzymatically crosslinked dextran-tyramine hydrogels as injectable scaffolds for cartilage tissue engineering. *Tissue Eng Part A*, 2010. 16(8): p. 2429-40.
135. Jin, R., et al., Chondrogenesis in injectable enzymatically crosslinked heparin/dextran hydrogels. *J Control Release*, 2011. 152(1): p. 186-95.
136. Jin, R., et al., Enzymatically-crosslinked injectable hydrogels based on biomimetic dextran-hyaluronic acid conjugates for cartilage tissue engineering. *Biomaterials*, 2010. 31(11): p. 3103-13.
137. Jiang, J., S.B. Nicoll, and H.H. Lu, Co-culture of osteoblasts and chondrocytes modulates cellular differentiation in vitro. *Biochem Biophys Res Commun*, 2005. 338(2): p. 762-70.
138. Nakaoka, R., S.X. Hsiong, and D.J. Mooney, Regulation of chondrocyte differentiation level via co-culture with osteoblasts. *Tissue Eng*, 2006. 12(9): p. 2425-33.



4



Chapter 4

4

GREM1, FRZB and DKK1 are key regulators of human articular cartilage homeostasis

Jeroen Leijten, Joyce Emons, Steffan Bos, Carsten Sticht, Bin Ma, Sandy van Gool, Eva Decker, Andre Uitterlinden, Gudrun Rappold, Albert Hofman, Fernando Rivadeneira, Sicco Scherjon, Jan Maarten Wit, Ingrid Meulenbelt, Joyce van Meurs, Clemens van Blitterswijk and Marcel Karperien

Opportunity is missed by most people because it is dressed in overalls and looks like work.
Thomas Edison

Abstract

Osteoarthritis (OA) is the most common form of arthritis and a leading cause of mobility associated disability. Recent evidence has shown that development of OA may be caused by activation of hypertrophic differentiation of articular chondrocytes. Healthy articular cartilage (AC) is highly resistant to undergo hypertrophic differentiation, in contrast to other types of hyaline cartilage such as growth-plate cartilage (GP). The natural mechanism that restricts healthy AC from undergoing hypertrophic differentiation is still unknown.

In this study, we set out to elucidate the underlying molecular mechanism that is responsible for the difference in propensity to undergo hypertrophic differentiation between human articular and growth plate cartilage. This approach identified the BMP- and Wnt-antagonists *GREM1*, *FRZB* and *DKK1*, which are highly enriched at the mRNA and protein level in AC. Supplementation of these antagonists, either individually or combined, to explant cultures of fetal tibiae or to chondrogenically differentiated MSCs prevented terminal hypertrophic differentiation and subsequent endochondral ossification without affecting chondrogenesis. Furthermore, *GREM1*, *FRZB* and *DKK1* were less transcribed in osteoarthritic cartilage compared to relatively preserved cartilage from the same osteoarthritic-joint. Additionally, we show that SNP-rs12593365, located in a genomic control region of *GREM1*, significantly associates with a 20% reduced risk for radiographic hip-osteoarthritis in two population-based cohorts.

Taken together, our data identifies *GREM1*, *FRZB* and *DKK1* as natural brakes of hypertrophic differentiation in articular cartilage. As hypertrophic differentiation is essential to development of osteoarthritis, these natural brakes of hypertrophy might open new avenues for therapeutic intervention.

4.1 Introduction

Arthritis is the leading cause of mobility associated disability. Of the more than 100 forms of arthritis, osteoarthritis (OA) is most common. OA is diagnosed in approximately 50 million people in the US alone and in 2007 health care costs raise up to 128 billion USD. Due to the aging of the population and increased life expectancy, these numbers are expected to raise substantial over the next two decades. The current management of OA is symptomatic, aimed at pain relief and coping with the disease and at the end stage joint replacement surgery as a successful treatment option. At present, there is no treatment that can intervene early in the disease process aiming at curing the disease. The pathophysiology of OA is complex, still largely unknown and has likely a multifactorial onset. Various risk factors for the development of OA including age, gender, overweight, trauma, sports and genetics have been identified [1].

Healthy articular cartilage is largely resistant to undergo hypertrophic differentiation in contrast to other forms of hyaline cartilage such as growth plate cartilage, which is responsible for bone elongation by hypertrophic differentiation of chondrocytes and their subsequent replacement by bone. The molecular mechanism underlying this discrepancy between these two types of hyaline cartilage is largely unknown. It has been postulated that articular cartilage secretes (a) factor(s) that inhibit(s) chondrocyte hypertrophy. This is based on the observation that articular cartilage explants efficiently block hypertrophic differentiation of growth plate cartilage explants in transwell co-culture experiments [2]. Interestingly, recent data obtained in transgenic mouse models has provided evidence that deregulated hypertrophic differentiation of articular chondrocytes may be a driving factor in the onset and progression of OA. A number of signaling pathways have been identified that can stimulate hypertrophic differentiation of chondrocytes including the Wnt/ β catenin [3], Bone Morphogenetic Protein (BMP) [4], Indian Hedgehog [5] and hypoxia induced signaling [6] pathways in growth plate cartilage. Interestingly, forced activation or conditional inactivation of these pathways in articular chondrocytes results in a relief in the break of hypertrophic differentiation and induces features of OA in mice [7-10]. Whether the same pathways are also involved in the pathogenesis of OA in man is still largely unclear. In this study, we set out to elucidate the underlying molecular mechanism that is responsible for the difference in the propensity to undergo hypertrophic differentiation between human articular and growth plate cartilage by making a detailed comparison of gene expression profiles of both types of cartilage. We hypothesized that this approach could reveal the identity of the articular cartilage secreted factor(s) that inhibit chondrocyte hypertrophy. We expected that this factor(s) should act up-stream of known pathways involved in the regulation of chondrocyte hypertrophy. Furthermore, since such (a) factor(s) would be of paramount importance for joint cartilage homeostasis, we anticipated that its expression should be disturbed in OA.

4.2 Materials and methods

4.2.1 Origin samples

The use of patient material was approved by the local hospital ethical committees and for all samples informed written consent was obtained. Samples were directly frozen in Cryomatrix (Cryomatrix, Shandon) or fixated, decalcified and embedded in paraffin. From some donors with primary OA undergoing total joint replacement surgery, cartilage specimens from areas visibly affected by the OA process (OA cartilage) and areas which appeared macroscopically intact (preserved cartilage) were taken for total RNA isolation.

4.2.2 Total RNA extraction

After removal of the bone, growth plate and articular snap frozen cartilage-samples were cut into 8 μm sections. Every fifth slide was stained with Haematoxylin to ensure that no bone contamination was present. Subsequently, from each slide cartilage was collected and homogenized in a 4M guanidine thiocyanate solution (Sigma). Total RNA isolation was performed by a method previously described [24].

4.2.3 Cell isolation and cultivation

After written consent was obtained, MSCs were isolated from fresh bone marrow samples and cultured as described previously [25]. MSCs pellets of 2.5×10^5 cells were cultured up to 35 days in a previously described chondrogenic culture medium [14]. On day 0, 11, 21 and 35 eight pellets were pooled for RNA isolation and two pellets for histological analysis. Chondrocytes were isolated from human articular cartilage, obtained after total joint replacement surgery, by collagenase digestion as previously described [26]. Isolated chondrocytes were seeded at 3000 cells per cm^2 and expanded in chondrocyte expansion medium as previously described [26]. Chondrocytes were expanded up to passage eight, isolating RNA from every second passage.

4.2.4 Organ cultures

All animal procedures were reviewed and approved by the animal care committee of the University of Utrecht. Tibiae were isolated from E17.5 fetal FVB mice (Harlan) and cultured in medium consisting of α -MEM supplemented with 10% heat inactivated fetal bovine serum (Biowhittaker) and 100 U/ml penicillin with 100 mg/ml streptomycin (Gibco). Medium was supplemented with 0, 50 or 500 ng/ml of murine Grem1, Frzb or Dkk1 recombinant proteins. After 7 days of culture, tibiae were fixated for histological analysis.

4.2.5 Histology and immunohistochemistry

Paraffin embedded samples were cut into 5 μm sections and stained either with haematoxylin and eosin, toluidine blue, toluidine blue combined with Von Kossa or Alcian

blue combined with Nuclear fast red solutions according to standard procedures. For immunohistochemistry, sections were incubated with 1:100 diluted primary antibodies against either *GREM1*, *FRZB* or *DKK1* (sc-28873, sc-13941 and sc-25516 respectively; Santa Cruz) and further developed using the rabbit ABC staining system (sc-2018; Santa Cruz) according to manufacturer's protocol. For image analysis ImageJ software was used.

4.2.6 Microarray processing and Quantitative real-time reverse transcriptase-polymerase chain reaction

Thirteen specimens, derived from eight articular and five growth plate specimens were analyzed on whole genome gene expression using Affymetrix HG-U133Plus2-type microarrays. Principal Component Analysis (PCA) with Pearson product-moment correlation was performed to compute correlations between gene expression of growth plates and articular cartilages. Changes of gene expression in pathways were analyzed using Genmapp2.0 [27]. Changes in gene ontology were investigated using PANTHER [28]. For gene expression analysis, cDNA was synthesized using 1 μ g total RNA (BioRad) in accordance with the manufacturer's instructions. 20 ng cDNA was amplified using iQ SYBR Green Supermix (BioRad, Hercules, CA, USA) on a MyIQ single color Real-time PCR detection system (BioRad) and analyzed using iQtm5 optical system software (Biorad). Primer sequences are available on request.

4

4.2.7 Genetic Study population

The Rotterdam Study is a population-based prospective cohort study that is comprised of men and women aged 55 years and older. A detailed description of the study design has been described previously [29]. The medical ethics committee of Erasmus University Medical School approved the study and written informed consent was obtained from each participant. The Rotterdam Study I (RSI) (N=5193) and RSII (N=1949) were investigated on associations between single nucleotide polymorphisms (SNPs) of *GREM1* and *DKK1* and radiographic OA. All SNPs from that were either in the coding region of or in 100Kb upstream or downstream of the two selected genes were used. The total number of SNPs that were analyzed was 116. Associations with OA phenotypes were tested using an allelic chi-square test (1 df) assuming an additive effect for each SNP tested. Analyses were carried out using MACH and GRIMP [30] and were adjusted for age, gender and BMI.

4.3 Results

4.3.1 Differential gene expression between articular and growth plate cartilage

Macroscopical and histological examination of growth plate and articular cartilage specimens from the same donor did not reveal indications for cartilage disease (figure 4.1A). From 4 donors, pairs of growth plate and articular cartilage tissue specimens

were collected and RNA was isolated. Samples were subjected to whole-genome gene expression profiling. In total, 2915 genes were found to be significantly differentially expressed of which 1321 were articular cartilage enriched and 1594 growth plate cartilage enriched. Of these, the fold change of only 418 genes was higher than two-fold and as few as 35 genes were expressed with a more than five-fold difference (figure 4.1B). Differential gene expression of 10 genes of interest was verified using RT-qPCR (figure 4.1C). Examination of the list of differentially expressed genes identified several BMP-related molecules including *GREM1*, *CHRD2*, *LTBP1*, *LTBP2*, *ID2*, *ID3*, *GDF10*, *SMAD3*, and *TGFB3* that were significantly higher expressed in articular chondrocytes. Furthermore, the expression of a number of extracellular matrix molecules was as well dissimilar with *COL3A1*, *COL5A2*, *KAL1*, *COL6A3*, *FBN1* and *COL14A1* being higher expressed in articular chondrocytes and *MATN1*, *COL12A1*, *COL4A5*, *MFAP3*, *FBN3* and *COL4A6* being higher expressed in growth plate chondrocytes. Growth plate and articular cartilage are both hyaline cartilage subtypes; traditional hyaline cartilage markers such as *COL2A1*, *COL9A1*, and *ACAN* were not found to be differentially expressed at the mRNA level.

4

4.3.2 Wnt signaling and cell cycle pathways are less active in articular cartilage

Pathway analysis, based on gene ontology, identified differential expression of the cell cycle pathway ($P < 0.001$) followed by the Wnt pathway ($p = 0.04$). Detailed analysis of the cell cycle pathway showed that the expression of the vast majority of the cell cycle related genes was higher in growth plate cartilage (figure 4.1D). Only four cell cycle related genes were more abundantly expressed in articular cartilage, of which three have an inhibitory role in cell proliferation. The higher activity of the cell cycle pathway is in line with the role of the growth plate cartilage in bone elongation. The changes in Wnt signalling suggested a higher activity in growth plate cartilage. This is based on i) higher expression of the Wnt agonists *WNT4*, *WNT5A* and *WNT11* in growth plate cartilage, ii) increased expression of the established Wnt target genes *CCND1*, *MMP2*, *PTTG1*, *LEF1*, *MYC*, *RUNX2*, *TIAM1*, *FST* and *WISP3* in growth plate cartilage, iii) the enriched expression of *TLE2*, an established transcriptional inhibitor of canonical Wnt-signaling in articular cartilage, and iv) the higher expression of the direct and indirect antagonists of Wnt-signaling *FRZB*, *DKK1* and *GREM1* in articular cartilage (figure 2). Furthermore, these three antagonists were the three most differentially expressed genes between growth plate and articular cartilage with an average fold change of 539, 205 and 97 respectively as determined by RT-qPCR. Notably, the BMP antagonist *GREM1* inhibits Wnt indirectly in contrast to *FRZB* and *DKK1* which are direct Wnt inhibitors. Protein expression of *GREM1*, *FRZB* and *DKK1* is predominantly present in articular cartilage and the resting zone of growth plate cartilage. We next performed immunohistochemistry to study protein expression of the BMP and Wnt antagonists in articular and growth plate cartilage specimens. Staining of all three antagonists was more intense in articular cartilage compared to growth plate cartilage, corroborating the mRNA expression patterns (figure 4.3). These antagonists were detected in all zones of articular cartilage in contrast

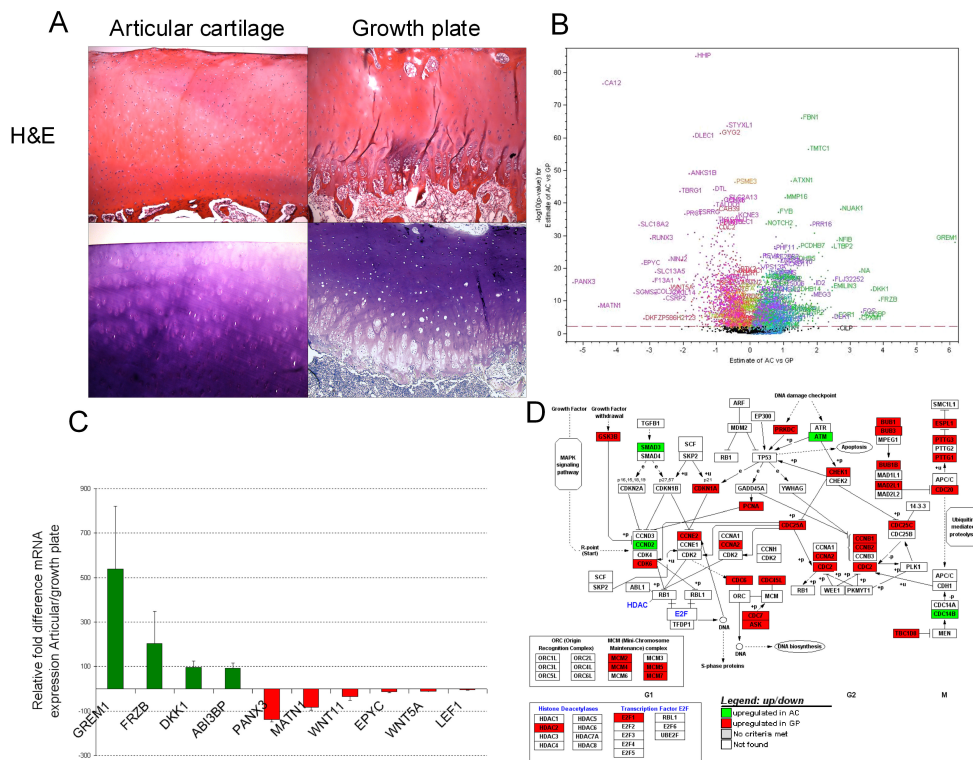


Figure 4.1: Gene expression analysis of healthy human growth plate and articular cartilage. (A) Representative histological sections of growth plate and articular cartilage from the same patient stained with either toluidine blue or haematoxylin and eosin confirm the healthy nature of both specimens. (B) Volcano plot depicting all 2915 differentially expressed genes between growth plate and articular cartilage of all donors as measured with whole genome gene expression analysis. The y-axis indicates the significance level, while the fold change after log₂ transformation is plotted on the x-axis. (C) 10 differentially expressed genes were selected for validation of the microarray data by using quantitative real-time PCR in all donor pairs. Data are expressed as mean +/- SEM. (D) Pathway analysis using the significantly differentially expressed genes between growth plate and articular cartilage demonstrated higher expression of many cell cycle genes in growth plate cartilage (red) compared to articular cartilage (green).

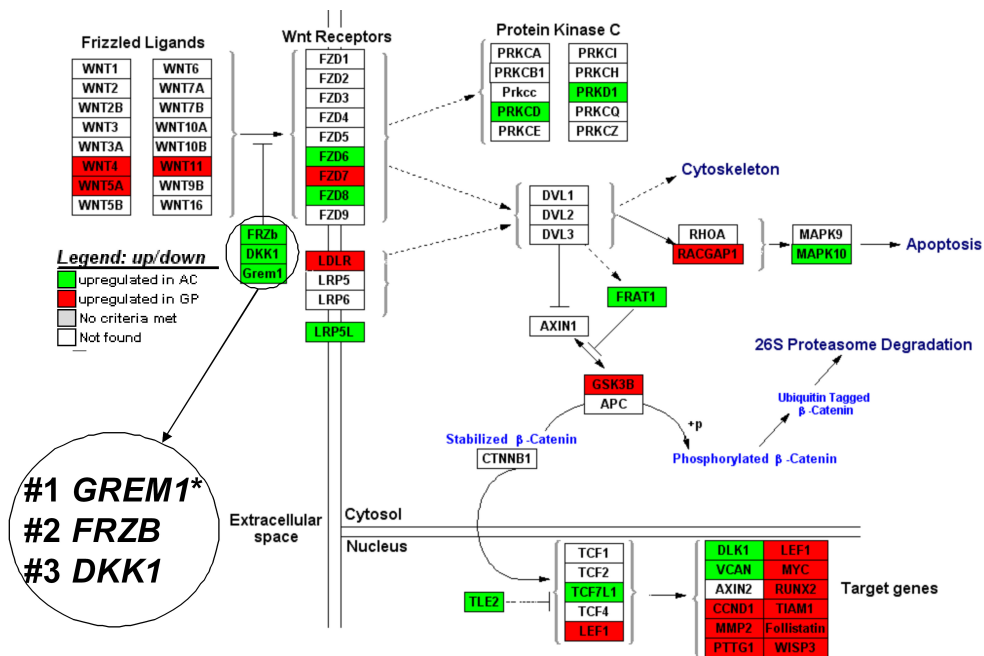


Figure 4.2: Differential expression of Wnt signaling related genes between growth plate and articular cartilage. Detailed pathway analysis of the Wnt pathway using the Genmapp2 software and the significantly differentially expressed genes as input, demonstrated differential expression of the Wnt-signaling pathway between growth plate and articular cartilage ($p=0.04$). *GREM1 indirectly inhibits Wnt signaling.

to growth plate cartilage. In the latter tissue, GREM1, FRZB and DKK1 staining was only witnessed in the resting zone and to a lesser extent in the late hypertrophic zone of growth plate cartilage, albeit at lower levels than in articular cartilage. To determine whether the differential expression of GREM1, FRZB and DKK1 was already present before the formation of the second centre of ossification, we investigated human femurs of two 20-week old fetal donors. The healthy and unaffected nature of the fetal femurs was confirmed by macroscopical and histological analysis (figure 4.4A). Immunohistochemistry revealed that GREM1 and DKK1 expression predominantly resided at the proximal resting zone, which is the region destined to become the articular cartilage (figure 4.4B). Although some GREM1 and DKK1 could still be detected in the distal resting zone, the staining was less intense. Moreover, no staining was detected in the proliferative and hypertrophic zones. FRZB was readily detected in the proximal resting zone and became progressively less intense in more distal zones.

RNA isolated from seven different regions of the fetal femur was subjected to qPCR gene expression analysis (figure 4.4C). Gene expression of *FRZB* steadily declined

	AC			GP			
	SZ	MZ	DZ	RZ	PZ	PHZ	HZ
GREM							
FRZB							
DKK1							
GREM	+++	++	++	+	-	-	+/-
FRZB	+++	++	+++	+/-	-	-	+/-
DKK1	+++	++	+++	+	-	-	+/-

Figure 4.3: GREM1, FRZB and DKK1 expression in growth plate and articular cartilage. Immunohistochemistry of articular and growth plate cartilage sections derived from the same patients with antibodies against GREM, FRZB and DKK1. More staining was witnessed for all three proteins in the articular cartilage compared to growth plate cartilage. (n=4 pairs of articular and growth plate cartilage specimens). Lower panel denotes a semi-quantitative scoring of the staining ranging from strong positive (+++) to undetectable levels (-). AC, articular cartilage. GP, growth plate cartilage. SZ, superficial zone. MZ, mid zone. DZ, deep zone. RZ, resting zone. PZ, proliferating zone. PHZ, prehypertrophic zone. HZ, hypertrophic zone. (Scale bar, 200 μ m.)

between the proximal resting zone and the hypertrophic zone. Although the gene expression of *GREM1* and *DKK1* also progressively declined, there was a stronger regional decline around the mid resting zone and the proliferative zone. Immunohistochemical analysis corroborated with the gene expression analysis as assessed by qPCR. Both analyses suggested the presence of a gradient in GREM1, FZRB and DKK1 expression, with highest expression in the region of the future articular cartilage and became progressively weaker towards the subchondral bone.

4.3.3 Chondrogenically differentiating MSCs resemble growth plate chondrocytes

We used the list of differentially expressed genes between growth plate and articular cartilage to determine whether differentiating MSCs acquire a gene expression fingerprint more characteristic of growth plate than articular chondrocytes. To investigate this, we performed a 3-dimensional principal component analysis, which involved expression profiles of growth plate and cartilage specimen as well as a previ-

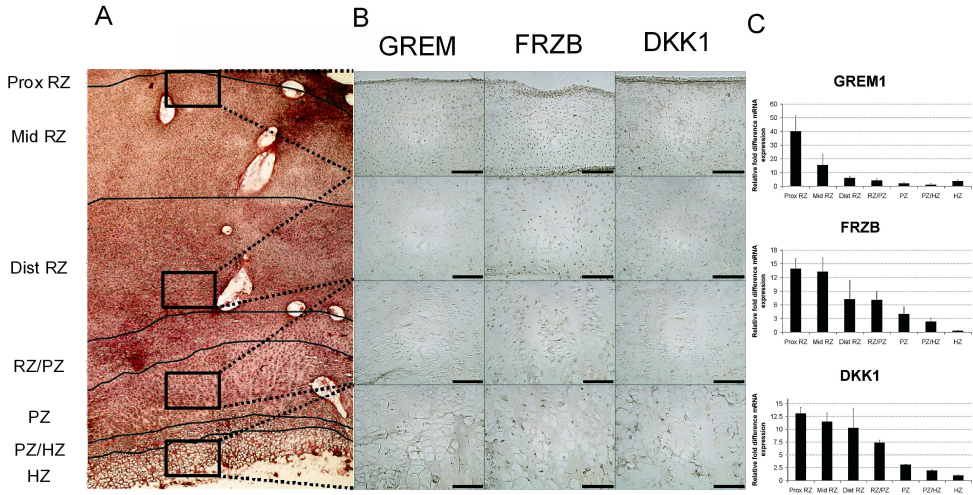


Figure 4.4: Figure 4. Expression of GREM1, FRZB and DKK1 in fetal cartilage. (A) Representative haematoxylin and eosin stained section of 20 weeks old human fetal distal femoral cartilage. Black boxes indicate respective locations of depicted immunohistochemical stainings. Lines denote the borders of the manually dissected zones of the primary growth plate from the proximal resting zone (RZ) to the distal hypertrophic zone (HZ) (B) Immunohistochemistry of fetal distal femoral cartilage sections with antibodies against GREM, FRZB and DKK1. All stainings showed positive cells near the joint-side. Staining became gradually less intense towards the subchondral bone. (C) Quantitative real-time PCR on cDNA belonging to seven manually dissected zones of the primary fetal growth plate demonstrated a gradual decrease in *GREM1*, *FRZB* and *DKK1* mRNA expression from the proximal resting zone towards the hypertrophic zone. Data are mean of $n=3$ donors \pm SEM. Abbreviations: Prox, proximal. Mid, middle. Dist, distal. RZ, resting zone. PZ, proliferative zone. HZ, hypertrophic zone. All pictures in panel B are taken using the same magnification. (Scale bar, 200 μ m).

ously established profile of chondrogenically differentiating fetal bone marrow derived MSCs (Van Gool et al, in preparation) (figure 4.5A). Growth plate and articular cartilage grouped distinctly from each other as well as from undifferentiated MSCs. Over time, chondrogenically differentiating MSCs gradually, but progressively, acquired a gene expression fingerprint more closely resembling growth plate rather than articular chondrocytes.

We then selected a panel of the differentially expressed genes and used this panel to assess cartilage lineage formation in chondrogenically differentiating adult bone marrow MSCs in pellet cultures in the presence of TGFB3 and BMP6. None of the AC specific genes were induced during 5 weeks of differentiation despite histological evidence of cartilage formation. More strikingly, both *GREM1* and *ABI3BP* were significantly down-regulated to levels normally found in GP-cartilage (figure 4.5B). In sharp contrast, growth plate enriched genes, such as *LEF1* and *PANX3*, were up-regulated almost matching the level of expression in the growth plate (figure 4.5C). Similar findings were made in MSCs cultured in pellets, discs or encapsulated in agarose hydrogels. This indicated that bone marrow derived MSCs in the presence of TGFB3 and BMP6 preferentially differentiate into a growth plate-like hyaline cartilage irrespective of the culture method.

4.3.4 *Grem1*, *Frzb* and *Dkk1* inhibit longitudinal growth of explanted fetal tibiae dose dependently

To investigate whether *GREM1*, *FRZB* and *DKK1* play a role in endochondral ossification and therefore in the longitudinal growth of long bones, we cultured explanted mouse fetal tibiae in the presence or absence of 50 or 500 ng/ml of recombinant *Grem1*, *Frzb* and *Dkk1*. Histological analysis showed no gross abnormalities in the metaphysis and diaphysis (figure 4.6A) nor in the epiphyseal cartilaginous heads (figure 4.6B) of all tibiae. Image analysis demonstrated that all tibiae grew over time.

Tibiae cultured in the presence of a single antagonist or a combination of all three antagonists grew more slowly compared to untreated controls in a dose-dependent manner, resulting in a lower total tibiae length at the end of culture. This was due to a decrease in length of the metaphysis and diaphysis with increasing dosages of *Grem1*, *Frzb* and *Dkk1*. In contrast, the combined length of the epiphyseal cartilaginous heads showed no difference (figure 4.6C). A more detailed analysis of the zonal distribution in the cartilage showed a significant decrease in length of the chondrocyte columns (proliferative zone), a modest but significant decrease in the height of the hypertrophic zone and a significant strong increase in length of the non-columnar (resting) zone ($p < 0.001$, $p = 0.013$, $p = 0.010$ respectively when comparing non-treated with treated explants (500 ng/ml)) (figure 4.6D). Taken together, these results suggest that the addition of recombinant *Grem1*, *Frzb* and *Dkk1* inhibits endochondral ossification and thus longitudinal growth of explanted tibiae by retarding the progressive differentiation of resting zone chondrocytes towards a terminally differentiated hypertrophic chondrocyte.

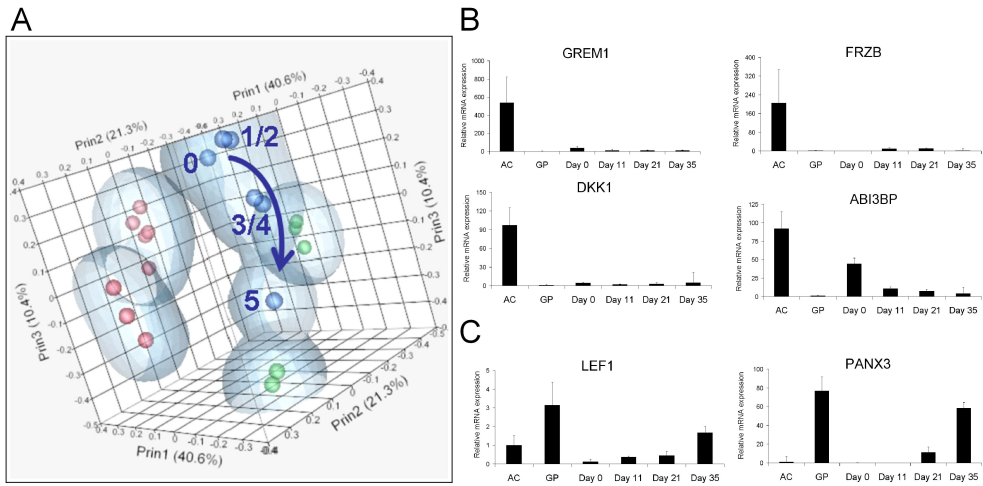


Figure 4.5: Chondrogenically differentiated MSCs resemble growth plate chondrocytes. (A) Three-dimensional principal component analysis based on whole genome gene expression analysis of articular cartilage (red spheres), growth plate cartilage (green spheres) and weekly time points of chondrogenically differentiating human fetal bone marrow MSCs up to five weeks (blue spheres). MSCs were differentiated in pellet cultures in the presence of TGFB3 and BMP6. Over time MSC derived cartilage progressively resembled more growth plate than articular cartilage. (B) Quantitative real-time PCR analysis of chondrogenically differentiating adult bone marrow MSCs (n=3) on articular enriched genes. Data are expressed as mean +/- SEM. Expression of none of these genes was induced during chondrogenic differentiation of the MSCs. (C) In marked contrast, gene expression of two growth plate chondrocyte enriched genes was induced. AC, articular cartilage. GP, growth plate cartilage.

4.3.5 Addition of GREM1, FRZB or DKK1 during chondrogenic differentiation of MSCs inhibits terminal hypertrophic differentiation

Since chondrogenically differentiated MSCs did not express GREM1, FRZB or DKK1, we reasoned that their addition during the differentiation period might steer the rather growth plate-like phenotype towards a more articular cartilage phenotype. To investigate this, chondrogenically differentiating MSCs were treated with 20 or 200 ng/ml recombinant human GREM1, FRZB and DKK1 from day 7 onwards. Histological analysis showed that after at least 3 weeks of culture all pellets stained positive for glycosaminoglycans (figure 4.7A). In line with previous observations, mineralization was first observed in the control cultures around week three, progressed over time and was almost exclusively present in the periphery of the pellets.

Addition of the antagonists at a concentration of 20 ng/ml resulted in slightly less

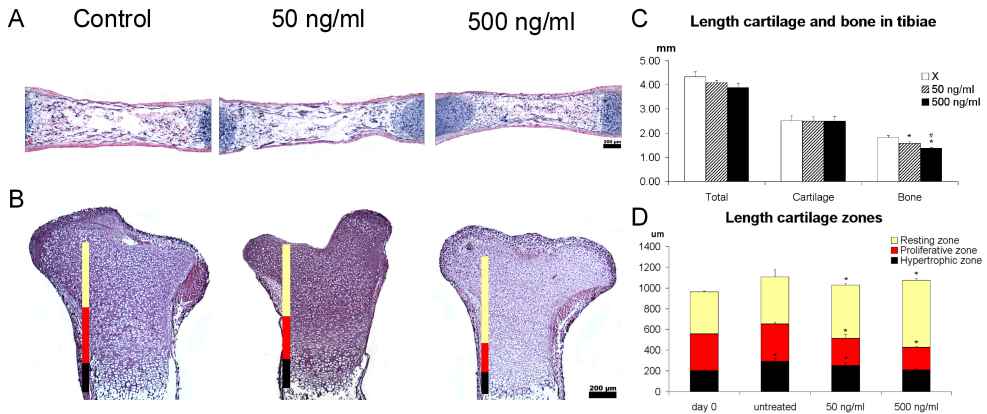


Figure 4.6: Grem1, Frzb and Dkk1 slow down longitudinal growth by inhibiting terminal differentiation. Explanted E17.5 mouse tibiae were cultured in the presence or absence of 50 or 500 ng/ml exogenous Grem1, Frzb and Dkk1. After 7 days of culture, midsagittal 5 μm paraffin sections were stained with (A) alcian blue and nuclear fast red or (B) haematoxylin and eosin. Using image analysis software the lengths of (C) the whole organ, the cartilaginous primary growth plates and bone shaft, and (D) the resting zone, proliferative zone and hypertrophic zone of the cartilage were determined. Yellow bars indicate the resting zone. Purple bars represent the proliferative zone and blue bars indicate the hypertrophic zone. Data represent the mean of 6 tibiae \pm SEM. (Scale bar, 200 μm).

intense toluidine blue staining after 5 weeks of differentiation (Figure 4.7A). Addition of 200 ng/ml of FRZB or DKK1 showed increased glycosaminoglycan staining, predominantly in the periphery of the pellet. This was not observed in GREM1 treated pellets. Importantly, addition of all three antagonists reduced matrix mineralization to undetectable levels (figure 4.7A). In line with this, treatment with the antagonists significantly down regulated the expression of genes traditionally linked to chondrocyte hypertrophy such as *ALP* and *COL10* (figure 4.7B).

Supplementation of 20 or 200 ng/ml recombinant GREM1, FRZB or DKK1 did not result in an increase in expression of the articular cartilage enriched genes *GREM1*, *FRZB* and *DKK1* and *ABI3BP* and only modestly decreased the expression of growth plate enriched genes such as *WNT5A*, *WNT11*, *EPYC* and *PANX3*, but this did not reach significance (figure 4.7C). Absence of a strong effect was not due to loss of biological activity as the expression of the Wnt-target gene *AXIN2* was significantly down-regulated. Taken together, these results demonstrated that exogenous GREM1, FRZB and DKK1 were able to inhibit hypertrophic differentiation and mineralization of chondrogenically differentiating MSCs, but were not able to steer the differentiation itself towards an articular cartilage phenotype.

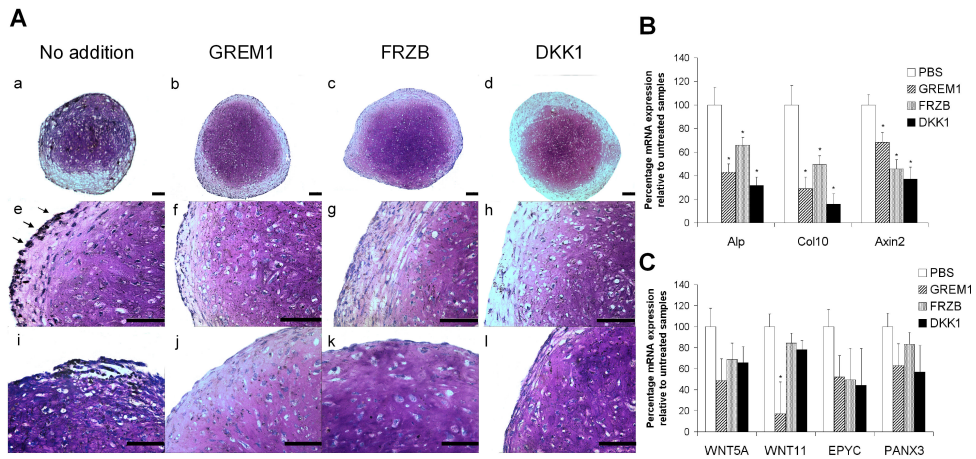


Figure 4.7: GREM1, FRZB and DKK1 inhibit matrix mineralization of chondrogenically differentiating MSCs. (A) Representative histological sections (n=6) of chondrogenically differentiated adult bone marrow MSCs stained with toluidine blue and Von Kossa cultured for either 3 weeks (i) or 5 weeks (a-h, j-l). Cells were supplemented with PBS (a,e,i), 20 ng/ml (b,f) or 200 ng/ml (j) of GREM1, 20 ng/ml (c,g) or 200 ng/ml (k) of FRZB or 20 ng/ml (d,h) or 200 ng/ml (l) of DKK1. After three weeks of chondrogenic differentiation low levels of mineralization are visible, while after five weeks mineralization is readily detected. Addition of GREM1, FRZB or DKK1 did not inhibit chondrogenesis, but did prevent mineralization. Arrows indicate nodules of mineralization. (B and C) Quantitative real-time PCR analysis was performed on MSCs chondrogenically differentiated for 5 weeks in the presence or absence of GREM1, FRZB or DKK1 (20 ng/ml). Investigated genes are enriched in hypertrophic differentiation (B) or the growth plate (C). Data are expressed as mean (n=3 donors) +/- SEM. (* = P<0.05). (Large scale, 100 μ m; short scale bar, 200 μ m).

4.3.6 Preserved antagonist expression in expanded articular chondrocytes

Expanded articular chondrocytes retain their ability to resist endochondral ossification [11]. To study whether this correlates with persistent expression of GREM1, FRZB and DKK1, we investigated the expression levels of these genes during extensive expansion. The expression of *GREM1* increased slightly over time. *FRZB* expression decreased progressively during expansion. However, this was counterbalanced by an almost equal increase in *DKK1* expression. Based on the steady decrease in expression levels of the direct Wnt target gene *AXIN2*, these data suggest that, canonical Wnt signalling slightly but progressively decreased during chondrocyte expansion (figure 4.8).

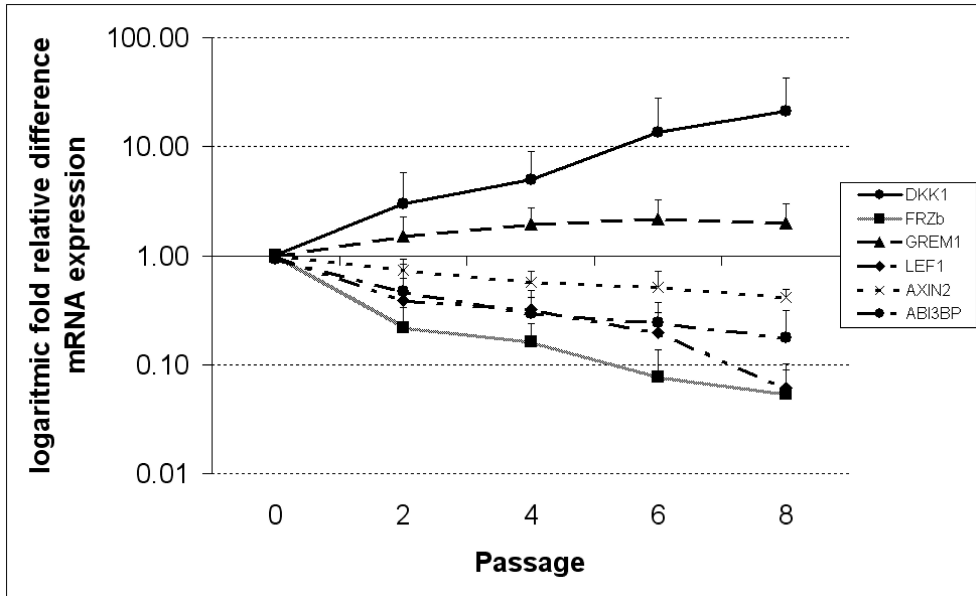


Figure 4.8: Continued Wnt inhibition during extensive expansion. Quantitative real-time PCR analysis of *GREM1*, *FRZB*, *DKK1*, *LEF1*, *AXIN2* and *ABI3BP* mRNA levels of human chondrocytes cultured up to passage eight. Data are the mean of n=6 observations after logarithmic transformation +/- SEM. Values of cells in passage 0 are set to 1.

4.3.7 *GREM1* transcription decreased in degenerating osteoarthritic cartilage

Osteoarthritic cartilage is characterized by evidence of increased hypertrophic differentiation [12]. Given the proposed role of the antagonists *FRZB*, *GREM1* and *DKK1* in preventing hypertrophic differentiation, we hypothesized that the expression of these genes was decreased in osteoarthritic cartilage. To investigate this, paired specimens of macroscopically relatively preserved and degenerating osteoarthritic cartilage were collected from a single osteoarthritic joint of 17 patients who had undergone a total knee arthroplasty. The mRNA was isolated and subjected to qRT-PCR analysis. In preserved cartilage, *GREM1*, *FRZB* and *DKK1* mRNA were expressed significantly higher compared to osteoarthritic cartilage, respectively 2.3, 3.0 and 2.7-fold change with corresponding P-values of <0.001, 0.004 and 0.002 (figure 4.9). Moreover, the expression levels of *GREM1*, *FRZB* and *DKK1* were all significantly positively correlated with each other.

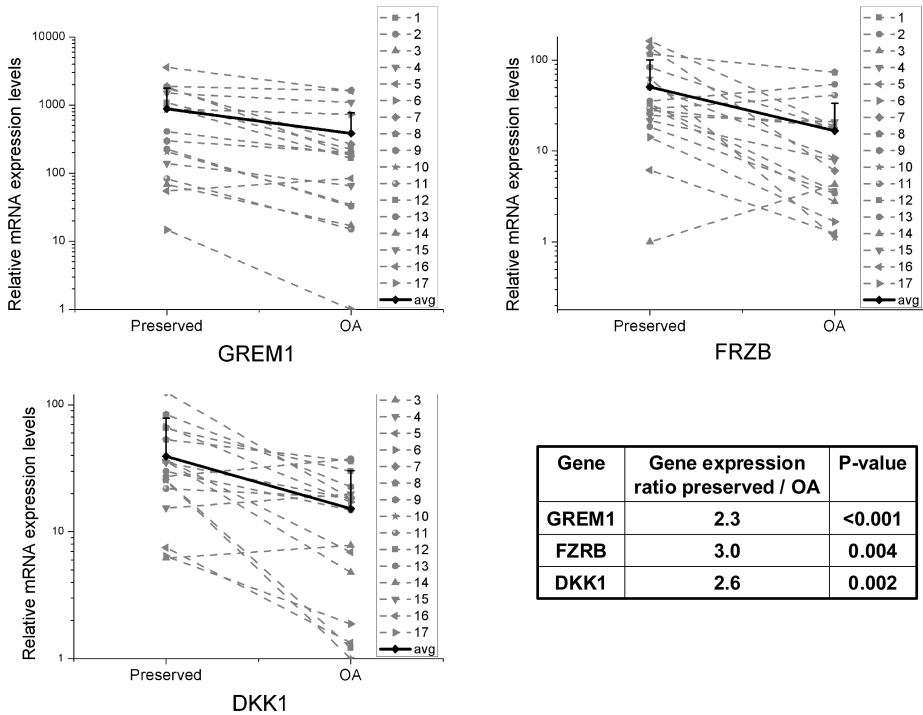


Figure 4.9: Correlation *GREM1*, *FRZB* and *DKK1* with OA. (A) Gene expression of *GREM1*, *FRZB* and *DKK1* was determined in preserved and degenerated cartilage from the same joint. All three antagonists are significantly less expressed in degenerated cartilage compared to preserved cartilage of the same joint. Dashed lines represent individual donors (n=17). Solid line represents the mean \pm SEM. (B).

4.3.8 SNP rs12593365 is associated with radiographic osteoarthritis

We next reasoned that articular cartilage enriched genes may be prime candidates for association with the development and progression of OA. To test this hypothesis, we selected 2 genes of interest, namely: *GREM1* and *DKK1* for which most common genetic variants were tagged by a total of 116 SNPs located in the annotated gene or within 100Kb up-stream or down-stream of the genes. These SNPs were analyzed for an association with radiographic knee or hip OA in the Rotterdam Study I, a large population cohort study. The study population comprised of in total 3243 controls, and 771 hip OA cases, and 1492 knee OA cases. We found a total of 12 SNPs nominally significant associated with hip OA, and 3 SNPs associated with knee OA

A				B							
RSI	Controls	Hip OA cases	Knee OA cases	SNP	minor allele	major allele	minor allele freq	RSI OR (95%CI)	P value RSI	RSII OR (95%CI)	P value RS2
Total nr	3243	771	1492	rs1881537	T	G	0.15	1.25 (1.08-1.45)	0.004	1.23 (0.90-1.66)	0.19
Nr Women	1642	499	1088	rs921510	A	C	0.20	1.21 (1.06-1.39)	0.005	1.21 (0.92-1.61)	0.17
Age (years)	66.9 ± 7.5	69.8 ± 8.0	69.8 ± 8.2	rs4779584	T	C	0.19	1.20 (1.05-1.38)	0.009	1.06 (0.79-1.42)	0.69
BMI	25.8 ± 3.4	26.8 ± 3.7	27.6 ± 3.9	rs1258726	C	T	0.22	0.83 (0.72-0.96)	0.009	0.81 (0.60-1.09)	0.16
				rs12593365	C	T	0.23	0.83 (0.73-0.96)	0.0099	0.69 (0.51-0.94)	0.02
				rs11636374	T	C	0.23	0.84 (0.73-0.96)	0.011	0.72 (53-0.98)	0.04
				rs12905294	A	G	0.41	1.16 (1.03-1.30)	0.011	1.10 (0.87-1.39)	0.44
				rs16959110	T	G	0.27	1.17 (1.04-1.33)	0.011	1.15 (0.89-1.48)	0.29
				rs16959022	T	C	0.05	1.34 (1.05-1.72)	0.018	0.92 (0.51-1.67)	0.78
				rs12593223	A	G	0.25	0.86 (0.75-0.98)	0.027	0.76 (57-1.02)	0.07
				rs11071936	G	A	0.33	0.87 (0.77-0.99)	0.029	0.92 (0.72-1.19)	0.53
				rs10318	T	C	0.17	1.17 (1.01-1.35)	0.035	1.04 (0.77-1.40)	0.81

Figure 4.10: Genetic association study. (A) Baseline characteristics of the study population RSI and RSII used in the genetic association study. (B) Genetic association study of *GREM1* and *DKK1* in two populations (RSI and RSII) for hip OA. RS, Rotterdam Study; OA, osteoarthritis, nr, number; BMI, body mass index; SNP, single nucleotide polymorphism.

(Figure 9.10).

We then tried to replicate these initial findings in a second population based cohort, the Rotterdam Study II, with in total 1466 controls, 158 hip OA cases and 369 knee OA cases. We observed that 11 of the 12 SNPs originally associated with hip OA in RSI were also associated with hip OA in RSII in the same direction (Figure 9.10), of which 2 SNPs reached nominal significance in RSII. A combined analysis of RSI and RSII for the top SNP rs12593365 showed that the C-allele was associated with 20% decreased risk for hip OA (OR:0.80 (95% CI: 0.71-0.92; p=0.001). SNP rs12593365 is located 80 KB downstream of the *GREM1* gene within a region that is known to be involved in its regulation of expression [13].

4.4 Discussion

In this study, we have reported on i) transcriptional markers distinctly present in either human growth plate or articular cartilage; ii) the identification of 3 antagonists *GREM1*, *FRZB* and *DKK1* which are enriched in articular cartilage and can mitigate hypertrophic differentiation and endochondral ossification; and iii) that the mRNA expression of these antagonists is decreased in severely affected osteoarthritic regions of joint cartilage.

The whole genome gene expressions analysis comparing donor paired articular cartilage and growth plate cartilage showed remarkably few genes expressed at a more than 2-fold difference. Only 35 genes were expressed with more than five-fold difference, which represents just 1.6% of all genes that were detected to be significantly differently expressed. This underlines the fact that both tissues, despite their distinct functions and fates, are both hyaline cartilage.

It should be noted that although our initial findings were made in hyaline cartilage specimens from preadolescent donors without macroscopic evidence of disease. Our

major findings were reproduced in healthy fetal hyaline cartilage. Although we cannot exclude that the gene expression patterns in growing donors might be different from that of adult donors, the gene expression analysis of articular cartilage of adult donors showed persistent expression of articular cartilage enriched genes while the expression of typical growth plate genes was invariably low.

It is well established that *in vitro* generated MSC derived cartilage is prone to undergo endochondral ossification when subcutaneously implanted in a suitable animal model [14]. Using our data set, we confirmed and at least partly explained this observation at the genetic level. We demonstrate that chondrogenically differentiating MSCs acquire a gene expression fingerprint more characteristic of a growth plate rather than an articular cartilage chondrocyte. We furthermore provide evidence that measuring the gene expression of four markers profoundly expressed in articular cartilage (*GREM1*, *FRZB*, *DKK1* and *ABI3BP*) and four markers enriched in growth plate cartilage (*PANX3*, *MATN1*, *EPYC* and *LEF1*) are sufficient to identify the hyaline cartilage subtype. This marker set can be used to develop and optimize differentiation protocols to help in obtaining articular-like cartilage from chondrogenically differentiating MSCs.

4

In contrast to osteoarthritic cartilage, healthy articular cartilage is largely resistant to undergo hypertrophic differentiation. It has been postulated that articular cartilage expresses one or more secreted factors that can prevent hypertrophic differentiation of growth plate cartilage or chondrogenically differentiating MSCs in co-cultures [2]. Moreover, this characteristic is retained over time in primary MSCs cultures of articular chondrocytes. Therefore, it is intuitive to assume that secreted molecules able to antagonize pathways known to be involved in hypertrophic differentiation would be of paramount importance in controlling the fate of hyaline cartilage and might be natural breaks preventing hypertrophic differentiation of normal articular cartilage. Indeed, the three most up-regulated genes in articular cartilage in comparison to growth plate cartilage were the secreted BMP- and Wnt antagonists *GREM1*, *FRZB* and *DKK1*. The Wnt- and BMP signaling pathways play both a stimulatory role in the tightly orchestrated process of hypertrophic differentiation [3, 15]. Indeed, inhibition of these pathways via supplementation of culture medium with recombinant *GREM1*, *FRZB* and *DKK1* led to an inhibition of hypertrophic chondrocyte differentiation and subsequent matrix mineralization in chondrogenically differentiated MSCs. In cultured mouse fetal explanted tibiae, they retarded endochondral ossification by keeping the chondrocytes in the resting zone. Additionally, the expression of these antagonists is preserved in expanded primary chondrocytes over time and these cells retain the propensity to inhibit hypertrophic differentiation of co-cultured MSCs. Therefore, *GREM1*, *FRZB* and *DKK1* are strong candidates for the above-mentioned secreted factors. We hypothesize that these articular cartilage enriched secreted factors act as a natural brake on terminal hypertrophic differentiation in healthy joint cartilage. Accumulating evidence suggests that activation of hypertrophic differentiation of articular chondrocytes is one of the underlying pathophysiological mechanisms of OA [7, 16]. This process is mediated amongst others via a shift in the balance between hypoxia inducible factor (HIF)1A and HIF2A, favoring the latter. Not only does this lead to up-regulation of catabolic genes such as *MMP3*, *MMP9* and *MMP13*, but also

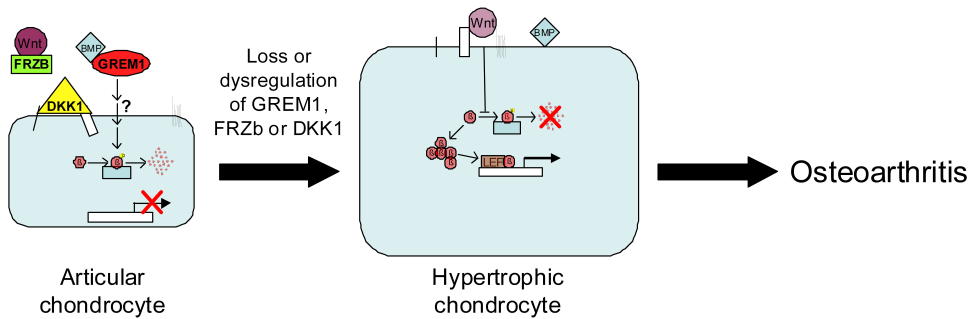


Figure 4.11: Schematic model of the role of GREM1, FRZB and DKK1 in articular cartilage homeostasis. Healthy articular chondrocytes express GREM1, FRZB and DKK1. By counteracting canonical Wnt signaling and / or BMP signaling they prevent hypertrophic differentiation of articular chondrocytes. Loss or dysregulation of these antagonists may relieve this natural break, which then may contribute to the pathogenesis of osteoarthritis by allowing hypertrophic chondrocyte differentiation.

genes that are involved in the stimulation of chondrocyte hypertrophy such as Indian hedgehog and runt-related transcription factor 2 [8, 17]. Additionally, Wnt/ β -catenin is able to alter HIF and IHH signaling [18, 19]. Moreover, induced conditional activation of Wnt/ β -catenin leads to the development of an osteoarthritic phenotype in mice via hypertrophic differentiation [20]. We postulate that GREM1, FRZB and DKK1 act as the natural brakes on hypertrophic differentiation of articular cartilage by directly or indirectly antagonizing the Wnt-signaling. Consequently, deregulation of their expression is likely to be associated with development of OA (figure 9.11). Indeed, we observed a significant decrease in expression of all three antagonists in severely affected osteoarthritic cartilage compared to relatively preserved cartilage from the same joint. Osteoarthritic cartilage show clear signs of increased chondrocyte hypertrophy, suggesting an association between decreased antagonist expression and signs of hypertrophy. More importantly, the expressions of these three secreted molecules are highly correlated. Previously it has been shown that DKK1 expression decreases in OA [9, 21]. FRZB has also been associated with OA; *FRZB*^{-/-} mice have a mild phenotype, but show accelerated cartilage destruction following exposure to OA inducing triggers [22]. Given the compensatory potential of other Wnt antagonists in articular cartilage, in particularly DKK1 and to a lesser extent GREM1, it seems feasible that they can compensate for the lack of FRZB under normal conditions. The compensatory roles may be unmasked by generating double or triple knock-out animals. The above mentioned lines of evidence are consistent with our hypothesis.

A possible important role for the identified genes in the etiology of OA is further corroborated by the results of the genetic association study. We demonstrated a significant association of polymorphisms near the *GREM1* gene with radiographic hip OA. Interestingly, these SNPs are located downstream of the *GREM1* gene in

a region that is known to regulate *GREM1* expression [13]. However, confirmation in additional study cohorts is necessary. *FRZB* polymorphisms have previously been described to be associated with osteoarthritis in some studies, but have not been replicated in others and a recently published meta-analysis found no overall effect of *FRZB* genetic variants on hip or knee OA [23]. Taken together, multiple lines of evidence support a role for *GREM1*, *FRZB* and *DKK1* in OA, and based on our data we postulate that they act as natural inhibitors of hypertrophic differentiation in healthy articular cartilage.

In summary, we used whole genome expression micro-array analysis to discriminate between two subtypes of hyaline cartilage, which are either resistant or prone to undergoing endochondral ossification. Using this dataset, we designed a panel of genetic expression markers able to distinguish between these two hyaline cartilages. We showed that the BMP antagonist *GREM1* and the Wnt antagonists *FRZB* and *DKK1* are highly enriched in articular cartilage and are likely to act as a natural mechanism in preventing terminal hypertrophic differentiation of chondrocytes and subsequent endochondral ossification of articular cartilage. Deregulation of this mechanism may disturb articular cartilage homeostasis by enabling hypertrophic chondrocyte differentiation, which may ultimately contribute to the pathogenesis of OA.

References

1. Felson, D.T., et al., Osteoarthritis: new insights. Part 1: the disease and its risk factors. *Ann Intern Med*, 2000. 133(8): p. 635-46.
2. Jikko, A., et al., Inhibition of chondrocyte terminal differentiation and matrix calcification by soluble factors released by articular chondrocytes. *Calcif Tissue Int*, 1999. 65(4): p. 276-9.
3. Tamamura, Y., et al., Developmental regulation of Wnt/beta-catenin signals is required for growth plate assembly, cartilage integrity, and endochondral ossification. *J Biol Chem*, 2005. 280(19): p. 19185-95.
4. De Luca, F., et al., Regulation of growth plate chondrogenesis by bone morphogenetic protein-2. *Endocrinology*, 2001. 142(1): p. 430-6.
5. Vortkamp, A., et al., Regulation of rate of cartilage differentiation by Indian hedgehog and PTH-related protein. *Science*, 1996. 273(5275): p. 613-22.
6. Stewart, A.J., B. Houston, and C. Farquharson, Elevated expression of hypoxia inducible factor-2alpha in terminally differentiating growth plate chondrocytes. *J Cell Physiol*, 2006. 206(2): p. 435-40.
7. Kawaguchi, H., Regulation of osteoarthritis development by Wnt-beta-catenin signaling through the endochondral ossification process. *J Bone Miner Res*, 2009. 24(1): p. 8-11.
8. Saito, T., et al., Transcriptional regulation of endochondral ossification by HIF-2alpha during skeletal growth and osteoarthritis development. *Nat Med*, 2010. 16(6): p. 678-86.
9. Tardif, G., et al., Differential gene expression and regulation of the bone morphogenetic protein antagonists follistatin and gremlin in normal and osteoarthritic human chondrocytes and synovial fibroblasts. *Arthritis Rheum*, 2004. 50(8): p. 2521-30.
10. Lin, A.C., et al., Modulating hedgehog signaling can attenuate the severity of osteoarthritis. *Nat Med*, 2009. 15(12): p. 1421-5.
11. Dell'Accio, F., et al., Expanded phenotypically stable chondrocytes persist in the repair tissue and contribute to cartilage matrix formation and structural integration in a goat model of autologous chondrocyte implantation. *J Orthop Res*, 2003. 21(1): p. 123-31.
12. Adams, S.L., A.J. Cohen, and L. Lasso, Integration of signaling pathways regulating chondrocyte differentiation during endochondral bone formation. *J Cell Physiol*, 2007. 213(3): p. 635-41.
13. Zuniga, A., et al., Mouse limb deformity mutations disrupt a global control region within the large regulatory landscape required for Gremlin expression. *Genes Dev*, 2004. 18(13): p. 1553-64.
14. Jukes, J.M., et al., Endochondral bone tissue engineering using embryonic stem cells. *Proc Natl Acad Sci U S A*, 2008. 105(19): p. 6840-5.
15. Nilsson, O., et al., Gradients in bone morphogenetic protein-related gene expression across the growth plate. *J Endocrinol*, 2007. 193(1): p. 75-84.
16. Bos, S.D., P.E. Slagboom, and I. Meulenbelt, New insights into osteoarthritis: early developmental features of an ageing-related disease. *Curr Opin Rheumatol*, 2008. 20(5): p. 553-9.
17. Kamekura, S., et al., Contribution of runt-related transcription factor 2 to the pathogenesis of osteoarthritis in mice after induction of knee joint instability. *Arthritis Rheum*, 2006. 54(8): p. 2462-70.
18. Kaidi, A., A.C. Williams, and C. Paraskeva, Interaction between beta-catenin and HIF-1 promotes cellular adaptation to hypoxia. *Nat Cell Biol*, 2007. 9(2): p. 210-7.
19. Mak, K.K., et al., Wnt/beta-catenin signaling interacts differentially with Ihh signaling in controlling endochondral bone and synovial joint formation. *Development*, 2006. 133(18):

p. 3695-707.

20. Zhu, M., et al., Activation of beta-catenin signaling in articular chondrocytes leads to osteoarthritis-like phenotype in adult beta-catenin conditional activation mice. *J Bone Miner Res*, 2009. 24(1): p. 12-21.

21. Diarra, D., et al., Dickkopf-1 is a master regulator of joint remodeling. *Nat Med*, 2007. 13(2): p. 156-63.

22. Lories, R.J., et al., Articular cartilage and biomechanical properties of the long bones in *Frzb*-knockout mice. *Arthritis Rheum*, 2007. 56(12): p. 4095-103.

23. Evangelou, E., et al., Large-scale analysis of association between GDF5 and FRZB variants and osteoarthritis of the hip, knee, and hand. *Arthritis Rheum*, 2009. 60(6): p. 1710-21.

24. Heinrichs, C., et al., Dexamethasone increases growth hormone receptor messenger ribonucleic acid levels in liver and growth plate. *Endocrinology*, 1994. 135(3): p. 1113-8.

25. Both, S.K., et al., A rapid and efficient method for expansion of human mesenchymal stem cells. *Tissue Eng*, 2007. 13(1): p. 3-9.

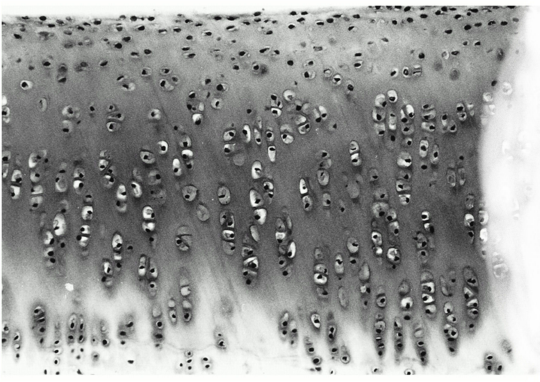
26. Jin, R., et al., Injectable chitosan-based hydrogels for cartilage tissue engineering. *Biomaterials*, 2009. 30(13): p. 2544-51.

27. Salomonis, N., et al., GenMAPP 2: new features and resources for pathway analysis. *BMC Bioinformatics*, 2007. 8: p. 217.

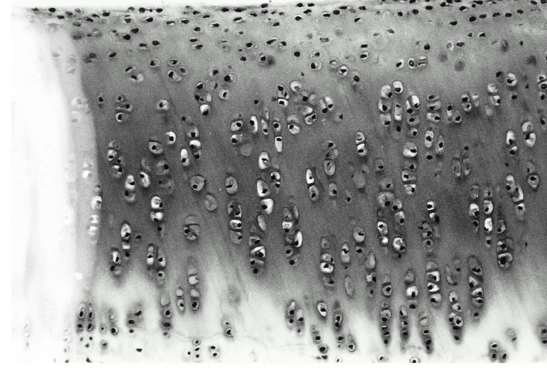
28. Thomas, P.D., et al., PANTHER: a library of protein families and subfamilies indexed by function. *Genome Res*, 2003. 13(9): p. 2129-41.

29. Hofman, A., et al., The Rotterdam Study: 2010 objectives and design update. *Eur J Epidemiol*, 2009. 24(9): p. 553-72.

30. Purcell, S., et al., PLINK: a tool set for whole-genome association and population-based linkage analyses. *Am J Hum Genet*, 2007. 81(3): p. 559-75.



5



Chapter 5

Grem1, Frzb and Dkk1 protein levels correlate with acute synovitis in equine joints

5

Jeroen Leijten, Janny de Grauw, Clemens van Blitterswijk, Rene van Weeren and Marcel Karperien

Science is simply common sense at its best.
Thomas Huxley

Abstract

There is an unmet need of biomarkers that can detect degenerative joint diseases with great sensitivity and specificity in an early stage of the disease. Recently, we hypothesized that the secreted BMP- and Wnt-antagonists Grem1, Frzb and Dkk1 are master regulators of joint homeostasis. Such regulators are prime candidates for biomarkers detecting cartilage disease.

In this study we investigated the effect of inflammation on the expression of Grem1, Frzb and Dkk1 in synovial fluid and in serum using an established horse model. Sterile inflammation was induced in the intercarpal joint by injecting 0.5 ng of lipopolysaccharide. Synovial fluid and serum were collected for analysis at several time points. Grem1, Frzb and Dkk1 were measured with ELISA. All three antagonists were significantly elevated in the synovial fluid of LPS injected intercarpal joints at 24 hours post injection. Values returned towards baseline at 168 hours post injection. Moreover, the protein levels of Grem1, Frzb and Dkk1 correlated with each other. In serum, Grem1 and Frzb, but not Dkk1, protein levels were affected. However, only the increase of Grem1 protein levels was statistically significant.

Taken together, our study reveals Grem1, Frzb and Dkk1 as informative biomarkers for inflammation of the synovial joint.

5.1 Introduction

The cartilage micro-environment is closely linked with joint homeostasis. Inflammation of the joint perturbs this homeostasis and induces cartilage catabolism [1]. Inflammation of the synovial membrane is common in several joint diseases including rheumatoid arthritis and osteoarthritis [2, 3].

We and others have identified the secreted Wnt- and BMP-antagonists Grem1, Frzb and Dkk1 as important regulators of cartilage homeostasis [4-6]. As Grem1, Frzb and Dkk1 are secreted soluble proteins, deregulation of cartilage homeostasis can result in detectable changes in synovial fluid or serum protein levels. In consequence, Grem1, Frzb and Dkk1 can be considered as interesting potential biomarkers for cartilage homeostasis. However, the effect of joint inflammation on the expression of these biomarkers is still largely unknown.

Injection of lipopolysaccharides in intercarpal horse joints is an established model to induce experimental synovitis [7, 8]. Advantageously, this model allows for collection of synovial fluid and blood for subsequent biomarker analysis. In addition, this model is highly suitable for the analysis of therapeutic intervention. For example, it has been demonstrated that intra-articular use of opioids effectively reduces pain and inflammation in this model [9].

The present study was designed to answer two intimately linked questions. Firstly, we examined whether the induction of experimental synovitis would affect the synovial fluid and serum protein levels of Grem1, Frzb and Dkk1. Secondly, we investigated whether intra-articular treatment with an opioid influences the expression of Grem1, Frzb and Dkk1 in synovial fluid.

5.2 Materials and methods

5.2.1 Experimental animals

All experimental procedures and protocols were previously approved by the Utrecht University Committee on the Care and Use of Experimental Animals in compliance with Dutch legislation on animal experiments. Two separate animal experiments were performed. Horses were stall-rested in separate box stalls of 3.6 m x 3.6 m on woodchip bedding and were fed silage ad libitum and one kg of maintenance concentrates b.i.d. with hay.

The first experiment was performed as previously described [7]. In short, sterile synovitis was induced in a randomly chosen intercarpal joint of six healthy skeletally mature Dutch Warmblood mares of ages between 5 and 8 years with no history of orthopedic disease. Blood and synovial fluid were collected 0, 8, 24 and 168 hours post injection.

The second experiment was a two-period randomized placebo-controlled crossover experiment, in which sterile synovitis was induced in a randomly chosen talocrural joint of eight Dutch Warmblood mares as previously described [9]. Horses were randomly assigned to receive morphine (n = 4) or placebo (n = 4) treatment. After a washout period of three weeks, the sterile synovitis was induced in the other joint

which received the opposite treatment. One hour after induction of synovitis, 20 ml of saline with or without 120 mg of morphine was administered intra-articularly. Synovial fluid was collected 0, 4, 8, 28, 52 and 168 hours post injection.

5.2.2 Induction of sterile synovitis

To induce sterile synovitis, the left or right tarsus of each horse was clipped and surgically prepared for dorsomedial arthrocentesis of the talocrural joint. Sterile LPS from *Escherichia coli* O55:B5 (Sigma-Aldrich) was diluted to a final concentration of 0.625 ng/ml. Horses were twitched and arthrocentesis was performed with a 21 gauge x 40 mm needle. After withdrawal of the baseline synovial fluid sample (T=0), 0.8 ml LPS solution (containing 0.5 ng LPS) was delivered aseptically into the talocrural joint.

5.2.3 Collection of blood and synovial fluid

Serum was isolated from EDTA treated blood from the left jugular vein before sedation for arthrocentesis at appointed time points. Serum was aliquoted and stored at -80°C until use. Synovial fluid was centrifuged in plain tubes at 10,000 g for 15 minutes, aliquoted and stored at -80°C until further analysis.

5.2.4 Quantification of Grem1, Frzb and Dkk1 protein levels

Grem1 (USCN Life Science), Frzb and Dkk1 (R&D Systems) protein levels in the collected serum and synovial fluid samples were measured by Enzyme-linked immunosorbent assay (ELISA) following manufacturer's instructions.

5.2.5 Statistical analysis

Statistical differences between two groups were analyzed by use of one-way analysis of variance on repeated measures. When a significant time effect was observed, levels at individual time points were compared with Tukey's post hoc tests. The level of significance was set at $P < 0.05$. Time points that compared to 0 hours post injection reached significance are indicated with an asterisk. Correlations between the expression levels of synovial fluid of Grem1, Frzb and Dkk1 during experimental synovitis were assessed using Pearson's correlation analysis.

5.3 Results

5.3.1 Synovial fluid protein levels of Grem1, Frzb and Dkk1 during sterile synovitis

Averaged Grem1, Frzb and Dkk1 concentrations in synovial fluid were 55 ng/ml, 41730 ng/ml and 425 ng/ml respectively (figure 5.1). Upon induction of sterile synovitis, Grem1, Frzb and Dkk1 protein levels increased in all tested horses. The induction of

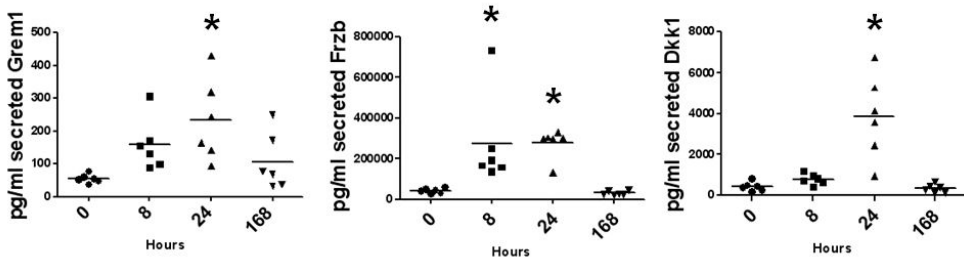


Figure 5.1: Synovial fluid protein levels of Grem1, Frzb and Dkk1 over time as measured in an intercarpal horse joint in which experimental synovitis is induced.

Table 1 Correlations between Grem1, Frzb and Dkk1 synovial protein levels

	r
Secreted Grem1 - Secreted Frzb	0.661**
Secreted Grem1 - Secreted Dkk1	0.580**
Secreted Frzb - Secreted Dkk1	0.457*

Correlations between changes in synovial fluid protein level during experimental synovitis in an intercarpal horse joint. (n=24); **P<0.01, *P<0.05.

Table 5.1: Correlations between Grem1, Frzb and Dkk1 synovial protein levels.

Frzb reached significance at 8 and 24 hours post induction. The increase in Grem1 and Dkk1 reached significance 24 hours post induction. The highest expression levels of all three proteins were measured at 24 hours post induction with an averaged protein level of 232 ng/ml, 275253 ng/ml and 3854 ng/ml for Grem1, Frzb and Dkk1 respectively. After 168 hours, the expression of the 3 antagonists returned towards baseline levels. Moreover, the expression levels of all three proteins correlated with each other (table 5.1).

5.3.2 Serum protein levels of Grem1, Frzb and Dkk1 during sterile synovitis

Grem1, Frzb and Dkk1 protein levels were detected in the serum with average concentrations of 83 ng/ml, 6786 ng/ml and 488 ng/ml respectively (figure 5.2). Upon induction of sterile synovitis, Grem1 protein levels in serum were statistically significant elevated compared to baseline levels after 8 hours with an increase of 102 % (+/- 173 ng/ml). Afterwards, Grem1 protein levels gradually returned to baseline levels, but even after 168 hours Grem1 levels were still 44.5 % (+/- ng/ml) increased compared to the baseline. Frzb protein levels were mildly decreased at 8 and 24 hours (+/- 6404 ng/ml and +/- 5985 ng/ml respectively) and slightly increased 168 hours

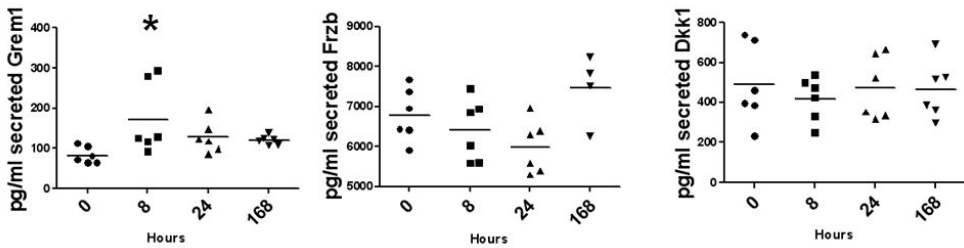


Figure 5.2: Serum protein levels of Greml1, Frzb and Dkk1 over time in a horse in which experimental synovitis is induced in one of its intercarpal joints.

post induction (+/- 7463 ng/ml). The average protein levels of Dkk1 in serum did not change significantly.

5.3.3 Effect of morphine treatment on synovial fluid protein levels of Frzb and Dkk1 during sterile synovitis

The induction of sterile synovitis resulted in the elevation of Frzb and Dkk1 levels in synovial fluid. Opioid treatment of sterile synovitis reduced pain, clinical lameness and inflammation [9]. Therefore, we investigated whether treatment of sterile synovitis with opioids mitigated the elevation of Frzb and Dkk1 protein levels in synovial fluid. Induction of sterile inflammation, increased Frzb and Dkk1 protein levels in synovial fluid, which was in agreement with experiment 1. Treatment with morphine did not affect LPS' effect on Frzb and Dkk1 protein levels compared to placebo treated joints (figure 5.3).

5.4 Discussion

Identification and characterization of joint homeostasis biomarkers is crucial for improving the accuracy of diagnosis and prognosis of joint diseases at an early stage [10]. The currently most frequently used biomarkers are derived from breakdown products of the extracellular cartilaginous matrix [11]. Although such biomarkers have proven to be reliable in advanced stages of joint disease, they lack the sensitivity and specificity in an early stage of disease. We postulated that secreted molecules that play a role in the maintenance of articular cartilage homeostasis may yield biomarkers that allow the detection of degenerative events in an early phase of the disease process. This potentially allows for preventive therapy, rather than symptomatic treatment at a late stage when joint function is already severely impaired. Previously, we and others have shown that GREM1, FRZB and DKK1 are potential candidates for such biomarkers [Chapter 4]. GREM1, FRZB and DKK1 are secreted soluble proteins able to inhibit BMP- or Wnt-signaling either directly or indirectly [12]. Circulating DKK1 protein levels have previously been reported to be increased in rheumatoid arthritis and de-

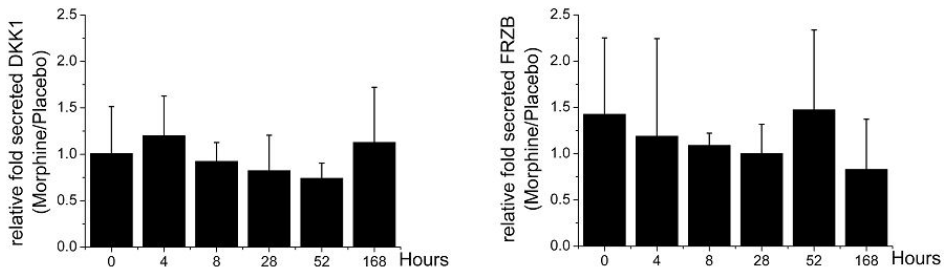


Figure 5.3: Effect of intra-articular morphine treatment on synovial fluid protein levels of Frzb and Dkk1 during experimental synovitis. Averaged protein level of each time point was normalized to protein levels of placebo treated intercarpal horse joints with experimental synovitis.

creased in osteoarthritis [4, 13]. Moreover, Dkk1 has been suggested to correlate with the severity of knee osteoarthritis [14]. Loss of Frzb expression in mice was associated with exacerbated cartilage destruction in experimental models for osteoarthritis [5]. Circulating FRZB protein levels were detected to be increased in early rheumatoid arthritis and decreased in response to disease-modifying antirheumatic drugs [15]. Furthermore, circulating FRZB protein levels were slightly increased in a FRZB haplotype variant that is associated with hip osteoarthritis [16]. FRZB protein levels in synovial fluid have remained largely uninvestigated. GREM1 was demonstrated to be differentially expressed between healthy and osteoarthritic human chondrocytes and synovial fibroblasts [6]. Moreover GREM1 protein levels are detectable in human serum (508 ng/ml) [17], which is considerably higher than serum values in horses (83 ng/ml in this study). However, Grem1 protein level in synovial fluid and the influence of cartilage related pathologies on Grem1's protein level in serum and synovial fluid have remained uninvestigated.

In the present study we demonstrated that the protein expression of Grem1, Frzb and Dkk1 in synovial fluid rapidly and transiently increased after induction of acute synovitis in equine joints. In addition, we showed that Grem1 protein levels were also increased in serum and were still elevated 168 hours after injection of LPS compared to baseline. At 8 and 24 hours after LPS injection Frzb expression in serum was slightly decreased and at 168 hours post injection slightly increased compared to baseline. Although articular cartilage produces and secretes Grem1, Frzb and Dkk1, it cannot be excluded that the measured differences in the synovial fluid and serum originated from other tissues. In particular, several other joint tissues such as bone and synovium express and secrete Grem1, FRZB and/or DKK1 [4, 5, 18]. Regardless, experimental synovitis elevated the level of all three proteins in the synovial fluid. As this increase in protein level is already detectable after eight hours, it might be speculated that this is due to a direct effect. In line with this, a previous study with an identical experimental set-up for the induction of experimental syn-

ovitis reported that the inflammation is most intense around 8 hours post injection as witnessed by lameness, joint effusion, carpal circumference and a sharp increase of prostaglandin E2, bradykinin and substance P in the synovial fluid. In contrast, collagen II turnover markers, collagenase-cleavage neopeptide of type II collagen (C2C) and carboxypropeptide of type II collagen epitope (CPII), only increased after 24 hours [19]. This suggests that the protein levels of the cartilage homeostasis markers Grem1, Frzb and Dkk1 are altered before collagen II degradation occurs.

Intra articular morphine injections results in analgesic effects via decreased cAMP formation, which lowers the neuronal excitability of the peripheral nerve endings [20]. Moreover, it also exerts an anti-inflammatory function via the inhibition of calcium-dependent release of proinflammatory mediators [21]. As a result, intra-articular injection of opioids strongly decreased the clinical lameness of horses caused by sterile inflammations of synovial joints [9]. However, of morphine have not been proven to inhibit cartilage degeneration. Moreover, intra-articular injection of morphine did not detectably influence Frzb and Dkk1 protein levels upon induction of sterile inflammation in synovial fluid. This suggests that the response in Frzb and Dkk1 protein levels, by the disturbance of joint homeostasis, is not influenced by symptomatic analgesic treatment and temporary mechanical unloading of the joint.

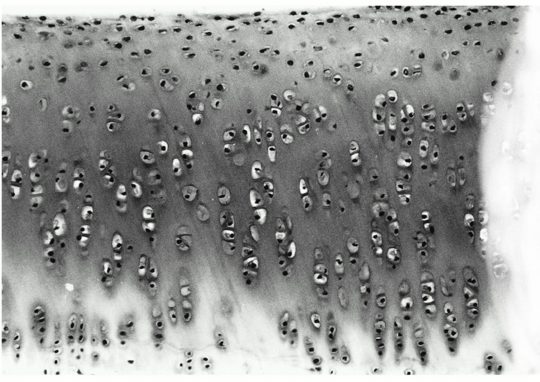
Secreted proteins that antagonize the same signaling pathway can have compensatory regulation; a decrease of one antagonist can be compensated by (altered expression of) other antagonists. Similarly, a decrease in antagonists might also lead to altered expression of stimulating agonists. Unfortunately, only limited data is available on these compensatory mechanisms in osteoarthritis. Deeper understanding of compensatory regulation in cartilage and its associated diseases is desirable, as it is known that many of its signaling pathways e.g. Wnt-signaling have the potency to autoregulate the expression of their own agonists and antagonists [Chapter 6].

Combinatorial testing of both candidate and established biomarkers might reveal a biomarker panel that possesses an increased diagnostic and prognostic potential compared to the traditional use of single cartilage biomarkers. The combination of biomarkers that are informative on the various phases of disease development might even allow estimating disease progression. In addition, the screening of multiple biomarkers can contribute to the discrimination of subgroups in heterogeneous diseases such as osteoarthritis. The present study reveals Grem1, Frzb and Dkk1 as putative informative biomarkers for inflammation of the synovial joint.

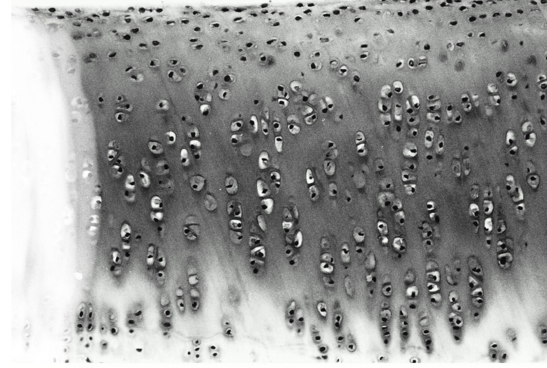
References

1. Kurz, B., et al., Pathomechanisms of cartilage destruction by mechanical injury. *Ann Anat*, 2005. 187(5-6): p. 473-85.
2. Sutton, S., et al., The contribution of the synovium, synovial derived inflammatory cytokines and neuropeptides to the pathogenesis of osteoarthritis. *Vet J*, 2009. 179(1): p. 10-24.
3. Hill, C.L., et al., Synovitis detected on magnetic resonance imaging and its relation to pain and cartilage loss in knee osteoarthritis. *Ann Rheum Dis*, 2007. 66(12): p. 1599-603.
4. Diarra, D., et al., Dickkopf-1 is a master regulator of joint remodeling. *Nat Med*, 2007. 13(2): p. 156-63.
5. Lories, R.J., et al., Articular cartilage and biomechanical properties of the long bones in Frzb-knockout mice. *Arthritis Rheum*, 2007. 56(12): p. 4095-103.
6. Tardif, G., et al., Differential gene expression and regulation of the bone morphogenetic protein antagonists follistatin and gremlin in normal and osteoarthritic human chondrocytes and synovial fibroblasts. *Arthritis Rheum*, 2004. 50(8): p. 2521-30.
7. de Grauw, J.C., et al., In vivo effects of meloxicam on inflammatory mediators, MMP activity and cartilage biomarkers in equine joints with acute synovitis. *Equine Vet J*, 2009. 41(7): p. 693-9.
8. Laverty, S., et al., Synovial fluid levels and serum pharmacokinetics in a large animal model following treatment with oral glucosamine at clinically relevant doses. *Arthritis Rheum*, 2005. 52(1): p. 181-91.
9. van Loon, J.P., et al., Intra-articular opioid analgesia is effective in reducing pain and inflammation in an equine LPS induced synovitis model. *Equine Vet J*, 2010. 42(5): p. 412-9.
10. Settle, S., et al., Cartilage degradation biomarkers predict efficacy of a novel, highly selective matrix metalloproteinase 13 inhibitor in a dog model of osteoarthritis: confirmation by multivariate analysis that modulation of type II collagen and aggrecan degradation peptides parallels pathologic changes. *Arthritis Rheum*, 2010. 62(10): p. 3006-15.
11. Patra, D. and L.J. Sandell, Recent advances in biomarkers in osteoarthritis. *Curr Opin Rheumatol*, 2011. 23(5): p. 465-70.
12. Gazzo, E., et al., Conditional deletion of gremlin causes a transient increase in bone formation and bone mass. *J Biol Chem*, 2007. 282(43): p. 31549-57.
13. Voorzanger-Rousselot, N., N.C. Ben-Tabassi, and P. Garnero, Opposite relationships between circulating Dkk-1 and cartilage breakdown in patients with rheumatoid arthritis and knee osteoarthritis. *Ann Rheum Dis*, 2009. 68(9): p. 1513-4.
14. Honsawek, S., et al., Dickkopf-1 (Dkk-1) in plasma and synovial fluid is inversely correlated with radiographic severity of knee osteoarthritis patients. *Bmc Musculoskeletal Disorders*, 2010. 11.
15. Corallini, F., et al., Circulating levels of frizzled-related protein (FRZB) are increased in patients with early rheumatoid arthritis and decrease in response to disease-modifying antirheumatic drugs. *Ann Rheum Dis*, 2010. 69(9): p. 1733-4.
16. Lane, N.E., et al., Frizzled-related protein variants are risk factors for hip osteoarthritis. *Arthritis Rheum*, 2006. 54(4): p. 1246-54.
17. Sha, G., et al., Elevated levels of gremlin-1 in eutopic endometrium and peripheral serum in patients with endometriosis. *Fertil Steril*, 2009. 91(2): p. 350-8.
18. Canalis, E., K. Parker, and S. Zanotti, Gremlin1 Is Required for Skeletal Development and Postnatal Skeletal Homeostasis. *Journal of Cellular Physiology*, 2012. 227(1): p. 269-277.

19. de Grauw, J.C., C.H. van de Lest, and P.R. van Weeren, Inflammatory mediators and cartilage biomarkers in synovial fluid after a single inflammatory insult: a longitudinal experimental study. *Arthritis Res Ther*, 2009. 11(2): p. R35.
20. Kalso, E., et al., No pain, no gain: clinical excellence and scientific rigour—lessons learned from IA morphine. *Pain*, 2002. 98(3): p. 269-75.
21. Stein, C., The control of pain in peripheral tissue by opioids. *N Engl J Med*, 1995. 332(25): p. 1685-90.



6



Chapter 6

Transcriptional regulation of GREM1, FRZB and DKK1 by hypertrophic differentiation-related factors

6

Jeroen Leijten, Ellie Landman, Nicole Georgi, Michelle Kip, Holger Jahr, Janine Post, Clemens van Blitterswijk and Marcel Karperien

Whoever ceases to be a student has never been a student.
George Iles

Abstract

Osteoarthritis is, at least in a subset of patients, associated with hypertrophic differentiation of articular chondrocytes. Recently, we have identified the BMP- and Wnt-signaling antagonists GREM1, FRZB and DKK1 as natural brakes of hypertrophic differentiation in healthy articular cartilage. Moreover, we demonstrated that deregulated transcription of these factors correlated with osteoarthritis. In this study we set out to investigate the influence of factors, which are important in the onset and progression of hypertrophic differentiation, on the gene transcription levels of *GREM1*, *FRZB* and *DKK1*.

Human articular chondrocytes were exposed to Wnt, BMP, IL1B, IHH, PTHrP, mechanical loading, different tonicities or distinct oxygen levels. We demonstrated that Wnt-, BMP-, IL1B-signaling and mechanical loading were capable of altering the mRNA levels of *GREM1*, *FRZB* and *DKK1*. IHH, PTHrP and tonicity influenced the mRNA levels of at least one antagonist, while oxygen levels did not demonstrate any statistical significant effect on the tested genes. IL1B strongly decreased *FRZB* and *DKK1* mRNA levels, which may account for IL1B's activating effects on canonical Wnt-signaling. Interestingly, our data demonstrated that both BMP- and Wnt-signaling up regulated the expression of each other's antagonists in a feedback loop.

Together, the current study provides insight in the transcriptional regulation of *GREM1*, *FRZB* and *DKK1* by conditions that are linked with the development and progression of osteoarthritis. Furthermore, we show that BMP and Wnt signaling are linked in a negative feedback loop effectively controlling the balance of BMP and Wnt activity, which is essential in articular cartilage homeostasis. As the mRNA expression of *GREM1*, *FRZB* and *DKK1* inversely correlated with hypertrophic differentiation and osteoarthritis, our data provides a deeper understanding of this pathology.

6.1 Introduction

Osteoarthritis is the main form of arthritis and the leading cause of mobility associated disability [1]. A growing body of evidence suggests that hypertrophic differentiation of articular chondrocytes underlies the pathogenesis of osteoarthritis, at least in a subset of patients. Healthy articular cartilage is largely resistant to hypertrophic differentiation. In recent years many factors that are able to influence, or correlate with, the development of osteoarthritis have been revealed. These include, but are not limited to, bone morphogenetic proteins (BMPs) [2], canonical wntless-type MMTV integration site family members (Wnts) [3], Hedgehog [4], interleukins [5] and the transcription factors HIF2A [6] and RunX2 [7]. Of these, BMPs [8], Wnt [9], IHH [10], HIF2A [11] and RunX2 [12] have also been identified as pro-hypertrophic factors.

Hypertrophic differentiation is a key characteristic of growth plate cartilage, another form of hyaline cartilage. This process is uncommon in healthy articular cartilage. The growth plate is instrumental in the process of longitudinal bone growth by endochondral ossification. Indeed, many of the aforementioned factors play a prominent role in the regulation of hypertrophic differentiation of growth plate chondrocytes [11,13,14,15]. Additionally, the pace of this process is controlled by the parathyroid hormone related peptide (PTHrP) and IHH negative feedback loop [16].

Regardless of the instigating factor(s), hypertrophic differentiation of chondrocytes induces a catabolic shift. Amongst others, interleukin 1 beta (IL1B) [17] and biomechanical stimulation, such as repetitive impulse loading [18] can also induce a catabolic shift. Additionally, tonicity might play a role in osteoarthritis, as it is significantly lower in osteoarthritic joints and is able to drive the expression of anabolic cartilage genes such as aggrecan (*ACAN*), SRY (sex determining region Y)-box 9 (*SOX9*) and collagen 2 (*COL2A1*) [19,20]. Healthy articular cartilage has an intrinsic mechanism that protects it from undergoing hypertrophic differentiation and subsequent catabolism [21]. Evidence suggests that articular cartilage secretes soluble factors that inhibit chondrocyte hypertrophy. This is based on the observation that articular cartilage conditioned medium is able to inhibit hypertrophic differentiation of growth plate cartilage or chondrogenically differentiated mesenchymal stromal cells [22,23]. Recently, we have identified the BMP and Wnt antagonists GREM1, FRZB and DKK1 as prime candidates for these articular cartilage secreted factors that inhibit chondrocyte hypertrophy [Chapter 4]. Moreover, we have demonstrated that the mRNA levels of these factors inversely correlated with osteoarthritis and that a SNP in the *GREM1* gene associates with hip-osteoarthritis. Based on these observations, we hypothesized that factors implicated in the development or progression of osteoarthritis are likely candidates for the regulation of *GREM1*, *FRZB* and *DKK1* mRNA expression in articular chondrocytes.

In this study, we have investigated the effect of important biochemical and biophysical stimuli, which have been implicated in hypertrophic differentiation of chondrocytes or in the development of osteoarthritis, to probe the transcriptional regulation of *GREM1*, *FRZB* and *DKK1* in articular chondrocytes.

6.2 Materials and methods

6.2.1 Chondrocyte isolation and culture

The use of human material was approved by a local medical ethical committee. After informed consent was obtained, human articular cartilage was obtained from macroscopically healthy looking areas of osteoarthritic femoral condyles from patients undergoing total knee replacement. Bovine cartilage was obtained from a local abattoir. Chondrocytes were isolated by cutting the cartilage tissue into small pieces and incubating these pieces in Dulbecco's modified Eagle's medium (Gibco) (DMEM) containing 0.2 % collagenase type II (Worthington) at 37°C for 8 hours. The isolated chondrocytes were subsequently washed, centrifuged and resuspended in DMEM (Gibco) containing 10 % heat inactivated fetal bovine serum (Biowhittaker), 0.01 M MEM nonessential amino acids (Gibco), 0.04 mM L-proline (Sigma), 0.2 mM ascorbic acid (Sigma) and 1 % Penicillin/Streptomycin (Gibco). Isolated Chondrocytes were seeded at 3000 per cm², cultured in a humid atmosphere with 5 % CO₂, passaged upon confluence using trypsin (Invitrogen) and had their medium refreshed thrice a week.

6.2.2 Oxygen levels

Freshly isolated human chondrocytes were seeded at 2,500 per cm² and cultured under conventional normoxic culture conditions (21 % Oxygen) or under hypoxic culture conditions (2.5 % oxygen) using a hypoxia incubator (proox model C21, Biospherix). Cells were culture until 95 % confluence was reached.

6.2.3 Tonicity

Chondrocytes were seeded at 7,500 cells/cm², expanded in culture medium that was adjusted to either 280 mOsm or 380 mOsm with sodium chloride and reseeded at 20,000 cells/cm². After 24 hours, 0 or 500 ng/ml of calcineurin inhibitor FK506 was supplemented to the culture medium. After six additional days the chondrocytes were lysed for gene expression analysis.

6.2.4 Mechanical stimulation

A medium suspension of passage two human chondrocytes was mixed in a 1:1 ratio with liquefied ultrapure agarose (Invitrogen) and loaded into a stainless steel bioreactor to create four 70 μ L constructs of two percent agarose containing 10×10^6 cells per ml. The insert, loaded with four constructs, was installed in a custom build previously described compression culture bioreactor. Using a custom designed compression plate, two out of 4 constructs were mechanically loaded with 0.5 MPa, while the other two constructs remained unloaded. Compression was applied in a cyclical fashion with a frequency of 0.33 Hz with a loading phase of 50 %. This loading was applied either without interruption (constant loading) or was followed every hour of

mechanical stimulation by an hour in which no compression was applied (intermittent loading). All samples were cultured for 48 hours.

6.2.5 Recombinant protein and compound stimulation

All cell types were seeded at 5,000 cells per cm^2 , grown to 95 % confluence and subsequently exposed to a single dose of recombinant proteins. In all experiments primary human or bovine chondrocytes, human MSCs and the cell lines MG63 and Saos-2 were used at passage 2. Cells received no medium refreshment after stimulation had occurred unless otherwise stated and were cultured up to 96 hours. Human chondrocytes were exposed to 4, 20, 100 or 200 ng/ml of recombinant human BMP2, 100 ng/ml of recombinant human WNT3A, 100 ng/ml of recombinant human DKK1, 3, 10 or 30 nM of the GSK3 β inhibitor GIN [24], 0.3, 1 or 3 μM of canonical Wnt inhibitor PKF115-584 [25], 10 or 100 ng/ml of recombinant human IL1B, 10 μM of the hedgehog signaling blocker cyclopamine, 2.5 $\mu\text{g}/\text{ml}$ of recombinant IHH or 5×10^{-7} M of recombinant human PTHrP. Passage two human and bovine chondrocytes, passage two human MSCs, MG63 and Saos-2 were stimulated with 10 nM of GIN. All recombinant proteins and compounds were purchased from R&D systems unless stated otherwise.

6.2.6 Quantitative real-time reverse transcriptase-polymerase chain reaction (qRT-PCR)

At designated time points, cells were washed with PBS and lysed using trizol reagent (Invitrogen). Total RNA was isolated using the Nucleospin RNA II kit (Bioke) according to manufacturer's instructions. RNA yields were measured using the Nanodrop 2000 (ND-1000 Spectrophotometer, Isogen LifeScience). Subsequently, cDNA was synthesized using the iScript Kit (BioRad) in accordance with the manufacturer's instructions. Expression levels of individual genes were analyzed using quantitative PCR by amplifying 20 ng cDNA using Sensimix SYBR (Bioline) on a MyIQ single color Real-time PCR detection system (BioRad) and analyzed using iQtm5 optical system software (Biorad). Amplifications were run under the following conditions: initial denaturation for 10 minutes at 95°C, then cycled 45 times at 95°C for 15 seconds, 60°C for 15 seconds and 72°C for 15 seconds and was followed by a melting curve. Gene expression is depicted as the relative fold change between treated samples and untreated controls and is normalized to 0 hours post-treatment unless stated otherwise. Primers sequences are available upon request.

6.2.7 Cell viability

Passage two human chondrocytes were seeded at 3,000 cm^2 . Upon reaching 95 percent confluence the chondrocytes were treated with 3, 10, 30 nM of GIN, 0.3, 1, 3 μM of PKF115-584, 100 ng/ml DKK1 or 100 ng/ml WNT3A. After 48 hours cell's total metabolic activity was measured using Alamar blue (Invitrogen) according to manufacturer's protocol.

6.2.8 Statistical analysis

Statistical differences between experimental treatments were analyzed using one-way ANOVA. Each group consisted of three different donors, each measured at least in triplicate unless specifically stated otherwise. Statistical significance was set to a $P < 0.05$ and has been indicated with an asterisk (*).

6.3 Results

6.3.1 BMP2 enhances transcription of Wnt antagonist *FRZB* and *DKK1*

Human chondrocytes were stimulated with a single pulse of BMP2 for up to 48 hours to investigate its effect on *GREM1*, *FRZB* and *DKK1* mRNA levels. Functionality of the recombinant protein was demonstrated by a dose dependent induction of the BMP target gene *ID1*. *GREM1* mRNA levels remained unaltered as compared to untreated chondrocytes after 48 hours. However, the expression of the Wnt-antagonists *FRZB* and *DKK1* were significantly up regulated in a dose dependent manner (figure 6.1). This suggested that BMPs were able to induce inhibition of canonical Wnt-signalling in a dose dependent manner. Indeed, the Wnt target gene *AXIN2* was down regulated in a dose dependent manner after BMP2 treatment.

6

6.3.2 Canonical Wnt-signaling down regulates *GREM1*, *FRZB* and *DKK1* expression

Chondrocytes were cultured in the presence or absence of either 100 ng/ml of recombinant WNT3A, or a dose range of the GSK3 β inhibitor GIN, which activates canonical Wnt-signaling. None of the conditions showed any signs of cytotoxicity as determined by phenotypical appearance and metabolic activity of the cells (figure 6.2). Both WNT3A and GIN up regulated *AXIN2* mRNA expression 48 hours after stimulation dose dependently (figure 6.3A).

Chondrocytes were then cultured in the presence or absence of 100 ng/ml of WNT3A or 10 nM of GIN up to 96 hours. Both GIN and WNT3A induced canonical Wnt signaling evidenced by an increase in *AXIN2* mRNA expression. The effect was first detected after six hours and peaked between 24 to 48 hours post stimulation (figure 6.3B). *FRZB* and *DKK1* mRNA levels started to decrease 48 hours after stimulation and were significantly lower after 72 and 96 hours compared to untreated samples. This suggested that activation of Wnt signaling resulted in the down regulation of Wnt antagonists (figure 6.3C and 6.3D). Activation of canonical Wnt signaling transiently decreased *GREM1* mRNA expression with lowest levels of mRNA expression 24 hours after treatment after which the expression levels gradually returned to control (figure 6.3E).

Additionally, we investigated the effects of enhanced canonical Wnt-signaling on the mRNA levels of *CHRD* and *CHRD2*, two BMP-antagonists which have been suggested to play an inhibitory role in hypertrophic differentiation of chondrocytes

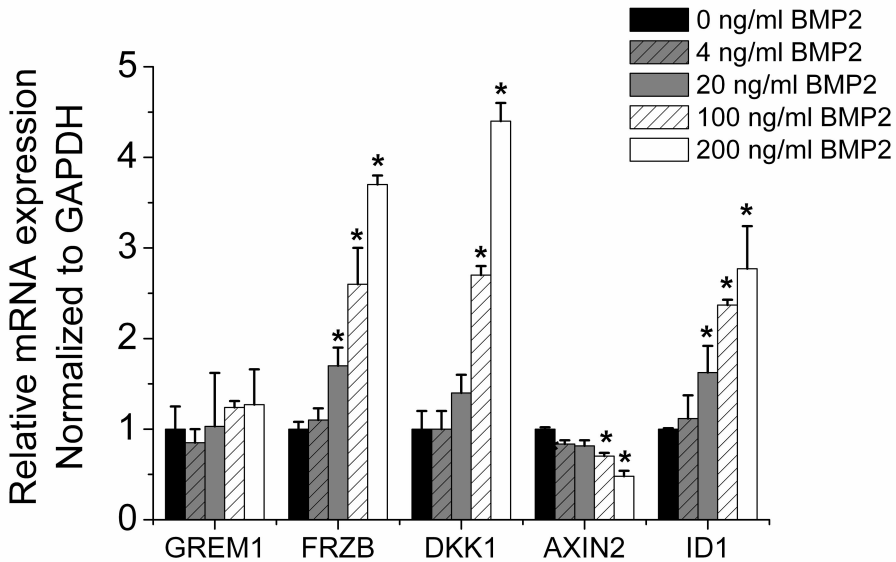


Figure 6.1: Effects of BMP signaling on the mRNA expression of *GREM1*, *FRZB* and *DKK1*. Chondrocytes were stimulated for 48 hours with different concentrations of BMP2 ranging from 0 to 200 ng/ml. Effects on gene expression of *GREM1*, *FRZB* and *DKK1*, *AXIN2* and *ID1* were analyzed using qPCR. Data is expressed as fold change relative to control and represents the mean of 3 donors +/- SEM. * = $P < 0.05$ compared to 0 ng/ml BMP2.

[26,27]. Activation of canonical Wnt-signaling reduced *CHRD* and *CHRD2* mRNA levels with a maximal effect after 72 hours (figure 6.4A and 6.4B). This suggested that activation of canonical Wnt signaling might be able to influence BMP signaling by decreasing the expression of BMP antagonists. Indeed, mRNA levels of the established BMP target gene *ID1* increased upon stimulation of canonical Wnt signaling. This increase was preceded by a decrease in BMP antagonists' gene transcription (figure 6.3F).

6.3.3 Canonical Wnt-signaling regulates *GREM1*, *FRZB* and *DKK1* mRNA levels in bovine chondrocytes, MG63, SAOS2, and MSCs

As activation of canonical Wnt is correlated with a catabolic response in cartilage, it is paramount for joint homeostasis that Wnt-signaling is tightly controlled. Typically, activation of critical pathways is accompanied by subsequent activation of negative

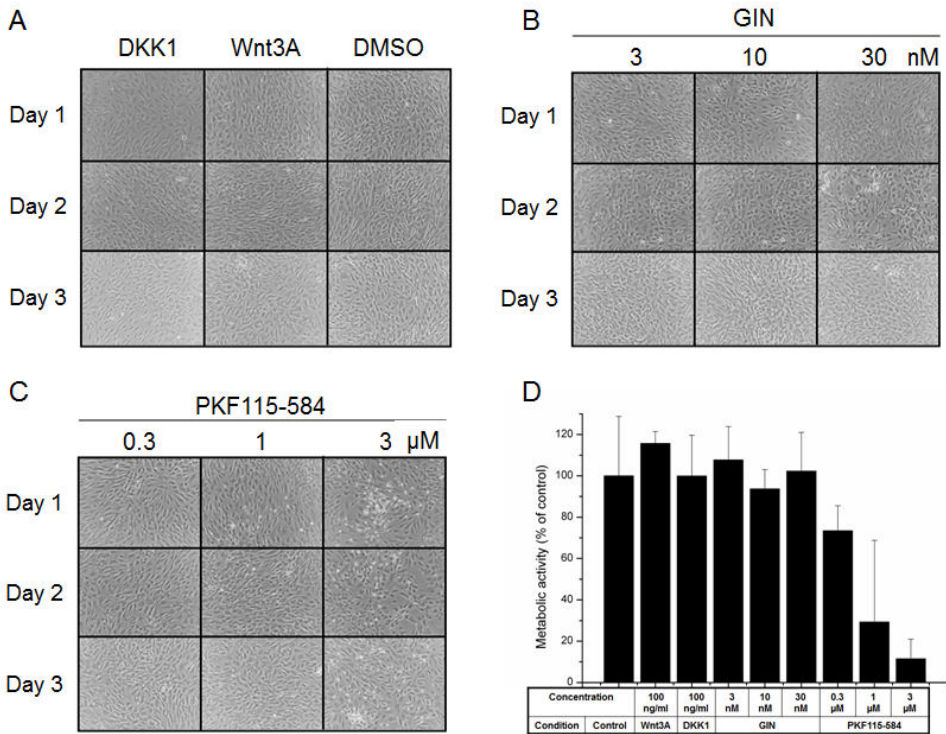


Figure 6.2: Cytotoxicity was phenotypically investigated by assessing chondrocyte morphology. Cells were exposed to DMSO, 100 ng/ml of WNT3A, and 100 ng/ml of DKK1 (A), a concentration range of GIN (B) and a concentration range of PKF115-584 (C). A representative picture of each condition over time is shown. To further investigate cytotoxicity, the metabolic activity of chondrocytes exposed to the different conditions was determined using Alamar Blue quantification. Data represent the mean of 3 donors \pm SEM.

feedback loops reducing pathway activity. Surprisingly, activation of canonical Wnt-signaling in primary human chondrocytes resulted in decreased *FRZB* and *DKK1* mRNA levels (Fig. 6.3C and 6.3D). We therefore tested whether this down regulation was restricted to articular chondrocytes or was a general response across different cell types. Bovine chondrocytes, MG63s, SAOS-2 and MSCs were exposed for 48 hours to 10 nM of GIN. Comparable to human chondrocytes, bovine chondrocytes down regulated *FRZB* and *DKK1* mRNA levels after activation of canonical Wnt-signaling. In contrast, MG63 and SAOS-2 did not respond to GIN with changes in expression of *FRZB* and *GREM1*, respectively (figure 6.5). Like chondrocytes, human bone marrow derived MSCs demonstrated a decrease in *FRZB* and *DKK1* mRNA levels upon stimulation of canonical Wnt-signaling. In contrast to human chondrocytes, *GREM1* mRNA expression was up regulated by activating Wnt-signaling. Together

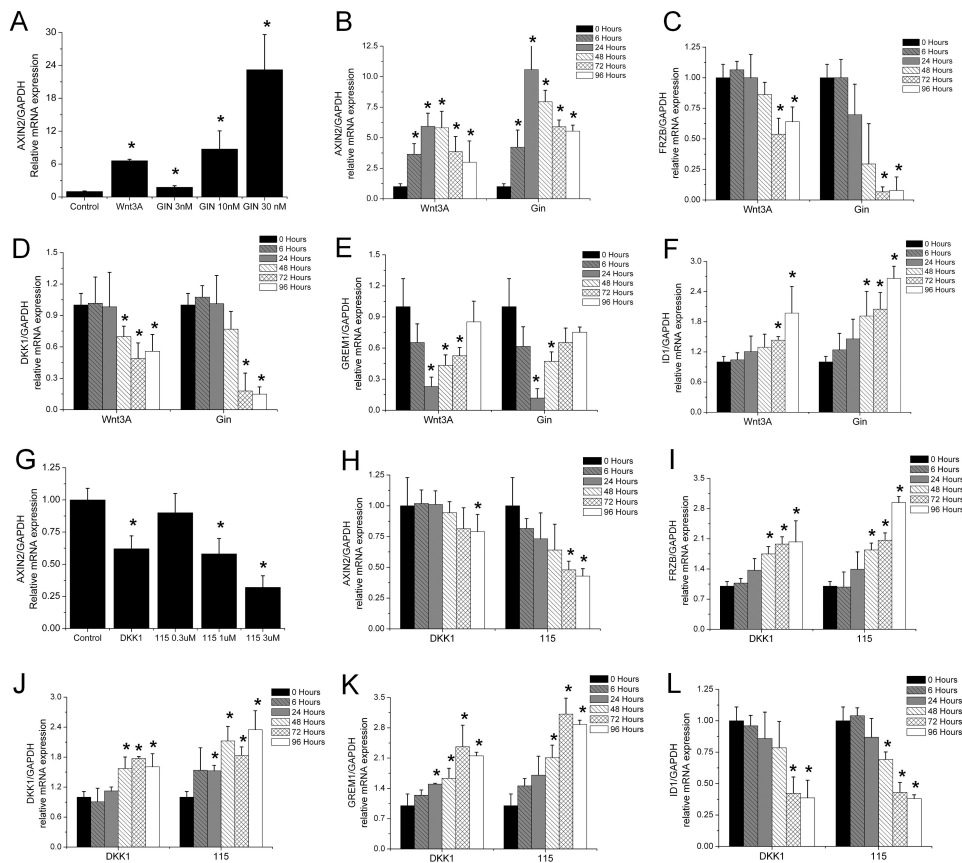


Figure 6.3: Effect of canonical Wnt signaling on the mRNA expression of *GREM1*, *FRZB* and *DKK1*. (A) Primary human chondrocytes were exposed to 100 ng/ml WNT3A or 3 different concentrations of GIN. After 48 hours *AXIN2* mRNA expression was analyzed by qPCR. (B-F) Chondrocytes were exposed to a single dose of 10 nM of GIN or 100 ng/ml of WNT3A. At indicated time points, mRNA expression was analyzed by qPCR of *AXIN2* (B), *FRZB* (C), *DKK1* (D), *GREM1* (E) and *ID1* (F). (G) Primary human chondrocytes were exposed to 100 ng/ml WNT3A or 3 different concentrations of PKF115-584 (115). After 48 hours *AXIN2* mRNA expression was analyzed by qPCR. (H-L) Primary human chondrocytes were exposed to 1 μ M of PKF115-584 or 100 ng/ml DKK1. At indicated time points gene expression was analyzed by qPCR of *AXIN2* (H), *FRZB* (I), *DKK1* (J), *GREM1* (K) and *ID1* (L). Data is expressed as fold change relative to control and represents the mean of 3 donors \pm SEM. * = $P < 0.05$ as compared to unstimulated cells (A, G) or 0 hours of stimulation (B-F, H-L).

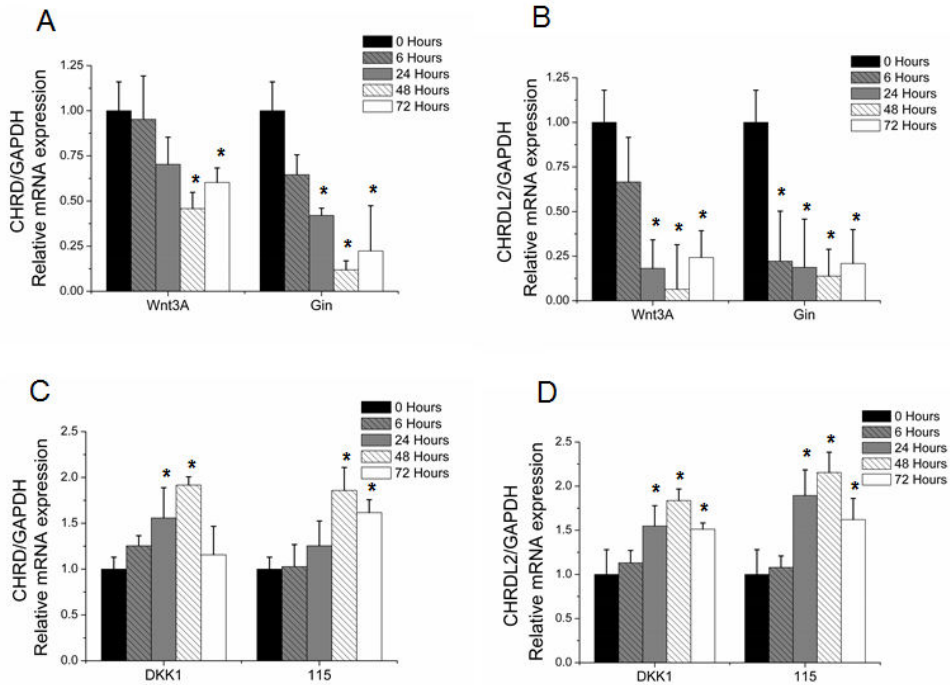


Figure 6.4: Wnt signaling decreases Chordin and Chordin-like 2 mRNA expression in primary human chondrocytes. Gene expression was measured by qPCR. Chondrocytes were exposed to a single dose of 10 nM of GIN, 100 ng/ml of WNT3A (A-B), 1 μ M of PKF115-584 or 100 ng/ml of DKK1 (C-D) for up to 72 hours and analyzed for the gene transcription of *CHRD* (A, C) and *CHRDL2* (B, D). Data represent the mean of 3 donors \pm SEM. * = $P < 0.05$ as compared to unstimulated cells

this suggested that the response to canonical Wnt-signaling stimulation with regards to the mRNA expression levels of Wnt and BMP antagonists is cell type dependent. The transcriptional regulation of *GREM1*, *FRZB* and *DKK1* upon activating canonical Wnt-signaling appeared to be conserved between human and bovine articular chondrocytes.

6.3.4 Inhibition of Canonical Wnt signaling induces mRNA expression of *GREM1*, *FRZB* and *DKK1*

We next investigated the effect of inhibiting canonical Wnt signaling on the mRNA expression levels of *GREM1*, *FRZB* and *DKK1* using 100 ng/ml of the Wnt-antagonist *DKK1* or 0.3, 1 or 3 μ M of the canonical Wnt inhibitor PKF115-584. Treatment of human chondrocytes for 48 hours with either Wnt-inhibitor significantly reduced

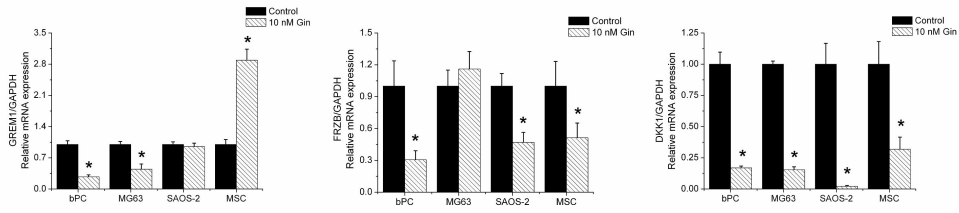


Figure 6.5: Effects of activation of canonical Wnt signaling on the mRNA expression of *GREM1*, *FRZB* and *DKK1* on other cells than human chondrocytes. A single dose of 10 nM of GIN was added to the culture media of bovine chondrocytes, the MG63 cell line, the SAOS-2 cell line and human bone marrow-derived mesenchymal stem cells. After 48 hours the gene transcription levels of *GREM1* (A), *FRZB* (B) and *DKK1* (C) were analyzed. Data represent the mean of 3 independent experiments (bovine chondrocytes, MG63 and SAOS-2) or 2 donors (MSCs) +/- SEM. * = $P < 0.05$ as compared to control.

AXIN2 mRNA levels, except for 0.3 μM of PKF115-584 (figure 6.3G). Treatment with 1 or 3 μM of PKF115-584 reduced the chondrocyte's metabolic activity and chondrocytes treated with 3 μM of PKF115-584 showed phenotypical signs of stress (figure 6.2). Therefore, a concentration of 1 μM of PKF115-584 was selected for further experimentation.

Treatment of chondrocytes up to 96 hours with a single dose of 100 ng/ml of *DKK1* or 1 μM of PKF115-584 resulted in a progressive decrease in *AXIN2* mRNA levels, which became statistically significant between 72 and 96 hours post treatment (figure 6.3H). In contrast, *FRZB* and *DKK1* mRNA levels steadily increased over time, which became significant between 24 and 48 hours post exposure (figure 6.3I and 6.3J). Treatment with *DKK1* or PKF115-584 increased *GREM1* mRNA levels and this coincided with a subsequent decrease in *ID1* mRNA levels (figure 6.3K and 6.3L). Taken together this data suggested that in human chondrocytes the *GREM1*, *FRZB* and *DKK1* mRNA levels were inversely related to the activity of canonical Wnt-signaling.

6.3.5 Effects of PTHrP, IHH and cyclopamine on *GREM1*, *FRZB* and *DKK1* mRNA expression

PTHrP and IHH expression in articular cartilage is correlated with osteoarthritis [4,28]. In addition, PTHrP and IHH critically regulate the pace of hypertrophic differentiation in growth plate cartilage in a negative feedback loop. As *GREM1*, *FRZB* and *DKK1* were able to inhibit hypertrophic differentiation in articular cartilage and mitigated longitudinal bone growth in explanted mouse fetal long bones [Chapter 4], we investigated whether PTHrP and IHH were able to influence their mRNA expression. Chondrocytes were cultured up to 96 hours in the presence or absence of PTHrP, IHH and the hedgehog signaling blocker cyclopamine. *GREM1* mRNA

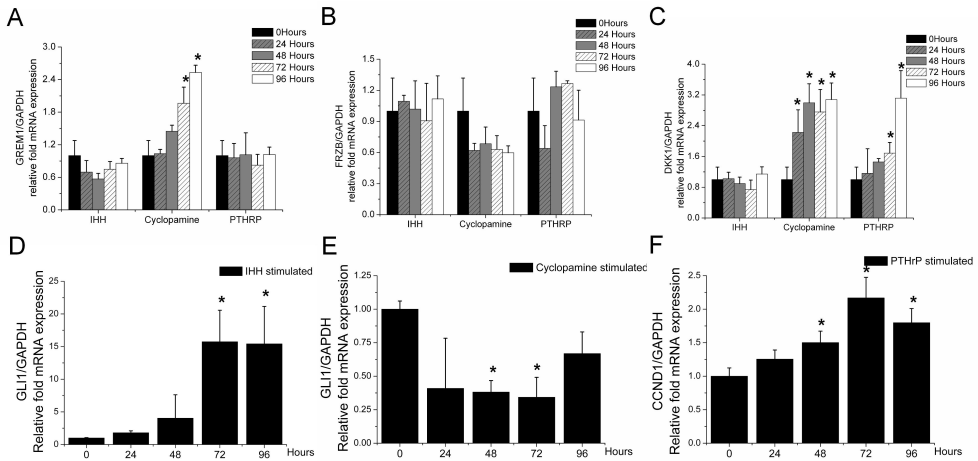


Figure 6.6: Effects of IHH or PTHrP mediated signaling on the mRNA expression of *GREM1*, *FRZB* and *DKK1*. Chondrocytes were exposed to 2.5 $\mu\text{g}/\text{ml}$ of IHH, 10 μM of cyclopamine, or 5×10^{-7} M of PTHrP for up to 96 hours. At the indicated time points mRNA expression was analyzed by qPCR of *GREM1* (A), *FRZB* (B), *DKK1* (C), *GLI1* (D-E) and *CCND1* (F). Data is expressed as fold change relative to control and represent the mean of 3 donors \pm SEM. * = $P < 0.05$ compared to unstimulated cells.

6

expression remained unchanged when stimulated with PTHrP, tended to transiently decrease after stimulation with IHH and was significantly increased by cyclopamine after 72 and 96 hours (figure 6.6A). PTHrP nor IHH affected *FRZB* mRNA levels. Cyclopamine tended to decrease *FRZB* mRNA expression but this did not reach significance (figure 6.6B). In contrast, *DKK1* mRNA expression was significantly increased by cyclopamine and PTHrP treatment from 24 and 72 hours, respectively but not by IHH (figures 6.6C). The expression of established hedgehog and PTHrP target genes was used to verify the biological activity of each stimulus. *GLI1* mRNA levels increased in the presence of IHH (figure 6.6D) and decreased in the presence of cyclopamine (figure 6.6E). *CCND1* mRNA levels increased in the presence of PTHrP (figure 6.6F). Taken together, this suggested that inhibition, but not activation, of IHH up regulated *GREM1* and *DKK1* mRNA levels. PTHrP only regulated *DKK1* mRNA levels.

6.3.6 Effects of IL1B stimulation on *GREM1*, *FRZB* and *DKK1* mRNA expression

Local injection of IL1B into mouse knee joints results in an osteoarthritis-like phenotype [29]. We previously demonstrated that degenerating osteoarthritic cartilage coincided with decreased *GREM1*, *FRZB* and *DKK1* mRNA levels. Therefore, we inves-

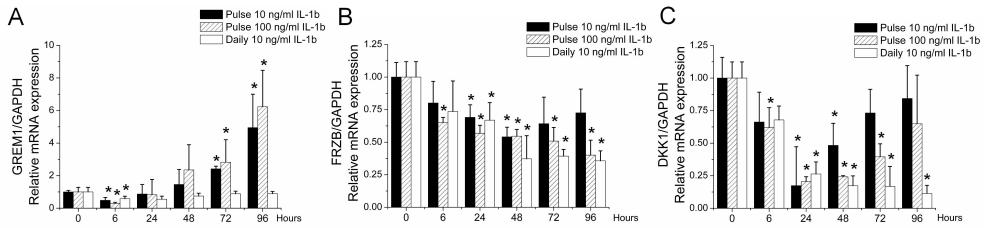


Figure 6.7: Effects of IL1B mediated signaling on the mRNA expression of *GREM1*, *FRZB* and *DKK1*. Chondrocytes received a single dose of 10 or 100 ng/ml of IL1B, or a daily medium refreshment containing 10 ng/ml of IL1B. Chondrocytes were stimulated up to 96 hours and at the indicated time points mRNA expression was analyzed by qPCR of *GREM1* (A), *FRZB* (B), and *DKK1* (C). Data is expressed as fold change relative to control and represent the mean of 3 donors +/- SEM. * = $P < 0.05$ as compared to unstimulated cells.

tigated whether stimulation of human chondrocytes with IL1B would affect *GREM1*, *FRZB* and *DKK1* mRNA levels. Chondrocytes were stimulated with either a single dose of 10 or 100 ng/ml of IL1B or with a daily repeated dose of 10 ng/ml of IL1B. Upon exposure to a single dose of IL1B *GREM1* mRNA levels decreased at 6 hours followed by a steady increase in mRNA expression, which became significantly higher than untreated samples after 72 hours. Interestingly, repeated treatment with of IL1B decreased *GREM1* mRNA expression after 6 hours which returned to base line after 24 hours (figure 6.7A). *FRZB* mRNA levels were dose-dependently down regulated after exposure to IL1B (figure 6.7B). Daily treatment with 10 ng/ml was as effective as a pulse treatment with 100 ng/ml. *DKK1* mRNA levels decreased after stimulation with IL1B. This down regulation was transient with a single dose, but persistent with a daily dose of IL1B (figure 6.7C).

6.3.7 Effects of physiological factors on *GREM1*, *FRZB* and *DKK1* mRNA transcription

Many physiological factors influence the homeostasis of articular cartilage. To determine if such stimuli have an effect on the mRNA expression levels of *GREM1*, *FRZB* and *DKK1*, chondrocytes were exposed to mechanical compression, oxygen tension and tonicity.

Chondrocytes encapsulated in three dimensional hydrogels were cultured in the presence or absence of cyclic loading of the construct with 0.5 MPa with a frequency of 0.33 Hz, which was either continuous or intermittently applied over a culture period of 48 hours. Both continuous and intermittent loading significantly elevated *GREM1* and *FRZB* mRNA levels compared to unloaded chondrocytes. *DKK1* mRNA levels were only significantly increased after intermittent loading of the construct (figure 6.8A). Interestingly, intermittent loading was more effective in up regulating *GREM1*,

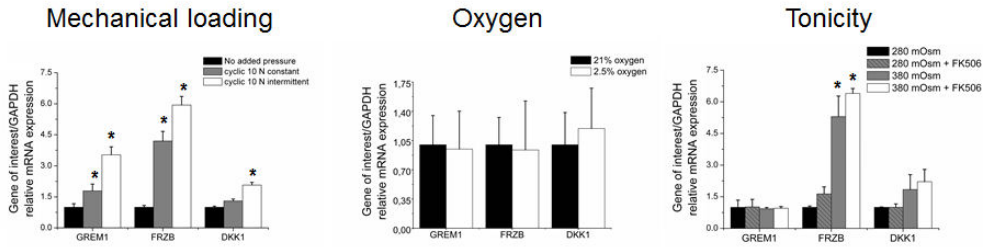


Figure 6.8: Effects of mechanical loading, oxygen level and medium tonicity mediated signaling on the mRNA expression of *GREM1*, *FRZB* and *DKK1*. Chondrocytes encapsulated in a hydrogel received no, intermittent or constant cyclical mechanical loading of 0.5 MPa with a frequency of 0.33 Hz and a loading phase of 50 % (A). Chondrocytes were exposed to normoxic or hypoxic culture conditions (B), or cultured in media with different tonicity with or without FK506 (C). All conditions were analyzed for the mRNA expression of *GREM1*, *FRZB* and *DKK1* by qPCR after 48 hours. Data is expressed as fold change relative to control and represent the mean of 3 donors \pm SEM. * = $P < 0.05$ as compared to unloaded samples or samples containing medium of 280 mOsm.

6

FRZB and *DKK1* mRNA expression than continuous loading.

Most of the articular cartilage persists in a continuous state of hypoxia, which allows for the stabilization of hypoxia-inducible factors that are able to influence cartilage homeostasis [30]. Therefore, chondrocytes were cultured under hypoxic or normoxic conditions by oxygenating the cultures with 2.5 percent or 21 percent oxygen respectively. No detectable changes in *GREM1*, *FRZB* and *DKK1* mRNA levels were observed between normoxic and hypoxic culture conditions (figure 6.8B).

Osteoarthritis is associated with a decrease in tonicity of the synovial fluid and cartilage [20]. Therefore, we investigated the effect of tonicity on the mRNA levels of *GREM1*, *FRZB* and *DKK1*. Tonicity did not detectably affect *GREM1* mRNA levels (figure 6.8C). In contrast, tonicity tended to increase *DKK1* mRNA levels and significantly increased *FRZB* mRNA levels. This effect was NFAT-independent as FK506, which indirectly inhibits NFAT nuclear translocation, had no significant effect on *GREM1*, *FRZB* and *DKK1* mRNA levels.

6.4 Discussion

Recently we have reported that *GREM1*, *FRZB* and *DKK1* are enriched in articular cartilage relative to other hyaline cartilage types and are potent inhibitors of hypertrophic differentiation and endochondral ossification [Chapter 4]. Moreover, the mRNA levels of *GREM1*, *FRZB* and *DKK1* proved to be inversely correlated with the level of cartilage degeneration. In the present study, we report on the effects of biochemical and biophysical stimuli, associated with or involved in hypertrophic dif-

ferentiation of chondrocytes in osteoarthritis, on the mRNA expressions of *GREM1*, *FRZB* and *DKK1*.

GREM1, FRZB and DKK1 are all three secreted soluble antagonists. FRZB and DKK1 are Wnt antagonists and GREM1 is a BMP antagonist. It has been demonstrated that GREM1 is also able to inhibit Wnt signaling via an unknown indirect mechanism [31,32]. It has been reported that BMP signaling is able to repress Wnt signaling [33]. Conversely, Wnt signaling is also able to repress BMP signaling [34]. It is well known that activation of Wnt signaling inhibits fibroblastic growth factor-dependent BMP repression [35]. More recently it was suggested that increased Wnt signaling corresponded with decreased expression of BMP antagonists [36]. Indeed, increased canonical Wnt signaling resulted in increased BMP/SMAD signaling [37]. Although the crosstalk between BMP- and Wnt signaling is suggested to involve SMAD4 and MAPK p38, the main mechanism has remained largely unknown [38,39,40].

Understanding the crosstalk between TGF β /BMP- and Wnt-signaling is desired as it has been reported to play important roles in the formation of several tissues including bone, cartilage and intestinal epithelium [37,38,39,41]. While in these studies the interplay is mainly characterized by activation of each other's ligands, in our study we have focused on antagonists. We provide evidence that these antagonists may play a central role in the cross talk as well. In particular, we demonstrated that in chondrocytes this crosstalk is mediated, at least partially, via reciprocal transcriptional control of each other's antagonists. Consequently, our data suggest that the crosstalk between TGF/BMP- and Wnt-signaling might act as a feedback loop that balances the activity of both pathways (figure 6.9A). Specifically, activation of Wnt signaling down regulates the expression of genes encoding BMP antagonists and is associated with the up regulation of BMP signaling. In turn, activation of BMP signaling results in increased expression of genes encoding Wnt antagonists, which is associated with decreased Wnt signaling. Furthermore, since we have only studied the cross talk in a model for cartilage homeostasis, it might be tantalizing to speculate whether the Wnt and BMP antagonists play an important role in maintaining homeostasis of other organs in which balanced Wnt and BMP signaling is crucial.

Stringent control over the Wnt pathway's activity is paramount for articular cartilage homeostasis as both exacerbated and repressed signaling results in an osteoarthritis-like phenotype, at least in animal models [42,43]. Perturbation of feedback loops that control the activity of Wnt signaling would therefore allow for the disturbance of the natural homeostasis. Factors associated with disturbed joint homeostasis include amongst others IL1 β , abnormal mechanical loading and hypotonicity. Although evidence suggests that short exposure to IL1 β results in minor joint inflammation without permanent joint destruction only, continuous exposure to IL1 β results in joint degradation which bears striking resemblance with osteoarthritis [5,29]. It has been shown that IL1 β activates Wnt signaling via an unknown mechanism [44]. Excessive mechanical loading of the joint induces the expression of IL1 β and catabolic proteins such as matrix metalloproteinases and aggrecanases [45]. Interestingly, reduced joint loading, by e.g. immobilization, also results in the up regulation of matrix metalloproteinases and aggrecanases [46]. In contrast, loading within the physiological range

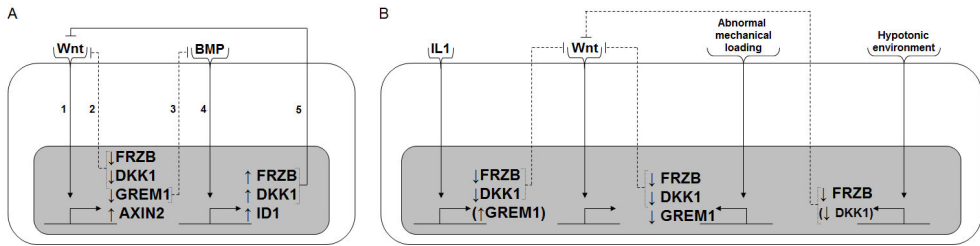


Figure 6.9: Working-model of feedback loop between Wnt- and BMP-signaling and its perturbation by factors correlated with osteoarthritis. Wnt- and BMP-signaling reciprocally regulate the transcription of each other antagonists (A). Exposure of Wnt agonists leads to activation of Wnt signaling [1]. This activation results in the down regulation of Wnt antagonists e.g. *FRZB* and *DKK1* leading to less inhibition of Wnt signaling [2]. Additionally, BMP antagonists e.g. *GREM1* are down regulated, leading to less inhibition of BMP signaling [3]. Stronger BMP signaling results in the up regulation of Wnt antagonists [4] establishing a negative feedback mitigating Wnt-signaling [5]. This feedback loop allows for tight control of both BMP and Wnt signaling in articular cartilage contributing to homeostasis. Established factors that influence cartilage homeostasis also perturb this feedback loop (B). IL1B, abnormal mechanical loading and tonicity all decrease the mRNA levels of Wnt and BMP antagonists possibly resulting in a reset of the feedback loop, and contributing to the loss of cartilage homeostasis. PTHrP and IHH have not been incorporated into the model as they only demonstrated marginal effects on *GREM1*, *FRZB* and *DKK1* mRNA levels.

inhibits the expression of catabolic genes and showed a chondroprotective effect in the presence of IL1B [47]. Additionally, mechanical loading is also able to regulate the activity of Wnt signaling via an unknown mechanism [48]. Tonicity is also able to regulate the expression of ILs [49]. However, its effect on Wnt signaling has remained largely uninvestigated. In the present study, we present data that imply that IL1B, mechanical loading and tonicity regulate the mRNA expression of *GREM1*, *FRZB* and *DKK1* (Figure 6.9B). Specifically, IL1, mechanical unloading and hypotonicity result in decreased expression of genes encoding Wnt antagonists.

Our data suggests that these factors might be able to perturb the balance between BMP- and Wnt-signaling by influencing the expression of both Wnt- and BMP antagonists in a manner that cannot be sequestered via their regular feedback loops. Consequently, it is tempting to speculate that these factors may generate an osteoarthritic-like phenotype, at least partially, via their ability to disturb this balance by deregulating the expression of Wnt and BMP antagonists. Although additional research is needed to sustain such a claim, recent evidence demonstrated that the addition of Wnt- and BMP antagonist sclerostin was able to prevent IL1 induced osteoarthritis-like phenotype [50]. During development PTHrP and IHH regulate the pace of hypertrophic differentiation in the growth plate by interacting with Wnt/ β -catenin signaling and with BMP/GDF5 signaling [51]. Moreover, PTHrP, IHH, BMP

and GDF5 have all been implicated in the development of osteoarthritis. However, in contrast to direct stimulation of the Wnt- and BMP signaling, the addition of the used concentrations of PTHrP and IHH to articular chondrocytes only demonstrated marginal regulation on *GREM1*, *FRZB* and *DKK1*. It cannot be excluded that this might, at least in part, be due to the concentrations of proteins used in the experiments or the fact that an *in vitro* cultured mono-layer of chondrocyte of might respond differently to identical stimuli than native chondrocytes.

Hypoxia inducible factors are both involved in the generation and the degeneration of cartilage as they are indispensable for chondrogenic differentiation during limb bud formation and are associated with the development of osteoarthritis. However, in the current study we did not detect any effect of the oxygen levels on the gene expression of *GREM1*, *FRZB* and *DKK1*. Nonetheless, HIFs interact further downstream with the Wnt signaling by forming complexes with β -catenin.

Although we previously have identified *GREM1*, *FRZB* and *DKK1* as key regulators of articular cartilage homeostasis, it is not unlikely that stimulation with BMPs, Wnts, IL1, IHH, PTHrP, oxygen concentrations, different tonicities and mechanical loading also influences the expression of other Wnt- and BMP antagonists. Moreover, it might also influence the expression of Wnt- and BMP agonists. Regardless, aberrant regulation of *GREM1*, *FRZB* and *DKK1* is inversely correlated with the level of degeneration of osteoarthritic cartilage and the current study grants insight in the transcriptional regulation of *GREM1*, *FRZB* and *DKK1* by regulators of chondrocyte hypertrophy. Together, this provides a deeper understanding of chondrocyte behavior, cartilage homeostasis and potentially osteoarthritis.

References

1. (2010) Prevalence of doctor-diagnosed arthritis and arthritis-attributable activity limitation — United States, 2007-2009. *MMWR Morb Mortal Wkly Rep* 59: 1261-1265.
2. Rountree RB, Schoor M, Chen H, Marks ME, Harley V, et al. (2004) BMP receptor signaling is required for postnatal maintenance of articular cartilage. *PLoS Biol* 2: e355.
3. Kawaguchi H (2009) Regulation of osteoarthritis development by Wnt-beta-catenin signaling through the endochondral ossification process. *J Bone Miner Res* 24: 8-11.
4. Lin AC, Seeto BL, Bartoszko JM, Khoury MA, Whetstone H, et al. (2009) Modulating hedgehog signaling can attenuate the severity of osteoarthritis. *Nat Med* 15: 1421-1425.
5. Martel-Pelletier J, Alaaeddine N, Pelletier JP (1999) Cytokines and their role in the pathophysiology of osteoarthritis. *Front Biosci* 4: D694-703.
6. Saito T, Fukai A, Mabuchi A, Ikeda T, Yano F, et al. (2010) Transcriptional regulation of endochondral ossification by HIF-2alpha during skeletal growth and osteoarthritis development. *Nat Med* 16: 678-686.
7. Kamekura S, Kawasaki Y, Hoshi K, Shimoaka T, Chikuda H, et al. (2006) Contribution of runt-related transcription factor 2 to the pathogenesis of osteoarthritis in mice after induction of knee joint instability. *Arthritis Rheum* 54: 2462-2470.
8. Nilsson O, Parker EA, Hegde A, Chau M, Barnes KM, et al. (2007) Gradients in bone morphogenetic protein-related gene expression across the growth plate. *J Endocrinol* 193: 75-84.
9. Wang L, Shao YY, Ballock RT (2007) Thyroid hormone interacts with the Wnt/beta-catenin signaling pathway in the terminal differentiation of growth plate chondrocytes. *J Bone Miner Res* 22: 1988-1995.
10. Minina E, Wenzel HM, Kreschel C, Karp S, Gaffield W, et al. (2001) BMP and Ihh/PTHrP signaling interact to coordinate chondrocyte proliferation and differentiation. *Development* 128: 4523-4534.
11. Stewart AJ, Houston B, Farquharson C (2006) Elevated expression of hypoxia inducible factor-2alpha in terminally differentiating growth plate chondrocytes. *J Cell Physiol* 206: 435-440.
12. Zheng Q, Zhou G, Morello R, Chen Y, Garcia-Rojas X, et al. (2003) Type X collagen gene regulation by Runx2 contributes directly to its hypertrophic chondrocyte-specific expression in vivo. *J Cell Biol* 162: 833-842.
13. Tamamura Y, Otani T, Kanatani N, Koyama E, Kitagaki J, et al. (2005) Developmental regulation of Wnt/beta-catenin signals is required for growth plate assembly, cartilage integrity, and endochondral ossification. *J Biol Chem* 280: 19185-19195.
14. De Luca F, Barnes KM, Uyeda JA, De-Levi S, Abad V, et al. (2001) Regulation of growth plate chondrogenesis by bone morphogenetic protein-2. *Endocrinology* 142: 430-436.
15. Provot S, Zinyk D, Gunes Y, Kathri R, Le Q, et al. (2007) Hif-1alpha regulates differentiation of limb bud mesenchyme and joint development. *J Cell Biol* 177: 451-464.
16. Vortkamp A, Lee K, Lanske B, Segre GV, Kronenberg HM, et al. (1996) Regulation of rate of cartilage differentiation by Indian hedgehog and PTH-related protein. *Science* 273: 613-622.
17. Daheshia M, Yao JQ (2008) The interleukin 1beta pathway in the pathogenesis of osteoarthritis. *J Rheumatol* 35: 2306-2312.
18. Radin EL, Paul IL, Rose RM (1972) Role of mechanical factors in pathogenesis of primary osteoarthritis. *Lancet* 1: 519-522.
19. van der Windt AE, Haak E, Das RH, Kops N, Welting TJ, et al. (2010) Physiological tonicity improves human chondrogenic marker expression through nuclear factor of activated

T-cells 5 in vitro. *Arthritis Res Ther* 12: R100.

20. Shanfield S, Campbell P, Baumgarten M, Bloebaum R, Sarmiento A (1988) Synovial fluid osmolality in osteoarthritis and rheumatoid arthritis. *Clin Orthop Relat Res*: 289-295.

21. Blanke M, Carl HD, Klinger P, Swoboda B, Hennig F, et al. (2009) Transplanted chondrocytes inhibit endochondral ossification within cartilage repair tissue. *Calcif Tissue Int* 85: 421-433.

22. Jikko A, Kato Y, Hiranuma H, Fuchihata H (1999) Inhibition of chondrocyte terminal differentiation and matrix calcification by soluble factors released by articular chondrocytes. *Calcif Tissue Int* 65: 276-279.

23. Fischer J, Dickhut A, Richter W, Rickert M (2010) Articular chondrocytes secrete PTHrP and inhibit hypertrophy of mesenchymal stem cells in coculture during chondrogenesis. *Arthritis Rheum*.

24. Miclea RL, Siebelt M, Finos L, Goeman JJ, Lowik CW, et al. (2011) Inhibition of Gsk3beta in cartilage induces osteoarthritic features through activation of the canonical Wnt signaling pathway. *Osteoarthritis Cartilage* 19: 1363-1372.

25. Lepourcelet M, Chen YN, France DS, Wang H, Crews P, et al. (2004) Small-molecule antagonists of the oncogenic Tcf/beta-catenin protein complex. *Cancer Cell* 5: 91-102.

26. Zhang D, Ferguson CM, O'Keefe RJ, Puzas JE, Rosier RN, et al. (2002) A role for the BMP antagonist chordin in endochondral ossification. *J Bone Miner Res* 17: 293-300.

27. Nakayama N, Han CY, Cam L, Lee JI, Pretorius J, et al. (2004) A novel chordin-like BMP inhibitor, CHL2, expressed preferentially in chondrocytes of developing cartilage and osteoarthritic joint cartilage. *Development* 131: 229-240.

28. Gomez-Barrena E, Sanchez-Pernaute O, Largo R, Calvo E, Esbrit P, et al. (2004) Sequential changes of parathyroid hormone related protein (PTHrP) in articular cartilage during progression of inflammatory and degenerative arthritis. *Ann Rheum Dis* 63: 917-922.

29. van de Loo AA, van den Berg WB (1990) Effects of murine recombinant interleukin 1 on synovial joints in mice: measurement of patellar cartilage metabolism and joint inflammation. *Ann Rheum Dis* 49: 238-245.

30. Lafont JE, Talma S, Hopfgarten C, Murphy CL (2008) Hypoxia promotes the differentiated human articular chondrocyte phenotype through SOX9-dependent and -independent pathways. *J Biol Chem* 283: 4778-4786.

31. Gaggero E, Smerdel-Ramoya A, Zanotti S, Stadmeier L, Durant D, et al. (2007) Conditional deletion of gremlin causes a transient increase in bone formation and bone mass. *J Biol Chem* 282: 31549-31557.

32. Gaggero E, Pereira RC, Jorgetti V, Olson S, Economides AN, et al. (2005) Skeletal overexpression of gremlin impairs bone formation and causes osteopenia. *Endocrinology* 146: 655-665.

33. Minear S, Leucht P, Miller S, Helms JA (2010) rBMP represses Wnt signaling and influences skeletal progenitor cell fate specification during bone repair. *J Bone Miner Res* 25: 1196-1207.

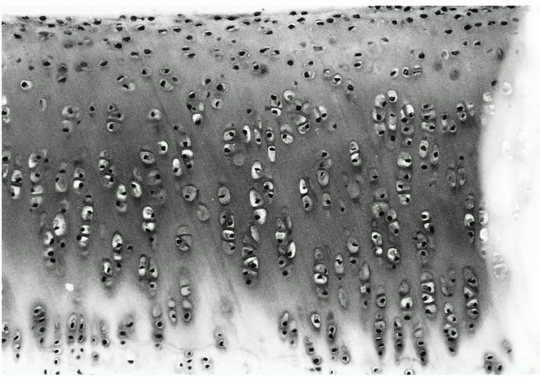
34. He XC, Zhang J, Tong WG, Tawfik O, Ross J, et al. (2004) BMP signaling inhibits intestinal stem cell self-renewal through suppression of Wnt-beta-catenin signaling. *Nat Genet* 36: 1117-1121.

35. Wilson SI, Rydstrom A, Trimborn T, Willert K, Nusse R, et al. (2001) The status of Wnt signalling regulates neural and epidermal fates in the chick embryo. *Nature* 411: 325-330.

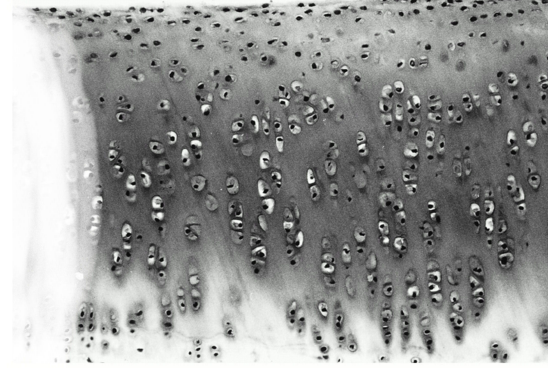
36. Guo X, Wang XF (2009) Signaling cross-talk between TGF-beta/BMP and other pathways. *Cell Res* 19: 71-88.

37. Miclea RL, van der Horst G, Robanus-Maandag EC, Lowik CW, Oostdijk W, et al.

- (2011) Apc bridges Wnt/beta-catenin and BMP signaling during osteoblast differentiation of KS483 cells. *Exp Cell Res* 317: 1411-1421.
38. Li J, Huang X, Xu X, Mayo J, Bringas P, Jr., et al. (2011) SMAD4-mediated WNT signaling controls the fate of cranial neural crest cells during tooth morphogenesis. *Development* 138: 1977-1989.
39. Tuli R, Tuli S, Nandi S, Huang X, Manner PA, et al. (2003) Transforming growth factor-beta-mediated chondrogenesis of human mesenchymal progenitor cells involves N-cadherin and mitogen-activated protein kinase and Wnt signaling cross-talk. *J Biol Chem* 278: 41227-41236.
40. Kamiya N, Kobayashi T, Mochida Y, Yu PB, Yamauchi M, et al. (2010) Wnt inhibitors Dkk1 and Sost are downstream targets of BMP signaling through the type IA receptor (BMPRIA) in osteoblasts. *J Bone Miner Res* 25: 200-210.
41. Kosinski C, Li VS, Chan AS, Zhang J, Ho C, et al. (2007) Gene expression patterns of human colon tops and basal crypts and BMP antagonists as intestinal stem cell niche factors. *Proc Natl Acad Sci U S A* 104: 15418-15423.
42. Zhu M, Tang D, Wu Q, Hao S, Chen M, et al. (2009) Activation of beta-catenin signaling in articular chondrocytes leads to osteoarthritis-like phenotype in adult beta-catenin conditional activation mice. *J Bone Miner Res* 24: 12-21.
43. Zhu M, Chen M, Zuscik M, Wu Q, Wang YJ, et al. (2008) Inhibition of beta-catenin signaling in articular chondrocytes results in articular cartilage destruction. *Arthritis Rheum* 58: 2053-2064.
44. Kaler P, Augenlicht L, Klampfer L (2009) Macrophage-derived IL-1beta stimulates Wnt signaling and growth of colon cancer cells: a crosstalk interrupted by vitamin D3. *Oncogene* 28: 3892-3902.
45. Saxon L, Finch C, Bass S (1999) Sports participation, sports injuries and osteoarthritis: implications for prevention. *Sports Med* 28: 123-135.
46. Haapala J, Arokoski JP, Hyttinen MM, Lammi M, Tammi M, et al. (1999) Remobilization does not fully restore immobilization induced articular cartilage atrophy. *Clin Orthop Relat Res*: 218-229.
47. Madhavan S, Anghelina M, Rath-Deschner B, Wypasek E, John A, et al. (2006) Biomechanical signals exert sustained attenuation of proinflammatory gene induction in articular chondrocytes. *Osteoarthritis Cartilage* 14: 1023-1032.
48. Sen B, Styner M, Xie Z, Case N, Rubin CT, et al. (2009) Mechanical loading regulates NFATc1 and beta-catenin signaling through a GSK3beta control node. *J Biol Chem* 284: 34607-34617.
49. Pan Z, Wang Z, Yang H, Zhang F, Reinach PS (2011) TRPV1 activation is required for hypertonicity-stimulated inflammatory cytokine release in human corneal epithelial cells. *Invest Ophthalmol Vis Sci* 52: 485-493.
50. Chan BY, Fuller ES, Russell AK, Smith SM, Smith MM, et al. (2011) Increased chondrocyte sclerostin may protect against cartilage degradation in osteoarthritis. *Osteoarthritis Cartilage* 19: 874-885.
51. Guo X, Mak KK, Taketo MM, Yang Y (2009) The Wnt/beta-catenin pathway interacts differentially with PTHrP signaling to control chondrocyte hypertrophy and final maturation. *PLoS One* 4: e6067.



7



Chapter 7

Hypoxia inhibits hypertrophic differentiation and endochondral ossification in explanted tibias

Jeroen Leijten, Nicole Georgi, Liliana Moreira Teixeira, Ellie Landman, Clemens van Blitterswijk and Marcel Karperien

7

You can go a long way with a smile. You can go a lot farther with a smile and a gun.
Al Capone

Abstract

Hypertrophic differentiation of growth plate chondrocytes induces angiogenesis which alleviates hypoxia normally present in cartilage. In the current study, we aim to determine whether alleviation of hypoxia is a downstream effect of hypertrophic differentiation or whether alleviation of hypoxia also plays an active role in regulating the hypertrophic differentiation process itself.

Fetal mouse tibiae (E17.5) explants were cultured up to 21 days under normoxic or hypoxic conditions (21 % and 2.5 % oxygen respectively). Tibiae were analyzed on growth kinetics, histology, gene expression and protein secretion. The oxygen level had a strong influence on the development of explanted fetal tibiae. Compared to hypoxia, normoxia increased the length of the tibiae, length of the hypertrophic zone, calcification of the cartilage and mRNA levels of hypertrophic differentiation-related genes e.g. *MMP9*, *MMP13*, *RUNX2*, *COL10A1* and *ALPL*. Compared to normoxia, hypoxia increased the size of the cartilaginous epiphysis, length of the resting zone, calcification of the bone and mRNA levels of hyaline cartilage-related genes e.g. *ACAN*, *COL2A1* and *SOX9*. Additionally, hypoxia enhanced the mRNA and protein expression of the secreted articular cartilage markers *GREM1*, *FRZB* and *DKK1*, which are able to inhibit hypertrophic differentiation.

Collectively our data suggests that oxygen levels play an active role in the regulation of hypertrophic differentiation of hyaline chondrocytes. Normoxia stimulates hypertrophic differentiation evidenced by the expression of hypertrophic differentiation related genes. In contrast, hypoxia suppresses hypertrophic differentiation of chondrocytes at least partially via the induction of *GREM1*, *FRZB* and *DKK1* expression.

7.1 Introduction

Longitudinal growth of long bones is a tightly regulated process that is driven by hypertrophic differentiation and endochondral ossification of hyaline cartilage [1]. During maturation, the cartilaginous ends of long bones can be divided into three general zones: the resting, proliferative and hypertrophic zone. The resting zone is located closest to the ends of the diarthrodial long bones and is populated by small and round chondrocytes. Adjacent to the resting zone is the proliferative zone, which is characterized by vertical columns of actively proliferating chondrocytes. At the end of the proliferative zone, chondrocytes start maturing into terminally differentiated enlarged chondrocytes, which are located in the hypertrophic zone. Before hypertrophic chondrocytes undergo apoptosis they partially degrade and mineralize the extracellular matrix. Additionally, hypertrophic chondrocytes produce large amounts of angiogenic factors, such as vascular endothelial growth factor (Vegf) that recruits invading blood vessels into the hypertrophic cartilage [2]. This not only allows for the infiltration of amongst others bone forming cells, but also the alleviation of hypoxic stress (less than 5 % oxygen) that occurs in most of the hyaline cartilage [3, 4].

Cells are able to adapt to hypoxia by means of hypoxia inducible transcription factors (Hifs) [5]. Hifs consist of heterodimers of two proteins: an α -protein (e.g. Hif1a) and a β -protein (e.g. Hif1b). While the β -protein is constitutively expressed, the stability of the α -protein is sensitive to hypoxia [6]. When oxygen levels are below five percent the hydroxylation of the α -protein is strongly mitigated. This prevents Hif1a's proteosomal degradation, allowing it to migrate into to the nucleus and bind the β -protein [7]. In the nucleus, Hifs regulate the expression of genes that contain hypoxia responsive enhancer elements in their promoter region [8]. Hypoxia regulated genes are amongst others involved in metabolism, bioenergetics and growth allowing cells to adapt to and survive in low oxygen tensions [9-11]. Additionally, hypoxia (in particular via Hif1a) stimulates chondrogenic behavior in both mesenchymal stromal cells (MSCs) and chondrocytes [12, 13]. This stimulation occurs through both Sox9 dependent and independent pathways [14]. Alleviating hypoxia, in cultures of chondrogenically differentiated MSCs, results in a strong catabolic response [15]. Based on these lines of evidence, we hypothesized that oxygen tension is an active regulator of hypertrophic differentiation and consequently longitudinal bone growth.

In this study, we have investigated the effects of normoxia and hypoxia on longitudinal growth of mouse fetal long bones. We show that hypoxia, compared to normoxia, mitigates longitudinal bone growth by inhibiting hypertrophic differentiation and subsequent endochondral ossification. Furthermore, normoxia stimulates the calcification of the hypertrophic zone. Together our data suggest that oxygen tension, in particular the transition from hypoxia to normoxia, is an active and potent regulatory factor in endochondral ossification and longitudinal growth.

7.2 Materials and Methods

7.2.1 Tibiae organ cultures

Tibiae were harvested from E17.5 fetal FVB-Type mice (Harlan) and cultured in medium consisting of α -MEM supplemented with 10 % heat inactivated fetal bovine serum (Biowhittaker) and 100 U/ml penicillin and 100 mg/ml streptomycin (Gibco). Tibiae were either cultured in a low oxygen incubator at 2.5 percent oxygen (proox model C21, Biospherix) or at 21 percent oxygen (Sanyo) up to 21 days receiving twice a week fresh medium.

7.2.2 Histological analysis

Tibiae were fixated using 10 % buffered formalin, dehydrated using graded ethanols and embedded in paraffin. Specimen were longitudinally cut at 5 μ m thickness using a microtome (Microm HM355S), deparaffinized in xylene and rehydrated by treatment with graded ethanols. Sections were stained with Alcian blue and Nuclear fast red or Alizarin red S according to standard procedures. For image analysis ImageJ software was used. Cartilage zones were judged as follows: small round chondrocytes were counted as the resting zone, stacked columnar chondrocytes were identified as the proliferative zone and the inflated chondrocytes following the proliferative zone were taken as hypertrophic zone. Length of the cartilaginous zones was determined as the shortest possible length as measured in midsaggital sections.

7.2.3 Total RNA isolation

Tibiae were washed in phosphate buffered saline. Both cartilaginous ends of the explanted tibiae were removed with a surgical blade under a stereomicroscope (Nikon SMZ800). Cartilage specimens were pooled (n=6) in a 2 ml tube and crushed using a Pellet stamp (Kontes) in the presence of Trizol (Invitrogen). Total RNA was isolated from the lysate using the Nucleospin RNA II (Macherey-nagel) according to manufacturer's protocol.

7.2.4 Quantitative real-time reverse transcriptase-polymerase chain reaction (qRT-PCR)

For each condition, one μ g of total RNA was reverse transcribed into cDNA using the iScript cDNA synthesis kit (BioRad) in accordance with the manufacturer's instructions. Subsequently, expression of various genes was investigated by qRT-PCR. In short, 20 ng cDNA was amplified using sensimix (GC Biotech) on a MyIQ single color Real-time PCR detection system (BioRad) and analyzed with iQ5 optical system software (Biorad). The cDNA was denatured for 10 minutes followed by 45 cycles of 15 seconds 95°C, 20 seconds 60°C and 20 seconds of 72°C after which a melting curve was generated. Primer sequences are available upon request.

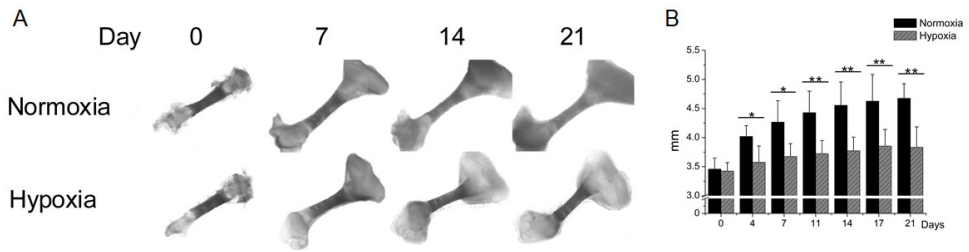


Figure 7.1: Explanted tibiae cultured 21 days under hypoxic or normoxic conditions. (A) Microphotographs of representative tibiae at different time points. (B) Using image analysis the average tibiae lengths were calculated. (N=18). * = $P < 0.05$. ** = $P < 0.01$

7.2.5 Enzyme-linked immunosorbent assay (ELISA)

Medium with or without explanted tibiae was cultured up to 7 days in either hypoxic or normoxic conditions after which it was collected. Protein concentrations of secreted Frzb and Dkk1 were determined by ELISA following the manufacturer's instructions (R&D Systems).

7.2.6 Statistical analysis

Statistical differences between two groups were analyzed using the Student's t-test or one-way ANOVA. Statistical significance was set to a $P < 0.05$ and indicated with an asterisk and/or hash-sign. Results are presented as mean of (how many repeats) standard deviation (SD).

7.3 Results

7.3.1 Hypoxia mitigates longitudinal growth

Biweekly macroscopical examination of explanted tibiae cultured up to 21 days in normoxia or hypoxia demonstrated longitudinal bone growth regardless in either condition (figure 7.1A). Tibiae cultured under normoxic conditions grew significantly larger than tibiae cultured under hypoxic conditions (figure 7.1B). The difference in longitudinal growth rate between both culture conditions was particularly dominant during the first week of the culture period. Remarkably, the shape of the cartilaginous heads under hypoxic conditions became more amorphous compared to the distinct cartilage shape of long bones cultured in normoxia. This suggested that the out-in gradient of oxygen was able to influence the shape of developing cartilage.

7.3.2 Normoxia stimulates endochondral ossification

To investigate whether the oxygen level dependent difference in growth was a result of endochondral ossification, midsagittal sections of tibiae cultured for 7 days under normoxic or hypoxic conditions were analysed histologically using Alizarin red S staining (figure 7.2A). All tibiae increased in mineralized bone length, defined as the length between the cartilaginous ends. However, the area of mineralized bone of tibiae cultured under normoxic conditions grew significantly larger than of tibiae cultured under hypoxic conditions (figure 7.2B). This suggested that normoxia increased the rate of endochondral ossification process. In contrast, semi-quantitative image analysis on midsagittal sections suggested that hypoxia resulted in higher absolute levels of calcification (figure 7.2C). Interestingly, while the bone was more calcified under hypoxic conditions, the hyaline cartilage showed a larger area of calcification under normoxic conditions (figure 7.2D).

7.3.3 Normoxia increases hypertrophic zone's length

The length of the resting, proliferative and hypertrophic zone was determined based on Alcian blue and nuclear fast red stained midsagittal sections of tibiae cultured up to 7 days (figure 7.3A). Freshly explanted uncultured tibiae showed similar zonal lengths compared to previously published observations [16]. All cultured tibiae showed a comparable increase in total cartilage length regardless of the culture conditions. However, we noted a remarkable difference in zonal organization of the primary growth plates: Tibiae cultured under normoxic conditions showed a progressive increase in length of the hypertrophic zone. In contrast, tibiae cultured under hypoxic conditions showed a progressive increase in the length of the resting zone (figure 7.3B). Additionally, the total cartilaginous surface area of midsagittal sections was significantly larger in tibiae cultured under hypoxic conditions compared to normoxic conditions (figure 7.3C).

7.3.4 Hypoxia decreases hypertrophy markers' mRNA expression

Gene expression analysis of the cartilaginous heads of tibiae cultured for 7 days in normoxia or hypoxia demonstrated higher levels of chondrogenic genes such as *Acan*, *Col2a1* and *Sox9* in hypoxic conditions compared to normoxic conditions (figure 7.4A). Matrix metalloproteinases (Mmps) mRNA levels responded diversely to different oxygen levels; hypoxia up regulated *Mmp3* mRNA, it down regulated *Mmp9* and tended to decrease *Mmp13* mRNA levels (figure 7.4B). The mRNA levels of genes related to hypertrophic chondrocytes such as *Runx2*, *Col10a1*, and *Alpl* were all expressed at a significantly lower level under hypoxic culture conditions (figure 7.4C). This suggested that hypoxia might be an important physiological factor preventing hypertrophic differentiation. Indeed, the mRNA levels of *Grem1* and *Frzb*, which we previously reported to be potent inhibitors of hypertrophic differentiation [Chapter 4], were significantly up regulated under hypoxic conditions compared to normoxic conditions. Moreover, the mRNA level of *Dkk1* tended to increase (figure 7.4D).

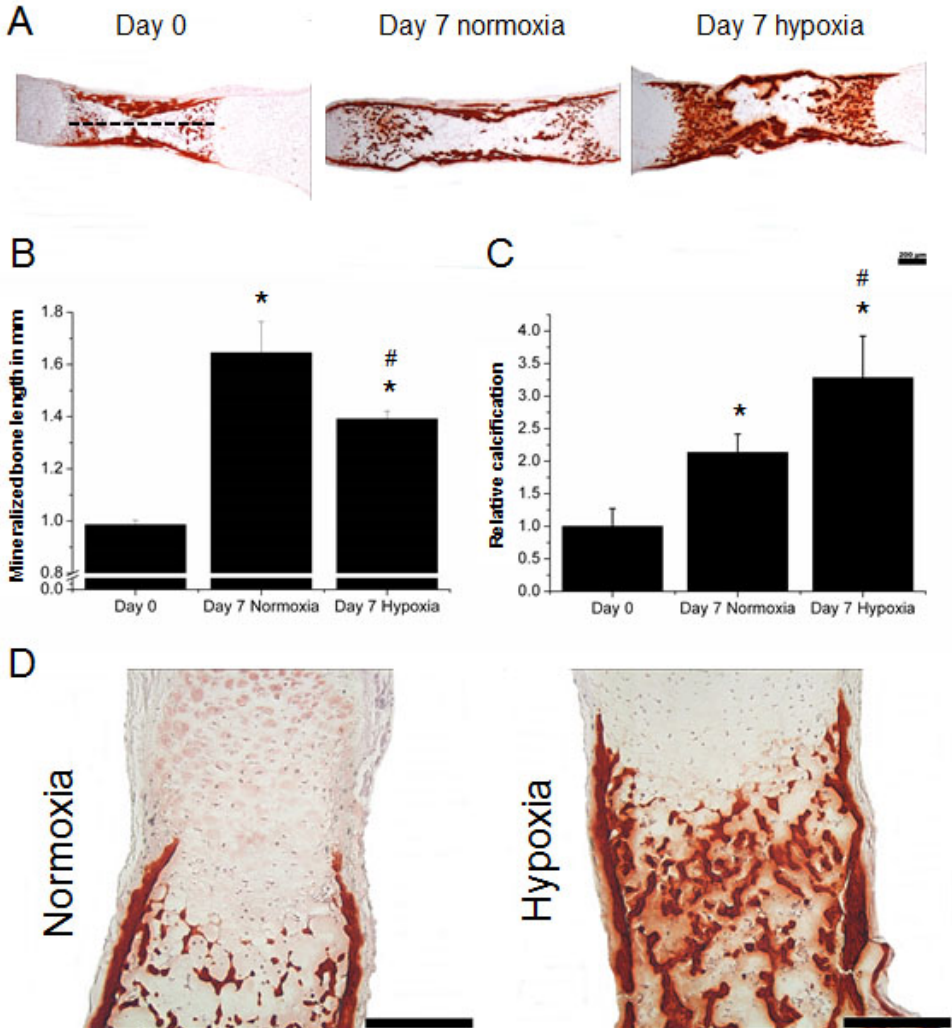


Figure 7.2: Histological analysis of calcification in explanted tibiae. (A) Midsagittal sections of tibiae were stained with Alizarin red after explantation or cultured seven days under hypoxic or normoxic conditions. (B) Image analysis was used to determine the length of the intensely calcified tissue, which was taken as the broken line indicated in 'A'. (C) The area of calcification was used to determine relative calcification of the samples. (D) Higher magnification microphotographs were used to investigate the calcification of the hypertrophic cartilage. (N=15). * = $P < 0.05$ compared to freshly isolated tibiae. # = $P < 0.05$ compared to normoxic condition of the same time point.

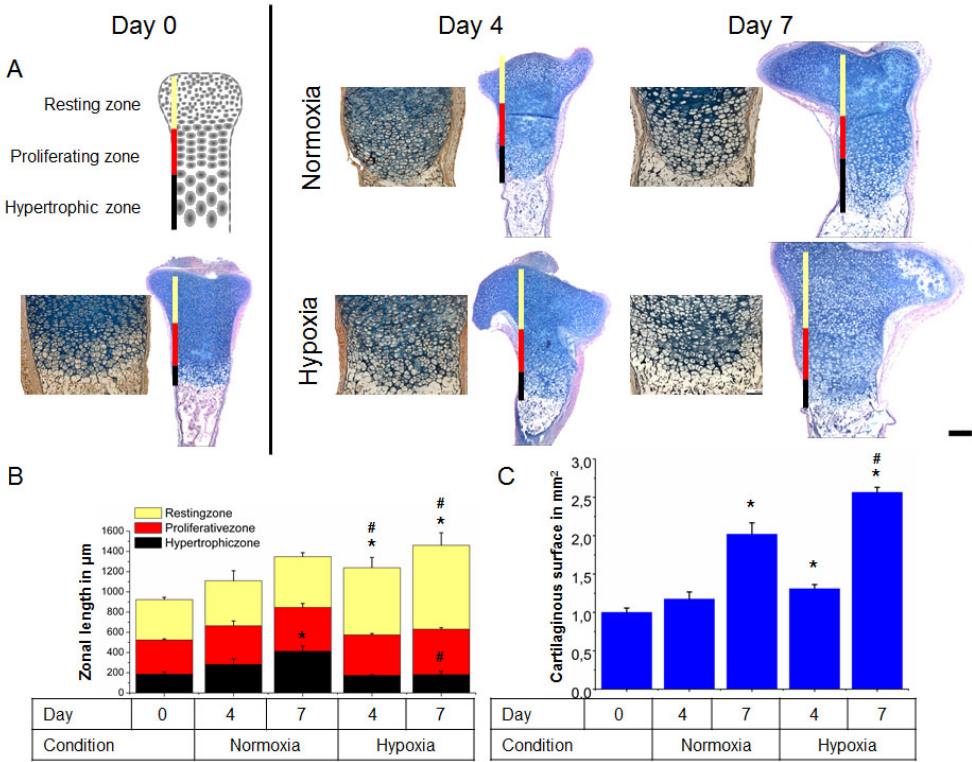


Figure 7.3: Histological analysis of zonal lengths in explanted tibiae. Mid-sagittal sections of tibiae were stained with Alcian blue and Nuclear fast red directly after explantation or after culture up to seven days under either hypoxic or normoxic conditions (A). Image analysis was used to measure the sizes of the different cartilaginous zones (B) and the surface of the cartilaginous area (C). (N=15). * = $P < 0.05$ compared to freshly isolated tibiae. # = $P < 0.05$ compared to normoxic condition of the same time point.

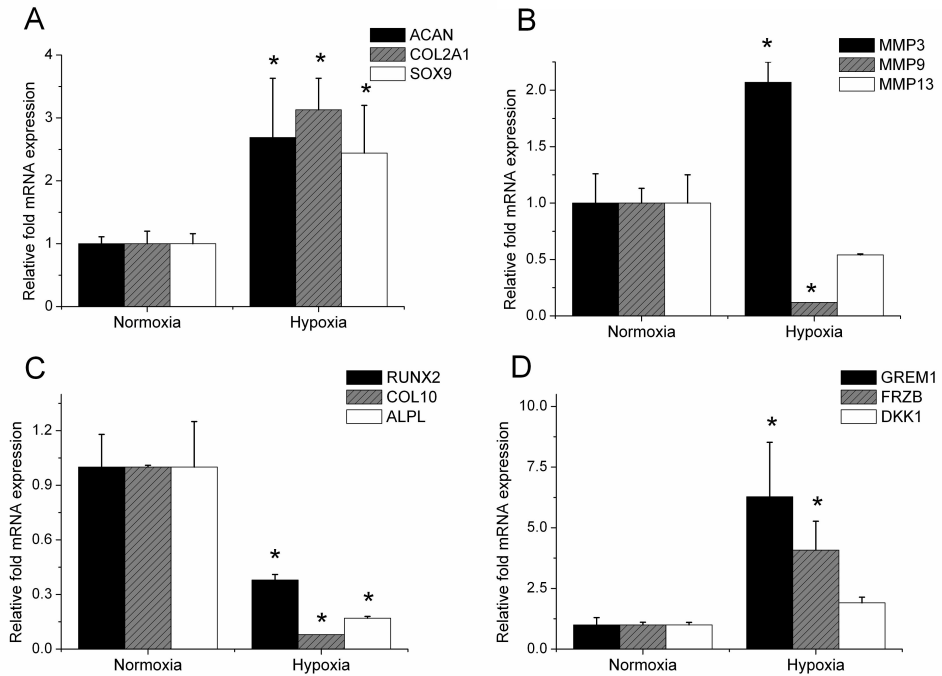


Figure 7.4: Gene expression in the cartilaginous heads of explanted tibiae. At 7 days mRNA was isolated and quantified using qPCR. Data are expressed as fold change relative to mRNA expression in normoxia. Effect of hypoxia on mRNA expression of (A) typical cartilage markers, (B) cartilage degrading MMPs, (C) hypertrophic markers and (D) secreted Wnt and BMP antagonists able to inhibit hypertrophic differentiation. (N=5). * = $P < 0.05$ compared to hypoxia.

7.3.5 Hypoxia enhances Frzb and Dkk1 protein levels

To investigate the effect of the oxygen level on Frzb and Dkk1 protein expression, tibiae were cultured for 7 days after which their protein levels were quantified. In line with mRNA expression, Frzb and Dkk1 protein levels were significantly higher under hypoxic conditions compared to normoxic conditions (figure 7.5A). Moreover, we investigated the effect of the oxygen level on Frzb and Dkk1 degradation. Fresh culture medium containing 10 % fetal bovine serum was incubated at 37°C for up to 7 days in the absence of tibiae. This demonstrated that Frzb and Dkk1 protein levels declined more rapidly under normoxic conditions compared to hypoxic conditions (figure 7.5B).

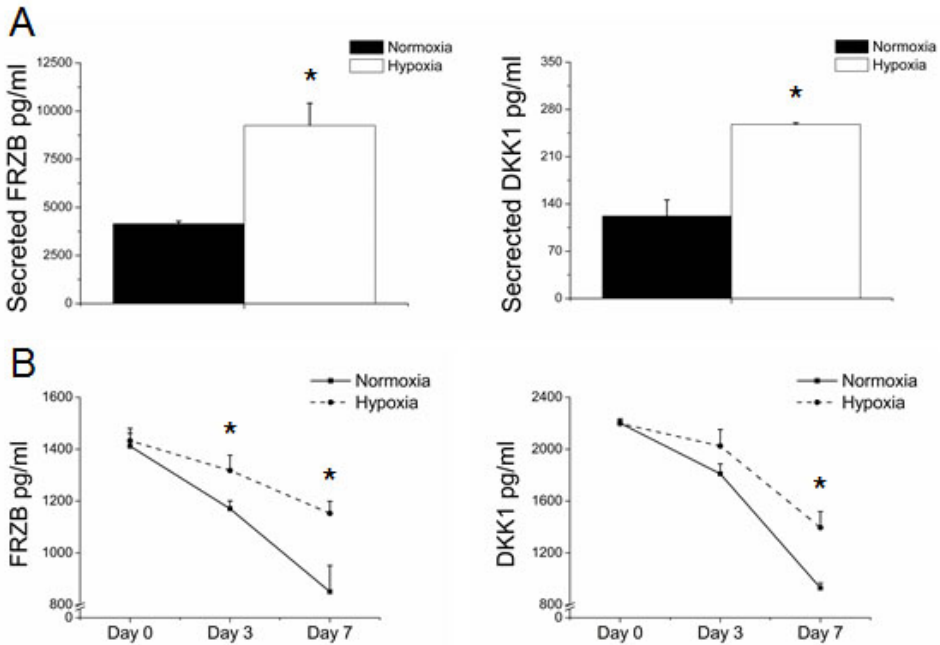


Figure 7.5: Effect of hypoxic and normoxic culture conditions on Frzb and Dkk1 protein levels under. (A) Tibiae were cultured for 7 days without receiving new medium in either hypoxia or normoxia (N=5). (B) Culture medium containing 10 % fetal bovine serum was incubated up to 7 days in 37°C. (N=4). Frzb and Dkk1 protein levels were analyzed using ELISA. * = P<0.05 compared to normoxic condition of the same time point.

7.4 Discussion

Longitudinal growth of long bones is driven by chondrocyte proliferation, chondrocyte hypertrophy and subsequent endochondral ossification of hyaline cartilage. This cartilage is predominantly avascular and its nutrient supply is dependent on diffusion from the surrounding tissue, being either the perichondrium or the blood vessels in the primary spongiosum. Consequently, out-in gradients of oxygen are present in hyaline cartilage [17]. The blood vessel formation at the osteochondral interface alleviates the terminally differentiated hypertrophic cartilage from its hypoxic stress [4, 11]. This effectively creates an oxygen gradient along the hypertrophic differentiating cartilage.

In this study, we have shown that oxygen levels were able to influence hypertrophic differentiation and subsequent endochondral ossification in explanted long bones cultured *ex vivo*. In particular, we demonstrated that normoxic conditions stimulate longitudinal growth compared to hypoxic conditions. This was, at least partly, explained by the difference in terminal differentiation; hypoxia retains chondrocytes

in the resting zone while normoxia stimulates them to progress towards the hypertrophic zone. Indeed, the length of the mineralized bone grew significantly larger under normoxic conditions compared to hypoxic conditions. Together, this suggests that the oxygen level is not just important for angiogenesis driven by hypertrophic differentiation, but also plays an active role in regulating the process of hypertrophic differentiation itself.

Oxygen levels inversely regulate the degradation rate of Hifs [18]. Accumulation of Hifs in hypoxic conditions allows for complex formation, nuclear translocation and transcriptional regulation, resulting in oxygen sensitive regulation of gene expression [19]. Interestingly, it has been shown that hypoxic stress is generated during the mesenchymal condensation that initiates the onset of long bone formation. Moreover, hypoxia induces Hif1a accumulation, which is essential for early chondrogenesis [13]. After the chondrocyte-lineage has been established, hypoxia induced Hif1a expression drives cartilage extracellular matrix production in the developing cartilage anlage [20].

Indeed, we also observed a significantly higher expression of *Acan*, *Col2a1* and *Sox9* when explanted tibiae were cultured under hypoxic conditions. Moreover, the shape of the tibiae became progressively more atypical under hypoxic conditions compared to normoxic conditions. This suggests that the out-in oxygen gradient, generated by the vascularized tissues surrounding the hyaline cartilage, as found *in vivo*, might contribute to defining the shape of the (cartilaginous ends of) long bones and controlling the direction of long bone elongation.

Blood vessels penetrate from the osteochondral regions into the hypertrophic zone. This process is driven by Vegf, which is expressed by hypertrophic chondrocytes and to a lesser extent by proliferative zone chondrocytes in response to the hypoxic conditions in the cartilage anlage [20]. This leads to vascularization of the cartilage, which results in normoxic conditions of the previously hypoxic cartilage. Compared to explants cultured in hypoxia, normoxic culture resulted in an increased expression of genes related to hypertrophic differentiation such as *Runx2*, *Col10a1*, *Mmp1* and *Mmp13* in the cartilaginous heads of the long bones [1, 15]. Increased expression of genes related to the terminal differentiation of hyaline cartilage coincided with an increased width of the hypertrophic zone in explants cultured in normoxia compared to explants cultured in hypoxia. In addition, we demonstrated that the mRNA levels of *Grem1* and *Frzb* as well as protein secretion of Frzb and Dkk1 were significantly lower under normoxia compared to hypoxia. Previously, we have shown that these three secreted antagonists are potent inhibitors of hypertrophic differentiation and subsequent endochondral ossification in explanted tibiae [Chapter 4]. Indeed, in this study we observed an inverse correlation between the expression of these antagonists and hypertrophic differentiation. Therefore it is tempting to suggest that the effect of oxygen levels on hypertrophic differentiation of chondrocytes is at least in part mediated via the expression of these antagonists.

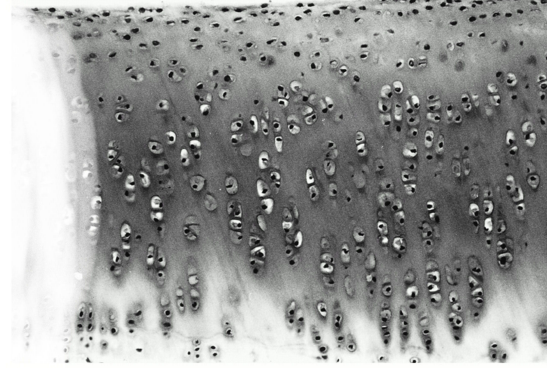
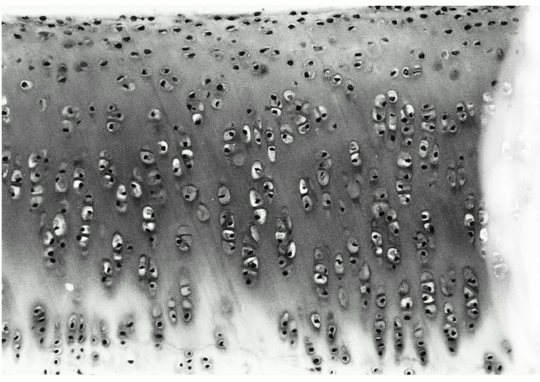
Hifs, in particular Hif2a, are associated with the expression of cartilage hypertrophy markers and the development of osteoarthritis [21]. In the current study, we demonstrated that oxygen levels regulated the expression and degradation of Grem1, Frzb and Dkk1. Moreover, we previously have identified Grem1, Frzb and Dkk1 as potent inhibitors of hypertrophic differentiation that are inversely correlated with

the level of degeneration in osteoarthritic articular cartilage [Chapter 4]. However, whether these two oxygen sensitive phenomena, which are both associated with osteoarthritis, are intertwined remains to be investigated.

Taken together, we have demonstrated that the oxygen levels are not just involved in the stimulation of angiogenesis, but also act as potent regulators of chondrocyte's hypertrophic differentiation and the endochondral ossification of developing long bones.

References

1. Hirao, M., et al., Oxygen tension regulates chondrocyte differentiation and function during endochondral ossification. *J Biol Chem*, 2006. 281(41): p. 31079-92.
2. Cramer, T., et al., Expression of VEGF isoforms by epiphyseal chondrocytes during low-oxygen tension is HIF-1 alpha dependent. *Osteoarthritis Cartilage*, 2004. 12(6): p. 433-9.
3. De Spiegelaere, W., et al., Detection of hypoxia inducible factors and angiogenic growth factors during foetal endochondral and intramembranous ossification. *Anat Histol Embryol*, 2010. 39(4): p. 376-84.
4. Brighton, C.T. and R.B. Heppenstall, Oxygen tension in zones of the epiphyseal plate, the metaphysis and diaphysis. An in vitro and in vivo study in rats and rabbits. *J Bone Joint Surg Am*, 1971. 53(4): p. 719-28.
5. Semenza, G.L. and G.L. Wang, A nuclear factor induced by hypoxia via de novo protein synthesis binds to the human erythropoietin gene enhancer at a site required for transcriptional activation. *Mol Cell Biol*, 1992. 12(12): p. 5447-54.
6. Bruick, R.K. and S.L. McKnight, A conserved family of prolyl-4-hydroxylases that modify HIF. *Science*, 2001. 294(5545): p. 1337-40.
7. Kaelin, W.G., Jr. and P.J. Ratcliffe, Oxygen sensing by metazoans: the central role of the HIF hydroxylase pathway. *Mol Cell*, 2008. 30(4): p. 393-402.
8. Wenger, R.H., D.P. Stiehl, and G. Camenisch, Integration of oxygen signaling at the consensus HRE. *Sci STKE*, 2005. 2005(306): p. re12.
9. Kim, J.W., et al., HIF-1-mediated pyruvate dehydrogenase kinase: a metabolic switch required for cellular adaptation to hypoxia. *Cell Metab*, 2006. 3(3): p. 177-85.
10. Cho, Y.S., et al., HIF-1alpha controls keratinocyte proliferation by up-regulating p21(WAF1/Cip1). *Biochim Biophys Acta*, 2008. 1783(2): p. 323-33.
11. Wang, Y., et al., The hypoxia-inducible factor alpha pathway couples angiogenesis to osteogenesis during skeletal development. *J Clin Invest*, 2007. 117(6): p. 1616-26.
12. Pfander, D., et al., HIF-1alpha controls extracellular matrix synthesis by epiphyseal chondrocytes. *J Cell Sci*, 2003. 116(Pt 9): p. 1819-26.
13. Provot, S., et al., Hif-1alpha regulates differentiation of limb bud mesenchyme and joint development. *J Cell Biol*, 2007. 177(3): p. 451-64.
14. Lafont, J.E., et al., Hypoxia promotes the human articular chondrocyte phenotype via SOX9-dependent and -independent pathways. *J Biol Chem*, 2008. 283(8): p. 4778-86.
15. Strobel, S., et al., Anabolic and catabolic responses of human articular chondrocytes to varying oxygen percentages. *Arthritis Res Ther*, 2010. 12(2): p. R34.
16. Zhou, Z., et al., Neogenin regulation of BMP-induced canonical Smad signaling and endochondral bone formation. *Dev Cell*, 2010. 19(1): p. 90-102.
17. Zhou, S., Z. Cui, and J.P. Urban, Factors influencing the oxygen concentration gradient from the synovial surface of articular cartilage to the cartilage-bone interface: a modeling study. *Arthritis Rheum*, 2004. 50(12): p. 3915-24.
18. Bunn, H.F. and R.O. Poyton, Oxygen sensing and molecular adaptation to hypoxia. *Physiol Rev*, 1996. 76(3): p. 839-85.
19. Liu, L. and M.C. Simon, Regulation of transcription and translation by hypoxia. *Cancer Biol Ther*, 2004. 3(6): p. 492-7.
20. Pfander, D., et al., Vhlh deletion in chondrocytes reduces proliferation increases matrix deposition during growth plate development. *Development*, 2004. 131(10): p. 2497-508.
21. Saito, T., et al., Transcriptional regulation of endochondral ossification by HIF-2alpha during skeletal growth and osteoarthritis development. *Nat Med*, 2010. 16(6): p. 678-86.



Chapter 8

Hypoxia steers chondrogenically differentiating human mesenchymal stromal cells towards an articular cartilage phenotype

Jeroen Leijten*, Nicole Georgi*, Clemens van Blitterswijk and Marcel Karperien

* Both authors contributed equally

8

The scientists of today think deeply instead of clearly. One must be sane to think clearly, but one can think deeply and be quite insane.

Nikola Tesla

Abstract

In vitro chondrogenic differentiation of multipotent cells results in the formation hypertrophic cartilage that is prone to undergo endochondral ossification when implanted. In contrast to current *in vitro* differentiation protocols, the embryological development of hyaline cartilage occurs under hypoxic conditions while its terminal hypertrophic differentiation is correlated with normoxic conditions.

In the current study we investigated whether a hypoxic environment steers chondrogenic differentiation of MSCs towards a more articular cartilage phenotype. Micromasses of human MSCs were chondrogenically differentiated up to 5 weeks under hypoxic (2.5 %) or normoxic (21 %) culture conditions. During the first 3 weeks hypoxia stimulated the expression of hyaline cartilage markers such as *COL2A1*, *ACAN* and *SOX9*. From the 3rd week onwards, hypoxia induced the expression of genes and proteins that are enriched in the articular cartilage compared to growth plate cartilage e.g. *GREM1*, *FRZB* and *DKK1*. Moreover, we demonstrated that relief of hypoxic stress down regulated the expression of these markers. Furthermore, hypoxia was only essential during the last three weeks to induce these factors.

Taken together, our data suggested that hypoxia stimulated the chondrogenic differentiation of MSCs towards the articular cartilage lineage once a hyaline cartilage phenotype was established. In consequence, variation of the oxygen tension might be a critical factor to consider in chondrogenic MSC differentiation protocols and is an promising target to augment articular cartilage repair therapies.

8.1 Introduction

The limited regenerative capacity of articular cartilage combined with its susceptibility to damage from high energy impacts and from repetitive shear and torsional forces has led to development of several therapeutic options [1]. Younger, more active patients with focal cartilage defects can be considered for regenerative procedures such as autologous chondrocyte implantation [2]. This procedure is based on the creation of a novel cartilaginous defect for the isolation of cells that after *in vitro* expansion are transplanted in the original defect site. To circumvent this drawback, alternative cell sources such as mesenchymal stromal cells (MSCs) are considered for implantation [3, 4].

MSCs can be isolated from a variety of tissues and are capable of forming hyaline-like cartilage upon chondrogenic differentiation [3, 5]. Unlike articular cartilage, this hyaline-like cartilage expresses typical hypertrophic markers and will undergo endochondral ossification when implanted in mice [6-9]. Indeed, accumulating evidence suggests that the current differentiation protocols are able to induce chondrogenesis of MSCs resulting in growth plate-like cartilage with the propensity to undergo hypertrophic differentiation but not in articular cartilage. This is supported by the observation, that standard chondrogenesis protocols do not induce the expression of genes that are enriched in articular cartilage compared to growth plate cartilage such as secreted soluble factors that inhibit hypertrophic differentiation [10-12].

During embryological development, MSCs condensate, undergo chondrogenic differentiation and giving rise to hyaline cartilage, which forms the anlage of a long bone. Upon birth the hyaline cartilage is physically separated by the formation of the secondary center of ossification, which results in the delineation of the growth plate and articular cartilage [13]. In contrast to *in vitro* chondrogenic differentiation protocols, the natural differentiation of MSCs occurs in a predominantly hypoxic environment [14]. Hypoxia occurs when oxygen levels become lower than five percent and results in the stabilization of hypoxia-inducible factors (HIFs). These transcription factors are able to bind hypoxia response elements of target gene promoters ([15]). It has been demonstrated that HIF expression is crucial to chondrogenesis [14, 16]. Moreover, the oxygen level regulates the expression of reactive oxygen species, which in turn drives hypertrophic differentiation and endochondral ossification of hyaline(-like) cartilage [17].

We hypothesized that oxygen levels play an influential role in differentiating MSCs towards either one of the hyaline cartilage subtypes. In the present study, we investigated the differences in whole genome gene expression profiles of MSCs undergoing chondrogenesis in either normoxic or hypoxic culture conditions. We provide new evidence that once MSCs have acquired a hyaline cartilage-like phenotype, hypoxia potently increases the expression of genes that are enriched in articular cartilage compared to growth plate cartilage, such as potent inhibitors of hypertrophic differentiation like GREM1, FRZB and DKK1.

8.2 Materials and Methods

8.2.1 Patient material

The use of patient material was approved by the local hospital ethical committees and for all samples informed written consent was obtained. Explanted articular cartilage was directly frozen in Cryomatrix (Cryomatrix, Shandon) using liquid isopentane and stored at -80°C . Human mesenchymal stromal cells (MSCs) were isolated from fresh bone marrow samples as described previously [18]. In short, aspirates were resuspended using a 20-gauge needle, plated at 500,000 cells/cm² and cultured in MSC proliferation medium consisting of α -MEM (Gibco), 10 % heat-inactivated fetal bovine serum (Biowhittaker), 0.2 mM ascorbic acid (Sigma), 2 mM L-glutamine (Gibco), 100 U/ml penicillin with 100 mg/ml streptomycin (Gibco) and 1 ng/ml basic fibroblast growth factor (Instruchemie, Delfzijl, The Netherlands).

8.2.2 Total RNA extraction

After removal of the subchondral bone, frozen articular cartilage samples were cut into 8 μm sections (Reichert Jung 2055 microtome, Leica). Every fifth slide was stained with Haematoxylin to validate that no bone contamination was present. Afterwards, the collected cartilage sections were homogenized in a 4 M guanidine thiocyanate solution (Sigma). Total RNA isolation was performed by a method previously described [19]. MSCs were lysed using Trizol reagent (Invitrogen). Total RNA of all specimens was isolated or purified using the Nucleospin RNA II kit (Bioke) according to manufacturer's instructions. Total RNA yields were measured using the Nanodrop2000 (ND-1000 Spectrophotometer, Isogen LifeScience). High Quality of the RNA was verified using the Agilent 2100 bioanalyzer (Agilent).

8.2.3 Chondrogenic differentiation of MSCs

MSCs were seeded at 2.5×10^5 cells per well in Cell star U-shaped 96 well plates (Greiner Bio-one), centrifuged for 3 minutes at 800 G and incubated at 37°C and 5 % CO₂ to induce pellet formation. Chondrogenic differentiation of MSCs was chemically induced by exposing cell pellets to a chondrogenic medium composed of DMEM high glucose supplemented with 100 $\mu\text{g}/\text{ml}$ sodium pyruvate (Sigma), 0.2 mM ascorbic acid, 50 $\mu\text{g}/\text{ml}$ insulin-transferrin-selenite (ITS+Premix, BD biosciences), 100 U/ml penicillin, 100 $\mu\text{g}/\text{ml}$ streptomycin, 0.1 μM dexamethason (Sigma) and 10 ng/ml transforming growth factor 3 (TGFB3, R&D system). MSCs were cultured up to 35 days under normoxic condition (21 % oxygen) or hypoxic condition (2.5 % oxygen), receiving biweekly medium refreshments. On day 7, 21 and 35 four pellets were pooled for RNA isolation and two were fixed in 10 % buffered formalin and subsequently embedded in paraffin.

8.2.4 Histological analysis

Paraffin embedded samples were cut into 5 μm sections, deparaffinized in xylene and dehydrated using graded ethanol steps. Sections were stained either with Alcian blue and counterstained with Nuclear fast red solutions according to standard procedures.

8.2.5 Quantitative glycosaminoglycan and DNA assay

Cell pellets ($n=4$) were washed with phosphate-buffered saline and frozen overnight at -80°C . After thawing, the constructs were digested for 16 hours with proteinase K (Sigma) at 56°C . Total DNA was quantified using the Cyquant dye kit (Molecular Probes) with a fluorescent plate reader (Perkin-Elmer). The amount of glycosaminoglycans (GAG) was measured spectrophotometrically after reaction with a DMMB dye (Sigma-Aldrich). The color intensity was quantified immediately in a microplate reader (Bio-TEK Instruments) by measuring the absorbance at 540 nm. The amount of GAG was determined using a calibration curve based on chondroitin sulfate A or B (Sigma-Aldrich). All values were normalized to their respective DNA amount (expressed as the GAG/DNA [$\mu\text{g}/\mu\text{g}$] ratio).

8.2.6 Determination of GREM1, FRZB and DKK1 protein levels

After 32 days of chondrogenic differentiation medium was conditioned for 3 days. GREM1, FRZB and DKK1 protein levels in the culture supernatant were measured by ELISA (USCN Life Science and R&D Systems) following manufacturer's instructions.

8.2.7 Microarray processing and statistical analysis

NuGEN Ovation PicoSL WTA System kit followed by Encore BiotinIL module was used to generate biotinylated sscDNA starting from 50 ng total RNA. 750 ng of the obtained samples was hybridized onto the Illumina HumanHT-12 v4 Expression BeadChips. The samples were scanned using the Illumina iScan array scanner. Gene expression profiling was performed using Illumina's Genomestudio v. 2010.3 software with the default settings advised by Illumina. The raw fluorescence intensity values were normalized applying quantile normalization. Differential gene expression was analysed using the commercial software package Genespring, version 11.5.1. (Agilent Technologies). Genes with at least a twofold difference being significantly differentially expressed according to an oneway ANOVA with a Benjamini-Hochberg FDR correction and TukeyHSD post hoc test using a cut-off rate of $P < 0.05$ were selected. Changes of gene expression in annotated canonical pathways and bio-functions were visualized using ingenuity pathway analysis software (Ingenuity Systems). Search Tool for the Retrieval of Interacting Genes/Proteins (STRING) was used to investigate the predicted gene-gene interaction network [20]. Clusters were formed using Markov clustering algorithms.

8.2.8 Quantitative real-time reverse transcriptase-polymerase chain reaction (qRT-PCR)

One μg of total RNA was reverse-transcribed using the iScript cDNA synthesis kit (BioRad) following manufacturer's instructions. 20 ng of cDNA was amplified using Sensimix (Bioline) and the MyIQ single color Real-time PCR detection system (BioRad). Analysis was performed on the iQ5 optical system software (Biorad). The qPCR amplifications were run under the following conditions: initial denaturation for 10 minutes at 95°C , then cycled 45 times at 95°C for 15 seconds, 60°C for 15 seconds and 72°C for 15 seconds and was finally followed by a melting curve. Sequences of primers are available upon request.

8.2.9 Statistical analysis

Statistical differences between two groups were analyzed using the Student's t-test or One-way ANOVA. Statistical significance was set to a $P < 0.05$ and indicated with an asterisk or hash sign. Results are presented as mean standard deviation.

8.3 Results

8.3.1 Hypoxia stimulates chondrogenic differentiation of MSCs

Pellet cultures of MSCs were differentiated into the chondrogenic lineage for up to 35 days in the presence of TGFB3 in either normoxic or hypoxic conditions. Histological analysis demonstrated little to no positive GAG staining after 7 days of culture in either normoxic or hypoxic conditions (figure 8.1A). In contrast, at 21 days of chondrogenic differentiation intense GAG staining throughout the pellet was noted in pellets cultured in hypoxia compared to a modest GAG staining in pellets cultured in normoxia. After 35 days, GAG staining intensified in the pellets cultured in hypoxia. Interestingly, in pellets cultured in normoxia positive staining for GAGs was predominantly found in the center of the pellet, the area with the lowest oxygen concentration, while the periphery of the pellet stained negative. Biochemical quantification corroborated enhanced GAG deposition in hypoxia compared to normoxia at 21 and 35 days of differentiation (figure 8.1B).

8.3.2 Effect of oxygen on gene expression profile of chondrogenically differentiating MSCs

Whole genome gene expression analysis was performed on MSCs that were chondrogenically differentiated for 7, 21 or 35 days under either hypoxic or normoxic culture conditions. A total of 503 genes were significantly differentially expressed with a more than two-fold change compared to undifferentiated cells in at least one of the conditions. Hierarchical clustering revealed that up to day 21 of culture the experimental conditions grouped according to culture time and not to oxygen exposure. After 35 days pellets cultured in normoxia showed more resemblance with pellets cultured for

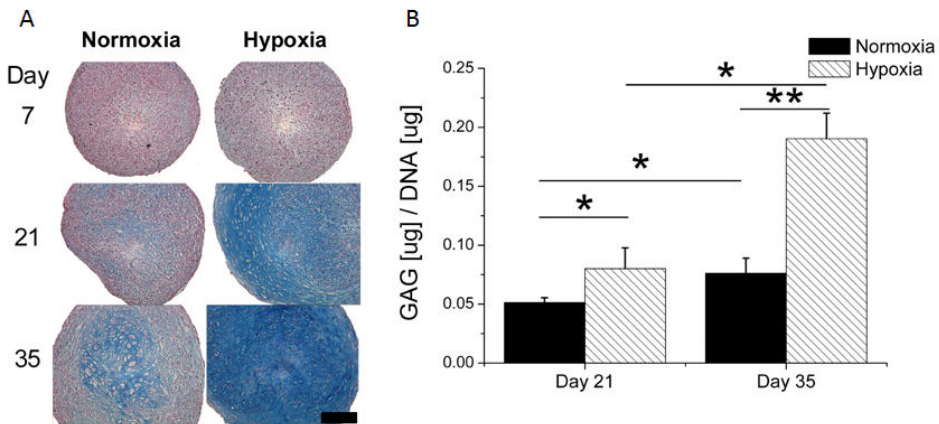


Figure 8.1: Hypoxia stimulates chondrogenic differentiation of MSCs. (A) Micromasses of MSCs were cultured up to 35 days under either normoxic or hypoxic conditions. Histological analysis of midsagittal sections using Alcian blue and Nuclear fast red was used to visualize chondrogenic differentiation. A representative example out of 3 donors is shown. (B) Biochemical analysis for GAGs was used to quantify chondrogenesis. Data represent the mean of 3 donors each measured in quadruplicate \pm SD. * = $p < 0.05$; ** = $p < 0.01$. Black bars indicate 100 μ m

21 days than with pellets cultured for 35 days in hypoxia (figure 8.2A). After 35 days of chondrogenic differentiation, 160 and 131 genes were up regulated more than twofold, under hypoxic and normoxic culture conditions respectively, compared to undifferentiated MSCs. 80 of these genes were present in both culture conditions. Similarly, 93 and 127 genes were down regulated after 35 days under hypoxic or normoxic respectively of which 76 genes were down regulated in both conditions (figure 8.2B). Comparing differences in gene expression between hypoxia and normoxia demonstrated that 26, 11 and 60 genes were up regulated and 8, 5 and 9 genes were down regulated more than twofold at day 7, 21 or 35 respectively (figure 8.2C).

Pathway analysis revealed that the differences between hypoxia and normoxia at day 7 were dominated by metabolism and cell cycle related functions. On day 21 this shifted towards differentiation/development of connective tissue and skeletal function. This shift towards skeletal and muscular systems and function intensified at day 35 as underlined by the strongly increased significance of this biofunction with according P values of $1.73E^{-2}$, $3.71E^{-5}$ and $1.34E^{-9}$ for day 7, 21 and 35 respectively (figure 8.2D). Taken together, this data suggested that in the first week hypoxia leads to a strong change in the metabolism of the MSCs, but only robustly enhances chondrogenesis at later time points.

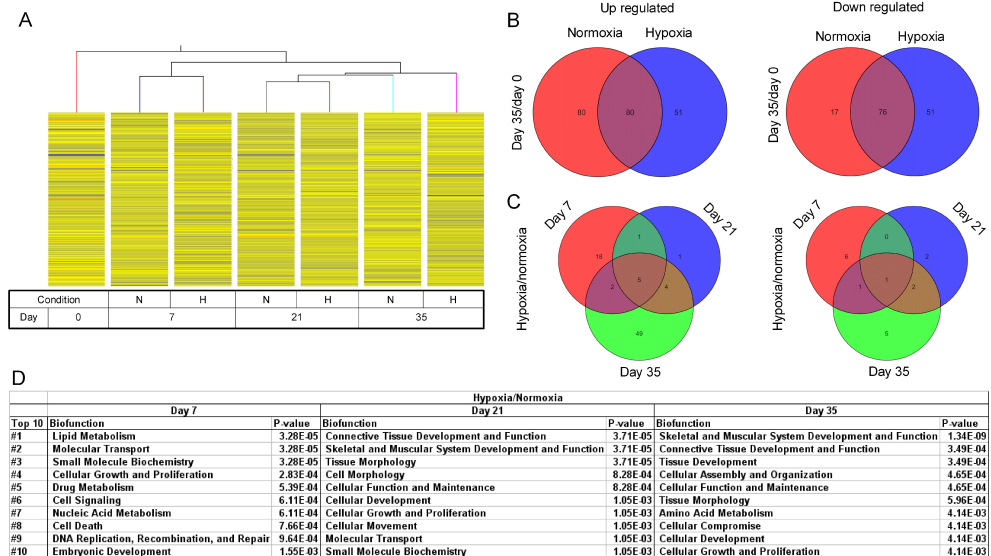


Figure 8.2: Whole genome gene expression analysis of chondrogenically differentiating MSCs under either normoxic or hypoxic conditions. (A) Normalized microarray data was hierarchical clustered. (B) Venn diagrams of genes with at least a twofold difference that were significantly differentially expressed between day 35 and day 0 under normoxic or hypoxic culture conditions, or (C) between normoxic and hypoxic culture conditions at day 7, day 21 or day 35. (D) Significantly different biofunctions between normoxic and hypoxic culture conditions at day 7, day 21 and day 35. Each data point is based on the gene expression analysis of 3 donors.

8

8.3.3 Gene networks regulated by oxygen levels

To reveal the gene networks underlying the differences in gene expression, the known and predicted gene/protein interactions were investigated for all genes more than twofold differentially expressed at day 35 between hypoxia and normoxia. Using Markov clustering algorithms two key nodes within the network were observed (figure 8.3). The relative smaller cluster was characterized by metabolism related genes, predominantly involving glycolysis. The larger node consisted predominantly of cartilage related genes, such as amongst others transforming growth factor beta 1 (*TGFB1*) and sex determining region Y-box 9 (*SOX9*), suggesting that these two genes might be key players in the observed enhanced cartilage formation in hypoxia.

8.3.4 Hypoxia induces chondrogenically differentiating MSCs to express hyaline cartilage-enriched genes

We next investigated whether hypoxia was able to steer chondrogenically differentiating MSCs into a more articular cartilage-like gene expression profile. For this

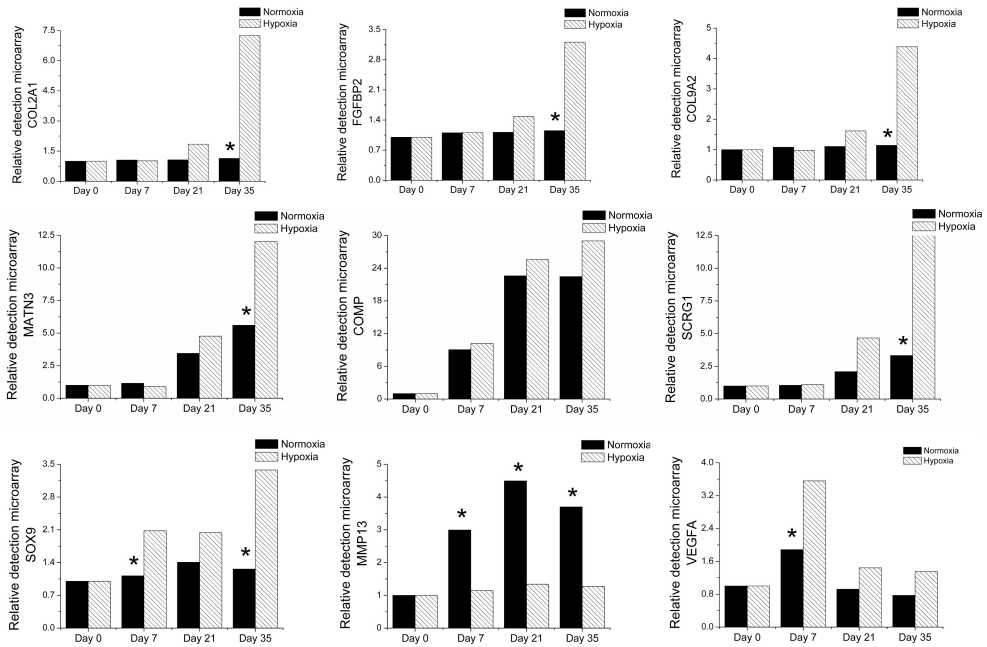


Figure 8.3: Network analysis of genes differentially expressed MSCs after 35 days of chondrogenic differentiation under either normoxic or hypoxic conditions. Genes with at least a twofold significant difference were analyzed on known or predicted gene or protein interactions. The red cluster contains predominantly genes involved glycolysis and the green cluster contains predominantly genes with a cartilage signature. Both clusters are up regulated in hypoxic conditions.

we first identified the difference in expression profiles between undifferentiated MSCs and healthy articular cartilage using a whole genome gene expression analysis. The six most differentially expressed genes were all expressed at higher levels in articular cartilage and established markers of hyaline cartilage, i.e. collagen type 2 alpha 1 (*COL2A1*), fibroblast growth factor binding protein 2 (*FGFBP2*), collagen, type IX alpha 2 (*COL9A2*), matrilin 3 (*MATN3*), cartilage oligomeric matrix protein (*COMP*) and Scrapie responsive gene (*SCRG1*; otherwise known as stimulator of chondrogenesis 1). In a previous study, we have shown that these markers showed comparable expression levels in the two hyaline cartilage subtypes derived from the same adolescent donors [Chapter 4]. Remarkably, all six genes were increased by hypoxia in chondrogenically differentiating MSCs compared to normoxia. Moreover several genes e.g. *FGFBP2* and *COL9A2* were not induced under normoxia, while hypoxia potentially activated their transcription (figure 8.4A). Additionally, the microarray data revealed responses typical to hypoxic conditions. For example, we detected

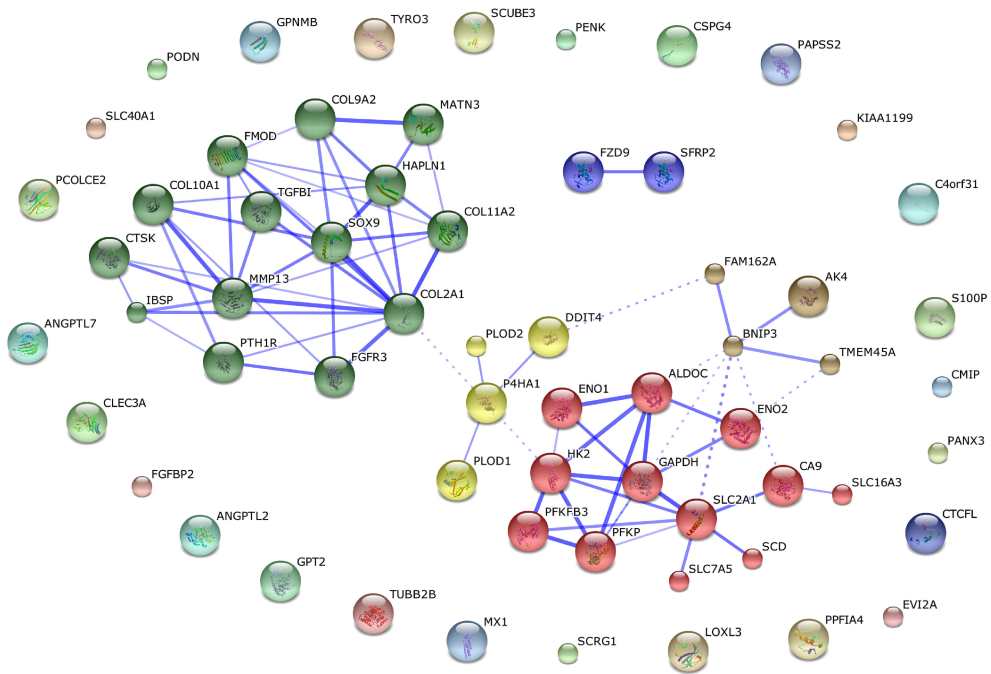


Figure 8.4: Hypoxia stimulated the expression of hyaline cartilage-enriched gene transcripts. (A) mRNA levels of six genes (*COL2A1*, *FGFBP2*, *COL9A2*, *MATN3*, *COMP* and *SCRG1*), which are most enriched in articular cartilage compared to MSCs, were investigated in chondrogenically differentiating MSCs using qPCR. (B) Additionally, the mRNA levels of *SOX9*, *MMP13* and *VEGFA*, which are known to be influenced by oxygen levels were investigated. Data represent the mean of 3 donors each measured in triplicate \pm SD. * = $P < 0.05$.

8

increased *SOX9* and vascular endothelial growth factor A (*VEGFA*) mRNA levels as well as relatively decreased matrix metalloproteinase 13 (*MMP13*) mRNA levels when MSCs were differentiated in hypoxia (figure 8.4B). Together this suggested that hypoxia could effectively stimulate transcription of hyaline cartilage specific genes during chondrogenic differentiation of MSCs, starting from 21 days of differentiation.

8.3.5 Hypoxia up regulates articular cartilage-enriched and decreases growth plate cartilage-enriched mRNA levels in chondrogenically differentiating MSCs compared to normoxia

qPCR analysis validated the microarray data showing that hypoxia enhanced transcription of typical hyaline cartilage markers such as *SOX9*, *COL2A1* and *ACAN*

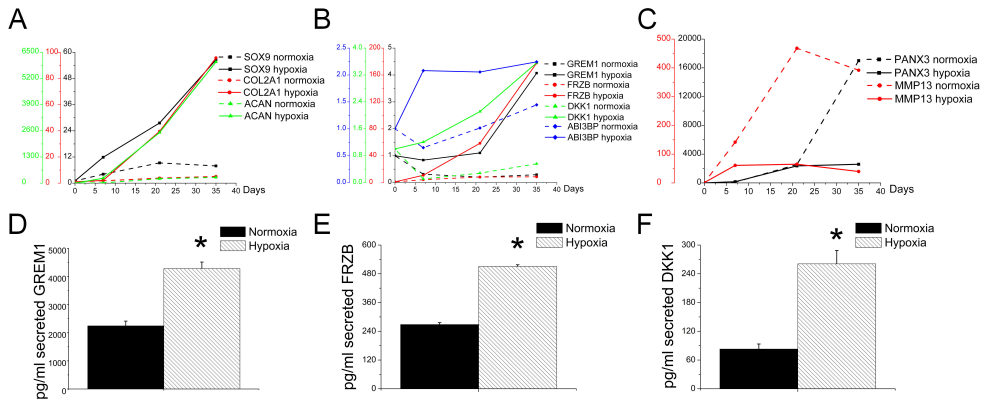


Figure 8.5: Hypoxia stimulated the expression of articular cartilage-enriched gene transcripts. (A) Chondrogenically differentiating MSCs under normoxic or hypoxic conditions were analyzed on gene expression of the cartilage markers *SOX9*, *COL2A1* and *ACAN*, (B) the articular cartilage markers *GREM1*, *FRZB*, *DKK1* and *ABI3BP* and (C) the growth plate markers *PANX3* and *MMP13* by qPCR. (D) Additionally, secretion of the articular cartilage-enriched markers *FRZB*, *GREM1* or *DKK1* was analysed using ELISA. Data represent the mean of 3 donors each measured in triplicate +/- SD. * = $P < 0.05$

(figure 8.5A). We next investigated whether the hypoxia also steered chondrogenic differentiation of MSCs specifically towards one of the hyaline cartilage subtypes e.g. articular cartilage or growth plate cartilage. In a previous study, we compared the whole genome gene expression profiles of articular cartilage and growth and demonstrated that *GREM1*, *FRZB*, *DKK1* and *ABI3BP* mRNA was strongly enriched in articular cartilage and *PANX3* and *MMP13* mRNA transcripts were enriched in growth plate cartilage. In the current study we investigated if the expression of these genes is different between MSCs undergoing chondrogenic differentiating in either hypoxic or normoxic culture conditions. *GREM1*, *FRZB*, *DKK1* and *ABI3BP* mRNA were robustly increased under hypoxic conditions, while under normoxic conditions these genes did not increase significantly (figure 8.5B). Furthermore, *PANX3* and *MMP13* mRNA levels were strongly increased under normoxic conditions compared to hypoxic conditions (figure 8.5C). ELISA assays demonstrated that *GREM1*, *FRZB* and *DKK1* protein levels corroborated with the found trends on the mRNA level. The protein levels of all three secreted proteins were significantly higher after 35 days of chondrogenic differentiation under hypoxia compared to normoxia (figure 8.5D). Together this suggested that compared to normoxia, hypoxia up regulated the expression of both typical hyaline cartilage markers and articular cartilage-enriched genes while decreasing the expression of growth plate cartilage-enriched genes in MSCs undergoing chondrogenesis.

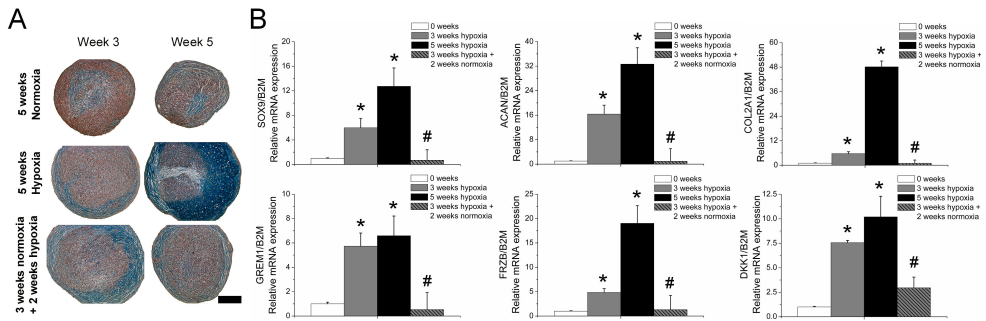


Figure 8.6: MSCs underwent chondrogenic differentiation for 5 weeks in normoxia, 5 weeks in hypoxia or in 3 weeks in hypoxia followed by 2 weeks of normoxia. (A) Histological analysis of GAGs using alcian blue and nuclear red on midsagittal sections of MSC micromasses, which were chondrogenically differentiated for 3 or 5 weeks. (B) Gene expression analysis of the articular cartilage markers *SOX9*, *ACAN* and *COL2A1* and (C) the articular enriched secreted antagonists *GREM1*, *FRZB* and *DKK1*. Data represent the mean of 3 donors each measured in triplicate \pm SD. * = $P < 0.05$. Black bars indicate $100 \mu\text{m}$

8.3.6 Continued hypoxia is needed to retain chondrogenic stimulus

We next explored whether transient exposure to hypoxia was sufficient to steer chondrogenically differentiating MSCs towards a more articular cartilage-like phenotype. MSCs were differentiated for 5 weeks in normoxia, 5 weeks in hypoxia or in 3 weeks in hypoxia followed by 2 weeks of normoxia. Hypoxia progressively enhanced GAG deposition and increased *SOX9*, *ACAN*, *COL2A1*, *GREM1*, *FRZB* and *DKK1* mRNA levels. However, when the hypoxic stress was alleviated after three weeks, it reversed the chondrogenic benefit generated by the initial exposure to hypoxia as witnessed by decreased GAG deposition (figure 8.6A). Moreover, when three weeks of hypoxic conditions were followed by two weeks of normoxic conditions, the increased mRNA levels of chondrogenic genes dropped to levels found in undifferentiated MSCs (figure 8.6B).

8.3.7 Delayed hypoxia stimulus is sufficient to induce a shift in gene expression profile

Next we investigated whether hypoxia during the first weeks was essential for the more robust chondrogenic differentiation when MSCs were differentiated under hypoxic conditions. Therefore, we compared mRNA levels of chondrogenically differentiating MSCs cultured for 5 weeks in normoxia, 5 weeks in hypoxia or 2 weeks in normoxia followed by 3 weeks in hypoxia. Again, *SOX9*, *ACAN*, *COL2A1*, *GREM1*, *FRZB* and *DKK1* mRNA levels were higher after 5 weeks of chondrogenesis under

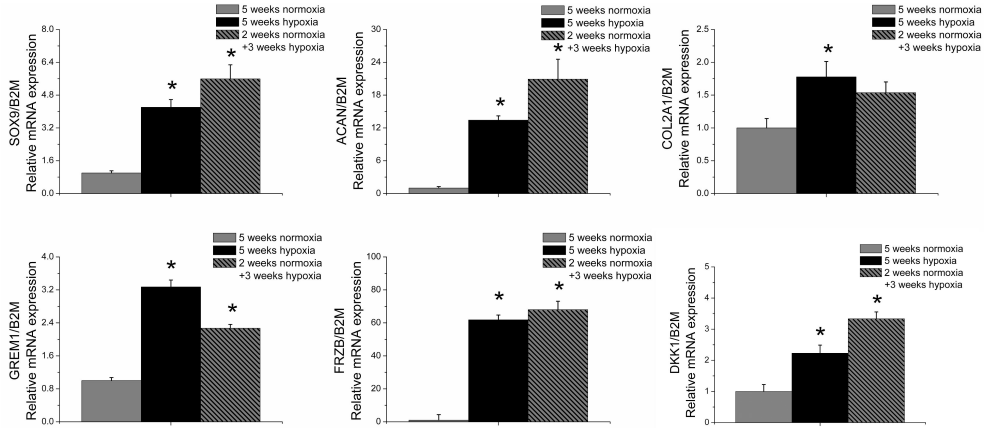


Figure 8.7: MSCs underwent chondrogenic differentiation in 5 weeks in normoxia, 5 in weeks hypoxia or 2 weeks in normoxia followed by 3 weeks in hypoxia. (A) mRNA levels of articular cartilage matrix components *SOX9*, *ACAN* and *COL2A1* and (B) the secreted antagonists *GREM1*, *FRZB* and *DKK1* were investigated using qPCR. Data represent the mean of 3 donors each measured in triplicate +/- SD. * = $P < 0.05$.

hypoxic conditions compared to normoxic conditions (figure 8.7). This underlined the reproducibility of our findings. Importantly, 2 weeks of normoxia followed by 3 weeks of hypoxia was as effective as culturing pellets for 5 weeks in hypoxia. This suggested that hypoxia stimulated the chondrogenic and articular cartilage-like phenotype only after the initial chondrogenesis had taken place.

8.4 Discussion

Embryological development of hyaline cartilage occurs under hypoxic conditions, while its terminal hypertrophic differentiation is correlated with normoxic conditions. Mimicking this environmental factor *in vitro* has shown similar effects. Specifically, chondrogenic differentiation under hypoxic conditions results in enhanced cartilage formation, while chondrogenic differentiation under normoxic conditions yields hypertrophic cartilage [9, 21, 22]. In fact, hypoxic culture conditions suppress hypertrophic differentiation [23, 24].

Indeed, in our study we demonstrated that hypoxia augmented hyaline cartilage formation. More importantly, we provided evidence that hypoxia steered the gene expression profile of chondrogenically differentiating MSCs towards a more articular cartilage-like than growth plate-like profile. In particular, we previously identified the factors *GREM1*, *DKK1* and *FRZB* that were enriched in articular cartilage compared to other forms of hyaline cartilage, and which were able to inhibit hypertrophic differentiation [Chapter 4]. Chondrogenic differentiation of MSCs under standard

culture conditions did not induce the expression of these genes. In fact, *GREM1* and *DKK1* mRNA levels were down regulated under normoxic culture conditions. Here, we demonstrated that hypoxic conditions were essential to induce these articular markers.

Varying environmental conditions like oxygen tension might present an efficient way to direct MSC differentiation into specific tissue subtypes. For example, by inducing cartilage formation under hypoxic conditions MSCs may generate a more articular cartilage-like tissue that could be used for treatment of articular cartilage defects. In contrast, by inducing cartilage formation in normoxia, cartilage with more growth plate like characteristics is formed which may be better suited for treatment of critical bone defects due to the propensity to undergo endochondral ossification. However, although oxygen levels efficiently generate gene expression profiles similar to those found in articular cartilage or hypertrophic growth plate cartilage, it remains to be proven whether a change in oxygen level is sufficient to ensure or prevent hypertrophic differentiation and subsequent endochondral ossification of the formed hyaline cartilage *in vivo*. Future studies should address this important and clinically relevant topic.

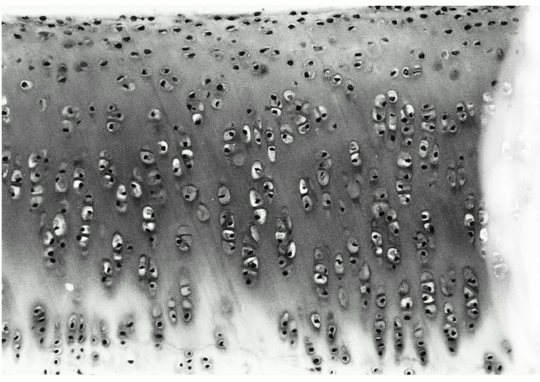
Alternatively, hypoxic culture conditions can be utilized for expanding or preconditioning MSCs. MSCs in hypoxic low density cultures displayed superior expansion capabilities compared to traditional methods [25]. Moreover, hypoxia maintained the multipotency of MSCs even in long term cultures [26]. This was emphasized by the increase in chondrogenic potential of MSC expanded under hypoxic conditions compared to those that were expanded under normoxic conditions [27].

Taken together, in the present study we demonstrated that reduction of oxygen tension boosted the chondrogenic differentiation of human bone-marrow derived MSCs in pellet cultures in the presence of TGF β 3. In addition, we showed that differentiation in hypoxia also steered the differentiation into a more articular cartilage-like tissue rather than a growth plate-like tissue. In conclusion variation of the oxygen tension might be a critical factor to consider in MSC differentiation protocols.

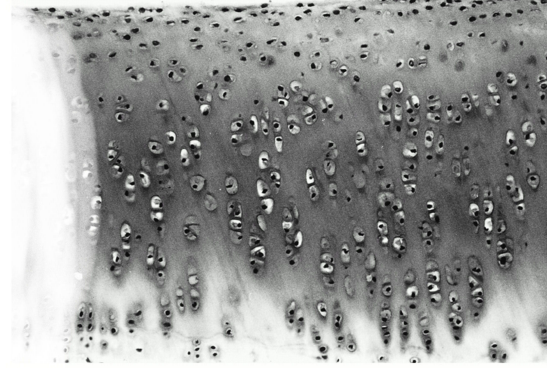
References

1. Jones, D.G. and L. Peterson, Autologous chondrocyte implantation. *J Bone Joint Surg Am*, 2006. 88(11): p. 2502-20.
2. Cole, B.J., C. Pascual-Garrido, and R.C. Grumet, Surgical management of articular cartilage defects in the knee. *J Bone Joint Surg Am*, 2009. 91(7): p. 1778-90.
3. Pittenger, M.F., et al., Multilineage potential of adult human mesenchymal stem cells. *Science*, 1999. 284(5411): p. 143-7.
4. De Bari, C., et al., Multipotent mesenchymal stem cells from adult human synovial membrane. *Arthritis Rheum*, 2001. 44(8): p. 1928-42.
5. Hass, R., et al., Different populations and sources of human mesenchymal stem cells (MSC): A comparison of adult and neonatal tissue-derived MSC. *Cell Commun Signal*, 2011. 9: p. 12.
6. Jukes, J.M., et al., Endochondral bone tissue engineering using embryonic stem cells. *Proc Natl Acad Sci U S A*, 2008. 105(19): p. 6840-5.
7. Steck, E., et al., Mesenchymal stem cell differentiation in an experimental cartilage defect: restriction of hypertrophy to bone-close neocartilage. *Stem Cells Dev*, 2009. 18(7): p. 969-78.
8. Koga, H., et al., Synovial stem cells are regionally specified according to local microenvironments after implantation for cartilage regeneration. *Stem Cells*, 2007. 25(3): p. 689-96.
9. Pelttari, K., et al., Premature induction of hypertrophy during in vitro chondrogenesis of human mesenchymal stem cells correlates with calcification and vascular invasion after ectopic transplantation in SCID mice. *Arthritis Rheum*, 2006. 54(10): p. 3254-66.
10. Jikko, A., et al., Inhibition of chondrocyte terminal differentiation and matrix calcification by soluble factors released by articular chondrocytes. *Calcif Tissue Int*, 1999. 65(4): p. 276-9.
11. Blanke, M., et al., Transplanted chondrocytes inhibit endochondral ossification within cartilage repair tissue. *Calcif Tissue Int*, 2009. 85(5): p. 421-33.
12. Fischer, J., et al., Human articular chondrocytes secrete parathyroid hormone-related protein and inhibit hypertrophy of mesenchymal stem cells in coculture during chondrogenesis. *Arthritis Rheum*, 2010. 62(9): p. 2696-706.
13. Zuscik, M.J., et al., Regulation of chondrogenesis and chondrocyte differentiation by stress. *J Clin Invest*, 2008. 118(2): p. 429-38.
14. Provot, S., et al., Hif-1alpha regulates differentiation of limb bud mesenchyme and joint development. *J Cell Biol*, 2007. 177(3): p. 451-64.
15. Schodel, J., et al., High-resolution genome-wide mapping of HIF-binding sites by ChIP-seq. *Blood*, 2011. 117(23): p. e207-17.
16. Malladi, P., et al., Hypoxia inducible factor-1alpha deficiency affects chondrogenesis of adipose-derived adult stromal cells. *Tissue Eng*, 2007. 13(6): p. 1159-71.
17. Morita, K., et al., Reactive oxygen species induce chondrocyte hypertrophy in endochondral ossification. *J Exp Med*, 2007. 204(7): p. 1613-23.
18. Both, S.K., et al., A rapid and efficient method for expansion of human mesenchymal stem cells. *Tissue Eng*, 2007. 13(1): p. 3-9.
19. Heinrichs, C., et al., Dexamethasone increases growth hormone receptor messenger ribonucleic acid levels in liver and growth plate. *Endocrinology*, 1994. 135(3): p. 1113-8.
20. Szklarczyk, D., et al., The STRING database in 2011: functional interaction networks of proteins, globally integrated and scored. *Nucleic Acids Res*, 2011. 39(Database issue): p. D561-8.
21. Khan, W.S., A.B. Adesida, and T.E. Hardingham, Hypoxic conditions increase hypoxia-

- inducible transcription factor 2alpha and enhance chondrogenesis in stem cells from the infrapatellar fat pad of osteoarthritis patients. *Arthritis Res Ther*, 2007. 9(3): p. R55.
22. Kanichai, M., et al., Hypoxia promotes chondrogenesis in rat mesenchymal stem cells: a role for AKT and hypoxia-inducible factor (HIF)-1alpha. *J Cell Physiol*, 2008. 216(3): p. 708-15.
23. Hirao, M., et al., Oxygen tension regulates chondrocyte differentiation and function during endochondral ossification. *J Biol Chem*, 2006. 281(41): p. 31079-92.
24. Ronziere, M.C., et al., Chondrogenic potential of bone marrow- and adipose tissue-derived adult human mesenchymal stem cells. *Biomed Mater Eng*, 2010. 20(3): p. 145-58.
25. Tsai, C.C., et al., Hypoxia inhibits senescence and maintains mesenchymal stem cell properties through down-regulation of E2A-p21 by HIF-TWIST. *Blood*, 2011. 117(2): p. 459-69.
26. Basciano, L., et al., Long term culture of mesenchymal stem cells in hypoxia promotes a genetic program maintaining their undifferentiated and multipotent status. *BMC Cell Biol*, 2011. 12: p. 12.
27. Sheehy, E.J., C.T. Buckley, and D.J. Kelly, Oxygen tension regulates the osteogenic, chondrogenic and endochondral phenotype of bone marrow derived mesenchymal stem cells. *Biochem Biophys Res Commun*, 2011.



9



Chapter 9

Trophic effects of mesenchymal stem cells increase chondrocyte proliferation and matrix formation

Ling Wu, Jeroen Leijten, Nicole Georgi, Janine Post, Clemens van Blitterswijk and Marcel Karperien

9

Given a choice between two theories, take the one which is funnier.
Blore's Razor

Abstract

Previous studies showed that co-culture of primary chondrocytes with various sources of multipotent cells results in a higher relative amount of cartilage matrix formation than cultures containing only chondrocytes.

The aim of this study is to investigate the mechanism underlying this observation. We used co-culture pellet models of human mesenchymal stem cells (hMSCs) and human primary chondrocytes (hPCs) or bovine primary chondrocytes (bPCs) and studied the fate and the contribution to cartilage formation of the individual cell populations during co-culture. Enhanced cartilage matrix deposition was confirmed by histology and quantification of total glycosaminoglycan (GAG) deposition. Species specific quantitative PCR (qPCR) demonstrated that cartilage matrix gene expression was mainly from bovine origin when bPCs were used. Short tandem repeat (STR) analysis and species specific qPCR analysis of genomic DNA demonstrated the near complete loss of MSCs in co-culture pellets after 4 weeks of culture. In co-culture pellets of immortalized MSCs (iMSCs) and bPCs, chondrocyte proliferation was increased, which was partly mimicked using conditioned medium, and simultaneously preferential apoptosis of iMSCs was induced.

Taken together, our data clearly demonstrate that in pellet co-cultures of MSCs and primary chondrocytes, the former cells disappear over time. Increased cartilage formation in these co-cultures is mainly due to a trophic role of the MSCs in stimulating chondrocyte proliferation and matrix deposition by chondrocytes rather than MSCs actively undergoing chondrogenic differentiation.

9.1 Introduction

Articular cartilage repair is a challenge due to the inability of cartilage to repair itself after damage. Autologous chondrocyte implantation (ACI) has become the golden standard treatment for large-size cartilage defects [1, 2]. However, ACI creates donor-site injury and is dependent on two-dimensional expansion of isolated chondrocytes resulting in chondrocyte dedifferentiation [3].

To reduce the number of chondrocytes needed in ACI, a partial substitution of chondrocytes with pluripotent stem cells is a promising strategy. It has been reported that co-culture of bone marrow mesenchymal stem cells (MSCs) and articular chondrocytes enhanced matrix deposition [4-6] even in absence of the chondrogenic factors Transforming Growth Factor β (TGFB) and dexamethasone (dex) [7]. Increased cartilage matrix formation was also found in co-culture of chondrocytes with other cell types, such as adipose-tissue derived stem cells, human embryonic stem cells and meniscus cells [8-11].

MSCs are promising for tissue repair because of their multi-lineage differentiation capacity [12]. Because of their importance in the development of articular cartilage, MSCs are a potential source for co-culture with chondrocytes. It is hypothesized that MSCs repair damaged tissue by differentiating into tissue specific cells replacing lost cells [13]. However, evidence suggests that differentiation into tissue specific cells cannot fully explain the benefits of transplanted MSCs in remodeling and recovery of damaged or lost tissue [14-16]. These studies point to a central role of MSCs in tissue repair as trophic mediators, secreting factors promoting tissue specific cells to restore the damaged or lost tissue [17, 18].

Two explanations have been proposed to explain increased cartilage formation in co-cultures of MSCs and articular chondrocytes. First, it has been suggested that increased cartilage formation in co-cultures is due to chondrogenic differentiation of MSCs stimulated by factors secreted by chondrocytes. Indeed, chondrocyte conditioned medium can induce chondrogenic differentiation of MSCs directly and in transwell cultures [19, 20]. However, it is unclear whether such an effect also occurs in co-cultures in which the cells are in direct cell-cell contact. Second, studies have hypothesized that the increased cartilage matrix formation is due to stimulation of the chondrocytes by MSCs [6]. Scientific evidence for this hypothesis is rather limited due to the inability to distinguish between the contributions of the individual cell populations to cartilage formation.

In this study we have addressed these issues by setting up pellet co-culture models of human MSCs (hMSCs) and either human (hPCs) or bovine primary chondrocytes (bPCs). Using a xenogenic system allowed us to determine the contribution of each cell population to the increased cartilage formation by using species specific gene expression analysis, whereas xenogenic specific effects were excluded in the human co-culture system. We examined chondrogenic gene expression, cell apoptosis and cell proliferation in human and bovine cell populations. Our data clearly demonstrates that the increased cartilage deposition in co-cultures is mainly due to a trophic role of the MSCs in stimulating chondrocyte proliferation and matrix deposition rather than MSCs actively undergoing chondrogenic differentiation.

9.2 Materials and Methods

9.2.1 Cell culture and expansion

Bovine primary chondrocytes (bPCs) were isolated from full-thickness cartilage knee biopsies of female calves of approximately 6 months old. Cartilage was separated and digested as previously described [21]. Human primary chondrocytes (hPCs) were obtained from full thickness cartilage dissected from knee biopsies of a patient undergoing total knee replacement as published previously [11]. Mesenchymal stem cells were isolated from aspirates as described previously [22]. The use of bone marrow aspirates and human knee biopsies was approved by a local Medical Ethical Committee. Donor information of human primary cells are available upon request. We define the primary cells (bPCs, hPCs and hMSCs) in this chapter as cells with low passage number without immortalization. iMSCs were kindly provided by Dr. O. Myklebost (Oslo University Hospital, Norway).

To form high density micro mass cell pellets, 200,000 cells per well were seeded in a round bottom 96 wells plate in chondrocyte proliferation medium (DMEM supplemented with 10% FBS, 1non-essential amino acids, 0.2 mM ascorbic acid 2-phosphate (AsAP), 0.4 mM proline, 100 U penicillin /ml and 100 $\mu\text{g}/\text{ml}$ streptomycin) or chondrogenic differentiation medium (DMEM supplemented with 40 $\mu\text{g}/\text{mL}$ of proline, 50 $\mu\text{g}/\text{mL}$ ITS-premix, 50 $\mu\text{g}/\text{mL}$ of AsAP, 100 $\mu\text{g}/\text{mL}$ of Sodium Pyruvate, 10 ng/mL of TGF-3, 10⁻⁷ M of dexamethasone, 100 U penicillin/ml and 100 $\mu\text{g}/\text{ml}$ streptomycin) and centrifuged for 3 min at 2000 rpm. Medium was refreshed twice a week. For co-cultures, iMSCs or hMSCs and bPCs or hPCs were mixed at ratios of 80/20% and 50/50%. All reagents used for were purchased from Invitrogen (Paisley, UK) unless otherwise stated. Common chemicals were purchased from Sigma-Aldrich (Germany).

9.2.2 Histology

Cell pellets were fixed with 10% formalin for 15 minutes and embedded in Paraffin using routine procedures. Sections of 5 μm were cut and stained for sulfated glycosaminoglycans (GAG) with alcian blue combined with counterstaining of nuclear fast red to visualize nuclei, or stained with toluidine blue alone.

9.2.3 Quantitative GAG and DNA assay

Cell pellets (N=6) were washed with PBS and frozen overnight at -80°C. Subsequently, they were digested and measured for GAG quantification as previously reported [11]. Relative cell number was determined by quantification of total DNA using a CyQuant DNA Kit, according to the manufacturer's instructions.

9.2.4 DNA isolation, RNA isolation and quantitative PCR

Total DNA was isolated from pellet cultures with the QIAamp DNA Mini Kit (Qiagen) according to the manufacturer's protocol. Total RNA was isolated from pellet culture

with the RNeasy Mini Kit (Qiagen). One microgram of total RNA was reverse-transcribed into cDNA using the iScript cDNA Synthesis kit (Bio-Rad). Primers sequences are available on request.

9.2.5 Cell tracking with organic fluorescent dyes

The organic fluorescent dyes, CM-DiI and CFSE were used for cell tracking in co-cultures. Cells were labeled according to the manufacturer's protocols.

9.2.6 EdU and TUNEL staining

For labeling of newly synthesized DNA, EdU (5-ethynyl-2'-deoxyuridine) was added to the culture media at a concentration of 10 μ M, 24 hours before harvesting the samples. Cell pellets were then washed with PBS and fixed with 10% formalin for 15 min. Samples were embedded in cryomatrix, and cut into 10 μ m sections with a cryotome (Shandon). Sections were permeabilized and stained for EdU with Click-iT EdU Imaging Kit. Cryosections were also stained for DNA fragments with DeadEnd Fluorometric TUNEL System (Promega). Nuclei were counterstained with Hoechst 33342.

9.2.7 Image acquisition and analysis

All fluorescent images were taken with a BD pathway 435 confocal microscope (BD Biosciences), unless otherwise stated. Using montage capture, images of high resolutions were obtained covering the entire section of a pellet. Separate images were captured using BP536/40 (Alexa 488), BP593/40 (DiI) and LP435 (Hoechst 33342) and pseudocolored green, red and blue respectively. ImageJ software [23] was used for cell counting. Briefly, we manually set a threshold to avoid artifacts. The number of green cells, red cells, green + red cells and total cells were counted by running plug-ins written in macro language of ImageJ (available on request). Values represent the mean +/- standard error of at least 3 biological replicates.

9.2.8 Preparation of conditioned medium

For conditioned medium, DMEM was incubated with iMSCs of 90% confluence for 48 hours, passed through a 0.22 μ m filter, and stored at -20°C. Upon usage, conditioned medium was thawed, transferred to Amicon Ultra-15 Centrifugal Filter Unites (Millipore, Billerica, MA) with a cut off of 3000D Nominal Molecular Weight Limit, and centrifuged at 4000 g for 40 minutes. The concentrated solute (still named conditioned medium) was supplemented with all chemicals needed for chondrocyte proliferation medium (see cell culture and expansion).

9.2.9 Short Tandem Repeats (STR) analysis

Genomic DNA samples were extracted from pellets with the QIAamp DNA Mini Kit (Qiagen). The sixteen loci of the kit PowerPlex 16 System (Promega) were amplified,

typed, sequenced and analyzed by ServiceXS B.V. (Leiden, the Netherlands). Specific alleles for the donor of hMSCs and the donor of hPCs were found in six loci (D7S820, D5S818, D13S317, D16S539, CSF1PO and Penta D). These alleles were used to define the origin of cells in allogeneic co-culture of hMSCs and hPCs. The amount of DNA present for each donor was calculated from the areas of the electropherogram for each locus of hMSCs' or hPCs' specific alleles and the ratio of hMSCs and hPCs was determined.

9.2.10 Statistical analysis

For the experiments using primary human cells (hMSCs and hPCs), three donors were tested, which showed similar results. Each experiment was performed at least in triplicate. So, only data from one representative donor is shown. Experiments using iMSCs and bPCs were performed at least in triplicate with similar data. A representative experiment is shown. Differences between different ratios of co-cultures of MSCs and primary chondrocytes were examined for statistical significance with one-way analysis of variance (ANOVA) followed by Tukey HSD Tests. Comparisons between iMSCs and bPCs in the same conditions were made using the Student's test. The level of significance was set at $P < 0.05$ unless stated otherwise.

9.3 Results

9.3.1 Co-culturing hMSCs with hPCs enhanced cartilage matrix formation

In order to study the contribution of MSC and chondrocytes on cartilage matrix formation we co-cultured human MSCs (hMSC) with human primary chondrocytes (hPCs) from different donors. After 4 weeks co-culture in chondrogenic differentiation medium, histology (Figure 9.1A) and GAG assay (Figure 9.1B) indicated that co-culture of hMSCs and hPCs increased cartilage formation. To determine the ratio of MSC and PC after prolonged co-culture we isolated genomic DNA, and STR loci with different repeat sizes in the different donors were analyzed. The results of locus D7S820 (Figure 9.1C) as well as analysis of other 5 STR loci (data not shown), indicated that the proportion of hMSCs decreased significantly. In order to elucidate the mechanisms behind the apparent loss of MSC in our co-culture system, we used xenogenic co-cultures of hMSCs and bPCs to enable identification of the role of each of the cell types in co-culture in pellet cultures. An advantage of these xenogenic co-cultures is that this system is more stable than co-culture systems that depend on donor hPCs isolated after total knee replacement surgery.

9.3.2 Xenogenic co-culture of hMSC and bPCs show enhanced chondroinduction

To allow long term cell tracking in co-cultures, we setup a pellet co-culture model of hMSCs and bPCs. Cells were mixed in different ratios and pellet culture was

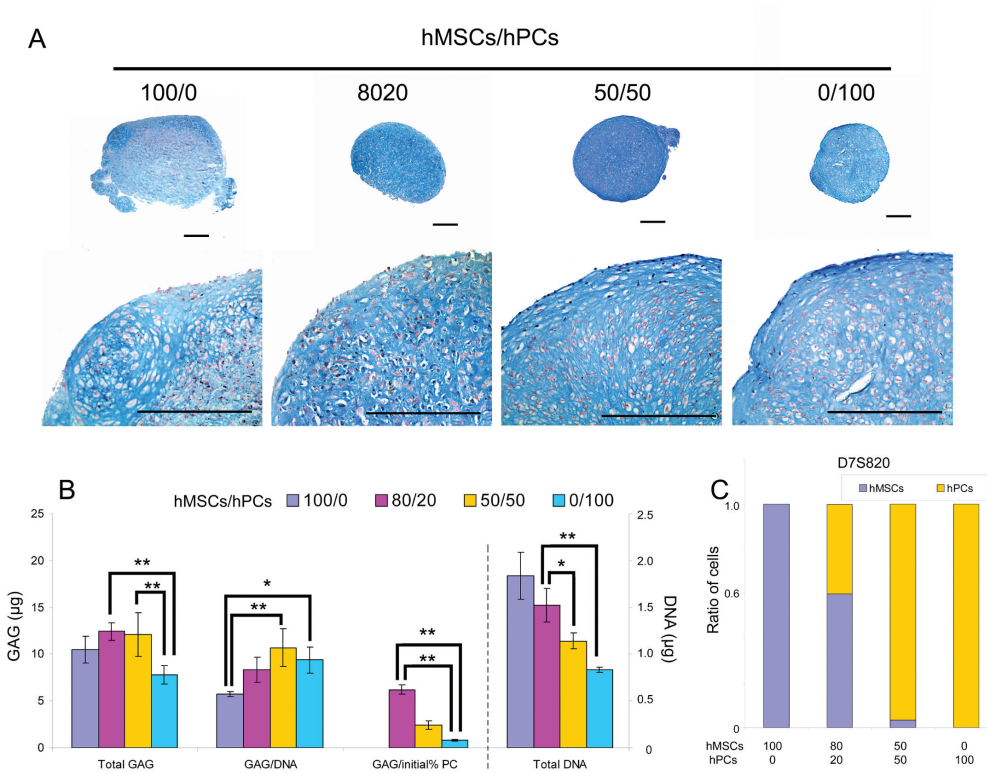


Figure 9.1: hMSCs / hPCs co-cultures enhance cartilage matrix formation and show decrease of MSCs after 4 weeks of culture. (A) Alcian blue staining indicates the presence of GAG. Pellets were cultured in chondrogenic differentiation medium (as described in supplementary materials) for 4 weeks before examination. Scale bar indicates 200 μm . (B) Biochemical assay shows an increase in GAG in co-culture pellets. Amount of GAG and DNA of pellets (N=6) were measured 4 weeks after culture in chondrogenic differentiation medium. Ratios of hMSCs and bPCs are indicated by different colors of bars. Scale on the left is for Total GAG, GAG/DNA and GAG/initial 10% PC, while scale on the right is for Total DNA. Asterisk represents $P < 0.05$. Double asterisk represents $P < 0.01$. NS=Not Significant. Error bar reflects Standard Deviation (S. D.). (C) Analysis of STR locus D7S820 reflects ratios of hMSCs and hPCs after 4 weeks coculture. Initial ratio of hMSCs and hPCs are indicated at the bottom of the bar chart.

performed in chondrocyte proliferation medium lacking TGF β and dexamethason. After 4 weeks, histology and GAG quantification were performed to evaluate cartilage formation. Alcian blue staining indicated the presence of GAG in all experimental groups except in the 100% hMSCs pellets (Fig. 9.2A left panel) in concordance with the absence of chondrogenic factors in the medium. In the positively stained areas at higher magnification (Fig. 9.2A right panel), cells showed a typical chondrocyte morphology and embedding in lacunae. Similar data were obtained by toluidine blue staining. GAG quantification showed a trend of decreased total GAG with increasing seeding percentage of hMSCs. However, when total GAG content was normalized to DNA or to the initial seeding percentage of bPCs, co-culture pellets showed significantly higher GAG content. Similar data were obtained when different MSC donors were used (data not shown). To avoid the effects of donor variation of primary cultured MSCs [24], we replaced hMSCs with a telomerase immortalized hMSC cell line (iMSCs). This cell line resembled primary cultured MSCs in their ability to differentiate into the adipogenic, osteogenic and chondrogenic lineages (data not shown), but had relatively low capacity of chondrogenic differentiation. As shown in Figure 9.2C and D, co-culture of bPCs with iMSCs for 4 weeks increased cartilage formation after correction for DNA content or initial seeding percentage of bPCs as compared to hMSCs. Despite the relatively low chondrogenic potential of iMSCs, increased cartilage matrix formation was observed in co-culture of bPCs and iMSCs. This demonstrated that iMSCs show comparable behavior to hMSCs in co-cultures with regard to enhanced cartilage formation, indicating that it is not the chondrogenic capacity of the MSCs that is responsible for enhanced chondroinduction.

9.3.3 Chondrocytes are located at the periphery of the cell pellet

We used organic fluorescent dyes to label individual cell populations in pellet co-cultures for short term cell tracking. Pellets were formed after 1 day of culture (Figure 9.3A). Rather than forming a homogenous pellet, both cell populations tended to segregate. This process continued in the following days and the dynamic cell pellets became more and more stable. After 4 days of co-culture, pellets were organized in a layer-like structure in which iMSCs resided predominantly in the core of the pellet and the bPCs, mixed with a sub-fraction of iMSCs, were predominantly found at the periphery. These observations are in agreement with the differential adhesion hypothesis which stipulates that mixed heterotypic cells rearrange to adopt a combination-specific anatomy [25]. From day 5 onwards, fluorescent dye transfer between labeled and non-labeled cells in the pellets became apparent as reported previously [26]. This made it impossible to perform long-term cell tracking in co-culture pellets using CM-DiI and/or CFSE labeling of cell populations. Enhanced cartilage matrix formation originates from bPCs.

After 1 day and 4 weeks of culture we isolated genomic DNA from the cell pellets and performed species specific qPCR for genomic GAPDH. As shown in figure 9.3B, after 1 day the ratio of genomic human and bovine DNA was in line with the seeding percentage of both cell populations. The percentage of human DNA was slightly higher which is most likely explained by faster aggregation of the iMSCs in pellets.

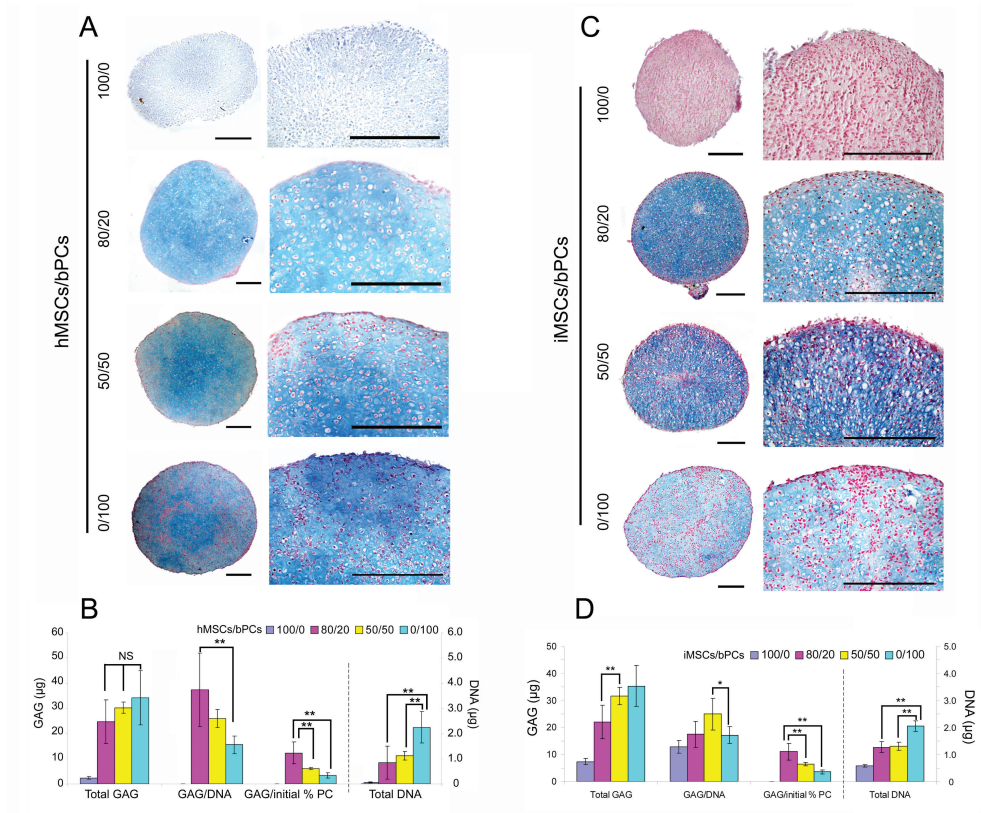


Figure 9.2: Co-culture of mesenchymal stem cells and chondrocytes increases cartilage matrix formation. (A) Alcian blue staining shows the presence of GAG in pellets cultured in chondrocytes proliferation medium. Ratios of hMSCs and bPCs are indicated on the left of the images. The left panel shows overviews of pellets, while the right panel shows magnified pictures. Scale bar indicates 200 µm. (B) Biochemical assay shows an increase in GAG in co-culture pellets. Amount of GAG and DNA of pellets (N=6) was measured 4 weeks after culture in chondrocyte proliferation medium. Ratios of hMSCs and bPCs are indicated by different colors of bars. Scale on the left is for Total GAG, GAG/DNA and GAG/initial 10% PC, while scale on the right is for Total DNA. Asterisk represents P<0.05. Double asterisk represents P<0.01. NS=Not Significant. Error bar reflects Standard Deviation (S. D.). (C) Alcian blue staining of pellets cultured in chondrocytes proliferation medium. Ratio of iMSCs and bPCs is indicated on the left of the images. The left panel shows overviews of pellets, while the right panel shows magnified pictures. Scale bar indicates 200 µm. (D) Biochemical assay of pellets (N=6) at 4 weeks after culture in chondrocyte proliferation medium. Ratios of iMSCs and bPCs are indicated by different colors of bars. Scale on the left is for Total GAG, GAG/DNA and GAG/initial 10% PC, while scale on the right is for Total DNA. Asterisk represents P<0.05. Double asterisk represents P<0.01. NS=Not Significant. Error bar reflects Standard Deviation (S. D.).

Remarkably, after 4 weeks of culture, the co-culture pellets contained predominantly DNA of bovine origin indicative for an overgrowth of bovine cells or a loss of human cells during the 4 week cell culture period. DNA analysis of co-culture pellets at 1, 2 and 3 weeks of culture demonstrated a steep drop in human DNA between 1 and 2 weeks with a further gradual decline at weeks 3 and 4 (data not shown).

An even more striking difference was found in mRNA isolated at 4 weeks. *Gapdh* mRNA in the co-culture pellets was from bovine origin (Figure 9.3C). Even in cell pellets with an initial seeding of 80% iMSCs, hardly any human mRNA was detected. Similar data were found in co-culture pellets of hMSCs and bovine chondrocytes after 4 weeks of culture also demonstrating the near absence of human DNA in the cell pellets, which is fully in line with the data obtained in co-culture pellets of iMSCs and bPCs (Figure 9.3D) and hMSC and hPC (Figure 9.1C). We next performed species specific qPCR to study the origin of the mRNA expression of chondrogenic genes in co-culture pellets (Figure 9.3F-G). At week 4, only expression of chondrogenic genes from bovine origin were detected in co-culture pellets. This data suggested that the cartilaginous matrix in co-culture pellets is from bovine origin. This observation, combined with the observation that in allogeneic co-cultures the percentage of MSCs decreased during prolonged culturing, suggests that the enhanced contribution of chondrocytes in the matrix formation may be due to PCs proliferation or MSC cell death.

9.3.4 iMSCs co-cultured with bPCs die via apoptosis

To determine whether MSC undergo apoptosis during prolonged cell culture we performed a fluorescent TUNEL assay. At week 1 and 2, high numbers of TUNEL positive cells were found in all cell pellets containing iMSCs, but not in pure bPCs cell pellets (Figure 9.4). TUNEL positive cells were predominantly present in the periphery of the pellets which is mostly composed of bPCs mixed with iMSCs (Figure 9.3A). Fewer TUNEL positive cells were found in the core of the pellet. Cell death in iMSC containing pellets started to increase significantly from day 5 onwards. From this time point cell tracking results by fluorescent labeling of cell populations became unreliable due to non-specific dye transfer. Since the TUNEL positive cells are predominantly found in iMSCs containing cell pellets and human DNA over time disappears from the cell pellets we concluded that cell death by apoptosis at least partially explains the disappearance of human DNA from co-culture cell pellets.

9.3.5 iMSCs stimulate chondrocyte proliferation in pellet co-cultures

We then examined cell proliferation in co-culture pellets using EdU incorporation. We focused on time points up to 3 days, in which organic fluorescent dyes are highly reliable for cell tracking [27]. bPCs were labeled with CM-DiI (red) to distinguish them from iMSCs. At day 1, EdU positive cells were evenly distributed over the pellet. At day 2 and day 3, EdU positive cells were predominantly found at the periphery of the pellets where red labeled bPCs resided (Fig. 9.5A). We determined

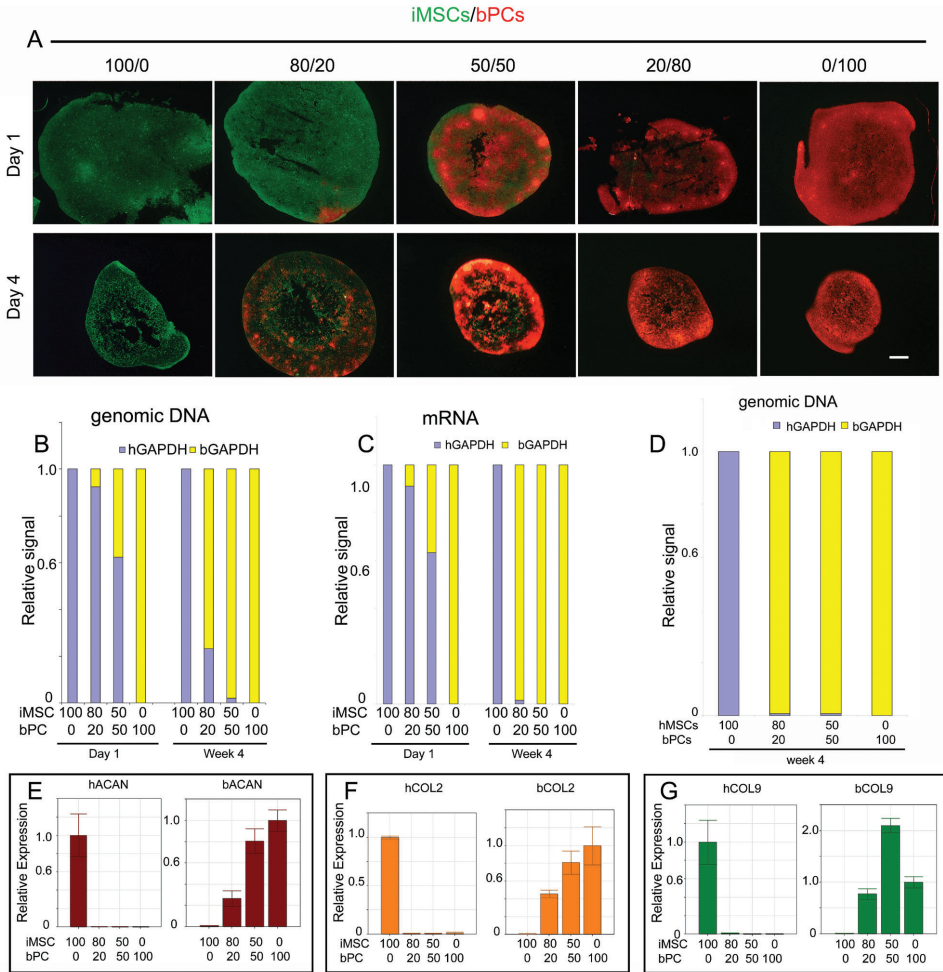


Figure 9.3: Cartilage matrix is from bovine origin. (A) Cell assembly of iMSCs and bPCs in co-culture pellets. iMSCs and bPCs were labeled with CFSE O (green) and CM-Dil (red) respectively, mixed at different ratios and then cultured in chondrocyte proliferation medium. At day 1 and day 4, pellets were harvested for cryosection. Images were made directly on the sections without any treatment, using a Nikon E300 fluorescent microscope. Scale bar represents 200 μm . (B) Species specific qPCR of GAPDH in co-cultures of iMSCs and bPCs at genomic DNA level. Genomic DNA was extracted from pellets (N=3) at day 1 and week 4. (C) Species specific qPCR of GAPDH in co-cultures of iMSCs and bPCs at mRNA level. RNA was extracted from pellets at day 1 and week 4. (D) Species specific qPCR of GAPDH in co-cultures of hMSCs and bPCs at genomic DNA level. Genomic DNA was extracted from pellets (N=3) at week 4. (E-G) Expression levels of *ACAN* (E), *COL2* (F) and *COL9* (G) were examined by species specific qPCR. RNA samples were extracted from pellets (N=3) cultured in chondrocyte proliferation medium for 4 weeks. Relative expression levels were obtained by normalization of human or bovine specific signals to cross species-specific *GAPDH* and β -*actin* signals. For human specific genes, values are relative amounts to 100/0 iMSC/bPC group. For bovine specific genes, values are relative amounts to 0/100 iMSC/bPC group. Error bar reflects Standard Deviation (S. D.).

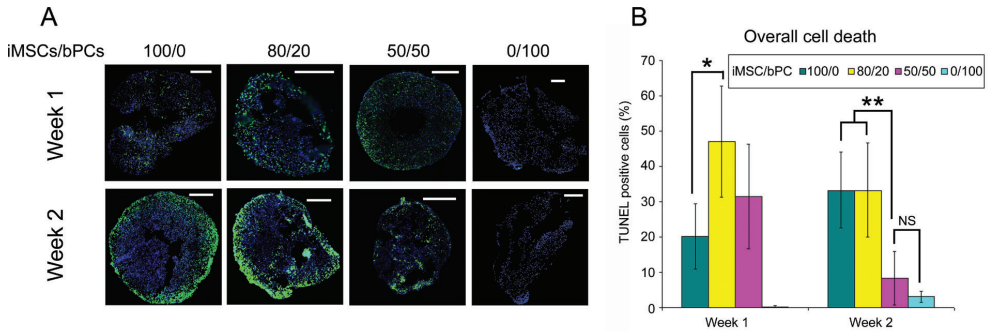


Figure 9.4: Preferential cell deaths of MSCs by apoptosis. (A) TUNEL staining of pellets. Cell pellets were cultured in chondrocyte proliferation medium for 1 week or 2 weeks before harvesting for cryosection. TUNEL positive cells were visualized with fluorescent labeling (green). Nuclei were counterstained with Hoechst 33342 (blue). Scale bar indicates 200 μm. (B) Quantification of TUNEL positive cells. Ratios of iMSCs and bPCs are indicated by bar colors. Data from 3 pellets were analyzed for statistic significance. Asterisk represents $P < 0.05$. Double asterisk represents $P < 0.01$. NS=Not Significant. Error bar reflects Standard Deviation (S. D.).

the percentage of EdU positive iMSCs or bPCs in co-cultures. Generally, co-culture increased the proliferation of both iMSCs and bPCs (Figure 9.5B and C). Interestingly, the percentage of EdU positive bPCs was higher than that of iMSCs in co-cultures of 80 % iMSCs and 20 % bPCs starting from day 2 onwards (Figure 9.5B).

Similar data were obtained in dye swap experiments in which iMSCs instead of bPCs were labeled with CM-DiI demonstrating that enhanced proliferation of bPCs in co-culture pellets was not an artifact of cell labeling. These data show that the change in ratio between MSC and PC during prolonged co-culturing is in addition to apoptosis also due to increased proliferation of chondrocytes in pellet cultures.

9.3.6 iMSC conditioned medium increases bPCs proliferation and matrix formation

To examine the effects of secreted factors, we compared proliferation and matrix formation of bPCs when cultured in proliferation medium or in 50 100 times concentrated iMSC conditioned medium. The concentrate was dissolved in chondrocyte proliferation medium. Pellets of bPCs cultured for 1 week in iMSCs conditioned proliferation medium showed higher EdU incorporation than cells cultured in non-conditioned proliferation medium (Figure 9.6A and B). Like in co-culture pellets EdU positive cells were predominantly found in the periphery of the pellet. Higher EdU incorporation was associated with increased DNA content. Additionally, total GAG content showed an increase, but GAG corrected for DNA was not significantly different between the two conditions (Figure 9.6C).

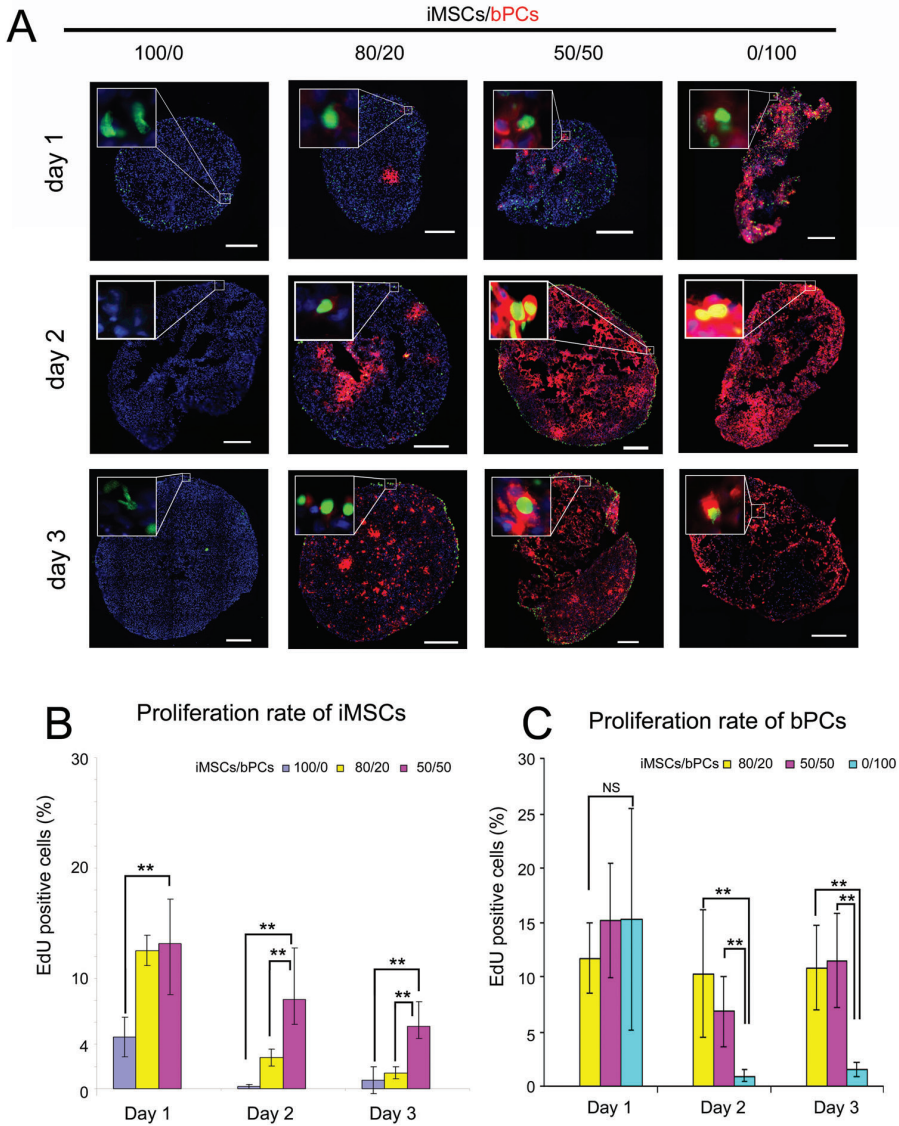


Figure 9.5: MSCs stimulate chondrocyte proliferation in co-culture pellets. (A) EdU staining of pellets at day 1, day 2 and day 3. bPCs were labeled with CM-DiI (red). EdU incorporation into newly synthesized DNA was visualized by Alexa 488 (green). Nuclei were counterstained with Hoechst 33342 (blue). Scale bar indicates 200 μ m. (B) Quantification of EdU positive iMSCs in all conditions. The initial ratios of MSCs and bPCs are indicated by bar colors. Asterisk represents $P < 0.05$. Data from 3 pellets were analyzed for statistic significance. Double asterisk represents $P < 0.01$. NS=Not Significant. Error bar reflects Standard Deviation (S. D.). (C) Quantification of EdU positive bPCs in all conditions. The initial ratios of MSCs and bPCs are indicated by bar colors. Data from 3 pellets were analyzed for statistic significance. Asterisk represents $P < 0.05$. Double asterisk represents $P < 0.01$. NS=Not Significant. Error bar reflects Standard Deviation (S. D.).

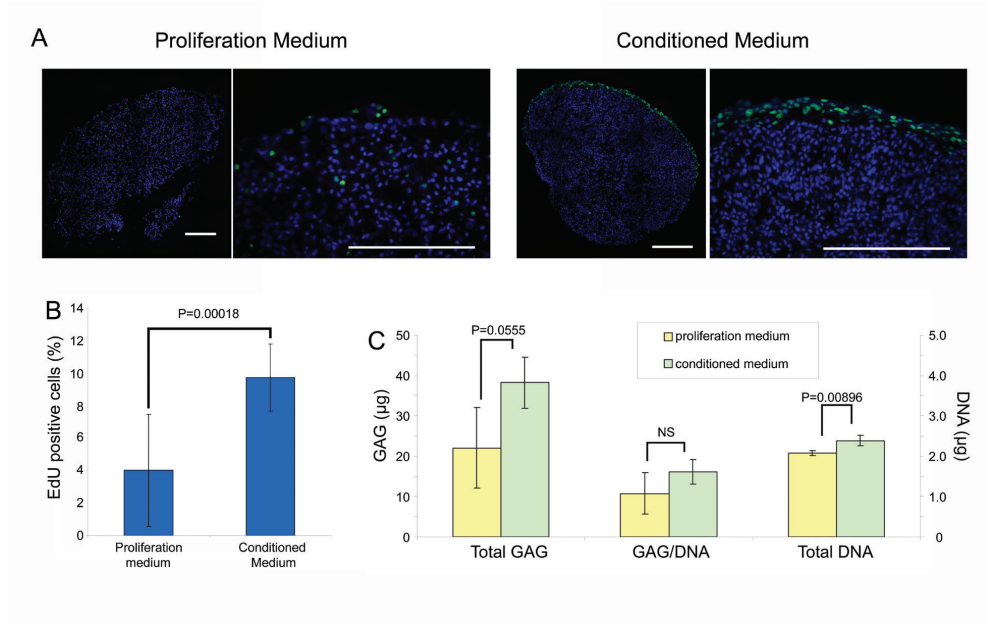


Figure 9.6: Conditioned medium of iMSCs enhances proliferation of chondrocytes. (A) EdU staining of bPCs pellets at day 2 after culturing in chondrocyte proliferation medium or conditioned medium of iMSCs. EdU incorporation into newly synthesized DNA was visualized by Alexa 488 (green). Nuclei were counterstained with Hoechst 33342 (blue). Scale bar indicates 200 μm . (B) Quantification of EdU positive cells. Data from 3 pellets were analyzed for statistic significance. P-value indicated in the bar chart is calculated by student's t-test. (C) GAG and DNA assay were performed at week 1 after culturing in chondrocyte proliferation medium or conditioned medium of iMSCs. The left scale is for Total GAG and GAG/DNA, while the right scale is for Total DNA. P-values indicate on the graph were calculated with the Student's t-test. NS=Not Significant. Error bar reflects Standard Deviation (S. D.).

9.4 Discussion

It has been shown that conditioned medium of chondrocytes induced osteo-chondrogenic differentiation of MSCs [19] and co-culture of MSCs and chondrocytes in 3-dimensional environments induced chondrogenic gene expression in MSCs [28]. Based on these studies, it was suggested that the beneficial effects of co-culturing chondrocytes and MSCs in cartilage matrix formation are largely due to the differentiation of MSCs into chondrocytes. In this study, we show that pellet co-cultures of chondrocytes and MSCs in chondrocyte proliferation medium benefit cartilage formation. Furthermore, we observe a significant decrease in MSCs caused by a preferential cell death of MSC. After 4 weeks of culture this results in an almost homogeneous cartilage construct, in which mainly chondrocyte-derived cells reside. The beneficial effects of the pellet co-culture are largely due to stimulation of proliferation and matrix formation of chondrocytes induced by a trophic effect of the MSCs. Our investigation distinguishes itself from comparable studies, the design of which did not allow discrimination between the contributions of individual cell populations to cartilage matrix formation [5, 6]. Although we cannot completely rule out the possibility that a subset of MSCs differentiated into chondrocytes and directly participated in cartilage formation, our data suggests that this may apply to a minority of cells only.

In pellet co-cultures of hMSCs and bovine chondrocytes, one may argue that our observations are due to a species difference which may hamper the response of bovine chondrocytes to human MSCs and vice-versa. However, species specificity cannot explain our findings since similar observations were made in a fully human co-culture model, indicating that in both models comparable mechanisms are likely operational. In addition, we show that the mechanisms underlying these observations are not donor specific, but are due to cell type specific contribution of MSCs as well as the chondrocytes. As shown in this study, as well as in many other studies [5, 6, 11], co-culture of hMSCs or other cell types [29, 30] with xenogenic chondrocytes appears a good model to study cell specific contributions to tissue formation.

In our studies, we have used hTERT immortalized hMSCs [31] as well as primary hMSCs. The iMSCs used in this study had a reduced chondrogenic potential. This lack of chondrogenic capacity did not impair their ability to stimulate cartilage formation in pellet co-cultures, furthermore providing evidence that chondrogenic differentiation of MSC does not significantly contribute significantly to the enhanced cartilage formation. Furthermore, similar results were obtained with primary hMSCs. Our data do indicate that chondrogenic capacity of cells used in co-cultures is not essential for stimulation of cartilage formation by chondrocytes in line with previous observations [11]. In addition, our data suggests that the relatively old age (60+ years) of the MSC donors does not affect their ability to simulate cartilage formation in co-culture.

Cell proliferation in pellet co-cultures was studied using EdU incorporation in DNA of proliferating cells. Cell proliferation was significantly increased in co-culture pellets compared to pellets of pure cell populations. By using cell specific labeling techniques and dye swap experiments, it was shown that EdU was preferentially incorporated in chondrocytes, which reside predominantly in the periphery of the cell

pellet. This suggests that the MSCs are potent stimulators of chondrocyte proliferation in pellet co-cultures. Limited proliferation of cells was found in the core of the cell pellet in which predominantly MSCs resided. Since EdU is extremely small (252 Dalton), this molecule is likely to penetrate with high efficiency in the pellet [32], suggesting that the preferential EdU labeling of cells in the periphery of the pellets is not an artifact caused by diffusion limitation. It is assumed that absence of proliferating MSCs in the center of the pellets is likely due to space limitation in the compacted core creating an environment which is not permissive for cell division [33, 34].

In co-culture pellets significant numbers of TUNEL positive MSCs were observed after 1 and 2 weeks of culture suggesting that MSCs most likely died via apoptosis. Also in pellets composed of 100 % MSCs but not 100 % bPCs, significant TUNEL staining was observed. Cell labeling experiments in pellet co-cultures demonstrated that the majority of the TUNEL positive cells were hMSCs. This is in line with the STR and genomic DNA analysis at the end of the culture period showing the disappearance of the MSCs from the co-cultures over-time. Our data suggest that the disappearance of MSCs in pellet co-cultures is most likely caused by apoptosis. Interestingly, TUNEL positive cells were predominantly found in the periphery of the pellet in which MSCs co-resided with chondrocytes. TUNEL positivity was higher in co-culture pellets compared to pellets of pure cell populations. This suggested that in addition to suboptimal culture conditions of MSCs in pellets, the presence of chondrocytes may have contributed to the death of MSCs. This may be caused by secreting apoptosis-inducing cytokines [35]. Furthermore, changes in extracellular matrix (ECM) in pellet cultures as compared to natural ECM of MSCs may influence the fate of MSCs [36-38] and this may have contributed to the increased cell death. Other explanations for death of MSCs in pellets could be cell compaction, and nutrition or space limitation in pellets [39, 40]. However, the relatively low levels of TUNEL positive cells in the core of the pellet compared to the periphery suggests that nutrient or oxygen limitation, which are likely most pronounced in the core of the pellet, are insufficient to induce cell death.

We provide evidence that the induction of chondrocyte proliferation by MSCs is most likely caused by (a) secreted factor(s), since this effect was at least partly mimicked by using MSC conditioned medium.. It has been reported that MSCs secrete a broad range of growth factors and cytokines including interleukin-6 (IL-6), hepatocyte growth factor (HGF), and vascular endothelial growth factor (VEGF), which enhance cell viability and proliferation *in vitro* and restore functions of damaged tissue *in vivo* [41, 42]. IL-6, for example, has been described to induce cartilage repair by increasing chondrocyte proliferation and stimulation of expression of cartilage matrix proteins and BMP-7 [43]. On the other hand (a) secreted factor(s) by MSCs cannot fully explain increased cartilage formation in co-culture pellets, since the relative deposition of glycosaminoglycans per DNA was not significantly different between pellets cultured in proliferation medium and that in conditioned medium. This indicates that conditioned medium only stimulated chondrocyte proliferation but not relative GAG amount per DNA, such as observed in co-culture pellets. This is in line with other reports demonstrating a role of cell-cell contact in cartilage formation improvement in co-cultures [44-46]. Therefore, it is likely that in addition to the trophic effects

of MSCs mediated by secreted factors, enhanced cartilage formation in co-culture with chondrocytes is due to additional stimuli such as direct cell-cell contact or other secreted factors.

Such a role of the MSCs as trophic mediators in cartilage formation in co-culture pellets is in line with their proposed role in tissue repair in other tissues, such as brain [47, 48], heart [49-52], and kidney regeneration [53, 54]. By providing nutrients and growth factors, MSCs increase proliferation and differentiation of host-derived cells to help them to repair damaged tissues [55]. The results of the present study are in line with and extend these observations to cartilage tissue formation. We are the first to show that MSCs have a prominent role as trophic mediators to stimulate cartilage matrix formation in pellet co-cultures with chondrocytes.

Despite the success of ACI in treatment of large-size cartilage defects, the requirement of two operations separated by several weeks' expansion of chondrocytes in vitro, is a major drawback of this procedure [56]. The results of this study imply that culture expansion of chondrocytes may benefit from co-culturing with MSCs. The MSCs may not only stimulate proliferation, thereby shortening culture time, but simultaneously may help the chondrocytes to retain their phenotype by counteracting chondrocyte dedifferentiation [41, 42]. They further imply that a substantial part of the chondrocytes needed for ACI may be substituted with MSCs without decrease in cartilage matrix formation. This may pave the road for a single step surgery to repair large-size cartilage defects, in which chondrocytes are isolated, mixed with bone marrow cells from the same patient, loaded on a scaffold and directly re-implanted into the patient. Based on our ex vivo results, one may expect that in a few weeks the implant will consist mainly of chondrocytes and cartilage specific matrix.

In conclusion, our data clearly demonstrate that in pellet co-cultures of MSCs and primary chondrocytes, MSCs disappear over time. Increased cartilage formation in these co-cultures is mainly due to a trophic role of the MSCs in stimulating chondrocyte proliferation and matrix deposition by chondrocytes rather than MSCs actively undergoing chondrogenic differentiation.

References

1. Brittberg M, Lindahl A, Nilsson A, Ohlsson C, Isaksson O, Peterson L. Treatment of deep cartilage defects in the knee with autologous chondrocyte transplantation. *N Engl J Med.*331:889-95. 1994.
2. Peterson L, Minas T, Brittberg M, Lindahl A. Treatment of osteochondritis dissecans of the knee with autologous chondrocyte transplantation: results at two to ten years. *J Bone Joint Surg Am.*85-A Suppl 2:17-24. 2003.
3. Schnabel M, Marlovits S, Eckhoff G, Fichtel I, Gotzen L, Vecsei V, et al. Dedifferentiation-associated changes in morphology and gene expression in primary human articular chondrocytes in cell culture. *Osteoarthritis Cartilage.*10:62-70. 2002.
4. Gruber HE, Deepe R, Hoelscher GL, Ingram JA, Norton HJ, Scannell B, et al. Human adipose-derived mesenchymal stem cells: direction to a phenotype sharing similarities with the disc, gene expression profiling, and coculture with human annulus cells. *Tissue Eng Part A.*16:2843-60. 2010.
5. Mo XT, Guo SC, Xie HQ, Deng L, Zhi W, Xiang Z, et al. Variations in the ratios of co-cultured mesenchymal stem cells and chondrocytes regulate the expression of cartilaginous and osseous phenotype in alginate constructs. *Bone.*45:42-51. 2009.
6. Tsuchiya K, Chen G, Ushida T, Matsuno T, Tateishi T. The effect of coculture of chondrocytes with mesenchymal stem cells on their cartilaginous phenotype in vitro. *Materials Science & Engineering C-Biomimetic and Supramolecular Systems.*24:6. 2004.
7. Hendriks J, Riesle J, van Blitterswijk CA. Co-culture in cartilage tissue engineering. *J Tissue Eng Regen Med.*1:170-8. 2007.
8. Bigdeli N, Karlsson C, Strehl R, Concaro S, Hyllner J, Lindahl A. Coculture of human embryonic stem cells and human articular chondrocytes results in significantly altered phenotype and improved chondrogenic differentiation. *Stem Cells.*27:1812-21. 2009.
9. Gunja NJ, Athanasiou KA. Effects of co-cultures of meniscus cells and articular chondrocytes on PLLA scaffolds. *Biotechnol Bioeng.*103:808-16. 2009.
10. Hildner F, Concaro S, Peterbauer A, Wolbank S, Danzer M, Lindahl A, et al. Human adipose-derived stem cells contribute to chondrogenesis in coculture with human articular chondrocytes. *Tissue Eng Part A.*15:3961-9. 2009.
11. Hendriks J, Miclea R, Schotel R, de Bruijn E, Moroni L, Karperien M, et al. Primary chondrocytes enhance cartilage tissue formation upon co-culture with a range of cell types. *Soft Matter.*in press:DOI: 10.1039/C0SM00266F. 2010.
12. Jiang Y, Jahagirdar BN, Reinhardt RL, Schwartz RE, Keene CD, Ortiz-Gonzalez XR, et al. Pluripotency of mesenchymal stem cells derived from adult marrow. *Nature.*418:41-9. 2002.
13. Bruder SP, Fink DJ, Caplan AI. Mesenchymal stem cells in bone development, bone repair, and skeletal regeneration therapy. *J Cell Biochem.*56:283-94. 1994.
14. da Silva Meirelles L, Caplan AI, Nardi NB. In search of the in vivo identity of mesenchymal stem cells. *Stem Cells.*26:2287-99. 2008.
15. Dai W, Hale SL, Martin BJ, Kuang JQ, Dow JS, Wold LE, et al. Allogeneic mesenchymal stem cell transplantation in postinfarcted rat myocardium: short- and long-term effects. *Circulation.*112:214-23. 2005.
16. Noiseux N, Gnecci M, Lopez-Ilasaca M, Zhang L, Solomon SD, Deb A, et al. Mesenchymal stem cells overexpressing Akt dramatically repair infarcted myocardium and improve cardiac function despite infrequent cellular fusion or differentiation. *Mol Ther.*14:840-50. 2006.
17. Crigler L, Robey RC, Asawachaicharn A, Gaupp D, Phinney DG. Human mesenchymal

stem cell subpopulations express a variety of neuro-regulatory molecules and promote neuronal cell survival and neuritogenesis. *Exp Neurol*.198:54-64. 2006.

18. Gnecci M, He H, Liang OD, Melo LG, Morello F, Mu H, et al. Paracrine action accounts for marked protection of ischemic heart by Akt-modified mesenchymal stem cells. *Nat Med*.11:367-8. 2005.

19. Hwang NS, Varghese S, Puleo C, Zhang Z, Elisseeff J. Morphogenetic signals from chondrocytes promote chondrogenic and osteogenic differentiation of mesenchymal stem cells. *J Cell Physiol*.122:281-4. 2007.

20. Chen WH, Lai MT, Wu AT, Wu CC, Gelovani JG, Lin CT, et al. In vitro stage-specific chondrogenesis of mesenchymal stem cells committed to chondrocytes. *Arthritis Rheum*.60:450-9. 2009.

21. Hendriks J, Riesle J, Vanblitterswijk CA. Effect of stratified culture compared to confluent culture in monolayer on proliferation and differentiation of human articular chondrocytes. *Tissue Eng*.12:2397-405. 2006.

22. Fernandes H, Dechering K, Van Someren E, Steeghs I, Apotheker M, Leusink A, et al. The role of collagen crosslinking in differentiation of human mesenchymal stem cells and MC3T3-E1 cells. *Tissue Eng Part A*.15:3857-67. 2009.

23. Abramoff M, Magelhaes P, Ram S. Image Processing with ImageJ. *Biophotonics International*.11:8. 2004.

24. Katopodi T, Tew SR, Clegg PD, Hardingham TE. The influence of donor and hypoxic conditions on the assembly of cartilage matrix by osteoarthritic human articular chondrocytes on Hyalograft matrices. *Biomaterials*.30:535-40. 2009.

25. Steinberg MS. Differential adhesion in morphogenesis: a modern view. *Curr Opin Genet Dev*.17:281-6. 2007.

26. Waschbisch A, Meuth SG, Herrmann AM, Wrobel B, Schwab N, Lochmuller H, et al. Intercellular exchanges of membrane fragments (trocytosis) between human muscle cells and immune cells: a potential mechanism for the modulation of muscular immune responses. *J Neuroimmunol*.209:131-8. 2009.

27. Tajbakhsh S, Vivarelli E, Cusella-De Angelis G, Rocancourt D, Buckingham M, Cossu G. A population of myogenic cells derived from the mouse neural tube. *Neuron*.13:813-21. 1994.

28. Vadala G, Studer RK, Sowa G, Spiezia F, Iucu C, Denaro V, et al. Coculture of bone marrow mesenchymal stem cells and nucleus pulposus cells modulate gene expression profile without cell fusion. *Spine (Phila Pa 1976)*.33:870-6. 2008.

29. Kuan WL, Hurelbrink CB, Barker RA. Increased capacity for axonal outgrowth using xenogenic tissue in vitro and in a rodent model of Parkinson's disease. *Xenotransplantation*.13:233-47. 2006.

30. Wang L, Li L, Menendez P, Cerdan C, Bhatia M. Human embryonic stem cells maintained in the absence of mouse embryonic fibroblasts or conditioned media are capable of hematopoietic development. *Blood*.105:4598-603. 2005.

31. Wolbank S, Stadler G, Peterbauer A, Gillich A, Karbiener M, Streubel B, et al. Telomerase immortalized human amnion- and adipose-derived mesenchymal stem cells: maintenance of differentiation and immunomodulatory characteristics. *Tissue Eng Part A*.15:1843-54. 2009.

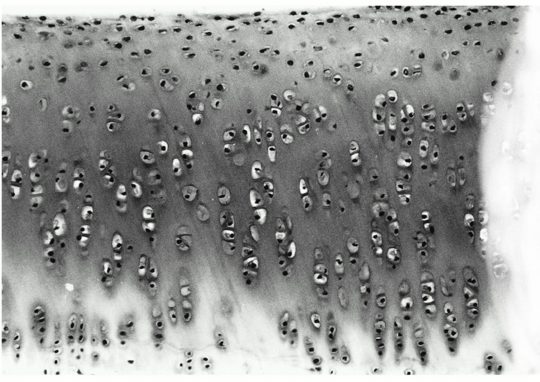
32. Salic A, Mitchison TJ. A chemical method for fast and sensitive detection of DNA synthesis in vivo. *Proc Natl Acad Sci U S A*.105:2415-20. 2008.

33. Foty RA, Steinberg MS. The differential adhesion hypothesis: a direct evaluation. *Dev Biol*.278:255-63. 2005.

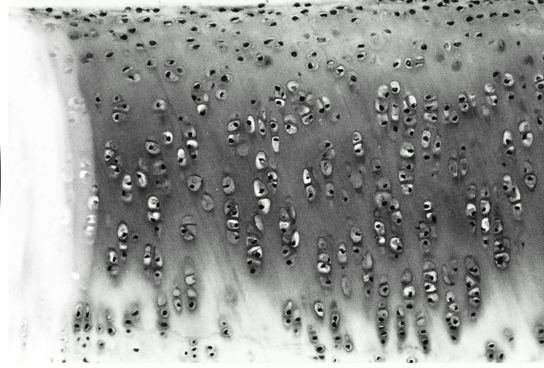
34. Nelson CM, Jean RP, Tan JL, Liu WF, Sniadecki NJ, Spector AA, et al. Emergent

- patterns of growth controlled by multicellular form and mechanics. *Proc Natl Acad Sci U S A*.102:11594-9. 2005.
35. Secchiero P, Melloni E, Corallini F, Beltrami AP, Alviano F, Milani D, et al. Tumor necrosis factor-related apoptosis-inducing ligand promotes migration of human bone marrow multipotent stromal cells. *Stem Cells*.26:2955-63. 2008.
36. Chen XD. Extracellular matrix provides an optimal niche for the maintenance and propagation of mesenchymal stem cells. *Birth Defects Res C Embryo Today*.90:45-54. 2010.
37. Choi KH, Choi BH, Park SR, Kim BJ, Min BH. The chondrogenic differentiation of mesenchymal stem cells on an extracellular matrix scaffold derived from porcine chondrocytes. *Biomaterials*.31:5355-65. 2010.
38. Werb Z. ECM and cell surface proteolysis: regulating cellular ecology. *Cell*.91:439-42. 1997.
39. Liu X, Hou J, Shi L, Chen J, Sang J, Hu S, et al. Lysophosphatidic acid protects mesenchymal stem cells against ischemia-induced apoptosis in vivo. *Stem Cells Dev*.18:947-54. 2009.
40. Song IH, Caplan AI, Dennis JE. Dexamethasone inhibition of confluence-induced apoptosis in human mesenchymal stem cells. *J Orthop Res*.27:216-21. 2009.
41. Banas A, Teratani T, Yamamoto Y, Tokuhara M, Takeshita F, Osaki M, et al. IFATS collection: in vivo therapeutic potential of human adipose tissue mesenchymal stem cells after transplantation into mice with liver injury. *Stem Cells*.26:2705-12. 2008.
42. Weil BR, Markel TA, Herrmann JL, Abarbanell AM, Meldrum DR. Mesenchymal stem cells enhance the viability and proliferation of human fetal intestinal epithelial cells following hypoxic injury via paracrine mechanisms. *Surgery*.146:190-7. 2009.
43. Namba A, Aida Y, Suzuki N, Watanabe Y, Kawato T, Motohashi M, et al. Effects of IL-6 and soluble IL-6 receptor on the expression of cartilage matrix proteins in human chondrocytes. *Connect Tissue Res*.48:263-70. 2007.
44. Csaki C, Matis U, Mobasheri A, Shakibaei M. Co-culture of canine mesenchymal stem cells with primary bone-derived osteoblasts promotes osteogenic differentiation. *Histochem Cell Biol*.131:251-66. 2009.
45. Xu J, Liu X, Chen J, Zacharek A, Cui X, Savant-Bhonsale S, et al. Cell-cell interaction promotes rat marrow stromal cell differentiation into endothelial cell via activation of TACE/TNF-alpha signaling. *Cell Transplant*.19:43-53. 2010.
46. Zhang B, Liu R, Shi D, Liu X, Chen Y, Dou X, et al. Mesenchymal stem cells induce mature dendritic cells into a novel Jagged-2-dependent regulatory dendritic cell population. *Blood*.113:46-57. 2009.
47. Chen J, Li Y, Katakowski M, Chen X, Wang L, Lu D, et al. Intravenous bone marrow stromal cell therapy reduces apoptosis and promotes endogenous cell proliferation after stroke in female rat. *J Neurosci Res*.73:778-86. 2003.
48. Li Y, Chen J, Zhang CL, Wang L, Lu D, Katakowski M, et al. Gliosis and brain remodeling after treatment of stroke in rats with marrow stromal cells. *Glia*.49:407-17. 2005.
49. Kinnaird T, Stabile E, Burnett MS, Shou M, Lee CW, Barr S, et al. Local delivery of marrow-derived stromal cells augments collateral perfusion through paracrine mechanisms. *Circulation*.109:1543-9. 2004.
50. Tang YL, Zhao Q, Zhang YC, Cheng L, Liu M, Shi J, et al. Autologous mesenchymal stem cell transplantation induce VEGF and neovascularization in ischemic myocardium. *Regul Pept*.117:3-10. 2004.
51. Zhang M, Mal N, Kiedrowski M, Chacko M, Askari AT, Popovic ZB, et al. SDF-1 expression by mesenchymal stem cells results in trophic support of cardiac myocytes after myocardial infarction. *FASEB J*.21:3197-207. 2007.

52. Kawada H, Fujita J, Kinjo K, Matsuzaki Y, Tsuma M, Miyatake H, et al. Nonhematopoietic mesenchymal stem cells can be mobilized and differentiate into cardiomyocytes after myocardial infarction. *Blood*.104:3581-7. 2004.
53. Baer PC, Geiger H. Mesenchymal stem cell interactions with growth factors on kidney repair. *Curr Opin Nephrol Hypertens*.19:1-6. 2010.
54. Imai N, Kaur T, Rosenberg ME, Gupta S. Cellular therapy of kidney diseases. *Semin Dial*.22:629-35. 2009.
55. Caplan AI, Dennis JE. Mesenchymal stem cells as trophic mediators. *J Cell Biochem*.98:1076-84. 2006.
56. Ruano-Ravina A, Jato Diaz M. Autologous chondrocyte implantation: a systematic review. *Osteoarthritis Cartilage*.14:47-51. 2006.



10



Chapter 10

High throughput generated micro-aggregates of chondrocytes stimulate cartilage formation in vitro and in vivo

Jeroen Leijten*, Liliana Moreira Teixeira*, Jorge Sobral, Rong Jin, Aart van Apeldoorn,
Jan Feijen, Clemens van Blitterswijk, Piet Dijkstra and Marcel Karperien

* Authors contributed equally

10

Reason has always existed, but not always in a reasonable form.

Karl Marx

Abstract

Cell-based cartilage repair strategies such as matrix-induced autologous chondrocyte implantation (MACI) could be improved by enhancing cell performance. We hypothesized that micro-aggregates of chondrocytes generated in high-throughput prior to implantation in a defect could stimulate cartilaginous matrix deposition and remodeling.

To address this issue, we designed a micro-mold to enable controlled high-throughput formation of micro-aggregates. Morphology, stability, gene expression profiles and chondrogenic potential of micro-aggregates of human and bovine chondrocytes were evaluated and compared to single-cells cultured in micro-wells and in 3D after encapsulation in Dextran-Tyramine (Dex-TA) hydrogels *in vitro* and *in vivo*.

We successfully formed micro-aggregates of human and bovine chondrocytes with highly controlled size, stability and viability within 24 hours. Micro-aggregates of 100 cells presented a superior balance in Collagen type I and Collagen type II gene expression over single cells and micro-aggregates of 20 and 50 cells. Matrix metalloproteinases 1, 9 and 13 mRNA levels were decreased in micro-aggregates compared to single-cells. Histological analysis demonstrated enhanced matrix deposition in constructs seeded with micro-aggregates cultured *in vitro* and *in vivo*, compared to single-cell seeded constructs. Whole genome microarray analysis and single gene expression profiles using human chondrocytes confirmed increased expression of cartilage-related genes when chondrocytes were cultured in micro-aggregates.

In conclusion, we succeeded in controlled high-throughput formation of micro-aggregates of chondrocytes. Compared to single cell-seeded constructs, seeding of constructs with micro-aggregates greatly improved neo-cartilage formation. Therefore, micro-aggregation prior to chondrocyte implantation in current MACI procedures, may effectively accelerate hyaline cartilage formation.

10.1 Introduction

Articular cartilage has a limited capacity for regeneration due to its avascular nature and deficiency on migrating or responding undifferentiated cell populations [1, 2]. Arthroplasty can be successfully used to treat degenerative joints at end stage disease. Due to the limited life-span of the prosthesis and the complications with revision surgery, this treatment option is less suited for young active patients with focal defects. Non-arthroplastic options include debridement, micro-fracture, osteochondral grafting, autologous chondrocyte implantation (ACI) or matrix-assisted autologous chondrocyte implantation (MACI). Both ACI and MACI are the most technically advanced procedures, representing promising treatment modalities, yet still with associated limitations [1, 3, 4]. The limited availability of autologous chondrocytes and their tendency to lose their phenotype during the required 2-D expansion phase to obtain sufficient cells for implantation are major drawback of these techniques. The current challenge to improve the therapeutic outcome of these techniques is to develop strategies that induce maximal cartilaginous matrix deposition per chondrocyte, avoiding the cost-prohibitive use of growth factors. Aggregation of chondrocytes is a well-studied phenomenon that enhances the chondrogenic phenotype. Traditionally it is employed by generating micromasses of 200.000-500.000 chondrocytes. More recently smaller aggregates are formed by culturing chondrocytes on agarose coated surfaces or micrometric patterns [5, 6]. However, such methods of aggregation are uncontrollable and yield insufficient amounts of aggregates needed for clinical application. In consequence, aggregation of chondrocytes prior to implantation has not been implemented in current MACI procedures.

To overcome these limitations, we designed a platform that enables the formation of highly controlled chondrocyte aggregates in a high-throughput fashion. We evaluated the effect of chondrocyte micro-aggregation *in vitro* and *in vivo*. We demonstrated that micro-aggregation enhanced sensitivity to chondrogenic stimuli and decreased the expression of catabolic factors, resulting in higher accumulation of cartilaginous matrix. We postulate that controllable high-throughput platforms such as described in this study enables the feasibility of the use of micro-aggregated chondrocytes in cell based cartilage repair strategies such as ACI or MACI. This might allow for improved therapeutic outcome by significantly boosting neocartilage formation.

10.2 Materials and Methods

10.2.1 Tissue source and preparation

The use of human material was approved by a local medical ethical committee. OA cartilage was obtained from the knee joints of adult patients suffering from late stage OA undergoing an arthroplasty, after informed consent. Bovine cartilage was obtained from a local abattoir. Human and bovine primary chondrocytes were isolated from knee articular cartilage by collagenase digestion and cultured in chondrocyte expansion medium composed of Dulbecco's modified Eagle's medium high glucose (Invitrogen), 10 % fetal bovine serum (Cambrex), 100 U/mL penicillin (Invitrogen),

100 mg/mL streptomycin (Invitrogen), 0.2 mM ascorbic acid (ASAP; Sigma), 0.1 mM non-essential amino acids (Sigma), and 0.4 mM proline (Sigma). Tissue samples were fixated, dehydrated and embedded in paraffin. Macroscopically OA cartilage was used to evaluate morphological features. Sections of 5 μm were collected and stained with H&E for further evaluation using light microscopy.

10.2.2 Mold design and micro-aggregate formation

Stainless steel molds were machined using a femto-second pulsed laser system to produce a negative replica of the micro-wells. The depth of the mold was designed to be 200 - 300 μm . The spacing between wells was 250 μm . To produce agarose micro-wells, autoclave-sterilized powder Ultrapure Agarose (Invitrogen) was dissolved via heating in sterilized PBS at 2 % w/v and added drop by drop into a previously sterilized O-Ring (with an area of 1.9 cm^2) placed on top of the micro-fabricated stainless steel mold. After drying, the gels were separated from the mold and transferred into 24 well culture plates. Each well of the 24-well culture plate contained 4×10^3 micro-wells (Figure 10.1). Different cell densities (20, 50, 100, 200, 300 and 500 cells per micro-well) were used to study the effect of cell number on the form and size of the micro-aggregates. Appropriate cell densities were seeded into each well of the 24-well plates containing 4×10^3 agarose micro-wells to obtain micro-aggregates of 50, 100 and 200 cells. Micro-aggregation was induced by gravity after seeding a single cell suspension on top of the micro-wells. Both expansion and chondrocyte differentiation medium (DMEM with 0.1 μm dexamethasone (Sigma), 100 $\mu\text{g}/\text{mL}$ sodium pyruvate (Sigma), 0.2 mm ascorbic acid, 50 mg/mL insulintransferrinselenite (ITS + 1, Sigma), 100 U/mL penicillin, 100 $\mu\text{g}/\text{mL}$ streptomycin, 10 ng/mL transforming growth factor $\beta 3$ (TGFB3, Invitrogen)) were used. The micro-aggregates were kept in culture in the micro-wells in a humidified atmosphere containing 5 % CO_2 at 37°C up to 7 days. Single cells were cultured in 2D on tissue culture plastic at the same cell density. Microscopic images were collected at several time points and morphometric analysis of the micro-aggregates was performed using ImageJ software.

10.2.3 Dextran-Tyramine hydrogels (Dex-TA)

10

Dex-TA with a degree of substitution of 15, defined as the number of tyramine (TA) moieties per 100 anhydroglucose (AHG) units in dextran, was prepared as described previously [7, 8]. Bovine chondrocytes (passage 2) either as micro-aggregates or as single cell suspension at a concentration of 10×10^6 cells per mL were mixed with the polymer solution. The hydrogel precursor/cell suspension was mixed with H_2O_2 (hydrogen peroxide, Sigma-Aldrich) and horseradish peroxidase (HRP type VI, 298 purpurogallin unit/mg solid, Aldrich) and gelation occurred within one minute (the final concentration of Dex-TA was 10 % wt). The amount of HRP used was fixed at 0.25 mg per mmol of TA moieties and the molar ratio of $\text{H}_2\text{O}_2/\text{TA}$ was 0.20 (mol/mol).

10.2.4 Metabolic activity and chondrocyte viability

Quantification of glucose consumption, as well as lactate and ammonia production by chondrocyte micro-aggregates of 100 cells on micro-wells and single cells cultured for 7 days in differentiation medium, was determined using a Vitros DT60 II medium analyzer (Ortho-Clinical Diagnostics, Tilburg, The Netherlands). The viability of the chondrocytes incorporated in the hydrogels either as single cells or as micro aggregates was assessed by a Live-dead assay. At day 7 and 14, the hydrogel constructs were rinsed with PBS and stained with calcein AM/ethidium homodimer using the Live-dead assay Kit (Invitrogen), according to the manufacturers' instructions and evaluated using fluorescence microscopy. Living cells fluoresce green and the nuclei of dead cells red.

10.2.5 In vivo implantation

Chondrocyte micro-aggregates of 100 cells were allowed to form for 24 hours in expansion medium. Afterwards, the aggregates were flushed out of the micro-wells and mixed with polymer precursor, as described above. Samples of each hydrogel type, containing either single cells or aggregates of 100 cells were cultured in vitro and at predetermined time points analyzed for cell viability, metabolic activity, matrix biosynthesis and gene expression analysis or were surgically implanted subcutaneously in 8 weeks old nude male mice (NMRI-Nude, Harlan) for a period of 2 or 4 weeks. The operative procedure and the care of the mice were performed under the regulation of the Central Laboratory Animal Institute (GDL), Utrecht University (Netherlands). The study was approved by a local animal ethical committee.

10.2.6 Histological analysis

At 14 and 21 days, hydrogel constructs seeded with single cells or aggregates of 100 cells and cultured in differentiation medium were fixed in 10 % buffered formalin for 1 hour. For the in vivo experiments, the samples were explanted after 2 and 4 weeks and allowed to fixate in 10 % buffered formalin overnight at 4°C. After embedding the samples in cryomatrix (Cryomatrix, Shandon), a cryo-microtome (Leica) was used to collect 10 μm sections onto gold-coated slides. The cryomatrix was washed off the slides by incubation in distilled water for 10 minutes. Afterwards, three histological stainings were performed: Picosirius Red staining for visualization of total collagen (processed according to the manufacturer's instructions (Polysciences) and both Toluidine blue (Fluka, 0,1 % in deionized water, 10 minutes incubation) and Safranin O (Sigma, 0,1 % in deionized water, 5 minutes incubation) for glycosaminoglycans (GAGs) visualization. The slides were then washed, dehydrated, mounted and analyzed using a bright field microscope (Nikon Eclipse E400).

10.2.7 Whole genome gene expression microarray analysis

Whole genome gene expression microarray analysis was performed on micro-aggregates of 100 cells and single cells incorporated in Dex-TA hydrogels, as described above,

and cultured in differentiation medium for 7 days. Three different human chondrocyte donors were used. NuGEN Ovation PicoSL WTA System kit followed by Encore BiotinIL module was used to generate biotinylate single stranded cDNA starting from 50 ng total RNA. 750 ng of the obtained samples was hybridized onto the Illumina HumanHT-12 v4 Expression BeadChips. Samples were scanned using the Illumina iScan array scanner. Gene expression profiling was performed using Illumina's Genomestudio v. 2010.3 software with the default settings advised by Illumina. Data was normalized by applying quantile normalization on the raw fluorescence intensity values. Differential gene expression was analysed using the commercial software package Genespring, version 11.5.1. (Agilent Technologies). Three-dimensional Principal Component Analysis (PCA) was used to demonstrate the differences in global gene expression between single cells and micro-aggregates. Hierarchical clustering was used to group all samples on similarity. Changes of gene expression in annotated canonical pathways and bio-functions were visualized using ingenuity pathway analysis software (Ingenuity Systems). Search Tool for the Retrieval of Interacting Genes/Proteins (STRING) was used to investigate the predicted gene-gene interaction network [9]. Markov clustering algorithm was used to identify interacting clusters of genes and encoded proteins within the microarray dataset.

10.2.8 Real time PCR analysis

Hydrogel/cell constructs cultured for either 7, 14 or 21 days in differentiation medium were washed with PBS and lysed using Trizol reagent (Invitrogen, Carlsbad, CA). Total RNA was isolated using the Nucleospin RNA II kit (Bioke) according to manufacturer's instructions. The RNA yields were determined using the Nanodrop2000 (ND-1000 Spectrophotometer, Isogen LifeScience). Subsequently, cDNA was synthesized using the iScript Kit (BioRad) according to the manufacturer's recommendations. Expression levels of individual genes were analyzed by quantitative PCR (MiQ, Bio-rad) and normalized on GAPDH. Primer sequences are available on request.

10.2.9 Statistical analysis

Statistical differences between two groups were analyzed using the Student's t-test or by one-way ANOVA. Statistical significance was set to $P < 0.05$ and indicated with an 'a'. Results are presented as mean standard deviation.

10

10.3 Results

10.3.1 High-throughput generated chondrocyte micro-aggregates resemble chondrocyte clusters in OA

Micro-fabricated molds were used as a tool to generate chips of identically shaped micro-wells in agarose. The procedure is outlined in Figure 10.1A. These chips were placed in 24-well plates and subsequently used to generate micro-aggregates similar to the ones observed in OA cartilage for further studies in high-throughput (Figure

10.1B). Shortly after seeding of a single cell suspension, gravitational force resulted in the concentration of chondrocytes at the bottom of the micro-wells. The chondrocytes contracted to a spherical aggregate thereby increasing intercellular contacts and minimizing free energy (Figure 10.1C). To study the effect of cell number in aggregation speed and stability of the micro-aggregates, pictures of the aggregates in the micro-wells were collected at different time points after seeding. The number of cells affected the speed of aggregate formation. We observed that lower cell densities demanded longer aggregation time, most likely due to limited contact opportunities (Figure 10.1C). After 24 hours, the aggregates were collected by flushing the non-cell adherent agarose chips with medium. The percentage of aggregate recovery was 96.6%. The aggregates could withstand centrifugation and resuspension in medium, as shown in Figure 1-D. Analysis of a correlation between cell seeding density, aggregate diameter and volume, demonstrated a linear correlation between seeding density and the aggregate volume assuming a spherical conformation (Figure 10.1D).

To evaluate aggregate stability after formation, the area and circularity of aggregates composed of 50, 100 and 200 cells were analyzed after 1, 3 and 7 days in culture. The area and circularity of the aggregates are represented in Figures 10.1E and F. As expected, the area of the aggregates decreased slightly over time due to condensation. The circularity of the aggregates provided information about stability and uniformity of the aggregates. Higher deviations in circularity were observed at later stages of culture and particularly in aggregates with lower cell densities. In subsequent experiments, aggregates were collected 24 hours after seeding, since this time point was sufficient to obtain stable micro-aggregates starting from single cell suspensions. Furthermore, extension of this culture time tended to result in migration of the micro-aggregates to neighboring wells and their subsequent merger suggesting a chemotactic attraction between the aggregates. This process resulted in an increased heterogeneity in size.

10.3.2 Micro-aggregation stimulates cartilage matrix formation

Gene expression of Aggrecan and Collagen type II was evaluated. Aggregates with densities of 50, 100 and 200 cells were cultured in the micro-wells and compared with single cells cultured in 2D using similar cell numbers. Figure 10.2A shows that aggregates cultured in expansion medium tended to slightly up-regulate the expression of both collagen type II and aggrecan, compared to single cells cultured in 2D. Figure 10.2B shows that, when the aggregates were chondrogenically stimulated with TGFB3, the gene expression of collagen type II and aggrecan significantly increased in micro-aggregates of 50 and 100 cells, compared to single cells and to aggregates of 200 cells. Overall, gene expression analysis demonstrated that micro-aggregates behaved similarly to single cells when cultured without stimulation. However, when the micro-aggregates were exposed to chondrogenic conditions containing stimulatory molecules alike found in native cartilage, cartilage matrix formation was significantly enhanced in aggregates of 50 and 100 cells with a less pronounced effect in aggregates of 200 cells. Given the higher stability of aggregates of 100 cells compared to aggregates of 50 cells, these cell clusters were selected for further experimentations.

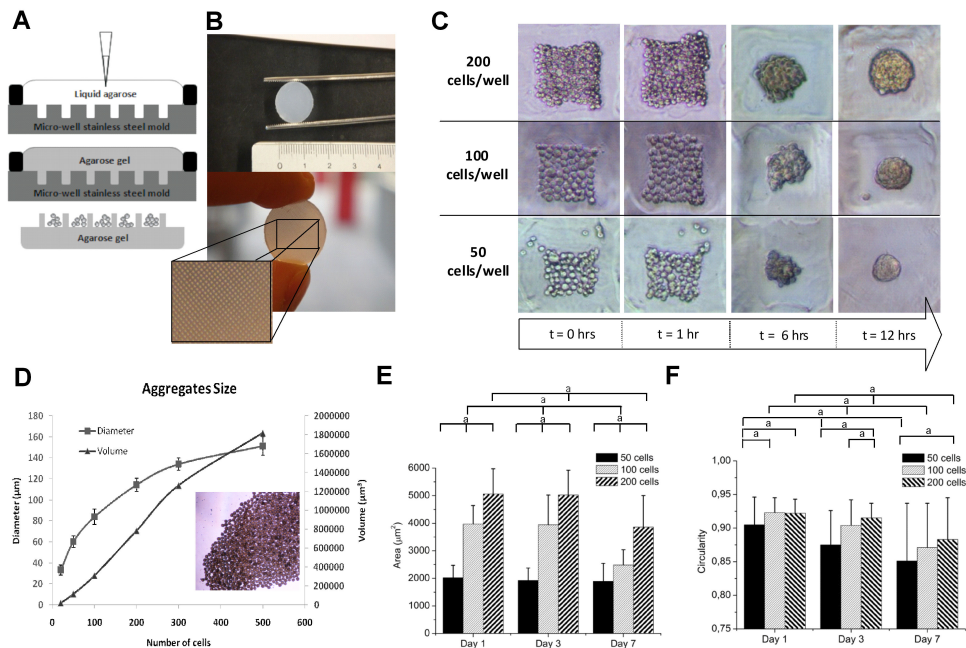


Figure 10.1: High-throughput formation of chondrocyte micro-aggregates. (A) Schematic representation of the micro-well technique for the formation of aggregates from single cell suspensions. A stainless steel mold was used to form micro-wells in agarose chips. (B) Each agarose chip contains 4×10^3 micro-wells. (C) Pictures at specific time points during aggregate formation. Each well of a 24 wells plate containing an agarose micro-well chip was seeded with the appropriate number of bovine chondrocytes to obtain micro aggregates of 50, 100 or 200 cells. Aggregation started to occur approximately 6 hours after seeding. After 12 hours, the aggregates had acquired a spherical shape, independently of aggregate size. (D) Correlation between the number of chondrocytes per micro well and the diameter (μm) and the volume (μm^3) of the obtained aggregates after 12 hours. Each data point represents the measurement of minimally 50 micro aggregates. At the lower right side of the graphic, aggregates obtained after flushing off the agarose chips are shown. (E) Micro-aggregate area (μm^2) slightly decreased over time most notably in aggregates bigger than 100 cells. Each data point represents the measurement of minimally 50 aggregates (F) Measurement of circularity of micro aggregates over time demonstrated a decrease in average circularity and an increase in spread. A perfect circle has a value of 1. Each data point represents the measurement of about 50 micro aggregates. Error bars were means SD.

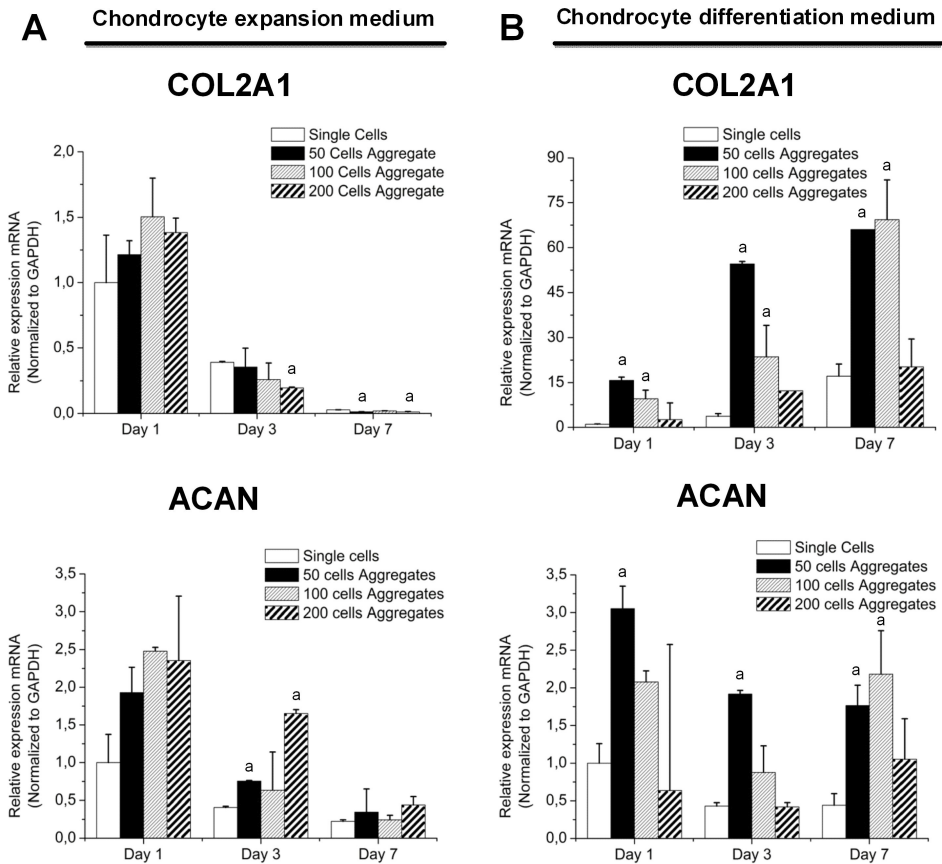


Figure 10.2: Micro-aggregation enhances collagen type II and aggrecan expression. (A) qPCR analysis of collagen type II (*Col2a1*) and aggrecan (*Acan*) gene expression at day 1, 3 and 7 of culture in chondrocyte expansion medium. Equal amounts of cells were cultured in micro-aggregates of 50, 100 and 200 bovine chondrocytes and compared with single cells cultured in a 2-D system. At day 7, no changes were observed between the different culture methods. (B) qPCR analysis of *Col2a1* and *Acan* gene expression was evaluated at day 1, 3 and 7 of culture in chondrogenic conditions. Micro-aggregated cell clusters of 50, 100 and 200 cells were compared with single cells cultured in a 2-D system. *Col2a1* and *Acan* expression was potently stimulated by culturing the cells in micro-aggregates of 50 and 100 cells. Error bars were means \pm SD (n=3/condition).

10.3.3 Micro-aggregated cell clusters remain viable after embedding in a hydrogel

We studied the effect of micro-aggregation on cell metabolism in comparison to equal numbers of single cells after embedding of the cells in a dextran based hydrogel. As shown in figure 10.3A, both single cells and micro-aggregates were uniformly distributed in the hydrogel and remained viable. The integrity of the micro-aggregates did not change over culture time. Micro-aggregated cell clusters were metabolically more active than single cell seeded constructs (Figure 10.3B). Micro-aggregates laden constructs had a significantly higher consumption of glucose and production of both lactate and ammonia. This suggested that aggregation of chondrocytes stimulated cell metabolism presumably due to higher cell-cell contacts. During glycolysis, oxidation of one molecule of glucose leads to two molecules of pyruvate and, subsequently, by anaerobic respiration, to two molecules of lactate. This expected 2:1 ratio of lactate:glucose was observed when single cells were cultured in the hydrogels. When cells were cultured in aggregates this ratio dropped to 1:1. This significant difference was suggestive for a metabolic shift suggesting that a part of the glucose may be used in biosynthesis of extracellular matrix molecules rather than energy consumption.

10.3.4 Cell cluster formation enhanced cartilage matrix deposition

Micro-aggregates of 100 cells or single cells suspensions with equal cell numbers were incorporated in a Dex-TA hydrogel and cultured in chondrocyte differentiation medium for 14 and 21 days. The relative fold expressions of chondrogenic related genes such as *Acan*, *Col2a1* and *Sox9* were up-regulated in hydrogels containing micro-aggregates compared to constructs seeded with equal numbers of single cells (Figure 10.4A to C). Figure 10.4G shows that the ratio of *Col2a1* and *Col1a1* is improved in constructs seeded with micro-aggregates. Over time, these differences became more pronounced. Additionally, no significant differences in gene expression of both *Col1a1* or *Col10a1* were observed between single cells and micro-aggregates, at any time point (Figure 10.4D and E). The expression of several MMPs was analyzed after 21 days in culture to evaluate the effect of cell clustering. As shown in Figure 4-F, a decrease in the expression of *Mmp1*, *Mmp9* and *Mmp13* was observed in hydrogels cultured with micro-aggregated cells. The expression of *Mmp3* was not detected in constructs seeded with micro-aggregates. The gene expression analysis was corroborated by histology (Figure 10.5A and B). Picrosirius red staining was more intense in hydrogels containing aggregated cells, suggesting the presence of more collagens (Figure 10.5A). The staining did not further increase by extending culture time from 14 to 21 days. The presence of GAGs was visualized by Toluidine blue and Safranin O staining (Figure 10.5A). Both stainings were more intense in hydrogels seeded with micro-aggregates compared to single cell seeded constructs. This difference was more striking at day 21. Additionally, mainly at day 14, a gradient of GAGs diffusing out of the micro-aggregates and into the hydrogel was visible. Similar results, and even more pronounced, were obtained 2 and 4 weeks after subcutaneous

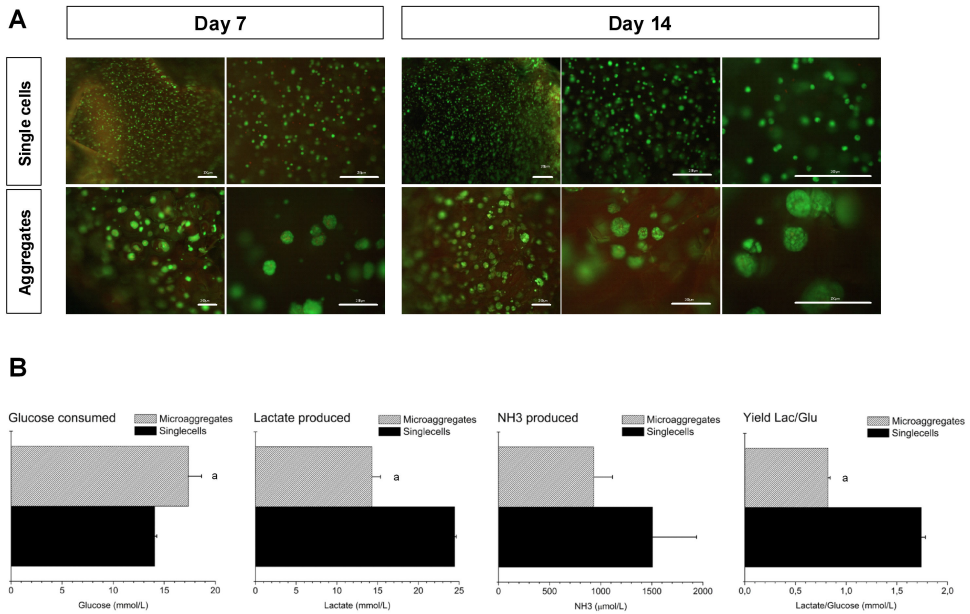


Figure 10.3: Micro-aggregation increases metabolic activity. (A) Equal numbers of cells, either as micro-aggregates or as single cells, were embedded in an in situ gelating Dex-TA hydrogel. After 7 and 14 days of culture, a viability assay was performed in which living cells were shown in green and dead cells in red. Incorporation of cells in the hydrogels did not affect viability nor did micro-aggregation. Clusters retained their spherical shape over time. (B) Glucose consumption and ammonia and lactate production were quantified after 7 days of culture of equal cell numbers of 100 cell micro-aggregates of bovine chondrocytes on agarose chips or as single cells in 2D. The ratio between lactate production and glucose consumption is represented in the lower right graphic. The clear difference between both culture systems was strongly suggestive for a shift in metabolic activity. Error bars represent means \pm SD ($n=3$ /condition).

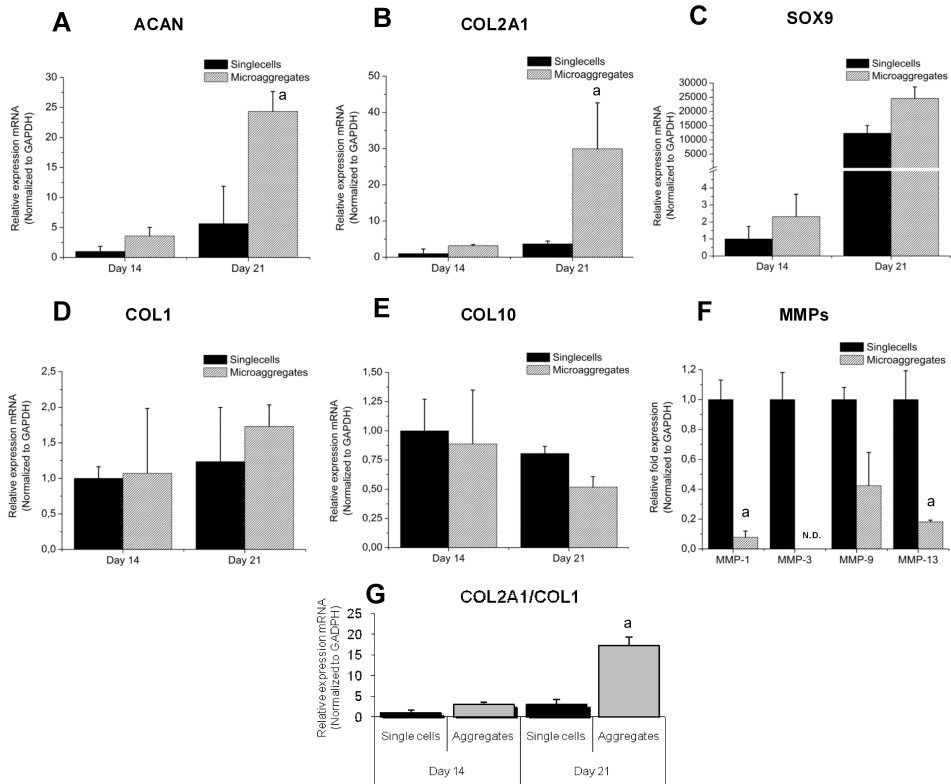


Figure 10.4: Micro-aggregation prior to seeding in hydrogels stimulates cartilage matrix gene expression. Relative mRNA levels for *Acan* (A), *Col2a1* (B), *Sox9* (C), *Col1a1* (D) and *Col10a1* (E), expressed by single bovine chondrocytes or micro-aggregated cell clusters incorporated into Dex-TA hydrogels, after 14 and 21 days in culture. Similar cell numbers were seeded in each construct. Relative mRNA levels for metalloproteinases (Mmp) 1, 3, 9 and 13 (F), expressed by single chondrocytes or micro-aggregated cell clusters incorporated into Dex-TA hydrogels, after 21 days in culture. (G) *Col2a1/Col1a1* ratio to elucidate chondrogenic phenotype development. Error bars were means \pm SD (n=3/condition).

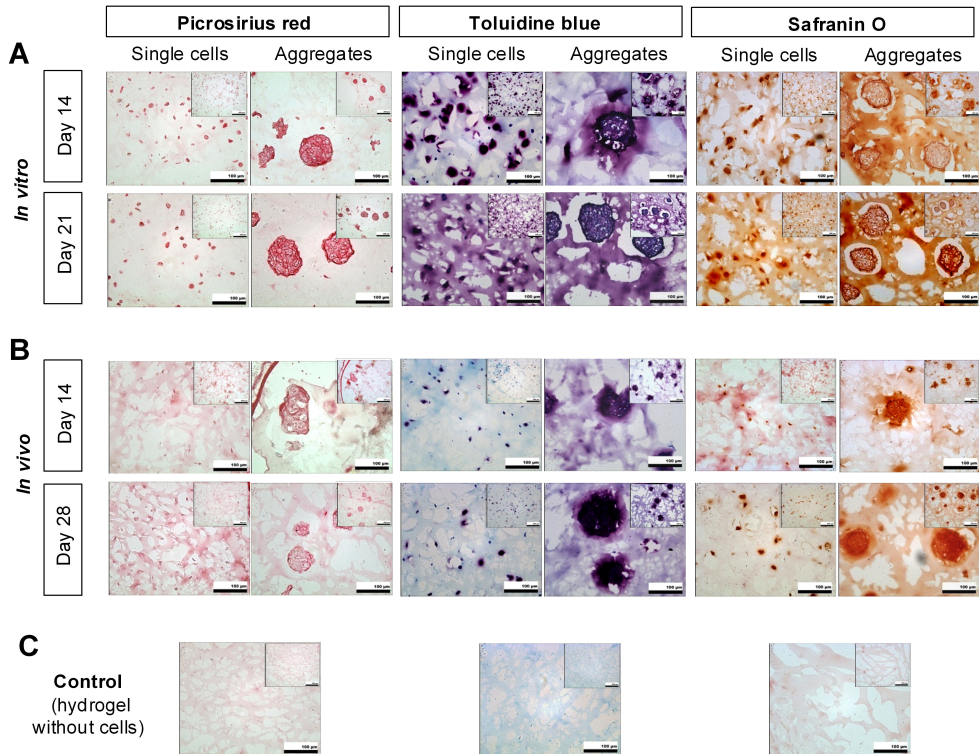


Figure 10.5: Micro-aggregation resulted in superior matrix production both *in vitro* and *in vivo*. (A) Histological evaluation of *in vitro* cultured hydrogels seeded with equal bovine chondrocyte numbers either as single cells or as micro-aggregates of 100 cells, for 14 and 21 days. Picrosirius red staining was performed to visualize total collagen content (red/pink colour). Both Toluidine blue (purple colour) and Safranin O (red/orange colour) stainings were performed to visualize glycosaminoglycans deposition. A more intense staining was observed in constructs seeded with micro-aggregates indicative for higher matrix production. (B) Histological evaluation of hydrogel constructs with encapsulated single cells or micro-aggregates of 100 cells implanted subcutaneously in nude mice for 2 and 4 weeks ($n=6$ mice per time point). Hydrogels with encapsulated micro aggregates showed more cartilage matrix. (C) Histological stainings of a representative control sample, consisting of the hydrogel without cells.

implantation of the cell seeded hydrogel constructs in nude mice (Figure 10.5B).

10.3.5 Microarray analysis confirmed increased expression of cartilage-related genes in human chondrocyte clusters

Whole genome gene expression profiling was used on human chondrocytes to validate our experimental model in a human system and to obtain a deeper understanding of the transcriptional effects of chondrocyte micro-aggregation. The formation of human chondrocyte clusters occurs similarly to bovine chondrocyte cell clusters and their incorporation in Dex-TA hydrogels was equally efficient. Gene expression profiles on constructs laden with identical cell numbers either as single cells or in micro-aggregates were distinct as demonstrated by 3-D principal component analysis (Figure 10.6A). Moreover, hierarchical cluster analysis demonstrated the presence of two main clusters: chondrocytes cultured as micro-aggregates or as single cells (Figure 10.6B). Gene and protein interactions analysis of the differentially regulated genes between single cells and micro-aggregates revealed one major central hub (Figure 10.6C). Interestingly, this intricate network contained the most highly differentially regulated genes such as connective tissue growth factor (*CTGF*) and extracellular matrix-related genes like *COL3A1*, *COMP* and *MMP3* (Figure 10.6D).

Indeed, bio-function analysis demonstrated significant differences in processes like 'cellular assembly and organisation', 'cellular functions and maintenance', 'connective tissue development and function' and 'skeletal and muscular system development and function' (Figure 10.7A). Gene expression patterns of 4 genes of interest were validated using qPCR (Figure 7-B). The selected genes were *COL2A1*, *ACAN*, *SOX9* and *COMP*, which are cartilage-related genes that were up regulated in the micro-aggregates. This data showed striking similarity with the experiments using bovine chondrocytes, suggesting that the effect of micro-aggregation on cartilage matrix formation is species-independent.

10.4 Discussion

In this study, we developed an *in vitro* micro cell-cluster platform that enabled the high-throughput formation of highly controllable micro-aggregates that can be harvested without enzymatic digestion or mechanical shearing. This allowed us to study the effect of micro-aggregation of chondrocytes on cartilage matrix formation and their potential as therapeutic cell source when combined with an *in situ* gelating injectable biomaterial. We demonstrated that formation of micro-aggregates resulted in enhanced cartilage matrix production and decreased MMPs transcription.

Cartilage repair strategies based on autologous chondrocyte implantation still rely on *in vitro* expansion to obtain sufficient cells, with all inherent drawbacks such as chondrocyte dedifferentiation [10]. Studies focusing on the self-aggregation potential of chondrocytes and its use for elastic cartilage reconstruction have been hampered due the problem of dedifferentiation and scarcity of starting material [11-13]. They have shown that by embedding aggregates in molded hydrogels, chondron-like clusters are formed and, thus, dedifferentiation of the chondrocytes is avoided, or at least delayed.

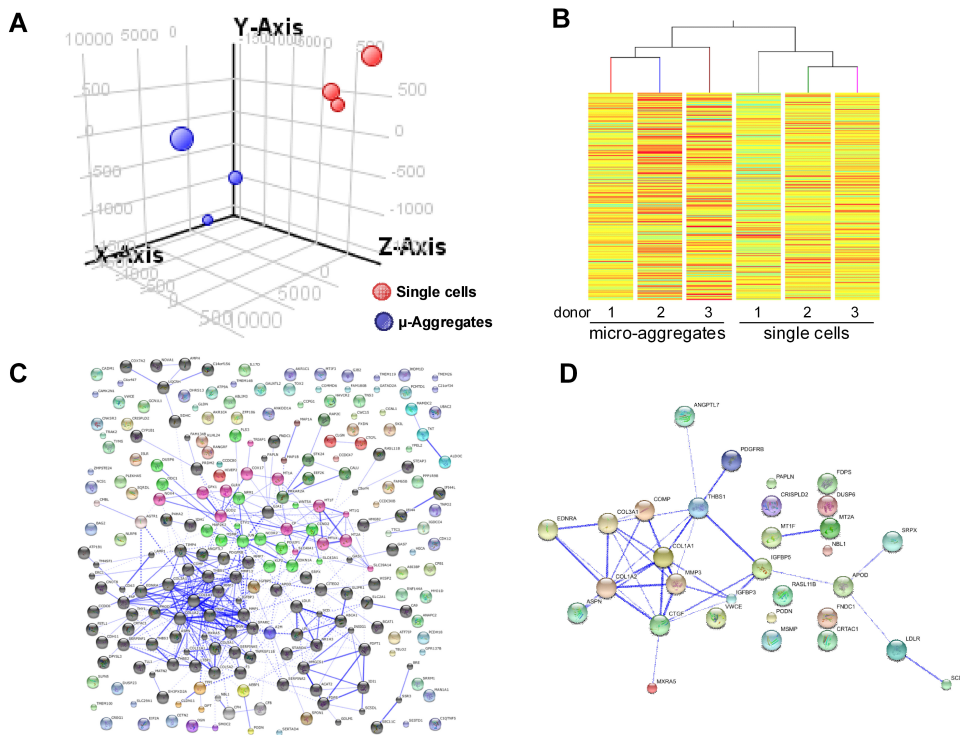


Figure 10.6: Whole genome gene expression analysis of micro-aggregates vs. single cells. (A) 3-D PCA plot of all detected probes of micro-aggregates (blue spheres) of human chondrocytes or of single cells (red spheres). (B) Hierarchical clustering of all significant differentially regulated genes between micro-aggregates (agg) and single cell chondrocytes (ss). (C) and (D) Gene and protein interaction networks of all selected significant differentially expressed genes or (D) and the subset of the higher differentially expressed genes.

Due to the cartilage's inherent low capacity to self-repair, the retention of cells in cell-based cartilage repair strategies at the defect site is of the highest importance. A myriad of biomaterials that provide an artificial extracellular matrix compatible with homogenous distribution of single cells or micro-aggregates are currently available for cartilage tissue regeneration strategies [6, 14]. Among the classes of biomaterials, hydrogels of natural polymers show promising features as defect filling scaffolds due to their similarity to the native cartilaginous extracellular matrix. *In situ* gelating injectable hydrogels have deserved much attention since they can be applied in a minimally invasive procedure and allow the possibility of cell incorporation during the gelation reaction [10]. Recently, we have developed a novel injectable enzymatically crosslinkable Dextran-Tyramine hydrogel (Dex-TA, 14kDa, DS=15). This fast gelating hydrogel is fully compatible with cell viability and has shown high potential for

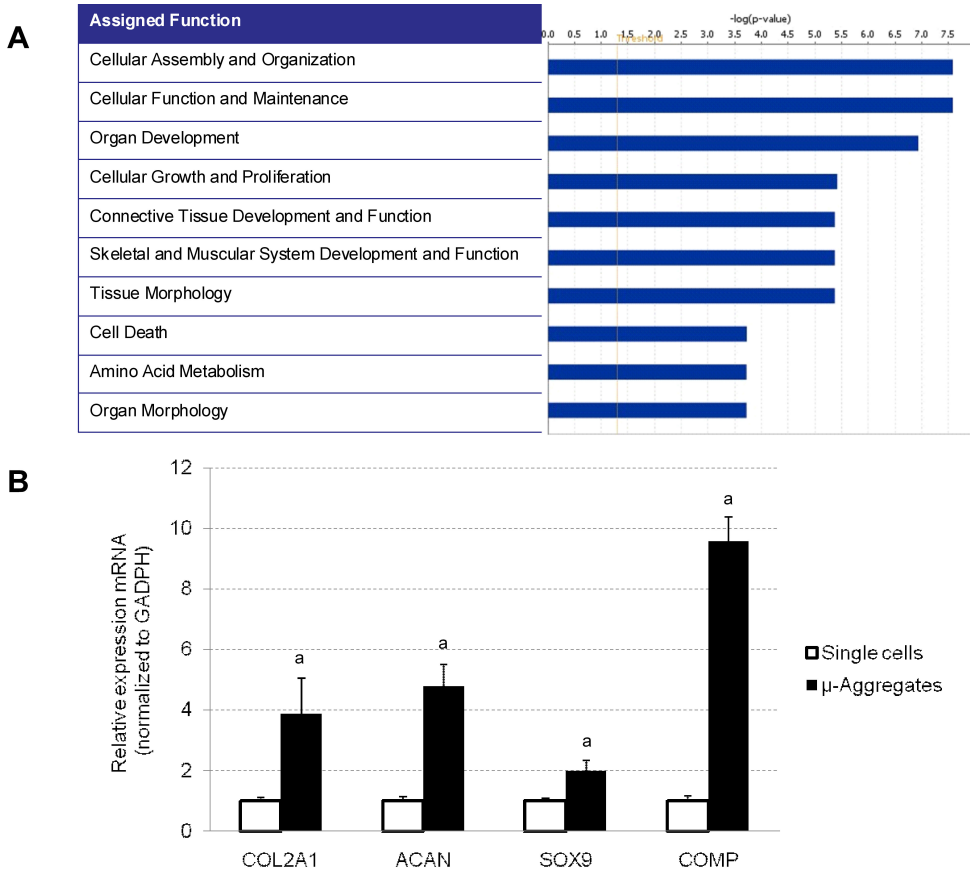


Figure 10.7: Differentially regulated bio-function list and qPCR validation of microarray data. (A) Differentially regulated bio-functions of micro-aggregates vs. single cells based on Ingenuity’s pathway analysis of whole genome gene expression microarrays. (B) qPCR validation of micro-array data. *COL2A1*, *ACAN*, *SOX9* and *COMP* showed up regulation in the micro-aggregated cells by microarray and qPCR. Error bars were means \pm SD (n=6/condition).

cartilage regeneration [7, 8]. We have chosen these hydrogels to evaluate whether seeding constructs with micro-aggregated cells rather than with single cells has a beneficial effect on cartilage matrix formation. Prior to incorporation of the micro-aggregates in the injectable Dex-TA hydrogels, different culture times and cell densities were evaluated to select the optimal micro-aggregate size. Interestingly we observed that larger micro-aggregates, such as 200 cells, were outperformed by smaller micro-aggregates, composed of 50 and 100 cells. Additionally, higher micro-aggregate stability was achieved in shorter formation time when aggregating 50 to 100 cells compared to 200 cells. After 3 days in culture, the micro-aggregates tended to merge due to cell migration, most likely facilitated by the increasing matrix that surrounded the aggregates. The merging of aggregates with increasing culture time has been previously reported [5, 11, 15]. Most probably, this process is driven by chemotactic factors secreted by the chondrocytes [16, 17]. Based on stability and formation characteristics, as well as expression of a chondrogenic gene profile, we selected aggregates of 100 cells as the optimal size for further experiments.

Micro-aggregates of 100 cells seeded in Dex-TA hydrogels proved to be viable and retained their integrity. Moreover, the aggregates could be easily uniformly distributed in the gel. Interestingly, when the chondrocytes were cultured in the aggregated form within hydrogels, a change in cell metabolism was observed. This might be due to a metabolic shift from a catabolic glycolysis pathway in single cell constructs to a more anabolic pathway in constructs seeded with aggregated cells. As cause or consequence of these events, glucose might have been directed to a greater extent to biosynthesis and, thus contributing to enhanced matrix production in micro-aggregates seeded constructs. Indeed this was supported by increased matrix deposition in hydrogels seeded with micro-aggregates. Likewise, the increase in biosynthesis in early cartilage lesions has been previously reported [18, 19]. Comparable shifts from catabolic to the anabolic responses have been recently reported to occur by varying the exposure of chondrocytes to different oxygen percentages [13]. Lower oxygen percentages, similar to physiological concentrations, significantly enhanced the chondrogenic capacity of chondrocytes cultured in micromass pellets. The enhanced chondrogenic behavior of the micro-aggregates might be at least in part explained by a relatively lower exposure to oxygen of cells in micro-aggregates compared to single cells in 2-D. However, other possibilities such as concentrating effects of both secreted soluble factors and extracellular matrix molecules cannot be excluded. Regardless of the cause, micro-aggregates of 100 cells outperformed single cells and showed therefore a greater potential for cell-based cartilage repair strategies.

Interestingly, morphometric analysis and gene expression profiles suggested that without addition of chondrogenic stimuli, both single cells and micro-aggregates behaved similarly suggesting that aggregation itself does not change cell behavior. However, when stimulated with a chondrogenic stimulus, such as TGFB3, micro-aggregated cells showed a very distinct response from single cells. A strong additional effect on cartilage matrix formation was obtained when cells were cultured in a micro-aggregated form.

Chondrocyte clusters are a histological hallmark of OA, the most prevalent form of degenerative joint diseases [20]. Interestingly, it has recently been suggested that this

clustering of chondrocytes are a self-reparative response of the cartilage, but experimental evidence is lacking [21]. The formation of chondrocyte aggregates or clusters in OA occurs by increased cell proliferation or active movement of the chondrocytes [22-24]. Chondrocyte clusters can be composed by more than 20 cells and are localized in the proximity of fissures in the upper cartilage layers [20, 25]. Although previous studies have investigated the effect of chondrocyte clustering on cartilage formation, these aggregates were formed either in insufficient quantity, with improper or poorly controlled size ranges, or attached to scaffold sheets [5, 11, 12, 26-28]. In contrast, the high throughput method described in this study allowed us to address this issue more systematically. Our data substantiates the hypothesis that micro-clusters of chondrocytes, such as observed in OA, may indeed be part of a regenerative response. To our knowledge, we are the first to address the function of micro-clusters by an experimental approach showing potent stimulation of cartilage matrix formation. Since we have not studied the function of micro-aggregates in an OA-like environment, e.g. in the presence of inflammatory cytokines, we cannot exclude that the OA-environment alters the behavior of the micro-aggregates. Using our model, the effect of various factors involved in OA can be easily addressed in a high-throughput approach. In addition, the potential to form these micro-aggregates in high-throughput potentially allows us to translate this method to a clinical application.

Considering the difference in expression ratio of collagen type II and collagen type X between clusters, it might be worthwhile to explore differential seeding of constructs with micro-aggregates of various sizes to reconstruct the zonal organization of cartilage. The role of microscale organization in a cartilage model has previously been investigated using cell clusters obtained by photo-immobilization of single cells in a hydrogel as described by Albrecht et al. [29]. In contrast to our study, no effect on cartilage matrix formation was observed. This difference might be explained by the cell-cell contact achieved with our approach of cell cluster formation, compared to the cell density approach in which cells are in close proximity, yet a couple of micrometers still apart. The two distinct outcomes suggest that close cell-cell contact and contraction forces during condensation of cell clusters strongly affect cell behavior [17, 30]. Thus, the system reported by Albrecht et.al. resembled more a 2D cell system within a hydrogel support. Our approach has the advantage of first enabling aggregate condensation while still retaining the possibility of combining these aggregates with an injectable hydrogel. Moreover, micro-aggregation prior to implantation in current ACI or MACI protocols might be highly beneficial for the clinical outcome. Thus, the extra simple step suggested herein might lead to a great improvement of current protocols.

Previous related studies have investigated the differences in gene expression using only a selection of genes. Consequently, the mechanism of action of the increased cartilage formation after micro-aggregation has remained largely unknown. To the best of our knowledge, this is the first comprehensive study that included a whole genome gene expression analysis elucidating gene regulatory networks involved in chondrocyte micro-aggregation. Our data suggested a central role for CTGF (also known as CCN2). It has been shown that CTGF is a potent mediator of chondrogenesis and is involved in the cell cycle [31]. Furthermore, CTGF is an established TGF β target

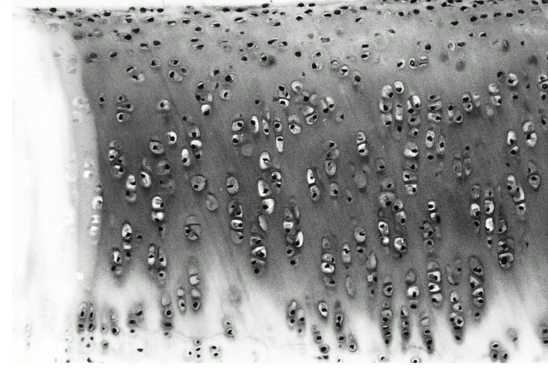
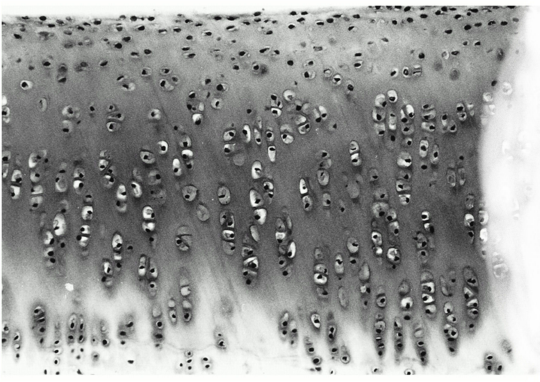
gene and mediates many of TGF β 's effects [32]. Indeed, the major changes in bio-functions were related to cellular function, proliferation and connective and skeletal tissue development. Moreover, our data demonstrated that the transcriptional effects of chondrocyte micro-aggregation are conserved between tested species.

Collectively, our data demonstrate that chondrocyte micro-aggregation prior to seeding of tissue engineered constructs has a beneficial effect on cartilage matrix formation compared to single cell cultures. Our experimental approach mimicking cell clusters, such as found in OA and other cartilage related diseases caused by chemical or mechanical injury, suggests that these clusters may indeed be part of an innate self-regenerative response of cartilage. Using our approach, it is possible to produce in high-throughput micro-aggregates with specific cell densities, using a simple and reproducible method. These micro-aggregates can be successfully incorporated into injectable *in situ* forming hydrogels, without affecting cell viability and the aggregates' spherical shape, while boosting cartilage formation compared to single cell-seeded constructs. Therefore, high-throughput formation of micro-aggregates prior to chondrocyte implantation in current ACI and MACI protocols may improve and accelerate hyaline cartilage formation.

References

1. Jones, D.G. and L. Peterson, Autologous chondrocyte implantation. *J Bone Joint Surg Am*, 2006. 88(11): p. 2502-20.
2. Buckwalter, J.A. and H.J. Mankin, Articular cartilage repair and transplantation. *Arthritis Rheum*, 1998. 41(8): p. 1331-42.
3. Batty, L., et al., Autologous chondrocyte implantation: an overview of technique and outcomes. *ANZ J Surg*, 2011. 81(1-2): p. 18-25.
4. Vavken, P. and D. Samartzis, Effectiveness of autologous chondrocyte implantation in cartilage repair of the knee: a systematic review of controlled trials. *Osteoarthritis Cartilage*, 2010. 18(6): p. 857-63.
5. Hamilton, D.W., et al., Chondrocyte aggregation on micrometric surface topography: a time-lapse study. *Tissue Eng*, 2006. 12(1): p. 189-99.
6. Wolf, F., et al., Cartilage tissue engineering using pre-aggregated human articular chondrocytes. *Eur Cell Mater*, 2008. 16: p. 92-9.
7. Jin, R., et al., Enzyme-mediated fast in situ formation of hydrogels from dextran-tyramine conjugates. *Biomaterials*, 2007. 28(18): p. 2791-800.
8. Jin, R., et al., Enzymatically Crosslinked Dextran-Tyramine Hydrogels as Injectable Scaffolds for Cartilage Tissue Engineering. *Tissue Eng Part A*, 2010. 16(8): p. 2429-40
9. Szklarczyk, D., et al., The STRING database in 2011: functional interaction networks of proteins, globally integrated and scored. *Nucleic Acids Res*, 2011. 39(Database issue): p. D561-8.
10. Kuo, C.K., et al., Cartilage tissue engineering: its potential and uses. *Curr Opin Rheumatol*, 2006. 18(1): p. 64-73.
11. de Chalain, T., J.H. Phillips, and A. Hinek, Bioengineering of elastic cartilage with aggregated porcine and human auricular chondrocytes and hydrogels containing alginate, collagen, and kappa-elastin. *J Biomed Mater Res*, 1999. 44(3): p. 280-8.
12. Fukuda, J., et al., Micromolding of photocrosslinkable chitosan hydrogel for spheroid microarray and co-cultures. *Biomaterials*, 2006. 27(30): p. 5259-67.
13. Strobel, S., et al., Anabolic and catabolic responses of human articular chondrocytes to varying oxygen percentages. *Arthritis Res Ther*, 2010. 12(2): p. R34.
14. Woodfield, T.B., et al., Scaffolds for tissue engineering of cartilage. *Crit Rev Eukaryot Gene Expr*, 2002. 12(3): p. 209-36.
15. Furukawa, K.S., et al., Rapid and large-scale formation of chondrocyte aggregates by rotational culture. *Cell Transplant*, 2003. 12(5): p. 475-9.
16. Martinez, I., et al., Differences in the Secretome of Cartilage Explants and Cultured Chondrocytes Unveiled by SILAC Technology. *Journal of Orthopaedic Research*, 2010. 28(8): p. 1040-1049.
17. DeLise, A.M., L. Fischer, and R.S. Tuan, Cellular interactions and signaling in cartilage development. *Osteoarthritis Cartilage*, 2000. 8(5): p. 309-34.
18. Aurich, M., et al., Differential matrix degradation and turnover in early cartilage lesions of human knee and ankle joints. *Arthritis Rheum*, 2005. 52(1): p. 112-9.
19. Poole, A.R., et al., Osteoarthritis in the human knee: a dynamic process of cartilage matrix degradation, synthesis and reorganization. *Agents Actions Suppl*, 1993. 39: p. 3-13.
20. Lotz, M.K., et al., Cartilage cell clusters. *Arthritis Rheum*, 2010.
21. Lee, G.M., et al., The incidence of enlarged chondrons in normal and osteoarthritic human cartilage and their relative matrix density. *Osteoarthritis Cartilage*, 2000. 8(1): p. 44-52.
22. Kouri, J.B., et al., Use of microscopical techniques in the study of human chondrocytes

- from osteoarthritic cartilage: an overview. *Microsc Res Tech*, 1998. 40(1): p. 22-36.
23. McGlashan, S.R., et al., Primary cilia in osteoarthritic chondrocytes: from chondrons to clusters. *Dev Dyn*, 2008. 237(8): p. 2013-20.
24. Pfander, D., et al., [Cell proliferation in human arthrotic joint cartilage]. *Z Orthop Ihre Grenzgeb*, 2001. 139(5): p. 375-81.
25. Schumacher, B.L., et al., Horizontally oriented clusters of multiple chondrons in the superficial zone of ankle, but not knee articular cartilage. *Anat Rec*, 2002. 266(4): p. 241-8.
26. Khademhosseini, A., et al., Microscale technologies for tissue engineering and biology. *Proc Natl Acad Sci U S A*, 2006. 103(8): p. 2480-7.
27. Penick, K.J., L.A. Solchaga, and J.F. Welter, High-throughput aggregate culture system to assess the chondrogenic potential of mesenchymal stem cells. *Biotechniques*, 2005. 39(5): p. 687-91.
28. Kelm, J.M. and M. Fussenegger, Microscale tissue engineering using gravity-enforced cell assembly. *Trends Biotechnol*, 2004. 22(4): p. 195-202.
29. Albrecht, D.R., et al., Probing the role of multicellular organization in three-dimensional microenvironments. *Nat Methods*, 2006. 3(5): p. 369-75.
30. Griffith, L.G. and M.A. Swartz, Capturing complex 3D tissue physiology in vitro. *Nat Rev Mol Cell Biol*, 2006. 7(3): p. 211-24.
31. Maeda, A., et al., CCN family 2/connective tissue growth factor modulates BMP signalling as a signal conductor, which action regulates the proliferation and differentiation of chondrocytes. *J Biochem*, 2009. 145(2): p. 207-16.
32. Song, J.J., et al., Connective tissue growth factor (CTGF) acts as a downstream mediator of TGF-beta1 to induce mesenchymal cell condensation. *Journal of cellular physiology*, 2007. 210(2): p. 398-410.



Chapter 11

Reflections and outlook: *complexities in articular cartilage tissue engineering*

I never did a day's work in my life. It was all fun.
Thomas Edison

11.1 Abstract

Cartilage tissue engineering requires an understanding of a variety of life science principles, and biomaterial chemistry, for the successful development of new therapeutic approaches. However, the current state-of-the-art knowledge is finite. Complexities at several levels provide challenges in current research and opportunities for future investigations. In this chapter the different levels of complexities are discussed in a bottom-up manner and emphasize how this thesis contributes to our understanding of these complexities.

11.2 Cell complexity

A cell is defined as the smallest structural unit of an organism that is capable of independent functioning, consisting of one or more nuclei, cytoplasm, and various organelles, all surrounded by a semipermeable cell membrane. The traditional tissue engineer approaches a cell as an input-output mechanism. For example, one expects that the inclusion of a single factor, such as a growth factor, would result in a singular cellular response that is based on the primary known function of the used growth factor. In recent years awareness has grown that such factors might not just have a single function [1]. They often have additional unknown, unforeseen or even contradictory effects. This can be due to unknown direct interaction, complex formation with other cellular components or secondary events that are caused by the original manipulation of the cell. Using this perspective, it seems intuitive that the mechanism of action of the secreted antagonists GREM1, FRZB and DKK1, which in chapter 4 were revealed to play important roles in the prevention of hypertrophic differentiation in hyaline cartilage, might not be solely mediated by their putative pathways. Indeed, in chapter 6 we demonstrated that changing the activity of either BMP or Wnt signaling results in a change in the activity of the other pathway via the regulation of each other antagonists e.g. GREM1, FRZB and DKK1. Regrettably, many of such cross-communications have remained largely uninvestigated and obscure our ability to understand and control cells.

Fortunately, this box of Pandora can be 'reverse-engineered' into a fire of Prometheus. This process would require an integrative network analysis [2]. Moreover, it has to transcend the traditional single level focus e.g. protein-protein or protein-gene interactions. Instead, it would entail an integrated analysis that includes many regulatory events that includes, but is not limited to, transcriptional activity, complex formation, functional redundancy, miRNA regulation, histone modifications and promoter silencing/activation. In the long term, this fundamental knowledge might allow for the generation of valuable predictive *in silico* cell models [3]. In shorter term, it can stimulate the understanding of complex diseases [4]. For example, osteoarthritis is a heterogeneous disease of which the underlying mechanism, in at least a subset of patients, might be hypertrophic differentiation of chondrocytes [5]. However, fundamental osteoarthritis research has indicated many different and seemingly unrelated pathways. Aberrant regulation of these pathways resulted in the development of an osteoarthritic phenotype via the hypertrophic pathway. Hypertrophic differentiation itself is a tightly orchestrated process that is based on intense cross-communication between multiple pathways. It is therefore tempting to speculate whether the pathological development of osteoarthritis might not be caused by deregulation of a single factor or pathway, but is mediated via the deregulation of several pathways, which can be instigated by deregulation by one of several pathways and is mediated via their cross communication. A development that might drive our understanding of such cellular behavior are the recent advances in promoter analysis, by which one predicts and validates which transcription factors control a particular gene or set of genes [6]. Consequently, one would be able to distill the essence of pathway activities from newly

acquired data or previously reported freely available datasets e.g. whole genome gene expression microarrays.

11.3 Tissue complexity

Tissue is defined as an aggregation of morphologically similar cells and associated intercellular matter acting together to perform one or more specific functions in the body. Mature articular cartilage appears to be a rather simple tissue compared to other tissues. It almost solely consists of a sparse population of chondrocytes that is surrounded by its matrix. However, it is complex in terms of its organization. Chondrocytes reside within a unique combination of matrix molecules that forms a specialized microenvironment that is commonly referred to as pericellular matrix [7]. Not only does this matrix convey mechanical stimuli from the extracellular matrix to the chondrocytes, it allows for the concentration of secreted factors [8]. In fact, in chapter four we describe that GREM1, FRZB and DKK1 expression is mostly restricted to the pericellular matrix.

Articular cartilage is comprised of several consecutive zones that not only are phenotypically distinct, but also perform unique functions. For example, the superficial zone is in contrast to the other zones essential to joint lubrication [9]. In addition, gradients permeate the articular cartilage, which can either be bound e.g. glycosaminoglycans or unbound e.g. oxygen and glucose [10]. Moreover, a robust osteochondral interface is indispensable for long term joint function [11]. Next to zonal differences, there are continuous elements that penetrate all zones of articular cartilage e.g. collagen fibers. The orientation of these fibers is dissimilar in different zones, which facilitates the transduction of mechanical stress [12]. The incorporation of such tissue complexities might augment the function of the engineered tissue by mimicking native tissue.

11.4 Organ complexity

Organs are defined as a group of tissues that perform a specific function or group of functions. Therefore, synovial joints are considered an organ as it is comprised of multiple tissues e.g. articular cartilage, synovium, meniscus, articular fat pads and tendons, which together allow for smooth and painless articulated motion of the diarthrodial joint. In fact, cartilage degenerative diseases such as osteoarthritis or rheumatoid arthritis are not cartilage specific but are considered joint diseases [13]. The altered behavior of several joint tissues contribute to the degeneration of the cartilage.

The foremost mechanism of communication between the different tissues that constitute the diarthrodial joint is mediated via the secretion of molecules into the synovial fluid. In normal homeostasis of the joint it functions as a portal that disseminates secreted factors that propagate continued function of the joint [14]. These factors are often referred to as master regulators'. These molecules are expected to function in, or even have their expression and/or activity influenced by, the local micro-environment.

Typically, deregulation of organ function correlates with aberrant expression or function of the master regulators. The secreted factors GREM1, FRZB and DKK1 fit this description. In chapter four we revealed that these antagonists are enriched in articular cartilage and prevent hypertrophic differentiation. In chapter five and six we describe that their expression is strongly influenced by stimuli correlated with pathological processes. In chapter seven and eight we demonstrate that the expression of these antagonists is driven by hypoxia, which an archetypal environmental factor of articular cartilage. The cross-communication between different tissues *in vivo* renders a challenge to the interpretation of *in vitro* experiments based on single cultures, as one cannot exclude that the data are confounded by this experimental artifact. Much knowledge has been derived from experiments based on non-human mammals. This approach provides specimens with low donor variation that are available on demand. Furthermore, they allow for experimentation that cannot be performed in humans due to ethical reasons. However, one has to be aware of the differences between species. For example, our understanding of both cartilage and joint homeostasis relies heavily on genetic mouse models. However, mouse joints are not fully comparable to their human equivalent. Not only are their genetic differences that result in (slightly) dissimilar proteins, they also do not undergo the same mechanical and nutritional stresses due to the animal's size and articular cartilage's height [15].

Further characterization of master regulators and cross-communication between tissues in humans might not only stimulates the acquisition of fundamental knowledge and drives the discovery of predictive and prognostic biomarkers, but also provides a solid theoretical framework containing the fundamental elements for successful cartilage repair strategies.

11.5 Valorization complexity

Although the traditional meaning of valorization is to give or ascribe value or validity to (something), the more modern annotation is slightly different as witnessed by the definition that the Dutch Innovation Platform employs: the process of value creation from knowledge by making it suitable and/or available for economic and/or social use by translating it into competitive products, services, processes or new commercial activities. In the current context it refers to the successful development of a clinically used/usable technique or product that is based on functional restoration of the joint by means of repairing the tissue by replacing the lost cells and/or matrix with a stable tissue engineered construct.

Repair of joint function or prevention of joint degeneration can be accomplished in various ways. One of these strategies is tissue engineering, which can be divided in two general approaches: those who include cells and those who do not. The most palpable contributions of this thesis relate to cell based approaches, as it is mainly focused on hypertrophic differentiation of chondrocyte(-like cells). When cells are used for cartilage repair, one is challenged to stimulate the used cells to rapidly form robust cartilage. This can typically be achieved by e.g. engineering implantable cartilage *in vitro*, stimulating cell *in vitro* prior implantation or including stimulating

factors within the optional biomaterial in which the cell can be laden. It is imperative to realize that some factors that boost neo-cartilage formation in the short term may hinder joint function in the long term, as they might alter the cellular behavior. For example, BMPs can stimulate chondrogenic differentiation of MSCs and enhance cartilage deposition by chondrocytes, but they also augment hypertrophic differentiation and endochondral ossification [16, 17]. Therefore, understanding of processes such as hypertrophic differentiation might prove invaluable for successful long term therapeutic outcome.

Engineering of cartilage and the use of large amounts of human compatible recombinant proteins is expensive and its clinical use might even prove to be cost-prohibitive for larger patient groups. It is therefore the challenge to design novel therapies that not only excel in overall complexity driven by technological developments, but rather also stand out by its elegant simplicity. In the current thesis we have explored two alternatives to the current treatments, which boost neo-cartilage formation in a cost-effective manner. In chapter nine we demonstrated that the addition of MSCs to chondrocyte provides an environment that induces more cartilage formation than just chondrocytes alone. In chapter ten we pioneered the chondrogenic effect of chondrocyte micro-aggregation using a newly designed highly controlled low cost high throughput platform.

Many novel strategies have shown to encompass advantages over the currently used clinical procedures. However, their true clinical relevance is yet to be determined. Although, most *in vitro* observations are frequently validated *in vivo*, they are frequently only performed in subcutaneous mouse models. Such a model is not representative for the micro-environment of the degenerating joint. Furthermore, the studies using orthotopic models are mostly only performed in small animals. These models do not possess the comparable mechanical stresses found in larger animals such as men. Moreover, most animal models are based on inbred animals and are therefore hard to extrapolate to (non-inbred) humans, particularly with heterogeneous diseases such as degenerative cartilage diseases. Consequently, it remains difficult to appraise the true clinical potential of many newly proposed cartilage repair strategies.

The development of new cell based tissue engineered strategies is further challenged by regulatory bodies. It is becoming increasingly difficult to obtain approval for marketing novel cell based treatments. The current European legislation for tissue engineered constructs belongs to Regulation '(EC) No 1394/2007' that regulates advanced therapy medicinal products. In contrast, cell-free strategies to repair diarthrodial joint are declared as class III medical devices according to Directive '2005/50/EC' [18]. As this affects the chance of successful deployment of the proposed product, it adds to the reasons why one would consider devising a cell-free-biomaterial cartilage repair strategy such as discussed in chapter two. This thesis further fuels the understanding of how implanted cell-free biomaterials should interact with the native cells. For example, combining a cell-free implant with native cells that are recruited via bone marrow stimulation techniques often results in hypertrophic differentiation and subsequent formation of endochondral bone within the articular cartilage [19, 20]. To prevent this undesired phenomenon one might include factors that are able to inhibit this process without interfering with the chondrogenesis. In this thesis we add to this

by revealing GREM1, FRZB, DKK1 and hypoxia mimicking molecules as potential candidates for these factors. Ultimately, the inclusion of stimulatory or inhibitory factors that are discovered in fundamental biology can be incorporated in biomaterial sciences to facilitate the rise of the next generation cartilage repair strategies.

References

1. Bussell, K., Adhesion and signalling - The many faces of beta-catenin. *Nature Reviews Molecular Cell Biology*, 2004. 5(12): p. 952-952.
2. Wu, J., et al., Integrated network analysis platform for protein-protein interactions. *Nat Methods*, 2009. 6(1): p. 75-7.
3. Lewis, N.E., et al., Large-scale in silico modeling of metabolic interactions between cell types in the human brain. *Nat Biotechnol*, 2010. 28(12): p. 1279-85.
4. Zheng, S., et al., Integrative network analysis identifies key genes and pathways in the progression of hepatitis C virus induced hepatocellular carcinoma. *BMC Med Genomics*, 2011. 4: p. 62.
5. Pitsillides, A.A. and F. Beier, Cartilage biology in osteoarthritis-lessons from developmental biology. *Nat Rev Rheumatol*, 2011. 7(11): p. 654-63.
6. Thomas-Chollier, M., et al., Transcription factor binding predictions using TRAP for the analysis of ChIP-seq data and regulatory SNPs. *Nat Protoc*, 2011. 6(12): p. 1860-9.
7. Toole, B.P., Hyaluronan: from extracellular glue to pericellular cue. *Nat Rev Cancer*, 2004. 4(7): p. 528-39.
8. Macri, L., D. Silverstein, and R.A. Clark, Growth factor binding to the pericellular matrix and its importance in tissue engineering. *Adv Drug Deliv Rev*, 2007. 59(13): p. 1366-81.
9. Neu, C.P., et al., Mechanotransduction of bovine articular cartilage superficial zone protein by transforming growth factor beta signaling. *Arthritis Rheum*, 2007. 56(11): p. 3706-14.
10. Heywood, H.K., M.M. Knight, and D.A. Lee, Both Superficial and Deep Zone Articular Chondrocyte Subpopulations Exhibit the Crabtree Effect But Have Different Basal Oxygen Consumption Rates. *Journal of Cellular Physiology*, 2010. 223(3): p. 630-639.
11. Dormer, N.H., et al., Osteochondral interface regeneration of the rabbit knee with macroscopic gradients of bioactive signals. *J Biomed Mater Res A*, 2011.
12. Ugrumova, N., et al., The collagen structure of equine articular cartilage, characterized using polarization-sensitive optical coherence tomography. *Journal of Physics D-Applied Physics*, 2005. 38(15): p. 2612-2619.
13. Martel-Pelletier, J. and J.P. Pelletier, Is osteoarthritis a disease involving only cartilage or other articular tissues? *Ekleml Hastaliklari Ve Cerrahisi-Joint Diseases and Related Surgery*, 2010. 21(1): p. 2-14.
14. Diarra, D., et al., Dickkopf-1 is a master regulator of joint remodeling. *Nat Med*, 2007. 13(2): p. 156-63.
15. Waterston, R.H., et al., Initial sequencing and comparative analysis of the mouse genome. *Nature*, 2002. 420(6915): p. 520-62.
16. Freyria, A.M., S. Courtes, and F. Mallein-Gerin, [Differentiation of adult human mesenchymal stem cells: chondrogenic effect of BMP-2]. *Pathol Biol (Paris)*, 2008. 56(5): p. 326-33.
17. Noel, D., et al., Short-term BMP-2 expression is sufficient for in vivo osteochondral differentiation of mesenchymal stem cells. *Stem Cells*, 2004. 22(1): p. 74-85.
18. Altenstetter, C., Medical Device Regulation and Nanotechnologies: Determining the Role of Patient Safety Concerns in Policymaking. *Law & Policy*, 2011. 33(2): p. 227-255.
19. Brown, W.E., et al., Magnetic resonance imaging appearance of cartilage repair in the knee. *Clin Orthop Relat Res*, 2004(422): p. 214-23.
20. Rubak, J.M., Reconstruction of articular cartilage defects with free periosteal grafts. An experimental study. *Acta Orthop Scand*, 1982. 53(2): p. 175-80.

Acknowledgements

As with all good things, this both scientific and very personal story has come to an end. As this thesis rests on the unyielding support of colleagues and friends, I would like to express my sincere gratitude, appreciation and respect to all involved. However, if this is the first page you read, please be kindly referred to chapter one.

First of all, Marcel you have been a great supervisor to me. I particularly appreciated our ‘open door meetings’, scientific discussions that very much transcended the confines of my own project and the freedom to explore adjacent topics. You uniquely contributed to my development as a scientist. Without you this thesis would not have been possible.

I would also like to acknowledge my promoter Clemens van Blitterswijk, for the opportunity and freedom to conduct my PhD research in the Tissue Regeneration group.

Moreover, I would like to thank Prof. Dr. Floris Lafeber, Prof. Dr. Gerjo van Osch, Dr. Peter van der Kraan, Prof. Dr. Leon Terstappen, Dr. Pieter Emans and Prof. Dr. Jan de Boer for taking place in the graduation committee.

To my paranymphs: Liliana and Jim. Thank you for standing behind me, although today it’s quite a bit more literal than usual. Please don’t forget to smile and look pretty.

It would have been impossible to have come to this point without being surrounded by a pleasant working atmosphere. Therefore, I would like to thank all direct and indirect colleagues. Nicole, please remain fluffy. Ellie, let’s go for another conference! Chris, you’re my favorite German supporter. Ling, looking at two cells interacting will never be the same without you. Karolina, please keep on killing people. Maciej and Sandra, thank you for keeping me well fed. Juan, thank you for sharing my geek-pride. Janine, as you noticed: cartilage does not regenerate, but it does grow (on you). André, you are the noblest person I ever met, please don’t be changed by the world. Sieger, I believe you can show that with small things you can accomplish great things. Bernke, let’s continue sharing stories over the years to come. Gizmo, Emma, Gobi and Ghandi thank you for spreading the love.

Dear Paula, Jim, Nathalie and Roos, although it is often not easy to synchronize our schedules, I am fully confident that we will always remain friends.

Naturally, I would like to thank my parents, brother and sister for their continued support, love and understanding. I would have never been able to come to this point if it weren’t for you. Thank you.

Lastly and above all else, I would like to thank my dear Dr. Lili. You are my muse, sounding board and slave-driver all in one loving little package. You complete me as I never imagined possible. Both this thesis and I are dedicated to you. Amo-te.

Curriculum Vitae

Jeroen Leijten was born on the 22nd of October 1982 in Breda, The Netherlands. In 2001 he received his diploma for pre-university education (VWO) from the Jan Tinbergen College in Roosendaal, The Netherlands. In August 2001 he started his study Biomedical Sciences at the University of Leiden, The Netherlands. During his studies he performed several traineeships in amongst others hematology, immunology and virus and stem cell biology at the LUMC, Leiden, The Netherlands. In December 2006 he graduated and obtained his MSc diploma. His master project was focused on improving the differentiation of stem cells into functional hepatocytes and was performed under the supervision of Dr. T. de Vries and Prof. Dr. R. Hoeben. Between 2003 and 2007 he worked initially as a student assistant and later as a senior assistant in teaching human physiology. In 2007, he started his PhD at the department of Tissue Regeneration at the University of Twente, MIRA Institute of Biomedical Technology and Technical Medicine, The Netherlands, under the supervision of Prof. Dr. C.A. van Blitterswijk and Prof. Dr. M. Karperien. The subject of his research was the prevention of hypertrophic differentiation in both the joint and cartilage tissue engineered constructs. For part of the work described in this thesis Jeroen Leijten has received a travel grant and abstract and poster awards on various international conferences. From November 2011, he will continue his scientific career as a post doctoral researcher at the department of Developmental Bioengineering, University of Twente, The Netherlands. During this period he will focus on improving tissue engineered constructs by combining traditional (molecular) cell biology with established biomaterials and microfluidic technology.

List of Publications

Peer-reviewed papers

Leijten JCH*, Moreira Teixeira LS*, Georgi N*, Wu L and Karperien M. Cartilage tissue engineering. *Endocrine Development*. 2011, vol 22, pp 102115.

Wu L, **Leijten JCH**, Georgi N, Post JN, van Blitterswijk CA, Karperien M. Trophic effects of mesenchymal stem cells increase chondrocyte proliferation and matrix formation. *Tissue Engineering Part A*. 2011 May;17(9-10):1425-36.

Moreira Teixeira LS, **Leijten JCH**, Wennink J, Ganguly A, de Boer J, Feijen J, van Blitterswijk CA, Dijkstra P, Karperien M. The effect of platelet lysate supplementation of a dextran-based hydrogel on cartilage formation. *Biomaterials*. 2012 May;33(14):3651-61.

Leijten JCH*, Chinnagounder Periyasamy P*, Dijkstra PJ, Karperien M, Post JN. Nanomaterials for the local and targeted delivery of osteoarthritis drugs. Accepted in *Journal of Nanomaterials*.

Leijten JCH, Emons J, Sticht C, van Gool S, Decker E, Uitterlinden A, Rappold G, Hofman A, Rivadeneira F, Scherjon S, Wit JM, van Meurs J, van Blitterswijk CA and Karperien M. GREM1, FRZB and DKK1 are key regulators of human articular cartilage homeostasis. Accepted in *Arthritis and Rheumatism*.

Leijten JCH*, Moreira Teixeira LS*, Sobral J, Jin R, van Apeldoorn AA, Feijen J, van Blitterswijk CA, Dijkstra PJ, Karperien M. High throughput generated micro-aggregates of chondrocytes stimulate cartilage formation in vitro and in vivo. Accepted in *European Cells and Materials*.

Van Gool SA, Emons JAM, **Leijten JCH**, Decker E, Yu X, Sticht C, van Houwelingen JC, Goeman JJ, Kleijburg C, Scherjon S, Gretz N, Wit JM, Rappold G, Karperien M. Fetal mesenchymal stem cells differentiating towards chondrocytes display a similar gene expression profile as growth plate cartilage. Submitted.

Higuera GA, Hendriks JAA, van Dalum J, Wu L, Schotel R, Moreira Teixeira LS, **Leijten JCH**, van den Doel M, Karperien M, Riesle J, van Blitterswijk CA and Moroni L. Three dimensional screening of cells and tissues in vivo decreases numbers of experimental animals required to bring novel regenerative therapies to the clinic. Submitted.

Leijten JCH*, Georgi N*, van Blitterswijk CA and Karperien M. Cell sources for articular cartilage repair strategies: shifting from mono-cultures to co-cultures. Submitted.

Ma B, **Leijten JCH**, Wu L, Kip M, Post JN, van Blitterswijk CA and Karperien M. Pathway Assessment of Human Articular Chondrocyte Dedifferentiation in Monolayer Culture by Gene Expression Profiling. Submitted.

Leijten JCH, Landman EBM, Georgi N, Kip M, Jahr H, Post JN, van Blitterswijk CA and Karperien M. Transcriptional regulation of GREM1, FRZB and DKK1 by hypertrophic differentiation-related factors. Submitted.

Spitters TWGM, **Leijten JCH**, Deus FD, Ferreira da Costa IB, van Apeldoorn AA, Blitterswijk CA, Karperien M. A novel dual flow bioreactor system with controlled mechanical stimulation: mimicking cartilages natural environment more closely. Submitted.

Wu L, **Leijten JCH**, van Blitterswijk CA and Karperien M, Mesenchymal stem cells increase chondrocytes proliferation in co-culture by secreting acidic fibroblast growth factor. Submitted.

Kunstar A, **Leijten JCH**, van Leuveren S, Hilderink J, Otto C, van Blitterswijk CA, Karperien M, van Apeldoorn AA. Systematic Raman analysis of the human fetal femur cartilage. Submitted.

Wu L, **Leijten JCH**, Prins H, Helder M, van Blitterswijk CA and Karperien M, Influence of in vitro expansion on trophic effects of adipose derived mesenchymal stem cells. Submitted.

Janeczek-Portalska KK, Moreira Teixeira LS, **Leijten JCH**, Feijen J, Dijkstra PJ, Boer J, Blitterswijk CA and Karperien M. Boosting angiogenesis and functional vascularization in injectable dextran-hyaluronic acid scaffolds by endothelial-like mesenchymal stromal cells. In preparation.

Leijten JCH, de Grauw J, van Weeren PR, van Blitterswijk CA and Karperien M. Grem1, Frzb and Dkk1 protein levels correlate with acute synovitis in equine joints. In preparation.

Leijten JCH*, Georgi N*, van Blitterswijk CA and Karperien M. Hypoxia steers chondrogenically differentiating human mesenchymal stromal cells towards an articular cartilage phenotype. In preparation.

Leijten JCH, Henke SJ, Kemna E, van Blitterswijk CA, van den Berg A and Karperien M. Dextran-tyramine microhydrogel formation by enzymatic crosslinking using a microfluidic device. In preparation.

Abstracts selected for oral presentation (non-exhaustive)

Leijten JCH, Emons J, van Gool S, Carsten C, Dekker E, Rappold G, van Blitterswijk CA, Wit JM and Karperien M. Comparing articular and growth plate cartilage gene expression profiles enables hyaline cartilage type determination. Gordon Research Conference, Cartilage biology and pathology, 2009, Les Diablerets, Switzerland. *Recipient travel grant award.*

Leijten JCH, Emons J, van Gool S, Carsten C, Dekker E, Rappold G, van Blitterswijk CA, Wit JM and Karperien M. Comparison of articular and growth plate cartilage gene expression profiles allows for hyaline cartilage type determination. NBTE, 2009, Lunteren, The Netherlands.

Leijten JCH, Emons J, van Gool S, Carsten C, Dekker E, Rappold G, van Blitterswijk CA, Wit JM and Karperien M. GREM1, FRZB and DKK1 are highly specific markers for articular cartilage which prevent hypertrophic differentiation. OARSI, 2010, Sitges, Spain.

Leijten JCH, Emons J, Sticht C, Bos S, Kerkhof HJ, Uitterlinden A, van Meurs J, Meulenbelt I, Dekker E, Rappold G, Wit JM, van Blitterswijk CA and Karperien M. GREM1, FRZB and DKK1 are enriched in articular cartilage, prevent hypertrophic differentiation and correlate with osteoarthritis. OARSI. ICRS, 2010, Brussels, Belgium.

Abstracts selected for poster presentation (non-exhaustive)

Leijten JCH, Emons J, van Gool S, Carsten C, Dekker E, Rappold G, van Blitterswijk CA, Wit JM and Karperien M. Identifying novel biomarkers able to discriminate between articular and growth plate cartilage. Highlights in biomedical technology symposium. 2008, Enschede, The Netherlands.

Leijten JCH, Emons J, van Gool S, Carsten C, Dekker E, Rappold G, van Blitterswijk CA, Wit JM and Karperien M. Comparing articular and growth plate cartilage gene expression profiles enables hyaline cartilage type determination. Gordon Research Conference, Cartilage biology and pathology, 2009, Les Diablerets, Switzerland. *Recipient best abstract award.*

Leijten JCH, Georgi N, Landman EBM, van Blitterswijk CA and Karperien M. Hypoxia inhibits hypertrophic differentiation and endochondral ossification in explanted tibias. NBTE, 2010, Lunteren, The Netherlands.

Moreira Teixeira LS*, **Leijten JCH***, Jin R, Dijkstra PJ, Feijen J, van Blitterswijk CA and Karperien M. Chondrocyte micro-aggregates enhance neo-cartilage formation. NBTE, 2010, Lunteren, The Netherlands. *Shared best poster award.*

Leijten JCH, Emons J, Bos S, Sticht C, Ma B, van Gool S, Dekker E, Uitterlinden A, Rappold G, Hofman A, Rivadeneira F, Scherjon S, Wit JM, Meulenbelt I, van Meurs J, van Blitterswijk CA and Karperien M. GREM1, FRZB and DKK1 are enriched in articular cartilage and prevent hypertrophic differentiation and endochondral ossification. Gordon

Research Conference, Cartilage biology and pathology, 2011, Ventura, USA. *Recipient best poster award.*

Leijten JCH, Georgi N, Landman EBM, van Blitterswijk CA and Karperien M. Hypoxia inhibits hypertrophic differentiation and endochondral ossification in tibia explants. OARSI, 2011, San Diego, USA.

Leijten JCH, Moreira Teixeira LS, Sobral J, Jin R, van Apeldoorn AA, Feijen J, van Blitterswijk CA, Dijkstra PJ, Karperien M. Chondrocyte cluster formation stimulates cartilage matrix deposition. OARSI, 2011, San Diego, USA.

Patent applications

Universiteit Twente, Karperien M, **Leijten JCH**. OSTEOARTHROSE MARKERS. PCT/NL2010/ P91430EP00.

* = shared first co-authorship